

Dissertation
submitted to the
Combined Faculties for the Natural Sciences and for Mathematics
of the Ruperto-Carola University of Heidelberg, Germany
for the degree of
Doctor of Natural Sciences

Presented by
Borja Garnelo Gómez, Master of Science
Born in Priaranza del Bierzo, Spain

Oral-examination: 17th November 2017

Phosphorylation of RLP44: Shifting between subcellular localization and receptor complexes

Referees: Prof. Dr. Jan Lohmann

Dr. Sebastian Wolf

Table of Contents

Table of Contents	I
List of Abbreviations	IV
Summary	1
Zusammenfassung	3
1. Introduction	5
1.1. The plant cell wall	5
1.1.1. General composition and synthesis.....	5
1.1.2. The role of pectins in cell growth and development	6
1.2. Plant Receptors	7
1.2.1. Receptor-like Kinases (RLKs)	8
1.2.2. Receptor-like Proteins (RLPs)	9
1.3. Cell Wall Signaling.....	10
1.3.1. RLKs implicated in the perception of cell wall perturbations	11
1.3.2. RLP44, a newly described sensor of CW pectin modifications	12
1.4. Brassinosteroid Signaling cascade.....	13
1.5. Phytosulfokine Signaling cascade	15
1.6. RLP44, BR and PSK- related signaling and Xylem development	16
1.7. Endocytosis and transmembrane circuits in plant cells.....	17
1.7.1. Clathrin-mediated endocytosis	17
1.7.2. Regulation of endocytosis by posttranslational modifications	18
1.7.3. Transmembrane circuits for PM proteins.....	20
Aim of this study	21
2. Results	22
Chapter 1: Phosphorylation of RLP44 controls protein function	22
2.1. Receptor-like protein 44 is a conserved receptor with a unique cytoplasmic domain.....	22
2.2. Phosphorylation is required for RLP44-mediated activation of BR signaling	24
2.3. Phosphorylation modifies RLP44 subcellular localization	26
2.4. Phosphorylation likely prevent RLP44 endocytosis.....	27
2.5. BRI1, but not Cell wall perturbation, partially influences RLP44 PM localization.....	31
2.6. RLP44 promotes BAK1 and BRI1 interaction.....	32
2.7. RLP44 activation of BR signaling requires the presence of BRI1	33
2.8. PSK signaling activation is independent of RLP44 phosphorylation.....	36
2.9. Gateway construct single phosphomutants show a nuclear localization	39
2.10. Putative phosphosites are not detected by LC-MS	41
2.11. RLP44 is phosphorylated in a Brassinosteroid (BR)-dependent manner	42
2.12. RLP44 phosphorylation depends on more than one kinase	44
2.13. RLP44 phosphorylation is PSKR1 independent.....	48

2.14.	(GS) ₁₁ -GFP linker is presumably hyperphosphorylated	50
2.15.	Phosphorylation of Ser-270 and Tyr-274 have a major effect on RLP44 function	52
2.16.	RLP44 phosphorylation influences the control of vascular fate by BL and PSK signaling	54
Chapter 2: RRE, a new saga of RLP44 suppressor mutants		58
2.17.	RRE mutants are uncouple in the integration of RLP44 signal into the BL cascade	58
2.18.	RRE mutants present changes on the CW properties	61
2.19.	RRE mutants could uncouple the integration of CW and PSK signaling	63
3.	Discussion.....	66
3.1.	RRE mutants suppose putative new player on the integration of CW signaling	66
3.1.1.	RRE 11.1 and RRE 38.6 have an altered CW	66
3.1.2.	RRE 24.1 and RRE 38.6 might participate in the control of vascular fate by RLP44....	67
3.2.	Phosphorylation of the highly conserved <i>At</i> RLP44 C-terminal domain impact on protein function	68
3.2.1.	RLP44 C-terminal domain is highly conserved	68
3.2.2.	Mutations on putative phospho-sites in RLP44 C-terminus domains alters protein function	69
3.2.3.	Specific phosphorylation of the RLP44 C-terminus is still unidentified	69
3.3.	Phosphorylation controls RLP44 clathrin-mediated endocytosis	70
3.3.1.	Phosphorylation does not interfere with protein vesicular trafficking	71
3.3.2.	RLP44 undergoes clathrin-mediated endocytosis	71
3.3.3.	Ser-268 and Ser-270 regulates the localization of RLP44	72
3.4.	RLP44 phosphorylation controls the integration of CW signals into the BL signaling cascade	73
3.4.1.	RLP44 phosphorylation is BL dependent	73
3.4.2.	RLP44 triggers the formation of BRI1 and BAK1 complex.....	75
3.4.3.	RLP44 phosphorylation modifies the interaction with BRI1 but not with BAK1.....	76
3.4.4.	RLP44 stabilization of BR signaling requires the presence of BRI1	77
3.5.	Activation of PSK signaling is independent of RLP44 phosphorylation	78
3.6.	RLP44 phosphorylation balance BL and PSK signaling in vascular fate control	79
4.	Conclusion	83
5.	Material and Methods.....	84
5.1.	Cloning procedures and Plasmid Construct	84
5.1.1.	Gateway™ Cloning	84
5.1.2.	GreenGate Cloning.....	86
5.1.3.	Transformation of competent <i>Agrobacterium tumefaciens</i>	89
5.1.4.	Stable transformation of <i>Arabidopsis thaliana</i>	90
5.2.	Plant material and growth conditions.....	91
5.2.1.	General growth conditions	91
5.2.2.	Crossing <i>A. thaliana</i>	91
5.2.3.	Transgenic lines	91
5.2.4.	gDNA Extraction	93

5.2.5. Genotyping	93
5.3. Root length measurements	93
5.4. Hypocotyl length measurements	94
5.5. Phosphorylation studies	94
5.6. EMS mutation mapping	95
5.6.1. EMS mutation procedure	95
5.6.2. Population creation for Next Generation Sequencing (NGS).....	95
5.6.3. Analysis of SNPs	95
5.7. RNA extraction and qPCR	95
5.8. Transient expression studies.....	96
5.9. BiFC (Bi-molecular Fluorescent Complementation)	96
5.10. Co-immunoprecipitation (Co-IP) and Western blotting	97
5.11. Confocal microscopy	99
5.11.1. Confocal laser scanning microscopy.....	99
5.11.2. Inhibitor treatments.....	99
5.11.3. FM4-64 staining	99
5.11.4. Basic Fuchsin staining.....	99
5.11.5. Cell Wall polysaccharides antibodies staining	99
5.12. Image analysis.....	100
5.12.1. Non-quantitative analysis	100
5.12.2. BFA compartments measurement.....	100
5.12.3. Plasma membrane-Intracellular signal ratio measurement.....	100
5.12.4. YFP/RFP ratio measurements for BiFC	101
5.13. Bioinformatics	101
5.13.1. <i>In silico</i> phosphorylation and ubiquitination prediction	101
5.13.2. Tree and protein alignments.....	101
5.14. Statistical analysis	101
5.15. Primers used in this study	102
6. Supplemental Figures	105
7. References	111
Acknowledgments	125

List of Abbreviations

All element abbreviations follow IUPAC nomenclature

Amino acids abbreviations follow standard single letter code

%	percent
$\mu\text{E m}^{-2} \text{s}^{-1}$	microEistein per square meter per second
μg	micrograme
μl	microlitre
μm	micrometer(s)
μM	micromolar
amiR	artificial micro RNA
ARF	ADP-ribosylation factor
BAK1	BRI1-ASSOCIATED KINASE 1
BFA	Brefeldin-A
BiFC	bimolecular fluorescence complementation
BL	Brassinolide
BR	Brassinosteroid
BRI1	BRASSINOSTEROID INSENSITIVE 1
BSA	bovine serum albumin
cDNA	complementary DNA
CIP	calf intestine phosphatase
CLE	CLAVATA3/EMBRYO SURROUNDING PEPTIDES
CLSM	confocal laser scanning microscopy
CLV2	CLAVATA-2
cm	centimeter
cm^2	square centimeters
CME	Clathrin-mediated endocytosis
<i>cnu2</i>	<i>comfortably numb 2</i>
CoIP	coimmunoprecipitation
Col-0	Columbia-0
CW	cell wall
dag	days after germination
DMSO	dimethyl sulfoxide
DNA	deoxyribonucleic acid
DTT	dithiothreitol
IV	

EMS	ethyl methanesulfonate
ER	endoplasmic reticulum
FLS2	FLAGELLIN-SENSING 2
FM4-64	(N-(3-triethylammoniumpropyl)-4-(6-(4-(diethylamino) phenyl) hexatrienyl) pyridinium dibromide)
gDNA	genomic DNA
GEF	guanine nucleotide exchange factors
GFP	GREEN FLUORESCENCE PROTEIN
h	hours
HG	homogalacturonans
IgG	immunoglobulin G
kDa	kilodalton(s)
LC-MS	liquid chromatography mass spectrophotometry
Ler	Landsberg erecta
LRR	leucine-rich regions
M	molar
min	minutes
ml	milliliter(s)
mM	millimolar
MS	Murashige & Skroog
MVB/LE	multivesicular bodies/ late endosome
ng	monogram(s)
NGM	next-generation mapping
NGS	next-generation sequencing
nm	nanometer(s)
nM	nanomolar
°C	degree Celsius
PCR	polymerase chain reaction
pH	potential of hydrogen/ <i>pondus hydrogenii</i>
PI3K	PHOSPHATIDYLINOSITOL 3-KINASE
PM	plasma membrane
PME	PECTIN METHYL ESTERASE
PMEI	PECTIN METHYL ESTERASE INHIBITOR
PMSF	phenylmethylsulfonyl fluoride
PPZ	propiconazol
PSK	phytosulfokine

PSKR1	PHYTOSULFOKINE RECEPTOR 1
RFP	red fluorescence protein
RLK	receptor-like kinases
RLP	receptor-like proteins
RLP44	RECEPTOR-LIKE PROTEIN 44
RNA	ribonucleic acid
ROI	region of interest
rpm	rounds per minute
RRE	RLP44-RFP EMS
RT	room temperature (22°C)
s	seconds
SD	standard deviation
SDS	sodium dodecyl sulfate
SERK	SOMATIC EMBRYOGENESIS RECEPTOR KINASE
SNP	single nucleotide polymorphism
T-DNA	transfer DNA
TGN/EE	trans-Golgi network/Early Endosome
TMM	TOO MANY MOUTHS
TPL	T-PLATE
WM	wortmannin
WT	wild-type
YFP	yellow fluorescent protein

Summary

In all organisms, tailoring development to the environment relies on the proper integration of intracellular and extracellular cues. The cell wall, the extracellular matrix of plants, directly influences the growth and shape of the cells. As a result, the biophysical properties of the cell wall are permanently controlled and the resultant information is transduced to the cell interior to accommodate the properties of the cell wall to growth. However, little is known about the cell wall signaling mechanisms or the molecular components that are part of them.

Recently, it was demonstrated that cell wall modifications could modulate the activity of the brassinosteroid (BR) signaling pathway, a feedback mechanism presumably mediating cell wall homeostasis. The integration of cell wall and BR signaling depends on the LRR receptor-like protein RLP44, which is able to interact with the BR receptor BRI1 and its co-receptor BAK1. In addition, RLP44 is important for the maintenance of procambial cell identity through PSK signaling by interacting with the PSK receptor, PSKR1. Therefore, RLP44 balances BR and PSK signaling to control vascular cell fate.

We could show that the RLP44 cytoplasmic domain is highly conserved and contains four amino acids predicted to be phosphorylated. Among those residues, Ser-268 and Ser-270 play an important role in shifting the localization of RLP44 and therefore control its function. Mechanistically, phosphorylation affects subcellular localization of the protein by exerting a negative effect on its clathrin-mediated endocytosis. Besides, RLP44 phosphorylation may alter its interaction with BR receptors, affecting signaling integration. Moreover, we demonstrated that RLP44 phosphorylation occurs in a BL-dependent manner and the phosphorylation of cytoplasmic RLP44 residues is required for activation of BR signaling. However, the kinases involved in RLP44 phosphorylation are not defined yet, although BRI1 and BAK1, but not PSKR1 might play a critical role. Contrary to the situation with BRI1, RLP44 phosphorylation is PSKR1-independent and modification of its cytoplasmic domain neither influences either the interaction with PSKR1 nor the RLP44 responsiveness to PSK. Taken together, we hypothesize that RLP44 phosphorylation might play a crucial role in regulating the integration of PSK and BL signaling in a BRI1- and Cell Wall-dependent manner. In addition, we identified in a suppressor screen of RLP44 overexpressing plants (RLP44ox), four mutants (RRE 9.2, RRE 11.1, RRE 24.1 and RRE 38.6) involved in the integration of CW changes into the BRI1- and/or PSKR1-dependent signaling. Those mutants possess an altered cell wall when compared to RLP44ox or wild-type, which might reflect an unbalanced cell wall signaling. In addition, RRE 24.1 and RRE 38.6 are PSK-insensitive and show an altered RLP44ox xylem phenotype, characterized by an increased number of xylem cell. Thus, RRE 24.1 and RRE 38.6 are promising candidates to study the integration of CW and PSK signaling and shed light on the biochemical mechanism that governs RLP44 function.

Zusammenfassung

In allen Organismen beruht die Anpassung der Entwicklung an die Umwelt auf der Integration von intrazellulären und extrazellulären Signalen. Die Zellwand, die extrazelluläre Matrix in Pflanzen, beeinflusst direkt das Wachstum und die Form der Zellen. Daher werden die biophysikalischen Eigenschaften der Zellwand permanent überwacht und die Information in die Zelle weitergeleitet, um die Eigenschaften der Zellwand anzupassen. Allerdings ist bisher wenig über diese Zellwand-vermittelten Signalprozesse oder die daran beteiligten Komponenten bekannt.

Kürzlich wurde nachgewiesen, dass die Modifikation der Zellwand die Aktivität des Brassinosteroid (BR)- Signalwegs beeinflussen kann. Dabei handelt es sich vermutlich um einen Rückkopplungsmechanismus der die Zellwandhomöostase aufrecht erhält. Die Integration der Zellwand und des BR-Signalweg hängt vom LRR Rezeptor-ähnlichen Protein RLP44 ab, das mit dem BR-Rezeptor BRI1 und dessen Co-Rezeptor BAK1 interagieren kann. Darüber hinaus ist RLP44 wichtig für die Aufrechterhaltung der prokambialen Zellidentität durch den Phytosulfokin (PSK)-Signalweg indem es mit dem PSK-Rezeptor, PSKR1, interagiert. Daher balanciert RLP44 die BR- und PSK-Signalwege, um das vaskuläre Zellschicksal zu bestimmen.

Wir haben gezeigt, dass die zytoplasmatische Domäne von RLP44 evolutionär hoch konserviert ist und vier Aminosäuren enthält, die basierend auf Vorhersagen phosphoryliert werden könnten. Insbesondere Ser-268 und Ser-270 spielen eine wichtige Rolle bei der Kontrolle der Lokalisierung von RLP44 und, daraus folgend, dessen Funktion. Mechanistisch beeinflusst die Phosphorylierung die subzelluläre Lokalisation des Proteins, indem sie eine negative Wirkung auf die Clathrin-vermittelte Endozytose ausübt. Außerdem hat die Phosphorylierung von RLP44 Auswirkungen auf die Interaktion mit BRI1, was wiederum direkt Einfluss auf die Signalweiterleitung hat. Darüber hinaus haben wir gezeigt, dass die Phosphorylierung von RLP44 BL-abhängig ist und für die Aktivierung der BR-Signalwegs erforderlich ist. Allerdings sind die an der Phosphorylierung beteiligten Kinasen nicht bekannt, obwohl BRI1 und BAK1, eine entscheidende Rolle spielen könnten. Hingegen ist die RLP44-Phosphorylierung PSKR1-unabhängig und diese Modifikation der zytoplasmatischen Domäne beeinflusst weder die Wechselwirkung mit PSKR1 noch die RLP44-Antwort auf PSK. Zusammengefasst vermuten wir, dass die RLP44-Phosphorylierung eine entscheidende Rolle bei der Regulierung der Integration der PSK- und BL-Signalwege in einer BRI1- und Zellwandabhängigen Weise spielen könnte. Des Weiteren konnten in einem Suppressor-Screen von RLP44 Überexpressionspflanzen (RLP44ox) vier Mutanten (RRE 9.2, RRE 11.1, RRE 24.1 und RRE 38.6) identifizieren, die an der Integration von Zellwandveränderungen mit den BRI1- und/oder PSKR1-Signalwegen involviert sind. Im Vergleich zu RLP44ox und dem Wildtyp besitzen diese Mutanten eine veränderte Zellwand, was ein Hinweis auf eine Abweichung in der Zellwandsignalweiterleitung darstellen könnte. Darüber hinaus waren RRE 24.1 und RRE 38.6 insensitiv gegenüber PSK und zeigten einen veränderten RLP44ox-Xylem-Phänotyp, der durch eine Erhöhung der Xylem-Zellen gekennzeichnet ist. Demnach sind RRE 24.1 und RRE 38.6 vielversprechende Kandidaten, um die Integration von Zellwand- und PSK-Signalwege zu untersuchen und den biochemischen Mechanismus, dem die RLP44-Funktion unterliegt, zu verstehen.

1. Introduction

1.1. The plant cell wall

1.1.1. General composition and synthesis

The plant cell wall plays a central role in building the architecture of the cell, participating in the defense mechanisms and also controlling growth and development of plants (Cosgrove 2005).

The plant cell wall comprised of a complex polysaccharide network, in which cellulose is an important load bearing structure interacting and intercalating other polysaccharides such as hemicelluloses and pectin (Wolf et al., 2012). In addition, various proteins also contribute to plant cell wall architecture. Moreover, in secondary cell walls that only appear in specialized tissues such as phloem and xylem after cessation of growth (Oda and Fukuda 2012), cell wall has a different composition, with changes in hemicelluloses types, reduction of pectin amount, appearance of lignin and an increase on cellulose content (Mellerowicz and Sundberg 2008).

Cellulose is a linear polymer of β (1 \rightarrow 4) linked glucan that is synthesized directly at the plasma membrane level and exported to the cell wall forming microfibrils and representing the most abundant component of the cell wall. Cellulose microfibrils are synthesized by Cellulose Synthase Complexes (CSC) directly at the plasma membrane (PM) (Arioli et al., 1998; Taylor et al., 2003). CSC form a rosette structure that is formed by six units and each individual unit is then comprised of three different CELLULOSE SYNTHASES (CESAs). Therefore, CESAs represent the fundamental elements involved in the formation of cellulose. The combination of CESAs within CSCs vary depending on the kind of cellulose that they need to produce either for the primary or the secondary cell wall. CSCs activity controls the movement of the complex and the distribution of microfibrils in the cell wall. In addition, the CSCs trajectory is controlled by cortical microtubules at the periphery of the cytoplasm (Paredez et al., 2006). In fact, disruption of microtubules has a direct effect on the CESAs mobility and therefore on the cell wall properties as it happens when in *Arabidopsis botero1* plants, where KATANIN - an enzyme that controls the length of microtubules (Bichet et al., 2001) - is mutated. The same phenotype can be reproduced pharmacologically though the use of oryzalin, an agent that depolymerize microtubules (Somerville 2006).

Hemicelluloses have a linear backbone of varying sugars, β (1 \rightarrow 4) glucan, xylan or mannan, (Scheller and Ulvskov 2010) that, in contrast with cellulose, these sugars are frequently interchanged along the hemicellulose fiber (Cosgrove 2005). Xyloglucan represents the main hemicellulose in primary cell wall of *Arabidopsis thaliana* and other dicots, whereas mannan and xylan are the main hemicellulose in the secondary cell wall (Scheller and Ulvskov 2010). Xyloglucans are synthesized in the Golgi apparatus by XYLOSYLTRANSFERASES (XXT1/XXT2) and exported by vesicles to the extracellular matrix (Cavalier and Keegstra 2006). Traditionally, it has been postulated that hemicelluloses act as the main compound tethering cellulose microfibrils and therefore strengthening the cell wall (Cosgrove 2005) although, in recent years the active role of hemicelluloses in development and in the response to pathogens, has been demonstrated (Xiao et al., 2016).

Pectins are formed by a large number of different sugar residues and therefore represents the most complex family of polysaccharides in nature (Wolf et al., 2009). Pectins consist of five different classes of polysaccharides: homogalacturonan (HG), xylogalacturonan (XGA), apiogalacturonan (AP), rhamnogalacturonan I (RGI) and rhamnogalacturonan II (RGII); all which vary in the type of sugars that form the main polysaccharide chain as well as on the type and complexity of the lateral chains (Hosmer and Mohnen 2009). HG is the most abundant pectin in all analyzed plant species. HG is a linear polymer of α (1 \rightarrow 4) linked galacturonic acid that are synthesized in the Golgi apparatus by GLYCOSYLTRANSFERASES and secreted to the cell wall in a highly-methylesterified status (Atmodjo et al., 2013). *In muro*, HGs can undergo modifications in their methylesterification levels by the activity of PECTIN METHYLESTERASES (PMEs) that are in turn controlled by PECTIN METHYLESTERASE INHIBITORS (PMEIs) (Pelloux et al., 2007). In the last decades, the notion of a pliant pectin gel has been challenged and it has been shown that pectins have indeed an active and dynamic role in controlling cell wall properties. Current research indicates that pectin down products and pectin modifications emerged as a player in the regulation of growth and development of the plant cell (Hocq et al., 2016).

1.1.2. The role of pectins in cell growth and development

As a rigid structure around cells, the cell wall actively participates in giving structure to the cell and, by extension, to the whole plant. Moreover, cell wall is the interface through which plant cells are glued together and it plays a vital role in cell-to-cell communication. In addition, due to its rigid structure, the cell wall supposes to be the first physical barrier against pathogens and it is involved in the activation of defense signaling cascades by acting as elicitor for the immune receptors. However, most importantly, the cell wall controls the direction and speed of the cell growth together with the turgor pressure.

Cellulose deposition driven by the CSC motility directly controls the direction of the growth. Cells grow anisotropically perpendicular to the orientation of the cellulose microfibrils (Suslov and Verbelen 2006). Perturbation of cellulose synthesis genes or cortical microtubules assembly produces a change on the cell growth anisotropy (Arioli et al., 1998; Bichet et al., 2001; Desprez et al., 2002). Furthermore, hemicelluloses might reinforce the structure of cellulose by their non-covalent interaction (Park and Cosgrove 2015) and a lack of proper xyloglucan, as in the *xxt1 xxt2* mutant, can influence the stability of cellulose under mechanical stress but without having a dramatic impact in growth (Cavalier et al., 2008; Xiao et al., 2016). However, the idea of hemicelluloses as the main structural companion of cellulose has been challenged and a model has been proposed in which cellulose and hemicellulose have limited interactions and pectin plays a more fundamental role (Cosgrove 2015; Hocq et al., 2016). Moreover, cellulose and hemicellulose interactions are believed to be the target of expansins, proteins that disrupt non-covalent bindings of the wall polysaccharides without a hydrolytic effect that ends up in an irreversible wall expansion (Cosgrove 2005) as well as endo-glucanases that hydrolase the glucosidic bonds and might facilitate new wall material integration (Perrot-Rechenmann 2010). It has been demonstrated that pectins have a direct and crucial role during the growth of plant cells (Hocq et al., 2016). Pectins are able to interact with cellulose and hemicellulose fibers, increasing the complexity of the cell wall structure (Hosmer and Mohnen 2009). Actually, it seems that pectins but not xyloglucan make the most contacts with cellulose (Wang et al., 2015). The most interesting role of pectins, and

more specifically homogalacturonan (HGs), in cell growth is based on the modifications they can experience once HG is secreted to the cell wall in a highly methylesterified form. *In muro*, HG can be demethylesterified by PME (Pelloux et al., 2007). This new conformation allow the production of HG-Ca²⁺ cross-links, which supposedly leads to cell wall rigidification (Cosgrove 2005). On the other hand, a random de-methyl esterification of HGs could imply a more accessible situation for different enzymatic proteins as pectin lyases or polygalacturonases that could cause cell wall loosening (Hocq et al., 2016; Ali and Traas 2016). Furthermore, inhibitors of PME (PMEIs) can prevent the activity of PMEs and regulate their effect on cell wall stability (Sénéchal et al., 2014). Therefore, the interplay between PMEs and PMEIs is responsible for controlling the balance between the rigidity and expansibility of the cell wall and this plays a role in multiple developmental processes such as control of organ initiation in the shoot apical meristem, hypocotyl growth or stomatal aperture (Peaucelle et al., 2011; Peaucelle et al 2015; Amsbury et al., 2016). In addition, a mutation in VANGUARD1 (VGD1), a pollen-specific PME, causes a premature burst of pollen tubes, reducing plant fertility (Jiang et al., 2005). Moreover, it was already demonstrated that overexpression of PME15 (PMElox) causes dramatic growth phenotypes in *Arabidopsis thaliana* (Wolf et al., 2012), demonstrating again that a balance between PME and PMEI is necessary for plant development. Taken all together, due to the importance of the balance established between PMEs and PMEIs, changes in the HGs conformation must be monitored by the cell in order to ensure proper development and environmental responses.

1.2. Plant Receptors

Multicellular organisms need to coordinate their growth and development as well as sense and respond to different stimuli by using extracellular signaling molecules that need to be perceived by other cells using plasma membrane (PM) receptors.

In animal cells, a big number of PM receptors are classified into the category of G-protein-linked receptors. Those, once the signal is perceived in the extracellular region, associates with a G protein (a trimeric GTP-binding protein) that activates the signal by interacting with GTP or switches it off by converting GTP in GDP and propagating a signal base in protein-protein interaction (Chow and Mccourt 2008). In addition, animal cells also possesses receptors linked to an intracellular kinase domain that can auto- or trans-phosphorylates at Tyrosine residues (Lemmon and Schlessinger 2010).

Similar to other multicellular organisms, plants are able to perceive cell-to-cell and long distance signals from the surroundings through the presence of receptors at the plasma membrane. Moreover, plants need to respond effectively to a variety of external cues. Therefore, a broad group of PM-associated receptors might reinforce adaptive processes and enable the characteristic plasticity of plant development. In the specific case of plant kingdom, a big number of PM receptors belonging to the enzyme-linked receptors group have been characterized (Wang et al., 2008). Since the characterization of the first plant plasma membrane receptor in maize (Walker and Zhang 1990), huge advances in the knowledge about plant receptors has been achieved. Most of the known plant PM receptors are categorized as Receptor-Like Kinases (RLKs) and Receptor-like proteins (RLPs).

1.2.1. Receptor-like Kinases (RLKs)

Various studies agree that the RLK family in *Arabidopsis thaliana* contains around 600 members that represent around 2.5% of the total genome (Ma et al., 2016). RLKs contains a signal peptide on its N terminal, a variable extracellular region, a unique transmembrane region flanked by two juxtamembrane regions, one inside and one outside of the PM, and a intracellular domain with a kinase activity (Afzal et al., 2008). Principally, the type of extracellular domain and the nature of the kinase activity is used to categorize RLKs. Kinases catalyze phosphorylation, a reversible modification that consist on the conjugation of a phosphate group in Serine (Ser), Threonine (Thr) and/or Tyrosine (Tyr) residues (Hashiguchi et al., 2017). Contrary to mammals, plant proteins preferentially phosphorylate Ser and Thr residues although, the less frequent Tyr phosphorylation also plays an important role for protein functionality (Afzal et al., 2008; Ghelis 2011). Phosphorylation mainly promotes changes on protein structure that modifies their capacity to interact with other proteins and enhances activation-deactivation of signaling pathways (Belkhadir and Jaillais 2015; Ma et al., 2016). In addition, the extracellular domain of RLKs influence the kind of interaction they undergo and the nature of the signal they sense. The extracellular domain of RLKs has been classified into different types such as CrRLK1-like, WAK1-like or LRR-like (Humphrey et al., 2007). Among those, the LRR-like extracellular domain is the most abundant and it characterized by the presence of a Leucine-Rich Region (LRR), a motif containing up to 25 leucines (Kajava 2002). Most importantly, the LRR domain is of crucial relevance for the recognition of the different signals as it commonly acts as the interface for the interaction with ligands and co-receptors (Zhang et al., 2016).

Functionally, LRR-RLKs are involved in the perception and activation of defense and/or developmental signaling (Ma et al., 2016) since plants continuously interact with multiple and varied pathogens and they need to respond to a putative infections fast and effectively. RLKs have evolved to be able to sense various pathogens elicitors (Couto and Zipfel 2016). For example, the two most studied LRR-RLKs, FLAGELLIN-SENSING 2 (FLS2) and ELONGATION FACTOR-TU RECEPTOR (EFR1), are able to sense directly the bacterial elicitors flagellin and EF-Tu, respectively, and provoke an immune response (Gomez-Gomez et al., 2000; Zipfel et al., 2006). In addition, other LRR-RLKs such as PEP1 RECEPTOR 1 and 2 (PEPR1, PEPR2) are able to sense endogenous plant elicitor peptides (PEPs), that act as damage-associated molecular pattern (DAMP) in a second wave of signaling to amplify defense responses (Yamaguchi et al., 2010; Yamaguchi et al., 2011). Moreover, plants are able to differentially respond to developmental stimuli in a tissue specific manner which also integrates their developmental and environmental contexts (Chow and Mccourt 2008). To this end, LRR-RLKs are also utilized for the sensing of different organic hormones and small signaling peptides in order to produce an accurate response based to the specific needs of the plant cell (Ma et al., 2016; Zhang et al., 2016). Among the characterized functions of LRR-RLKs in developmental signaling are: i) the perception and signal transduction of the plant hormone Brassinosteroid (BR) by BRASSINOSTEROID INSENSITIVE 1 (BRI1) (Li and Chory 1997), ii) the regulation of the apical meristem maintenance by the perception of the small peptide CLAVATA3 (CLV3) by CLAVATA1 (CLV1)(Clark et al., 1997; Brand et al., 2000), iii) the control of the organ abscission by the perception of the peptide INFLORESCENCE DEFFICIENT IN ABCISSION (IDA) by HAESA (HAE) (Santiago et al., 2016), iv) the patterning regulation of stomata

in leaves by the recognition of EPPIDERMAL PATTERNING FACTORS (EPFs) by ERECTA (ER); and v) the control of root growth by the peptide PSK and its receptor PHYTOSULFOKINE (PSK) RECEPTOR 1 (PSKR1) (Ladwig et al., 2015).

Interestingly, all these LRR-RLKs, with the exception of ER, have been shown to require the presence of a Somatic Embryogenesis Receptor Kinases (SERKs), a family of LRR-RLKs consisting in five members that act as co-receptors (Chinchilla et al. 2009). SERKs have a fundamental role in the integration of simultaneous signaling events through the heterodimerization with other LRR-RLKs upon signal perception. As a consequence, activation of downstream signaling is mediated by differential auto- and trans-phosphorylating upon the binding of SERKs to different members of the signal cascade (Ma et al., 2016).

1.2.2. Receptor-like Proteins (RLPs)

Another interesting group of PM-associated receptors in *Arabidopsis thaliana* are those belonging to the RLP family. RLPs are single transmembrane domain proteins with an extracellular domain that contains one of various motifs among which LRR is the most common, with 57 known members in *Arabidopsis* (Wang et al., 2008). However, the most important characteristic of RLPs is the varied structure of their cytoplasmic domain, which lack any obvious active motif for intracellular signaling (Wang et al., 2008).

Of all the LRR-RLPs described so far, a large number of them are involved in perceiving defense-related signals (Liebrand et al., 2014). The first examples of defense-associated LRR-RLPs Cf-9 and Ve which were described to perceive fungal elicitors in *Solanum lycopersicum* (tomato) (Wang et al., 2008; Liebrand et al., 2014). Similarly, several LRR-RLPs have been found to be required for pathogen defense in *Arabidopsis thaliana*, such as RLP3, RLP23 or RLP30. All these RLPs recognize specific elicitors from different fungi species and activate a specific signaling cascade (Shen and Diener 2013; Zhang et al., 2013; Albert et al., 2015).

Strikingly, although the majority of the characterized RLPs involved in immune responses, only small number of them have also been described to be involved in the regulation of plant development (Wang et al., 2008). Notably, and in line with expectations, those RLPs are well-conserved throughout the plant kingdom (Wang et al., 2008). In this class of RLPs, we find CLAVATA2 (CLV2/RLP10), which perceives CLV3 to regulate apical meristematic populations and maintains the root apical meristem through its perception of various signal peptides (Müller et al., 2008; Hazak et al. 2017). Moreover, TOO MANY MOUTHS (TMM/RLP17) participates in the regulation of stomatal patterning by interacting with ERECTA (ER) receptors and modulating the affinity of ER for different EPFs (Nadeau and Sack 2002; Lin et al., 2017).

Due to the lack of an enzymatically active cytoplasmic domain, all RLPs presumably need to interact with other PM-localized protein kinases to transduce the signal into the cell since RLPs need a co-receptor to correctly bind a ligand and convey signaling. (Ma et al., 2016). However, this is not always true as some RLPs have been shown to directly bind ligands and promote or specify a signaling response (Yamaguchi et al., 2016). CLV2 can interact with CLV3 in the apical meristem independently of CLV1 (Müller et al., 2008) but also with different peptides in the root (Hazak et al. 2017). TMM interacts

with ER to form a pocket that allows for the selective recognition of EPFs therefore specifying ER signaling (Lin et al. 2017). RLP23 also interacts *in vivo* with the small peptide *nlp20* to enhance immune responses against fungal pathogens (Albert et al. 2015)

As observed with LRR-RLKs, many LRR-RLPs can also interact with SERKs. For example, RLP30 and RLP23 have both been shown to interact with BAK1/SERK3 in order to transduce the signal they perceive (Zhang et al., 2013; Albert et al., 2015). In addition, several RLPs have shown to also interact with the adaptor kinase SUPPRESSOR OF BIR1-1 (SOBIR1) (Liebrand et al., 2013). To date, interaction of SOBIR1 has only been shown between RLPs, an interaction that can be independent of BAK1, as it with CLV2, or in concomitance, as it with RLP23 and RLP30 and it can be either independent or in concomitance with BAK1 (Liebrand et al., 2013; Zhang et al., 2013; Albert et al., 2015; Gust and Felix 2014). Moreover, a cytoplasmic pseudokinase, CORYNE1 (CRN), has been described to be fundamental for function of some RLPs, such as CLV2 function (Zhu et al. 2010; Somssich et al., 2016). In addition, the interaction of CRN with BARELY ANY MERISTEM3 (BAM3), a LRR-RLKs involved in perception of CLE45 has been recently demonstrated to control phloem development (Hazak et al., 2017).

In conclusion, the biochemical complexity of the signal perception by PM-associated proteins, from signal perception to complex formation and signaling, reflects the capacity of plants to respond and coordinate multiple stimuli; transforming those signals into immediate physiological responses which allow for continued growth and survival.

1.3. Cell Wall Signaling

The cell wall is the plant cell's direct interface with the outside world and therefore should be able to relay information regarding external conditions. It has already been shown that breakdown products of the CW are perceived as damage-associated patterns (DAMPs), alerting the cell to a possible pathogen attack (Ferrari et al., 2013). Furthermore, plant CWs are known to be plastic structures, changing their composition and structural properties throughout the growth and development of the plant (Cosgrove 2005). Perturbing the synthesis or modification of CW greatly impacts the growth of plants (Fagard et al., 2000; Wolf et al., 2012; Xiao et al., 2016). For many years, these growth defects were believed to be attributed to a physiological attempt to compensate for a lack of CW integrity through the enhanced deposition of other CW elements (Manfield et al., 2004; Castro et al., 2014). Recently, it has been shown that the growth phenotypes of many CW mutants can be attributed to perturbed signaling of plasma membrane (PM) receptors as THESEUS1 (THE1) (Hématy et al., 2007). THE1 was discovered in a suppressor screen using a mutant of CELLULOSE SYNTHASE 6/PROCUSTE1 (CESA6/PCR1). The mutant *cesa6^{prc1-1}* is characterized by a dwarf phenotype and a reduction of cellulose content that it is compensated for by increased pectin and callose ectopic deposition (Fagard et al., 2000). Strikingly, the THE null mutant, *the1-1*, is able to restore the normal growth of *cesa6^{prc1-1}* without restoring the cellulose content (Hématy et al., 2007) indicating that the reduction in growth is a secondary effect produced by signal perception from the wall.

1.3.1. RLKs implicated in the perception of cell wall perturbations

In the last decades, different putative CW signaling receptors have been described. As mentioned previously, the receptor-like kinases (RLKs) comprise a big part of the PM-associated receptors and are single transmembrane domain proteins with predicted cytoplasmic catalytic activity, normally a Ser/Thr kinase (Afzal et al. 2008). Although the downstream signaling cascades are not well resolved some components have been described, such as intracellular protein kinases (RLCKs), mitogen-activated protein kinases (MAPKs) and calcium dependent kinases (CDKs) (Wolf 2017). In contrast to previously described PM-associated receptors involved in developmental processes, receptors associated with cell wall surveillance often have a more varied architecture of their extracellular domains (ECD) and do not rely mainly on LRR-motifs. Among them, we can find CrRLK1L or wall associated kinases (WAKs).

The most studied group of CW receptor-like kinases are the *Cantharanthus roseus* receptor-like kinase1-like proteins (CrRLK1L) (Boisson-Dernier et al., 2011), a family of 17 predicted receptors that contain a domain homologous to Malectin from *Xenopus laevis*. Malectin is a protein able to interact with di-glucose motifs (Schallus et al., 2008). Therefore, it is possible that the Malectin-like domains in CrRLK1L potentially interact with cell wall polysaccharides. FERONIA (FER) is a CrRLK1L involved in the perception of the pollen tube by the female gametophyte, a mechanism that relies on FER sensing CW perturbations caused by the approaching of the pollen tube (Huck et al., 2003). In addition, FER is a key component to responses involving intrinsic and extrinsic mechanical signals (Shih et al., 2014). In line with these functions, *fer* mutants have altered cell wall composition (Yeats et al., 2016). FER contains a Ser/Thr kinase domain that is phosphorylated upon the direct interaction with the secreted peptide RAPID ALKALIZATION FACTOR1 (RALF1) (Haruta et al., 2014). Intriguingly, RALF1 does not seem to possess any carbohydrate moiety but it is possible that the Malectin-like domain binds signal molecules with various motifs or that RALF1 is interacting with a different region of FER. In any case, FER signaling seems to have an important role in the regulation of the cell wall integrity during development (Höfte et al., 2015). Furthermore, the closest FER homologous ANXUR1 and 2 (ANX1/2) have been also implicated in cell wall regulation (Boisson-Dernier et al., 2009; Boisson-Dernier et al., 2013). Similarly, the previously mentioned RLK, THESEUS 1 (THE1), also contains a malectin-like domain on its ECD and a predicted cytoplasmic Ser/Thr kinase domain (Boisson-Dernier et al., 2011). THE1 mutant is able to restore the dwarf phenotype of *cesa6^{prc1-1}* without restore the cellulose contents. That observation meant that on those mutants the dwarf phenotype was not depending on the lack of cellulose but on a signal produced as response to the changes in the cell wall composition (Hématy et al. 2007). In any way, the signaling process in which THE1 is involved as well as the kind of signal THE1 could sense from the Malectin-like domain are still unknown.

Wall-associated kinases (WAKs) are members of a different RLK family. They contain an ECD with an epidermal growth factor (EGF)-like domain and an intracellular domain with a predicted Ser/Thr kinase activity. WAKs are the only PM-associated receptors whose direct binding to the cell wall has been demonstrated (Decreux and Messiaen 2005) and they seem to have an important role in plant development (Wagner and Kohorn 2001). Although, the complete signaling pathway of WAKs is still unknown, it has been suggested that WAKs might convey the information into the cell by activating

MAPKs upon pectin perception (Kohorn 2016). QUASIMODO1/GAUT8 and QUASIMODO2/TUMOROUS SHOOT DEVELOPMENT 2 are a galacturonosyltransferase and a putative pectin methyltransferase, respectively. The mutants have a reduction of homogalacturonans (HG) in their cell walls and, as a consequence, a loss of cell adhesion (Mouille et al., 2007; Krupková et al., 2007). Recently, ESMERALDA1 (ESMD1) has been discovered from a suppressor screen of *qua1-1 qua2-1* (Verger et al., 2016). ESMD1 is able to rescue the cell adhesion problems of the mutant without restoring the HG content. ESMD1 encodes a putative o-fucosyltransferase similar to the previously described FRIABLE1 (FRB1) (Neumetzler et al., 2012). This putative o-fucosyltransferase is predicted to act on EGF-like domains, like those present in the ECDs of WAK-like proteins, Therefore, it could be possible that changes in pectin composition found in QUASIMODO1/2 mutants could activate ESMD1 and FRB1 to act on the EGF-like domains of WAKs and therefore activate signaling (Verger et al., 2016; Wolf 2017).

1.3.2. RLP44, a newly described sensor of CW pectin modifications

RLPs such as CLV2 and TMM can engage in other signaling pathways in a similar fashion as when they are involved in developmental processes, via direct interaction with LRR-RLKs (Jeong et al., 1999; Nadeau et al., 2002). As previously mentioned, the methyl-esterification status of HGs *in muro* by PME and PME1 is maintained at equilibrium in order to preserve the normal development of the (Jiang et al., 2005; Wolf et al., 2012). Research to unravel how this balance is maintained is still ongoing but there is evidence suggesting that RLPs play a major role in this regulation.

Perturbing pectin methylation through the overexpression of PME15 (PMElox) causes severe root and rosette phenotypes, which include: root waving, organ fusion and reduced fertility (Wolf et al., 2012). A forward genetic screen performed on PMElox plants allowed the identification of the suppressor mutant, *comfortable numb1 (cnu1)*, that is able to restore a Col-0 (WT) phenotype. A map based cloning approach determined that the mutation was located in the kinase domain of the BR-receptor, BRASSINOSTEROID INSENSITIVE1 (BRI1) suggesting that the brassinosteroid signaling pathway was involved in the PMElox phenotype. From the same screen, the *comfortable numb2 (cnu2)* suppressor mutant, was also found to suppresses the PMElox phenotype, *cnu2* was later discovered to contain a mutation in the LRR-RLP RLP44 (At3g49750). Thus, RLP44 constitutes a new putative signaling component required for the integration of CW and BR signaling (Wolf et al., 2014).

RLP44 is a PM-localized protein with a short LRR extracellular domain, a single transmembrane domain and a small cytoplasmic tail. RLP44 is able to activate the BR signaling downstream of hormone perception via BRI1. The *cnu2* mutant and *rlp44^{cnu2}* mutant (*cnu2* point mutation in a stable segregated line devoid of PMElox) both respond normally to BL-treatment and the overexpression of RLP44 (RLP44ox) produces a BRI1ox-like phenotype characterized by longer petioles and leaves. However, these mutations are not able to rescue the *bri1^{cnu1}* (*cnu1* mutation in a stable, segregated line devoid of PMElox) (Friedrichsen et al., 2000; Wolf et al., 2014). Furthermore, comparative microarray between PMElox and *cnu2* plants shows that the loss of RLP44 prevents the activation of BR signaling by PMElox and restores to normal the expression of around 90% of all misexpressed genes found in the PMElox background. As similar restoration of gene expression was also observed with *cnu1*, suggesting that

RLP44 and BRI1 act in the same CW-signaling pathway (Wolf et al., 2014). Not surprisingly, RLP44 has been shown to interact with BAK1 (Wolf et al., 2014) and BRI1 (Holzwardt et al., in revision) and is presumably phosphorylated within the cytoplasmic domain (Wolf et al., 2014). As RLP44 lacks the ability to initiate its own kinase-signaling cascade, the formation of the complex with the BAK1 and BRI1 kinases might allow for activation of RLP44-mediated signaling pathways.

No other LRR-RLP as of yet, has been characterized as a putative CW receptor. However, other RLPS conserved across many plants among species could play a role in CW-signaling. RLP57 is the closest homologous to RLP44 in *Arabidopsis thaliana* and its role has yet not be characterized (Wang et al., 2008). Furthermore, RLP4 is also highly conserved, is able to interact with RLP44, and has both an LRR and a malectin-like domain (Schallus et al., 2008; Sebastian Augustin, Master thesis 2015).

1.4. Brassinosteroid Signaling cascade

In order to tailor growth to the environmental cues, plants make use of a wide range of signaling molecules such as phytohormones and signaling peptides, which can be sensed, and acted upon, by different cellular tissues. The brassinosteroids (BR) group of phytohormones is found ubiquitously in a plant and known to influence photomorphogenesis, cell elongation and cell differentiation events to name a few (Belkhadir and Chory 2006; Jaillais and Vert 2012). Brassinolide (BL), the most active BR compound, is synthesized in the Endoplasmic Reticulum (ER) and exported to the apoplast where it can act as a signaling molecule. BR synthesis is regulated by a negative feedback loop and its synthesis is inhibited in the presence of high concentrations of BL (Belkhadir and Jaillais 2015). The importance of BR-signaling in plants is reflected in the severe morphological phenotypes of BR mutants, which is characterized by dwarfism, impaired photomorphogenesis and altered vascular development, among others (Jaillais and Vert 2016).

The LLR-RLK BRI1 perceives BRs at the cell surface (Li and Chory 1997). In the vasculature, BRs are perceived by two functional BRI1 homologs BRI1-LIKE1 AND BRI1-LIKE 3 (BRL1, BRL3) (Caño-Delgado et al., 2004). Structurally, BRI1 binds BL via a hydrophobic pocket within an LRR island domain of the extracellular domain (ECD) of BRI1. Upon binding to BRI1, BL promotes the association of BRI1 with the LRR-RLKs co-receptor BRI1-ASSOCIATED KINASE 1 (BAK1), through the ECD (Jaillais et al., 2011; Santiago et al., 2013). As mentioned previously, BAK1 is a member of the somatic embryonic receptor family (SERK) (Ma et al., 2016). BAK1 recognizes the BRI1 BL-binding island domain and coordinates the stable binding of BL to BRI1 but it is not able to bind BL independent of BRI1 (Santiago et al., 2013). This aforementioned association activates a cascade of phosphorylation and de-phosphorylation events that results in transcriptional changes within the nucleus.

In absence of BL, BRI1 is negatively controlled by BRI1-KINASE INHIBITOR (BKI1), a cytosolic protein that remains close in proximity to the cell PM (Wang et al., 2015). BKI1 inhibits BL-signaling by interacting with the kinase domain of BRI1 and competing with BAK1 for the formation of the complex (Jaillais et al., 2011). This scenario changes upon BL treatment. Firstly, BKI1 dissociates from BRI1 after the transphosphorylation BKI1 by BRI1 on residue Y211 (Jaillais et al., 2011). Immediately after

the dissociation from BKI1, BRI1 interacts with BAK1 to form a BRI1-BL-BAK1 complex. In order to activate the signaling cascade, BRI1 phosphorylates BAK1 and BAK1 reciprocally phosphorylates BRI1 (Wang et al., 2005b; Wang et al., 2008). Presumably, specific phosphorylation of BRI1 and BAK1 kinase domains facilitate the interaction with PROTEIN PHOSPHATASE 2A and 2B (PP2A, PP2B) which consequently act to inactivate the signal pathway (Wu et al., 2011; Segonzac et al., 2014; Wang et al., 2016). Subsequent to the BRI1 and BAK1 activation, BRI1 SUBSTRATE KINASE (BSK1/CDG1), a PM associated Receptor-like kinase is phosphorylated (Tang et al., 2009). BSK1 then phosphorylates BRI1 SUPPRESSOR 1 (BSU1) and BSU LIKE-1 (Kim et al., 2011a) and in turn, BSU1 de-phosphorylates the GSK3-like kinase BRASSINOSTEROID INSENSITIVE 2 (BIN2) (Kim et al., 2009).

BIN2 is considered as a signaling hub since it integrates and links out to different pathways. The BL-responsive transcription factors (TFs) BRASSINAZOLE RESISTANT 1 (BZR1) and BR-INSENSITIVE-EMS-SUPPRESSOR 1 (BES1) are both under the direct control of BIN2 (Kim et al., 2009; Tang et al., 2009). In the absence of BL, BIN2 is activated via auto phosphorylation and acts to inactivate BR-signaling through the phosphorylation of BZR1 and BES1. Upon phosphorylation, the TFs interact with 14-3-3 and remain in the cytosol, targeting them for ubiquitination and protein degradation. Moreover, BIN2 directly inhibits the *in vitro* DNA binding activity of BZR1/BES1 (He et al. 2002; Gampala et al. 2007; Vert and Chory 2006). In the presence of BL, BIN2 is de-phosphorylated by active BSU1 allowing unphosphorylated BZR1 and BES1 to be targeted to the nucleus. Once there, BZR1 and BES1 modify gene expression by directly interacting with promoter regions of BL-response genes (Sun et al., 2010; Guo et al., 2013).

One important aspect of BR signaling is its crosstalk and integration with other pathways, especially at the level of BIN2 and BZR1/BES1. BIN2 can be activated by the TDIF RECEPTOR (TDR) upon the perception of its ligand, TRACHEARY ELEMENT DIFFERENTIATION INHIBITORY FACTOR (TDIF) (Cho et al., 2014). This BR-independent activation of BIN2 initiates the phosphorylation of AUXIN RESPONSE FACTORS (ARFs), promoting auxin-mediated responses during lateral root development (Cho et al., 2014). Furthermore, the same TDIF-TDR-BIN2 signaling cascade inhibits BZR1 and BES1 in a BR-independent manner. As a consequence, procambium cells maintain their stemness, inhibiting their differentiation into xylem cells (Kondo et al., 2014). Moreover, BIN2 can regulate the phosphorylation status of other cytoplasmic kinases such as YODA (YDA) or MITOGEN-ACTIVATED KINASE KINASE 4 (MKK4) and influences the stomata development (Kim et al. 2012; Khan et al. 2013).

BZR1 and BES1, like BIN2, play an important role in the integration of different BR-dependent/-independent pathways. An example of BR-independent regulation of BZR1 is that of the kinase TARGET OF RAPAMYCIN (TOR) which stabilizes and prevents its degradation, and allowing BZR1-mediated gene transcription (Zhang et al., 2016). In addition, BZR1 interacts with the transcription factor PHYTOCROME-INTERACTING FACTOR 4 (PIF4), integrating environmental and hormonal signals. They are inhibited by the DELA proteins which are they themselves degraded through gibberellin-mediated proteasomal targeting (Oh et al., 2012; Gallego-Bartolome et al., 2012).

1.5. Phytosulfokine Signaling cascade

In addition to classical plant hormones, a large number of small peptides have been shown to participate and influence different developmental and growth programs (Delay et al., 2013). These peptides are categorized into two main families: secreted and non-secreted peptides (Matsubayashi 2014). Among secreted peptides, RNA translation form pre-peptides (around 100 amino acids) that can undergo different posttranslational processes that define their nature. Cysteine-rich pre-peptides are processed to generate disulfide bonds. Some other pre-peptides can also undergo sulfation or hydroxylation for the modification of Tyr, Lys or Pro. In addition, pre-peptides are also cleaved to finally generate short peptides with normally less than 20 amino acids (Matsubayashi 2014).

Among secreted peptides, the CLAVATA 3 (CLV3)/EMBRYO SURROUNDING REGION-related (CLE) family is the best-characterized one having a crucial role in the differentiation of shoot and root meristems (Yamaguchi et al., 2016). For instance, CLV3 negatively regulates stem cells maintenance in the shoot apical meristem (Brand et al., 2000), CLE40 maintains QC and columella stem cell identity (Stahl et al., 2009), whereas TDIF/CLE41/CLE44 regulates vascular stem cell fate (Hirakawa et al., 2008). However, CLE peptides are not the unique posttranslational secreted peptides; also, Phytosulfokine (PSK) peptide family belongs to this group (Matsubayashi 2014).

PSK was initially characterized as secreted peptide in *Asparagus officinalis* cell cultures capable of produce cell proliferation (Matsubayashi et al., 1996). PSK family include 5 pentapeptides formed after the cleavage of a pre-peptide and a posttranslational modification based on the addition of sulfate (SO₃H) groups to two tyrosines of the pentapeptide to finally have the mature form Tyr(SO₃H)-Ile-Tyr(SO₃H)-Thr-Gln (Matsubayashi et al., 1996; Yang et al., 1999).

PSK is perceived at plasma membrane by LRR-RLKs PSK RECEPTOR 1 and 2 (PSKR1/PSKR2) which interact with the co-receptor BAK1/SERK3 and presumably activate a cation-translocating channel formed by the H⁺-ATPases AHA1/2 and the CYCLIC NUCLEOTIDE-GATED CHANNEL (CNGC17) (Matsubayashi et al., 2002; Matsubayashi et al., 2006; Ladwig et al., 2015). PSK interacts with a β-strand of the island domain of the PSKR1 extracellular domain (ECD) while the two sulfations in PSK help to keep the interaction with the receptor (Wang et al., 2015). This interaction site in PSKR1/2 is conserved along the orthologs where the main structural difference is observed at the transmembrane domain (TMD) or kinase domain (KD) (Wang et al., 2015). Interestingly, PSK also promotes the interaction of PSKR1 with the N-terminus of SERK1 and SERK3, an interaction that is structurally similar to the interaction between BRI1 and BAK1 promoted by BL (Wang et al., 2015). After perception, PSK signal activates a cascade that, in *Arabidopsis thaliana*, is involved in root cellular proliferation and expansion, tracheary element differentiation as well as defense responses (Matsubayashi et al., 1999; Kutschmar et al., 2009; Igarashi et al., 2012; Hartmann et al., 2013). Treatment of Col-0 seedlings with PSK potentiate the root growth when compared to mock treatments (Hartmann et al., 2013). The single and double mutants of the receptor, *pskr1-3*, *pskr2-1* and *pskr1-3 pskr2-1* loss the capacity to respond to PSK reflected in shorter roots (Kutschmar et al., 2009) and reduction of above-ground growth that is translated into smaller plant rosettes and shorter shoots (Hartmann et al., 2013). In addition, ubiquitous overexpression of PSKR1 increases length of roots and hypocotyls and is able to rescue the mutant

phenotype (Hartmann et al., 2013). Interestingly, the expression of PSKR1 only in root epidermis cells of *pskr1-3 pskr2-1* is enough to restore the response to PSK and normal root growth indicating that PSK might control the root growth in the epidermis in a non-cell autonomous way (Hartmann et al., 2013).

Moreover, PSK signaling seems to be BR-signaling dependent. TYROSILPROTEIN SULFOTRANSFERASE-1 (TPST1) is required for a proper sulfation of PSK, and the lack of it like in *tpst-1* mutant produce a similar phenotype as *pskr1-3 pskr2-1* and it can be restored upon PSK application (Hartmann et al., 2013). When PSK is applied together with the inhibitor of endogenous BR biosynthesis Brassinazole (BZ), *tpst-1* short root phenotype is not restored, the effect is only reverted when BL is additionally applied to the system (Hartmann et al., 2013). Moreover, application of BZ to PSKR1 overexpression lines also blocks the increase of root growth and *det2-1* (a mutant in BR synthesis) or *bri1-9* (mutation on BRI1) are insensitive to PSK treatment (Hartmann et al., 2013). All these data suggest that the effect of PSK requires proper BR synthesis and perception and the two signaling cascades might interact at some point.

1.6. RLP44, BR and PSK- related signaling and Xylem development

The vascular tissue is fundamental for plant physiology as it allows transport of water, nutrients and small molecules throughout the plant. *Arabidopsis thaliana* primary root vascular tissue is typically formed by five xylem cells aligned in a median axis and four phloem cells each at opposite poles with procambium cells disposed between the xylem and phloem (De Rybel et al., 2015). Phloem is specialized in the transport of nutrients, xylem in the transport of water and procambium is the source for the lateral meristem during the secondary growth. Main characteristic of xylem cells is the presence of a secondary cell wall enriched in lignin that allows the transport of water and provide the stiffness during growth (Lucas et al., 2013). This vascular pattern is created and maintained by antagonistic auxin and cytokinin signaling during embryo development (De Rybel et al., 2015). Post-embryonically, the maintenance of xylem identity is auxin-dependent and once the xylem cells are positioned, the transition into tracheary cells (the ones containing a lignified cell wall) is regulated by a complex regulatory network controlled by HD-ZIP III transcription factors (De Rybel et al., 2015). Besides, brassinosteroid signaling pathway also participates in xylem differentiation (Ibañes et al., 2009). Another interesting observation is that PSK is able to promote the differentiation from mesophyll to tracheary cells in cell culture (Matsubayashi et al., 1999).

Interestingly, PSK signaling is BR-dependent (Hartmann et al., 2013) and crosstalk between BR signaling and other developmental cascades is described. Furthermore, it has been shown that BR signaling promotes the transcriptional activation of PSK5 through the promotion of the ERF115 activity to enhance QC proliferation (Heyman et al. 2013). Besides, BRI1 and PSKR1 are structurally similar and both interact with the LRR-RLK BAK1 (Kim et al., 2011b; Wang et al., 2015; Ladwig et al., 2015). However, the connection between these two pathways are poorly known.

RLP44, a receptor that integrates CW with BR signaling (Wolf et al., 2014) is mainly expressed in epidermis and mature vasculature, specifically to xylem (Holzwardt et al., In revision). Strikingly, RLP44

mutant shows an increase of xylem cell number that is also observed in loss-of-function BRI1 mutants as *bri1-null* or the *bri1 bri1 bri3* but absent in BL synthetic mutants as *cpd* or hypomorphic mutants as *bri1^{enu1}* or *bri1-301* (Jaillais et al., 2011; Vragović et al., 2015, Holzward et al., In revision). RLP44 is able to interact with the two BR receptors BAK1 (Wolf et al., 2014) and BRI1 (Holzward et al., In revision). Unexpectedly, RLP44 also interacts with the PSK receptor PSKR1 and the application of PSK to *rlp44-3* restores the observed xylem deficiency (Holzward et al., In revision). These data support the idea that RLP44 shifts the interaction with BRI1 and PSKR1 and, in this way, RLP44 controls the vascular cell fate by balancing BR and PSK signaling. Therefore, RLP44 could integrate the changes sensed at the level of the CW into two independent signaling pathways and modulate different and/or combined responses although the nature of the signal perceived by RLP44 is still unknown.

1.7. Endocytosis and transmembrane circuits in plant cells

A big group of plant plasma membrane receptors have an important role to keep plant cells in shape. However, they need to be constantly regulated to avoid an excess of its activity (Reyes et al., 2011). One way to control their activity is via endocytosis of the proteins. Once proteins are endocytosed into the cell via vesicles, these vesicles fuse with the Trans Golgi Network/Early Endosome (TGN/EE). The TGN/EE is a unique plant vesicle system that incorporates vesicles coming from Golgi carrying newly synthesized cargo with vesicles coming from the PM that, from the TGN/EE, might either be recycled to the PM or be subjected to degradation in the vacuole via multivesicular bodies (MVB) (Reyes et al., 2011).

1.7.1. Clathrin-mediated endocytosis

Clathrin mediated endocytosis (CME) is the best-characterized endocytic pathway in eukaryotes (McMahon and Boucrot 2011). Clathrin is a vesicle coat scaffold protein with a “three-leg” structure called triskelion where each of the legs contains a heavy (CHC) and light chain (CLC) (Fujimoto et al., 2010). CME consists on a series of events: nucleation, cargo selection, coat assembly, scission and the final formation of a vesicle in the cytosol.

Nucleation, the first step in CME, starts with invagination of the region that is subjected to internalization. ADAPTOR PROTEIN 2 (AP2) complex is the main actor in the nucleation in mammals and yeast, recognizing the region by directly interacting with cargo-sorting motifs, phosphatidylinositol 4,5-bisphosphate (PtdIns(4,5)P₂), and accessory proteins (McMahon and Boucrot 2011). However, not all mammalian AP2 subunits are present in plants and the accessory proteins have not been identified so far (Paez Valencia et al., 2016). Interestingly, plants harbor a conserved additional and plant-specific protein localized at the plasma membrane, TPLATE, that interacts with another seven proteins (TWD40-1, TWD40-2, AtEH1, AtEH2, LOLITA, TML, TASH3) to form the core of the TPLATE complex (TPC) (Gadeyne et al., 2014). The TPLATE is essential since its mutation, in contrast to AP2 mutations, is lethal for the plant (Fan et al., 2013; Gadeyne et al., 2014). In fact, TPLATE seems to be the first element to anchor to the PM during the nucleation, allowing the assembly of the rest of TPC elements and finally

recruiting AP2 (Gadeyne et al., 2014). In any case, even if TPLATE and AP2 overlap during CME, they seem to have also different roles along the process (Gadeyne et al., 2014).

Once a plasma membrane pit is formed, the elements at the PM to be part of the cargo are selected by the direct interaction with AP2 or TPC members. AP2 specifically recognizes two kinds of cargo consensus sequences in PM proteins: a di-Leu-based motif or a Tyr-based motif (McMahon and Boucrot 2011). For instance, the boron transporter BOR1 contains a Tyr-based motif on a cytosolic loop (Takano et al., 2010). In addition, posttranslational modifications such as ubiquitination are also used as signals for endocytosis such as in the case of the iron transporter IRT1 (Barberon et al., 2011). On the other hand, members of the TPC as TW40-2 have been also characterized to cooperate with AP2 on the selection of CESAs complex for CME (Bashline et al., 2015).

Subsequently, AP2 and TPC recruit Clathrin triskelia from the cytosol to the PM where the vesicle is created. This recruitment facilitates the polymerization and stabilization of Clathrin structure. In turn, a stable Clathrin lattice strengthens the invagination and promotes the creation of a fully formed vesicle (Sweitzer et al., 1998; McMahon and Boucrot 2011). Finally, the vesicle is cut from the PM by the action of GTPases DYNAMIN RELATED PROTEIN 1 and 2 (DRP1/2) (Fujimoto et al., 2010). DRP1/2 form a helix structure on the neck of the vesicle and pinch the PM in order to liberate the vesicle (Fujimoto et al., 2010). In addition, it has been hypothesized that some members of the TPC such as TML, TASH3 or TWD40-2 could also participate in the recruitment of DRPs and in the membrane scission (Gadeyne et al., 2014; Bashline et al., 2015). Once the vesicle is released, all the proteins rapidly disassemble and the vesicle is uncoated and transported to the TGN/EE (Paez Valencia et al., 2016).

Strikingly, degradation or recycling of PM proteins are not the only functions of endocytosis, signaling cues at the PM require endocytosis for its propagation upon ligand binding (Irani and Russinova 2009). For instance, *flg22* interacts with its receptor FLS2 and activates the signaling cascade but also promotes the endocytosis of the receptor (Khaled et al., 2015). *AtPeps* also promote CME of PEPR1/2 upon the interaction with the ligand to expand the signaling (Ortiz-Morea et al. 2016) similarly to what it is observed for CLV1 that also undergoes endocytosis in a ligand-dependent manner (Nimchuk et al. 2011). On the other hand, presence of auxin stabilizes the PM localization of the PIN-FORMED (PIN1) auxin transporter (Robert et al., 2010).

1.7.2. Regulation of endocytosis by posttranslational modifications

A posttranslational modification (PTM) is defined as a covalent processing event result of a cleavage or modification in one or more of the protein amino acids that balances protein function by modifying their activity, localization or interaction with other proteins (Offringa and Huang 2013). More than 200 different PTMs has been described so far but most frequent in eukaryotic proteins are phosphorylation, acetylation, glycosylation, hydroxylation, methylation and ubiquitination (Khoury et al., 2011).

Phosphorylation enhances activation-deactivation of signaling pathways although, and especially for PM proteins, phosphorylation is also important for protein localization. Usually, phosphorylation is used as a signal for cargo selection for CME (Traub and Bonifacino 2014). For instance, FLS2 is subjected to a low range of endocytosis in absence of the ligand. Upon application of *flg22*, FLS2 is auto- and

trans- phosphorylated, promoting subsequent ubiquitination and endocytosis (Schulze et al. 2010; Lu et al. 2011). Oppositely, BRI1 is on a continuous turnover between the PM and the endosomes and this ratio is not altered by the presence of BL. In any case, upon BL perception, consequent phosphorylation of BRI1 is essential to keep BRI1 active on the endosomes and transduce the signal (Irani et al. 2012; Belkhadir and Jaillais 2015). On the other hand, there is not too many examples where phosphorylation stabilize proteins at the PM in plant and only the example of PIN1 has been described. PIN1 is phosphorylated by PID1 and this event increases the tendency of PIN1 for an apical localization in the PM, essential for its correct function. Loss of phosphorylation in PIN1 produces a change to basal positioning, affecting the correct efflux of auxin (Huang et al., 2010; Offringa and Huang 2013). In humans, there is some more cases known where phosphorylation stabilize proteins at the PM. AQUAPORIN 2 (AQP2) need to be phosphorylated to localize at the PM. However, upon channel aperture, a subsequent phosphorylation enhances the CME of both PM proteins (Offringa and Huang 2013). In addition, two specific phosphorylation of the polymeric Immunoglobulin receptor (pIgR) will facilitate the dual function of the protein. One phosphorylation will promote the endocytosis of the protein whereas a different one will facilitate the specific pIgR apical PM localization and promote transcytosis (Offringa and Huang 2013).

Ubiquitination is another posttranslational modification with a strong importance for endocytosis. Ubiquitination consist in a reversible conjugation of a 73-aa-protein Ubiquitin (Ub) to Lys residues of targeting proteins by the consecutive activity of a Activating enzyme (E1), conjugating enzyme (E2) and a Ub-ligase (E3) (Zientara-rytter and Sirko 2016). Ubiquitination is used to target misfolded proteins for degradation in the proteasome but it is also a signal for cargo selection for CME (Paez Valencia et al., 2016). PM proteins are labelled with one Ub (monoubiquitination) or a chain of Ub (polyubiquitination), both acting both as a sorting signal. Depending on the position of the Ub chain formation, polyubiquitination is classified in Lys-48 linked or Lys-63 linked chains. This difference has also an impact on sorting signals since Lys-48 polyubiquitination is commonly associated as target for degradation whereas Lys-63 is related with non-proteolytic functions (Dubeaux and Vert 2017). In plants, there are several examples of PM proteins where ubiquitination leads to a change of its localization and the control of their function. For instance, the monoubiquitination of IRON-REGULATED TRANSPORTER (IRT1) promotes its endocytosis and sorting to keep low levels of protein at the PM and avoid plant stress. Modification of the Lys involved in monoubiquitination stabilizes the protein at the PM which leads to the lethality of the plant (Barberon et al., 2011). In the case of FLS2, internalization by ubiquitination is essential for the propagation of the signal transduction. Upon *flg22* perception and activation, BAK1 phosphorylates and activates E3-Ub-ligases (PUB2 and PUB3) that ubiquitinates FLS2, which is subsequently sorted by CME (Lu et al., 2011). Furthermore, BRI1 is Lys63-polyubiquitinated to control the internalization and recycling of the protein. Absence of BRI1-polyubiquitination impairs the normal localization of the protein and affects the BR signaling in a BL independent manner (Martins et al., 2015). Finally, all those PM proteins that are not recycled and remain ubiquitinated, are recognized by ESCRTs complexes in the MVB and proteins are targeted to degradation in the vacuoles (Dubeaux and Vert 2017).

Overall, Phosphorylation and Ubiquitination are important for protein sorting in PM and endosomes. However, a pattern of events during CME cargo labeling is yet not clear and the contribution of the two posttranslational modifications need to be sorted out (Nakagami et al., 2010).

1.7.3. Transmembrane circuits for PM proteins

Once the vesicles arrive to the TGN/EE, cargo can be recycled to the PM or targeted for degradation in the vacuole. It is assumed that plants do not have specific vesicles for recycling and instead, recycled vesicles are speculated to be directly formed from the TGN/EE or MVB compartments (Paez Valencia et al., 2016). In the first case, specific ADP-ribosylation factors (ARFs) machinery is involved. ARFs contain a small myristoylated N-terminal helix capable to interact with different membranes (Donaldson and Jackson 2011). ARF-membrane interaction is controlled by GUANINE NUCLEOTIDES EXCHANGE FACTORS (GEFs) that interchange a GDP in ARFs with a GTP and allows cited interaction and GTPase ACTIVATING PROTEINS (GAPs) that negatively control ARFs by catalyzing the hydrolysis of the GTP (Donaldson and Jackson 2011). ARF interaction allows the recruitment of coat proteins that promote sorting of cargos as well as lipid-modifying enzymes such as phosphatidylinositol (PtdIns) and other effector molecules that influence membrane trafficking (Donaldson and Jackson 2011). *Arabidopsis thaliana* contains 8 ARF-GEFs including GNOM, sensitive to the drug Brefeldin-A (BFA), and BIG5 (Richter et al. 2007). The mutation or inhibition of ARF-GEFs directly affects recycling to the PM of different proteins as the case of GNOM that affects the proper localization of PIN1 (Doyle et al., 2015). Interestingly, ARF-GEFs and ARF-GAPs are not randomly distributed among the vesicles and they are used to define a polar recycling pathway and activate specific trafficking pathway (Richter et al., 2007).

In addition, movements of vesicles from MVBs to the TGN/EE can also be controlled by a retromer-mediated system (Burd and Cullen 2014). Retromer system is formed by VACUOLAR PROTEIN SORTING (VPSs) that are able to recognize specific cargos in the vesicle and SORTING NEXINs (SNXs) that bind to the lipids at the vesicle membrane, stabilize the retromer structure, and recruit lipid modification enzymes (Kang et al., 2012; Robinson et al., 2012). Retromer-system formation can be inhibited by applying the drug Wortmannin (WM) that inhibits PI-3 kinases and directly affect the attachment of the different retromer subunits (Fernandez-Borja et al., 1999; Robinson et al., 2008). The retromer system localizes to the MVBs and presumably facilitates the return of vesicles to the TGN/EE to be recycle to the PM, since there is no evidence of a direct connection between MVBs and PM (Robinson et al., 2008). In addition, Retromer-mediated system is fundamental for the recovery of PM proteins as PIN2 (Kleine-Vehn et al., 2008).

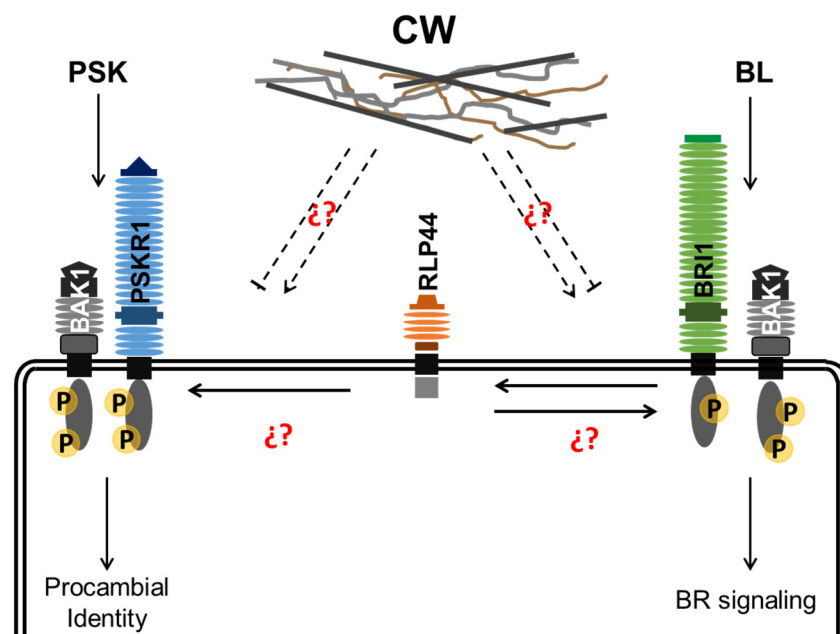
Aim of this study

The mechanism of the RLP44 mediated activation of BR and PSK signaling as well as the nature of the interdependence between both is still unknown. Therefore, the main objective of this thesis is to:

Reveal the mechanism of signaling integration between cell wall, BR and PSK signaling

RLP44 has a small and highly conserved cytoplasmic domain, which contains four amino acids (a threonine, two serines and a tyrosine) that are predicted to be phosphorylated. Furthermore, previous results suggest that after immunopurification, RLP44-GFP gives rise to a signal with anti-phosphoserine antibodies (Wolf et al. 2014). This posttranscriptional modification has been shown to have an effect on the function and localization of plasma membrane proteins (Wu et al., 2011; Offringa et al., 2013). Therefore, signal transduction of cell wall changes might be influenced by phosphorylation state of the C-terminal cytosolic domain of RLP44. Hence, we aim to analyze the effect of phosphorylation for RLP44 function and its impact on the integration with BR signaling. Furthermore, attending to recent findings of the lab, we want to address the role of RLP44 phosphorylation in xylem development and its role in PSK signaling.

Besides, to understand how RLP44 interacts and activates BR signaling, seed of the RLP44-RFP (RLP44ox) line were mutagenized to identify suppressors which are specifically impaired in signaling integration between the pathways but not in BL sensing. Therefore, plants in which the RLP44ox phenotype was suppressed have been selected for further studies including, in a first stage, BL sensitivity and RLP44ox expression analysis. The identification of new mutants would be useful to gain insight into the molecular connection between these three signaling pathways as well as new players for CW signal perception and its influence on RLP44 balance between BR and PSK signaling.



Initial model of the thesis. Reveal the mechanisms that integrate CW, BR and PSK signaling.

2. Results

Chapter 1: Phosphorylation of RLP44 controls protein function

2.1. Receptor-like protein 44 (RLP44) is a conserved receptor with a unique cytoplasmic domain

The Receptor-like protein (RLP) family consists of 57 members in *Arabidopsis thaliana* (Wang et al., 2008), some of which were shown to be involved in pathogen perception or developmental signaling. Among them, only a few members of the family have been thoroughly characterized such as TOO MANY MOUTHS (TMM) (Nadeau and Sack 2002), CLAVATA 2 (CLV2) (Jeong et al., 1999) or RECEPTOR-LIKE PROTEIN 23 (RLP23) (Albert et al., 2015).

RECEPTOR-LIKE PROTEIN 44 (RLP44) has been discovered in a suppressor screen of *Arabidopsis thaliana* (Col-0) plants overexpressing PECTIN METHYL ESTERASE INHIBITOR 5 (PMEIox) (Wolf et al., 2014). RLP44 is presumably sensing changes on the cell wall homeostasis and conveying this information into the cell by interacting with the two brassinosteroids co-receptors BRASSINOSTEROIDS INSENSITIVE1-ASSOCIATED KINASE (BAK1) (Wolf et al., 2014) and BRASSINOSTEROID INSENSITIVE1 (BRI1) (Holzwardt et al., In revision).

Whether RLP44 is conserved in the plant kingdom is still not known, therefore we searched for putative orthologs among different species within the plant kingdom. We were able to identify putative orthologs to the division of mosses where *Physcomitrella patens* represents the group (Figure 1.A). This finding is in line with previous reports of other RLPs such as TMM that are highly conserved during evolution (Peterson et al., 2010). Since genes related with developmental processes are prone to be conserved, the sequence analysis might suggest an important role of RLP44 in development. Interestingly, even though RLP44 shares 80% of identity with RLP57 (Wang et al., 2008), *Arabidopsis thaliana* RLP44 is closer to RLP44 orthologs from other *Brassicaceae* than to RLP57 (Figure 1.A).

Interestingly, RLP44 contains a small cytoplasmic domain that differs from those of other RLPs by its chemical properties. RLP44 cytoplasmic domain shows a basic nature, whereas the rest of RLPs are predominantly acidic (Gust and Felix 2014). In addition, the RLP44 cytoplasmic domain is more conserved in the different orthologs than their LRR region in the extracellular domain, characteristic among RLKs and RLPs (Figure 1.B). A closer look into the RLP44 cytoplasmic domain showed that it contains four aminoacids that are predicted *in silico* to be phosphorylated (one threonine, one tyrosine and two serines) as well as three lysines, two of which are predicted to be ubiquitinated (Figure 1.C, Supplemental Figure 1). Protein phosphorylation can have wide-ranging functions from governing protein-protein interaction to controlling activity of enzymes, to the regulation of subcellular localization (Offringa and Huang 2013). Ubiquitination plays a decisive role in labelling PM proteins as target for protein degradation or as a signal for endocytosis (Dubeaux and Vert 2017). Because of the importance of these modifications for protein function and the high conservation of the cytoplasmic domain, we decided to investigate the conservation among RLP44 of the posttranslational predicted peptides.

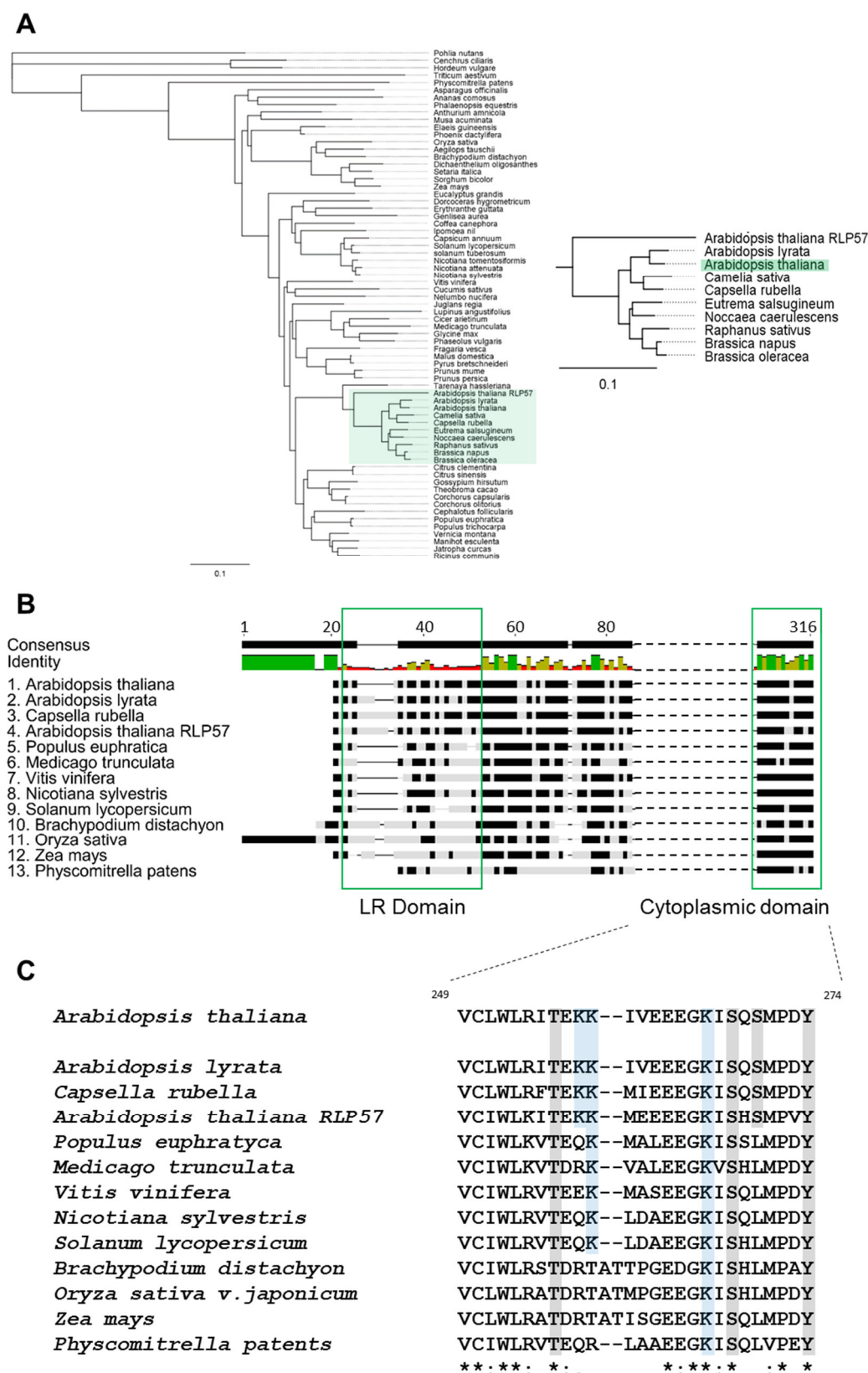


Figure 1. Cytoplasmic domain of the receptor-like 44 protein is conserved among species. A. Phylogenetic tree representing RLP44 orthologs. *Pohlia nutans* RLP44 protein sequence has been used as out-group. Bar represents the length of branch that correspond with a genetic change of 0.1. Area labelled in green correspond with the enlarged image to the right. **B.** Comparison of sequence identity between LR and Cytoplasmic domain of selected RLP44 orthologs. **C.** Alignment of orthologs RLP44 cytoplasmic domains. In grey, putative phosphorylated residues. In blue, putative ubiquitinated residues. * Show fully consensus among sequences. : shows partial consensus.

Thr-256, Lys-266, Ser-268 and Tyr-274 are highly conserved among the different RLP44 of different species (Figure 1.C) whereas Lys-258 and Ser-270 are present only in Brassicaceae species, detail that could indicate a specific function of those residues for the function of *At*RLP44. Furthermore, previous work in the lab showed that RLP44 could be phosphorylated in, at least, serine residues (Wolf et al., 2014). Therefore, we decided to study if phosphorylation of the cytoplasmic domain of RLP44 is playing a decisive role for the function of the protein.

2.2. Phosphorylation is required for RLP44-mediated activation of BR signaling

Proteins can undergo different post-transcriptional modifications, phosphorylation being the most studied one since it impacts on protein function on a multitude of developmental and defense signaling processes (Frost 1981). In plants, phosphorylation has been commonly described for serine and threonine residues (Afzal, Wood, and Lightfoot 2008). Recently, phosphorylation in tyrosine has been also described, but in much less frequency (Ghelis 2011). In addition, RLP44 is possibly phosphorylated on its conserved cytoplasmic domain, which contains four putative phospho-residues: T256, S268, S270 and Y274 (Figure 1.C).

To gain mechanistic insight into the role of phosphorylation on RLP44 function, mutated versions of those four phospho-residues were generated using Gateway® cloning system. Specifically, a phospho-dead RLP44 version (RLP44^{Pdead}-GFP) where these residues have been changed to alanine or phenylalanine was generated, deleting the capacity to be phosphorylated and phospho-mimic RLP44 version (RLP44^{Pmimic}-GFP) where these residues have been changed to glutamic acid creating chemical properties similar to a phosphorylated residue (Figure 2.A). These constructs were used to transform the PMElx suppressor mutant *cnu2* to assess their capacity to function in RLP44's BR signaling promoting role (Wolf et al., 2014).

A comprehensive analysis of homozygous lines expressing RLP44-GFP, RLP44^{Pdead}-GFP and RLP44^{Pmimic}-GFP has been performed starting by the characterization of their macroscopic growth phenotype. PMElx plants are characterized by a defective directional growth (seedling root waving, organ fusion and reduced fertility) (Wolf et al., 2012). By contrast, *cnu2* plants (*rlp44* mutation in a PMElx background) suppress PMElx phenotype being phenotypically indistinguishable from Col-0 (Wolf et al., 2014). Even though these constructs had the same protein expression (Figure 2.D), their capability in rescuing the phenotype differed dramatically. As expected, RLP44-GFP was able to restore PMElx phenotype in *cnu2* background showing the characteristic root waving, organ fusion and reduced fertility (Figure 2.B; Supplemental Figure 2.A, 2.B). Likewise, RLP44^{Pmimic}-GFP version was also able to restore this phenotype. However, RLP44^{Pdead}-GFP failed to rescue the PMElx phenotype and was indistinguishable from *cnu2* at a macroscopic level (Figure 2.B; Supplemental Figure 2.A).

Moreover, the response to BL in terms of directional growth of etiolated hypocotyls was studied. WT etiolated hypocotyls grow upright in normal conditions, whereas an increase of BL in the medium changes the direction of growth along the surface of the medium (agravitropic growth) (Gupta et al., 2012). Interestingly, it has been shown that PMElx also increases the agravitropic growth of dark-

grown hypocotyls similarly to the BL effect (Wolf et al., 2012). As expected, etiolated Col-0 seedlings increased its agravitropic response increase BL in the agar medium. In contrast, PMElox grows agravitropically over the agar plate due to its enhanced brassinosteroid signaling (Wolf et al., 2012). Accordingly, *cnu2* suppresses PMElox agravitropic phenotype and is indistinguishable from Col-0. As expected, RLP44-GFP and RLP44^{Pmimic}-GFP were able to restore the agravitropic growth of PMElox when complemented *cnu2* plants, but not RLP44^{Pdead}-GFP (Supplemental figure 2.D).

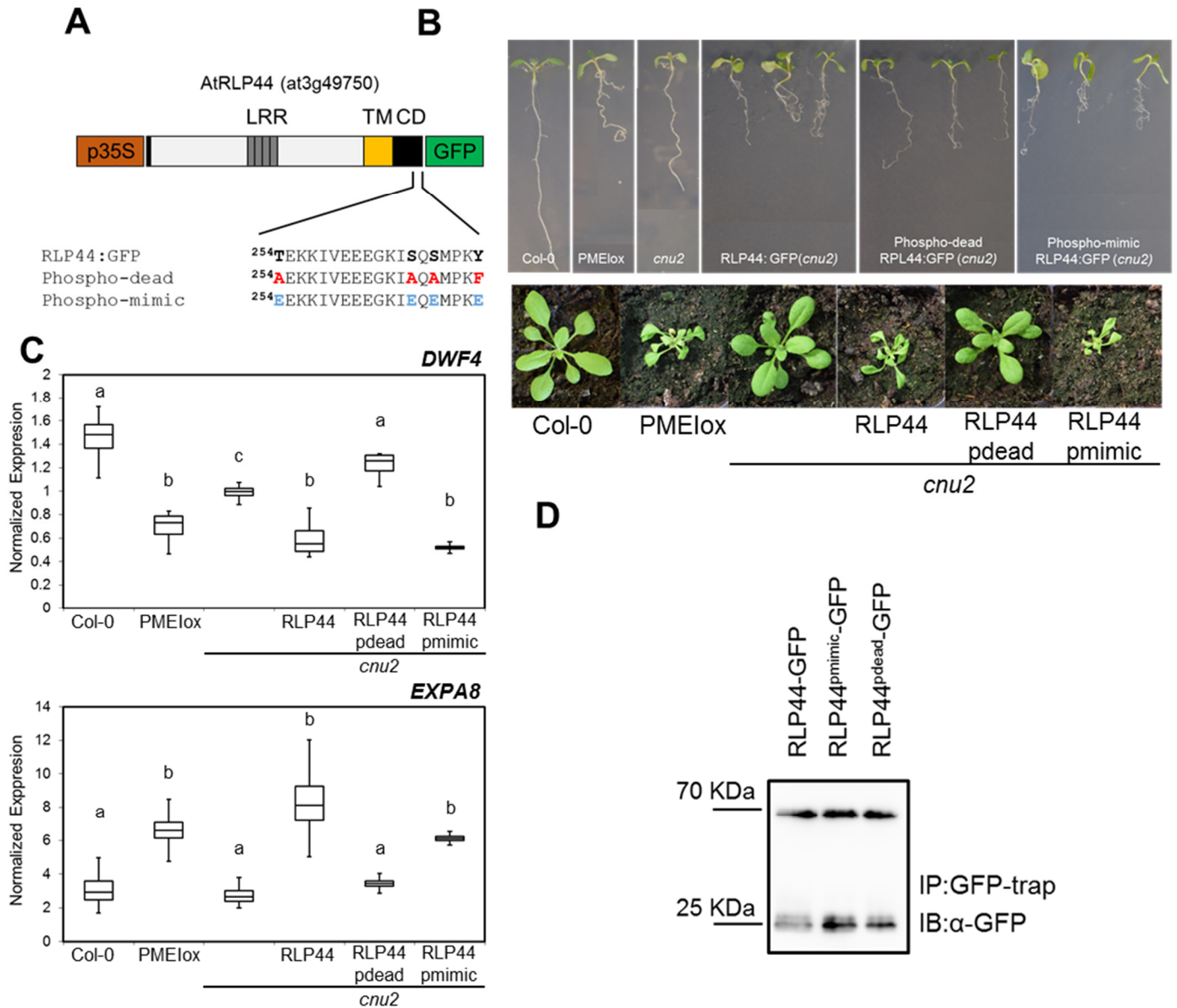


Figure 2. Modification of RLP44 phospho-residues influence protein function. A. Schematic representation of Gateway® constructs highlighting modified phosphoresidues in the cytoplasmic domain. **B.** Phenotype of 7dag seedlings and 21 dag plants. RLP44^{pmimic}-GFP and not RLP44^{pdead}-GFP rescue PMElox phenotype in *cnu2* background **C.** RLP44^{pmimic}-GFP restores to PMElox levels the expression of BR-regulated genes *DWF4* and *EXPA8* in the *cnu2* background. Normalized expression (n=3). Letters indicated significant differences (p<0.05) determined by Tukey's test (ANOVA) **D.** RLP44-GFP lines are equally expressed in *cnu2* plants. IP: Immunoprecipitation, IB: Immunoblotting.

In addition, RLP44-GFP (*cnu2*) and RLP44^{Pmimic}-GFP (*cnu2*) rescued the PMElox phenotype in terms of expression of BR-regulated genes. PMElox enhances BR signaling as can be observed by the reduction in expression of BR-negatively-regulated gene *DWF4* or the increase of the BR-positively-regulated gene *EXPA8*. This effect was reverted by the *cnu2* mutation which restores Col-0 expression levels (Figure 2.C). In line with the previous data, *cnu2* plants transformed with RLP44-GFP or RLP44^{Pmimic}-GFP were able to restore the expression pattern of *DWF4* and *EXPA8* similarly to PMElox whereas RLP44^{Pdead}-GFP did not alter *cnu2* BR-regulated genes expression.

All data together suggest that the four potential phosphorylated amino acids for the cytoplasmic domain seem to have a crucial role for the correct function of RLP44 in promoting BR signaling.

2.3. Phosphorylation modifies RLP44 subcellular localization

Plasma membrane (PM) proteins are decisive elements for sensing and translating different signaling cues into the cell. Therefore, levels of proteins at the PM have to be closely controlled and endocytosis is one of the processes that help to keep PM proteins regulated (Geldner and Robatzek 2008; Luschnig and Vert 2014). Furthermore, protein modifications influence their localization and, consequently, their functionality (Barberon et al., 2011; Martins et al., 2015). RLP44 is localized in the plasma membrane and intracellular vesicles and it has been shown to co-localize with the endocytic tracer dye FM4-64 (Wolf et al., 2014) as well as with the late endosome marker ARA7 (Andreas Kolbeck, master thesis 2015; Geldner et al., 2009) suggesting the endocytosis of RLP44 through the Trans-Golgi Network (TGN).

To gain insight on the effect of phosphorylation in RLP44 localization, GFP fluorescence in 6 days-old seedlings of *cnu2* mutants complemented with RLP44-GFP, RLP44^{Pdead}-GFP and RLP44^{Pmimic}-GFP was studied. RLP44-GFP showed a PM and vesicular fluorescence as previously described (Wolf et al., 2014). Surprisingly, the RLP44^{Pdead}-GFP showed strongly reduced PM fluorescence and an increase in intracellular fluorescence (Figure 3.A). In contrast, the RLP44^{Pmimic}-GFP showed a strongly increased PM signal (Figure 3.A). This signal was confirmed by FM4-64 staining. In addition, ratio between the PM and intracellular signal of the three different lines was measured and it could be confirmed the increase on the ratio for RLP44^{Pmimic}-GFP about three folds (Figure 3.B). Furthermore, the same pattern on PM and endocytic fluorescence was seen on independent Col-0 plants transformed with the same constructs (Supplemental Figure 3.A and 3.B).

These observations revealed the importance of phosphorylation on these four residues for the subcellular localization of RLP44. In addition, these results suggested that either RLP44 phosphorylation retains the protein at the PM or, alternatively, that the lack of phosphorylation prevents the protein to be transported or anchored to the PM (Figure 3.C).

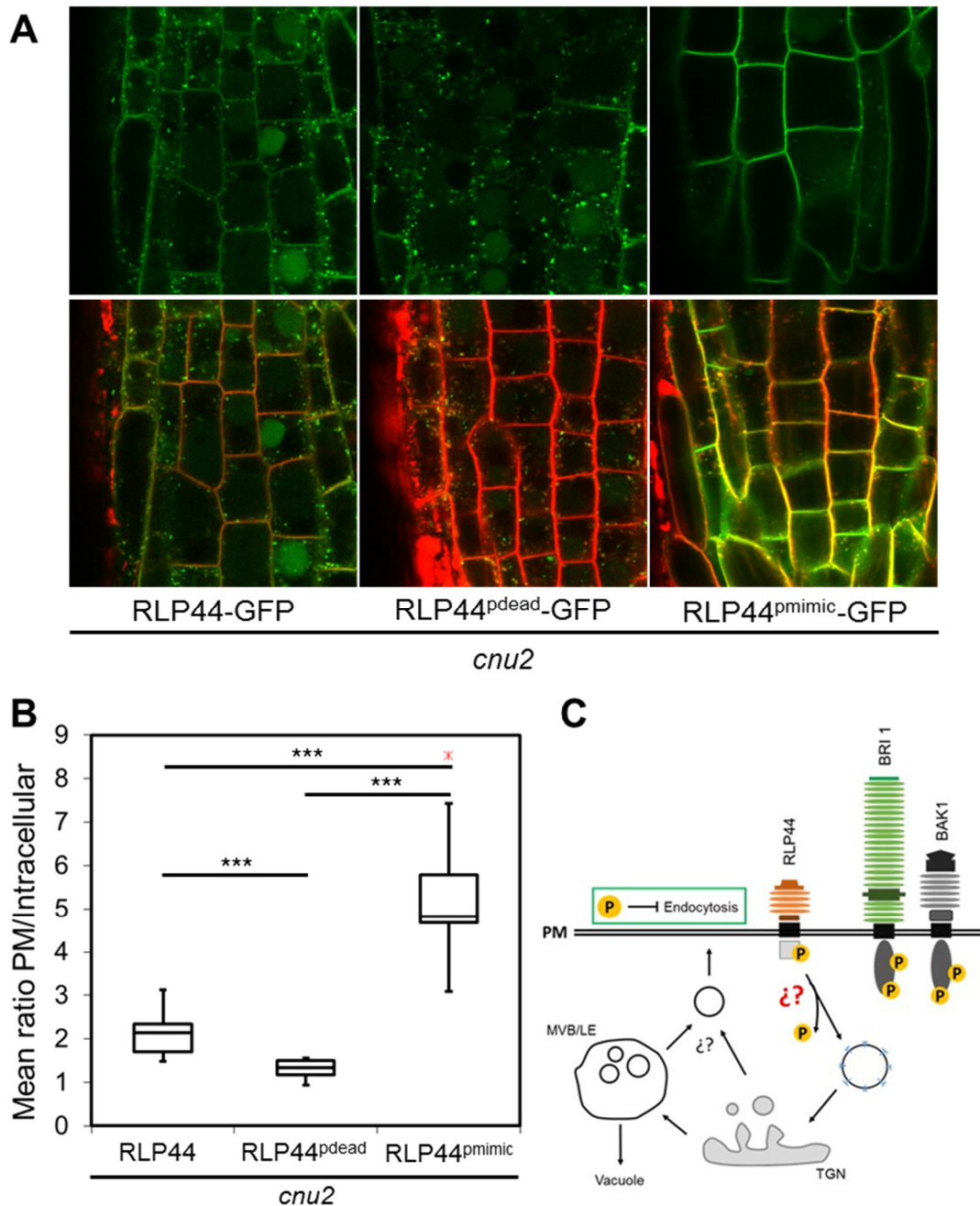


Figure 3. RFP44^{pmimic}-GFP strongly increase PM localization. **A.** RFP44^{pmimic}-GFP fluorescence signal of 7-day-old seedlings roots and merged fluorescence after 10 min of staining with endocytic tracer dye FM4-64 shows an enrichment on PM localization when compares WT. **B.** RFP44^{pmimic}-GFP increases the ratio of PM and intracellular fluorescence whereas RFP44^{pdead}-GFP reduces it. Bars indicate mean \pm SD (n=3), Asterisks indicate results of a two-tailed t-test with $p < 0.05$ (*), $p < 0.01$ (**), $p < 0.001$ (***) **C.** Working cartoon: RFP44 phosphorylation blocks endocytosis.

2.4. Phosphorylation likely prevent RFP44 endocytosis

The majority of PM receptors in eukaryotic cells are taken up into the cell via Clathrin-mediated Endocytosis (CME) where the cargo is internalized into vesicles that are covered by a clathrin coat (McMahon and Boucrot 2011). Once they are internalized, vesicles are fused with into the Trans-Golgi Network (TGN) where cargo can then be redirected to the PM or driven to degradation in the vacuole via the late endosome (LE) as intermediate compartment (Robinson et al., 2008).

We hypothesized that phosphorylation of RLP44 might retain the protein at the PM or that the lack of phosphorylation could prevent the transport to the PM. In order to elucidate which of the two possibilities was the correct one, the endocytosis of RLP44 was studied by using an inhibitor treatment and a genetic approach, both based on the blockage of the endocytosis and/or endomembrane pathway.

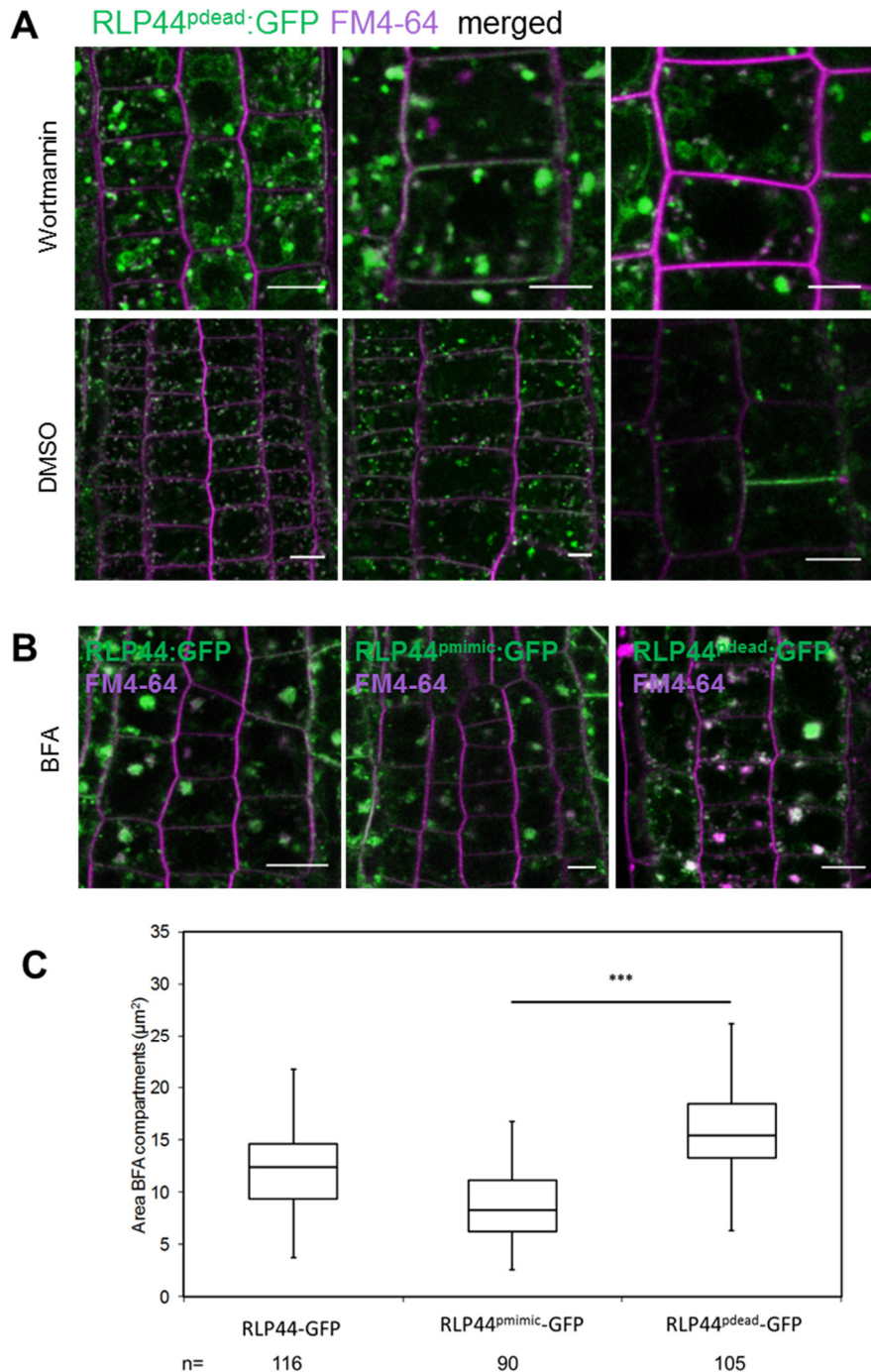


Figure 4.A. Phosphorylation does not affect VB formation. **A.** 7day-old RLP44^{pdead}-GFP *cnu2* seedlings are affected in an ordinary way by the treatment with 30 μ M Wortmannin for 165 min or DMSO for 165 min ; followed by the staining with the endocytic tracer dye FM4-64 for 20min (n=18) bars= 10 μ m. **B and C.** 7 day-old RLP44-GFP, RLP44^{pmimic}-GFP and RLP44^{pdead}-GFP show differential BFA bodies areas upon treatment with 50 μ M BFA for 120 min or DMSO for 165 min; followed by the staining with the endocytic tracer dye FM4-64 for 20min, bars=10 μ m. Asterisks indicate results of a two-tailed t-test with $p < 0.05$ (*), $p < 0.01$ (**), $p < 0.001$ (***) n= number of cells measured in 18 independent roots.

First, Brefeldin A (BFA) and Wortmannin (WM) were used, two chemical inhibitors that interact and block endosomal compartments at different levels (Robinson et al., 2008). BFA inhibits the activity of GNOM, an GEF involved in the activation of ARFs, in turn implicated in the formation of vesicles from the TGN/EE (Donaldson and Jackson 2011). Therefore, BFA produce the blockage of vesicles formation and therefore secretory trafficking and form a characteristic BFA body, defined as an aggregation trans-Golgi and endosomal vesicles (Robinson et al., 2008). Therefore, endocytosed proteins accumulates in BFA bodies. On the other hand, WM inhibits PI3K activity, essential for the attachment of nexins (SNXs) to the membrane of MVBs (Fernandez-Borja et al., 1999). Thus, WM inhibit the function of the retromer system, involved in the creation of vesicles that presumably move from the MVB to TGN/EE (Robinson et al., 2012). As a consequence, trafficking from the MVB to the TGN as well as endocytosis is minimized and the MVB shows an apparent ring-like structure (Robinson et al., 2008).

Seven-day-old seedlings of RLP44-GFP, RLP44^{Pmimic}-GFP and RLP44^{Pdead}-GFP (*gnu2*) were treated with 30 μ M WM for 165 minutes and 50 μ M BFA for 120 minutes followed by 20 minutes of staining with the endocytic tracer FM4-64. Upon the treatment with WM, RLP44^{Pdead}-GFP fluorescence was visible in the characteristic ring-like structures (Figure 4.A), suggesting that many of the intracellular punctate structures positive for RLP44^{Pdead}-GFP are MVBs, consistent with increased endocytosis. Furthermore, WM treatment slightly increased plasma membrane localization of RLP44^{Pdead}-GFP (Figure 4.A and Supplemental figure 4.A and 4.B). These data suggests that phosphorylation allowed retaining RLP44 on the plasma membrane and the lack of phospho-residues would produce a faster uptake of the protein into the endosomal system (Figure 3.C). Moreover, upon BFA treatment, RLP44^{Pdead}-GFP showed an increased signal in the BFA bodies when compared to RLP44-GFP (Figure 4.B and 4.C). In addition, GFP signal in BFA bodies of RLP44^{Pmimic}-GFP was weaker than the RLP44-GFP signal (Figure 4.B and 4.C). This observation suggested that the rate of endocytosis could depend on the phospho-status of RLP44.

To validate this observation, a different approach was performed using estradiol-inducible expression of an artificial microRNA (amiRNA) against the TPLATE complex (amiRNA:TPLATE, amiR-TPL), a major adaptor complex for clathrin-mediated endocytosis in plants (Gadeyne et al., 2014) (Figure 5.B). Lines carrying this construct were crossed with plants carrying RLP44-GFP and RLP44^{Pdead}-GFP. We hypothesized that phosphorylation determines residence time at the plasma membrane. If this is correct, interference with endocytosis should lead to increased PM localization of phospho-dead RLP44-GFP upon blocking CME. Therefore, subcellular localization of RLP44-GFP and RLP44^{Pdead}-GFP in amiR-TPL seedlings two-days upon the induction of amiRNA by transferring 3-days-old seedlings from normal agar plates to plates containing 5 μ M β -Estradiol. Therefore, the ratio of the mean signal of PM and intracellular GFP was analyzed and measured. As induction control, the same ratio for FM4-64 staining on β -Estradiol induced amiR-TPL was measured and compared with mock controls (Figure 5.A and Figure 5.C). In accordance with the hypothesis, the PM/intracellular GFP signal ratio was increased upon induction of amiRNA in both RLP44^{Pdead}-GFP and RLP44-GFP (Figure 5.A and Figure 5.C). Moreover, the ratio of β -Estradiol induced RLP44^{Pdead}-GFP raised the levels of the mock-treated ratio of RLP44-GFP and, in any of the lines studied, application of β -Estradiol produced a reduction of total root length in accordance with a reduction on cell growth (Supplemental figure 5.A). Moreover, when mock-

treatment and β -Estradiol induced-seedlings were treated with 50 μ M BFA, a drastic reduction on the presence of BFA bodies on the amiTPL lines upon induction was observed, as well as a strong reduction on BFA bodies in the RLP44^{Pdead}-GFP (Supplemental Figure 5.B).

Taken together, these data indicate that phosphorylation of RLP44 is associated with the membrane localization of the protein. RLP44 might arrive to the PM where, after being phosphorylated, it is retained in order to sense changes in the cell wall. RLP44^{Pdead}-GFP presumably arrives to the PM and is quickly taken up via clathrin-mediated endocytosis due to its inability to be phosphorylated.

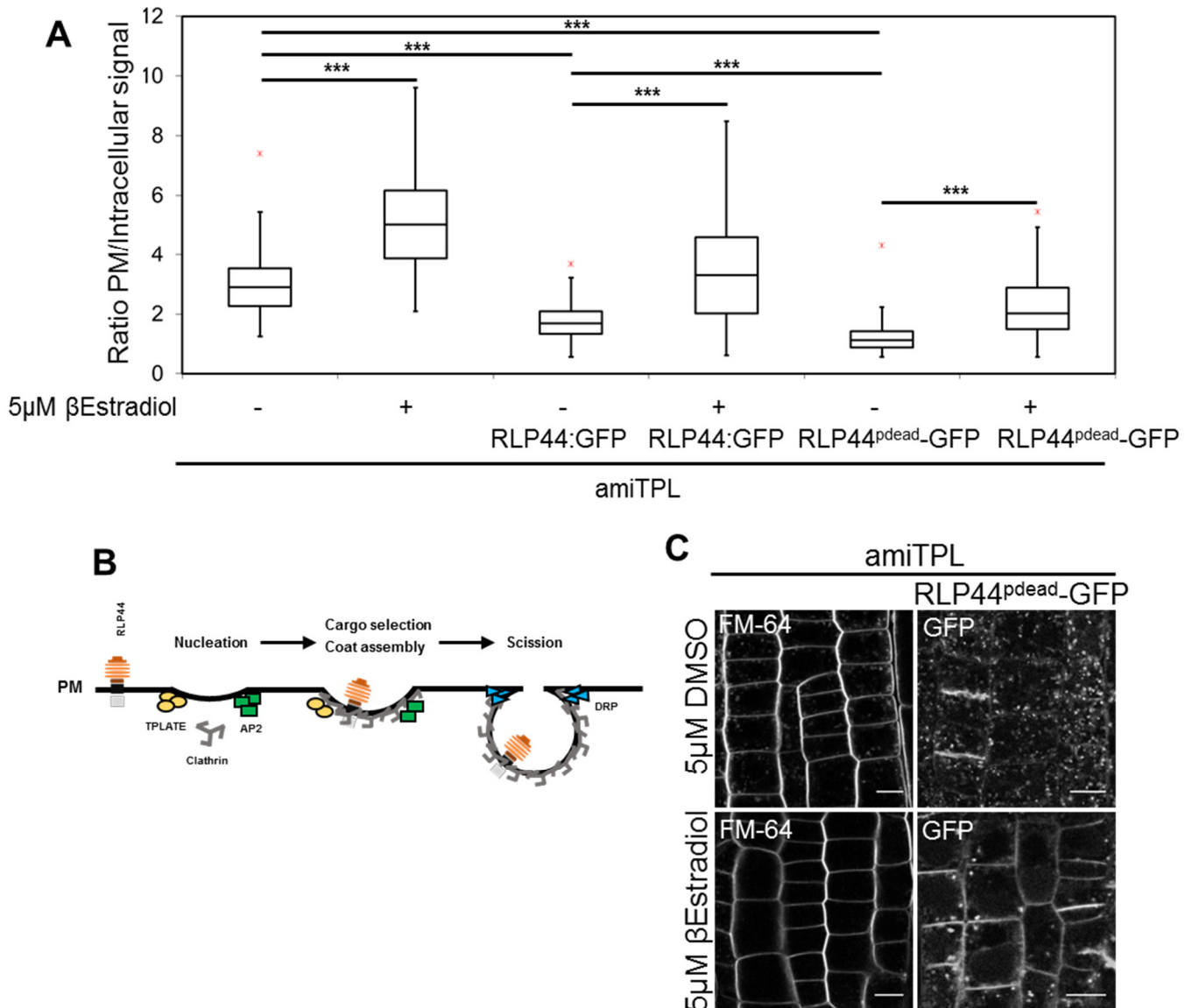


Figure 5. Inhibition of CME retains RLP44^{pdead}-GFP in the PM. **A.** Upon the inhibition of CME endocytosis by the induction of amiR-TPL, 5 days-old RLP44^{pdead}-GFP (amiR-TPL) seedlings increase GFP localization at the PM. Box-plot quantifies the ratio of the PM and intracellular signal for the same cell (n= 60-82 from 15-18 independent roots). Asterisks indicate results of a two-tailed t-test with p<0.05 (*), p<0.01 (**), p<0.001 (***). **B.** Cartoon of the RLP44 CME. **C.** RLP44^{pdead}-GFP (amiR-TPL) and amiR-TPL seedlings imaged upon 3 days of induction with 5 μ M β -estradiol bars=10 μ m.

2.5. BRI1, but not Cell wall perturbation, partially influences RLP44 PM localization

Plant signaling processes are highly regulated by the subcellular compartmentalization of the receptors (Reyes et al., 2011), including BRI1 in which the blockage of its constitutive endosomal recycling impacts on the activation of BR cascade (Irani et al., 2012).

Since the creation of a phospho-mimic version of RLP44 leads to a strong increase of the PM localization of the protein and the function of RLP44, and RLP44 signal is integrated into the BR cascade, it was interesting to check if the absence of BRI1 would influence the localization of the protein.

Therefore, subcellular imaging of 7-days-old seedlings expressing RLP44-GFP, RLP44^{pmimic}-GFP and RLP44^{pdead}-GFP, in both Col-0 and *bri1*-null background was performed. The PM/intracellular signal ratio was measured and compared between the different constructs in the two different backgrounds. Intriguingly, RLP44-GFP PM/intracellular signal ratio was slightly increased in *bri1*-null mutant when compared to wild-type (Figure 6.A, 6.B).

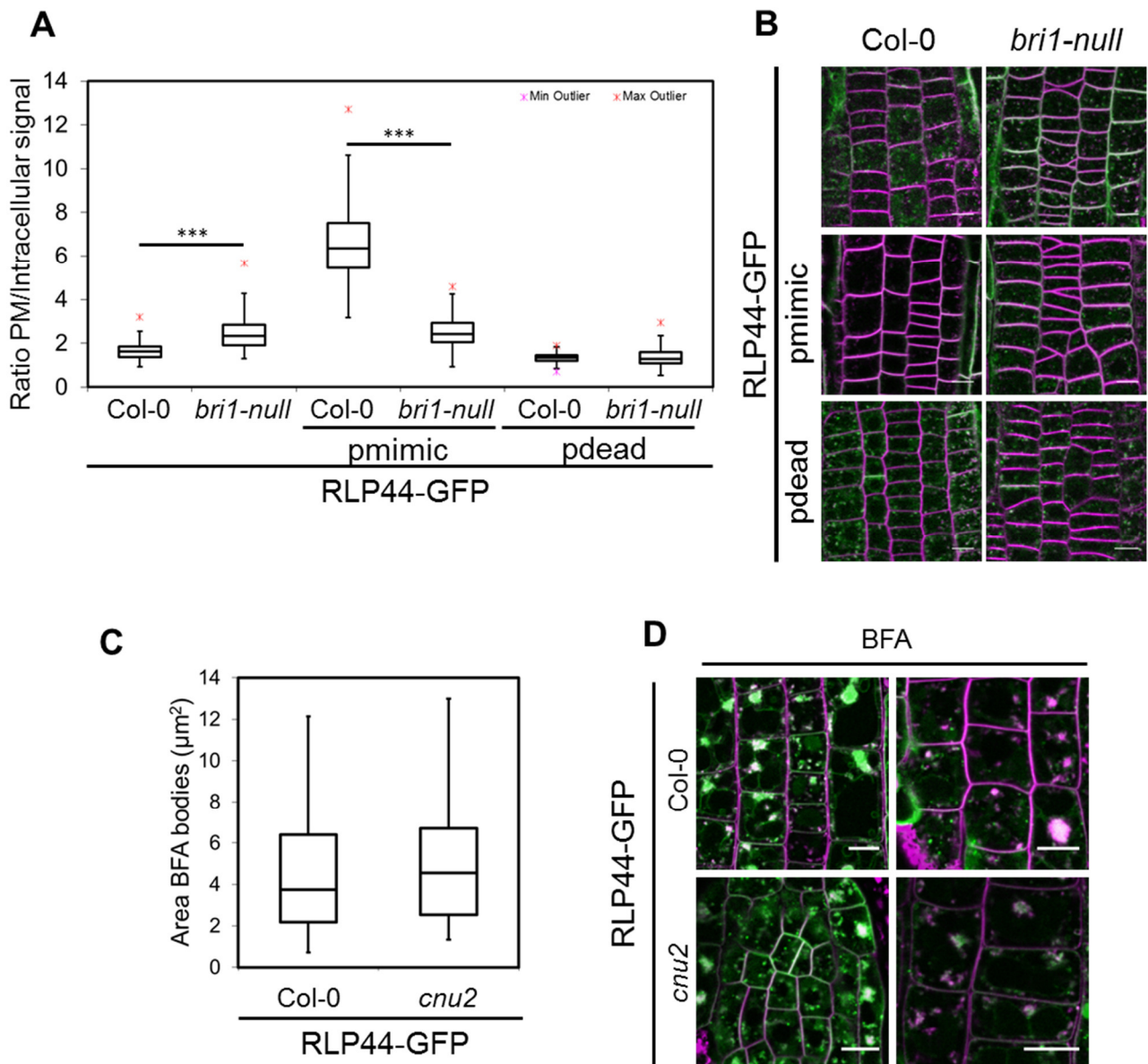


Figure 6. (previous page) RLP44 subcellular localization depends on BRI1. **A.** RLP44^{pmimic}-GFP strongly increase intracellular localization in absence of BRI1. Box-plot quantifies the ratio of the PM and intracellular signal for the same cell (n=48-62 cells from 12 independent roots). Asterisk indicate results of a two-tailed t-test with p<0.05 (*), p<0.01(**), p<0.001(***) **B.** Representative images 6 days-old RLP44-GFP, RLP44^{pmimic}-GFP and RLP44^{pdead}-GFP seedlings in Col-0 and *bri1*-null background. Bars= 5 μ m. **C.** Perturbation of the cell wall cause by PMElox did not modify endocytosis of RLP44. Box-plot quantifies area of BFA bodies in root cells (n=42-56 cells from 15 independent roots) **D.** Representative images of 6-days old RLP44-GFP seedlings in Col-0 and *cnu2* background. Bars= 5 μ m.

However, RLP44^{pmimic}-GFP experienced a strong reduction on the PM/intracellular ratio when the constructs was expressed in *bri1*-null background and compared to Col-0 (Figure 6.A, 6.B). Interestingly, this reduction reached a ratio value similar to the values of RLP44-GFP in *bri1*-null background instead of Col-0. RLP44^{pdead}-GFP did not show any variation on its localization in the absence of BRI1 and it showed in both cases a lower ratio value than RLP44-GFP and RLP44^{pmimic}-GFP RLP44 in the two backgrounds (Figure 6.A, 6.B).

These data suggested that plasma membrane localization of RLP44 is partially dependent on the presence of BRI1. Alternatively, other PM or PM-related proteins could influence the localization and endocytosis of RLP44. Thus, it was interesting to unravel if the CW signaling perceived by RLP44 would influence its localization at the plasma membrane and its endosomal recycling. To address this question, RLP44-GFP expressed in a Col-0 or in a *cnu2* background were used. RLP44-GFP was able to complement *cnu2* and restore the strong characteristics produced by PMElox (Figure 2.B). On the other hand, RLP44-GFP in Col-0 presented a normal subcellular localization and did not have a strong overexpression phenotype (Supplemental Figure 3.A, 3.B). Thus, 7-days-old seedlings of RLP44-GFP (Col-0) and RLP44-GFP (*cnu2*) were BFA-treated for 120 min and seedlings were stained with FM4-64 for 15 min to track endocytosis. Afterward, seedlings were imaged to compare and measure the differences of RLP44-GFP signal in BFA bodies. Interestingly, there was no difference on GFP signal in BFA bodies when RLP44-GFP in Col-0 and *cnu2* were compared (Figure 6.C, 6.D). These data suggested that RLP44 vesicular trafficking might not change by the signal produced in the presence of PMElox. In any case, these observation need to be tested in other cell wall mutants.

2.6. RLP44 promotes BAK1 and BRI1 interaction

BRI1 and BAK1, the two co-receptors of BR signaling, only interact and auto- and trans-phosphorylate each other when BL is perceived (Belkhadir and Jaillais 2015). BAK1 also interacts with other different RLKs and RLPs modulating more than one signaling process in the same PM context (Ma et al., 2016). RLP44 interacts with BAK1 (Wolf et al., 2014) and BRI1 (Holzwardt et al., In revision) which suggests that the formation of a ternary complex between RLP44, BAK1 and BRI1 is necessary to transduce the information into the cell. Nevertheless, the biochemical nature and mechanism of the interaction and complex formation remains unknown (Figure 7.A).

To gain insight into the effect of RLP44 on the formation of BRI1 and BAK1 complex, we used two transgenic lines: p35S:BRI1-GFP (Col-0) and pBRI1:BRI1-mCit pBAK1:BAK1-HA (*bri1-null*) and generated a third stable line expressing pBRI1:BRI1-mCit, pBAK1:BAK1-HA and p35S:RLP44-RFP in a *bri1-null* background. BRI1-mCit was immunopurified from 7 days-old seedlings using GFP-trap. After immunodetection with BAK1 and HA antibodies, a slight increase of BAK1 pull-down in presence of RLP44 was observed compared to the transgenic line without carrying p35S:RLP44-RFP (Figure 7.B), suggesting that the presence of RLP44 could promote the interaction between BAK1 and BRI1.

2.7. RLP44 activation of BR signaling requires the presence of BRI1

RLP44 might form a complex with BRI1 and BAK1 in order to transduce the information perceived at cell wall level into the cell. Since previous work in the lab suggested that the cytoplasmic domain of RLP44 alone and not the extracellular domain was sufficient to pull down BRI1 in co-immunoprecipitation assays, we wanted to disentangle whether the phosphorylation of RLP44 cytoplasmic domain could have an impact on the interaction with BRI1-BAK1 complex. Therefore, changes in the interaction with BRI1 and BAK1 were tested for the phospho-mutants by using co-immunoprecipitation and ratiometric bimolecular fluorescence complementation (BiFC) (Grefen and Blatt, 2014).

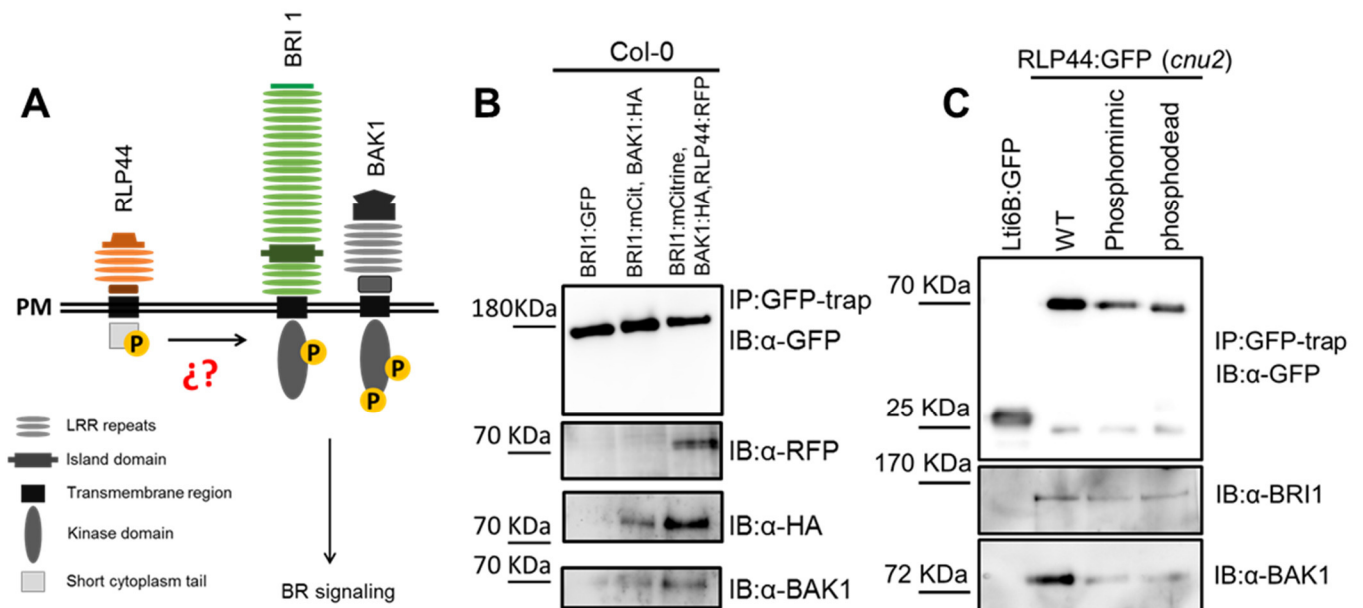


Figure 7. RLP44 positively influence BRI1 and BAK1 interaction. **A.** Hypothesis model cartoon. **B.** Immunoprecipitation of BRI1mCit in presence of RLP44-RFP increases co-immunoprecipitation of endogenous BAK1 and BAK1-HA. **C.** Modifications on cytoplasmic phospho-residues of RLP44 did not interfere on the complex formation with BAK1 and BRI1. IP: immunoprecipitation. IB: Immunoblotting.

For the first approach, the two available phospho-mutant lines (RLP44^{Pdead}-GFP and RLP44^{Pmimic}-GFP) were used together with RLP44-GFP as a positive control and LOW TEMPERATURE INDUCE PROTEIN 6B (Lti6B)-GFP as negative control (Cutler et al., 2000). RLP44-GFP versions and Lti6B-GFP were immunopurified from 7 days-old seedlings by GFP-trap. After immunodetection with antibodies directed against GFP, BRI1 and BAK1, it was observed that both phospho-mutant versions were able to pull down BRI1 and BAK1 similarly to the WT version (Figure 7.C). These data suggest that the

mutation of the putative phospho-residues do not interfere with the formation of the complex *per se* even if RLP44 phosphorylation status changed their time of residence in the plasma membrane (Figure 3.B). These results do not necessarily mean a direct interaction and there might be rearrangements in higher-order complexes that might be missed with CoIP.

Furthermore, a ratiometric BiFC analysis (Grefen and Blatt 2014) was performed to study the interaction of the different phospho-mutants with BAK1 and BRI1. In our Ratiometric BiFC essays, the 2in1 plasmid generated by Gateway® was used. The plasmid incorporates in the same construct the sequence of the two proteins to test the interaction anchoring to the cYFP and nYFC, respectively. In addition, it also contains the full RFP sequence under the control of the constitutive 35S promoter which can be used not only as a proof for transformation but also it can be used to normalized the YFP signal and obtain quantifiable values. As a positive control, a plasmid carrying BRI1-BAK1 sequences was used. Moreover, as negative control, interaction with FLS2 was used in the combinations depicted in Table 1. After infiltration of *Nicotiana benthamiana* leaves, they were imaged for both YFP and RFP signals. Afterwards, the mean value of the of the YFP and RFP signals of the same leaf region was measured and afterwards the ratio of the two mean signals was calculated to acquire a comparable value between the different protein combinations.

Table 1. List of combinations used for BiFC experiment in transiently transformed *N.benthamiana* leaves.

	nYFP	cYFP
Positive Control	BAK1	BRI1
Negative Control	BRI1	FLS2
WT sample	BAK1	RLP44
Phospho mimic sample	BAK1	RLP44 ^{pmimic}
Phospho dead sample	BAK1	RLP44 ^{pdead}
WT sample	BRI1	RLP44
Phospho mimic sample	BRI1	RLP44 ^{pmimic}
Phospho dead sample	BRI1	RLP44 ^{pdead}
WT Negative control	FLS2	RLP44
Phospho mimic negative control	FLS2	RLP44 ^{pmimic}
Phospho dead negative control	FLS2	RLP44 ^{pdead}

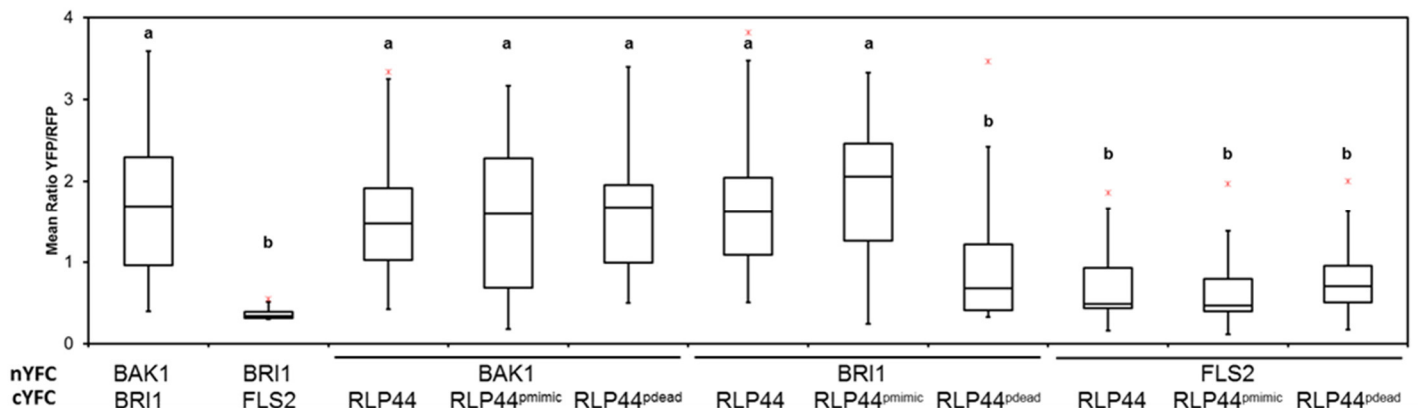


Figure 8. RLP44 phosphorylation interferes on the interaction with BRI1 but not BAK1. BiFC analysis of in vivo interaction between RLP44, RLP44^{pmimic} and RLP44^{pdead} with BAK1, BRI1 and FLS2. RLP44 and RLP44^{pmimic} interacts with BAK1 and BRI1 whereas RLP44^{pdead} is only able to interact with BAK1. Interaction of all RLP44 versions with FLS2 has been used as a negative control. Box-plot quantifies ratio of the mean value of YFP and RFP fluorescent signal. Letters indicated significant differences ($p < 0.001$) determined by Tukey's test (ANOVA) ($n = 30-80$ from 2-6 independent leaves).

2.8. PSK signaling activation is independent of RLP44 phosphorylation

Phytosulfokine (PSK) is a disulfated pentapeptide (Matsubayashi et al., 1996) with a general role in plant growth and development (Matsubayashi et al., 2014). PSK is perceived at the plasma membrane by the PHYTOSULFOKINE RECEPTOR 1 (PSKR1) and its homologous PSKR2, both leucine-rich repeat Receptor-Like Kinases (LRR-RLK) (Matsubayashi et al., 2002; Matsubayashi et al., 2006). Interestingly, PSKR1/2 are members of the same LRR-RLK family as BRI1 (Amano et al., 2007) and interact with SERKs co-receptors (Ladwig et al., 2015). Recent results in the lab showed that RLP44 is able to interact with PSKR1 (Holzwarth et al., in revision). Therefore, we wanted to investigate if RLP44 phosphorylation might also impact on the interaction with PSKR1.

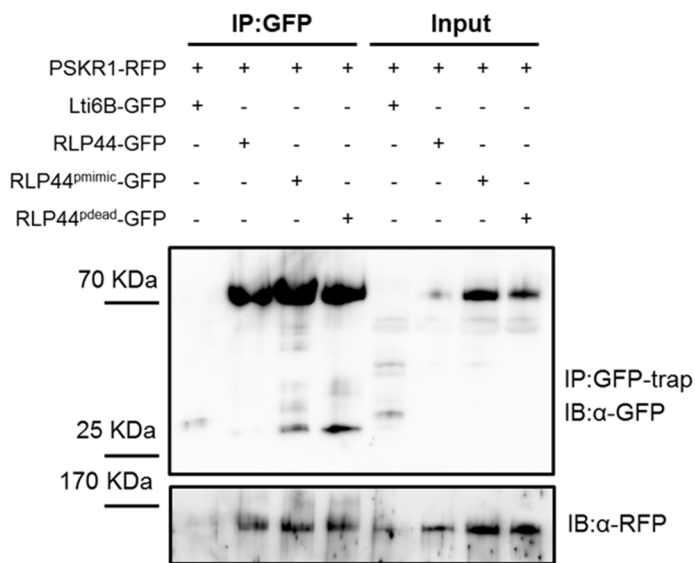


Figure 10. PSKR1 form a complex with all RLP44 phospho-versions. Immunopurification of RLP44-GFP, RLP44^{pmimic}-GFP or RLP44^{pdead}-GFP but not Lti6B-GFP transiently expressed in *N.benthamiana* leaves produce the co-immunopurification of PSKR1-RFP, co-expressed on the same leaves. IP: immunoprecipitation against GFP. IB:Immunoblotting using GFP or RFP anti-serum

First, the interaction of PSKR1-RFP with each of RLP44^{pmimic}-GFP and RLP44^{pdead}-GFP was tested, together with RLP44-GFP and Lti6B-GFP as positive and negative control, respectively, by transiently co-expressing the constructs in *Nicotiana benthamiana* leaves. Two days after co-infiltration, positive expression was checked and plant material was harvested. After immunopurification by GFP beads, presence of RLP44 versions and PSKR1 using anti GFP and RFP antibodies were immunodetected. Interestingly, RLP44^{pmimic}-GFP and RLP44^{pdead}-GFP were able to pull down PSKR1-RFP in the same manner as RLP44-GFP (Figure 10.A). Notably, PSKR1 interact with BAK1 (Ladwig et al., 2015) and phospho-mimic and phospho-dead versions of RLP44 were able as well to pull down the co-receptor (Figure 10.A). Therefore, it cannot be excluded that the co-immunopurification was due to the presence of a complex of PSKR1 together endogenous BAK1. In addition, results in the lab showed that the cytoplasmic domain alone of RLP44 directly interacted with PSKR1. Thus, further studies are needed to understand the biochemistry of the complex formation.

Consequently, the effect of PSK in RLP44^{pmimic}-GFP and RLP44^{pdead}-GFP has been checked. Previous observations showed that RLP44 overexpression increases the response to PSK when compares to Col-0 in terms of root length promotion. Col-0, *pskr1-3*, *pskr1-3 pskr2-1*, RLP44-GFP (Col-0), RLP44^{pmimic}-GFP (Col-0) and RLP44^{pdead}-GFP (Col-0) seedlings were grown for 6 days in agar medium supplied by 1 μ M PSK and DMSO as mock control independently. Phytosulfokine promoted root length in Col-0 and RLP44-GFP (Col-0) whereas *pskr1-3* and *pskr1-3 pskr2-1* were insensitive to the peptide

(Figure 11.B). RLP44^{pmimic}-GFP (Col-0) had a similar effect than RLP44-GFP (Col-0), in line with previous results (Figure 11.B). Unexpectedly, RLP44^{pdead}-GFP (Col-0) was insensitive to PSK even if endogenous RLP44 was present (Figure 11.B). These results suggest that RLP44^{pdead}-GFP has a dominant negative effect on the endogenous RLP44, which might interfere with the response to PSK. Interestingly, when it comes to the response to BL, RLP44^{pdead}-GFP (Col-0) does not differ of the response of Col-0 (Supplemental figure 3.C).

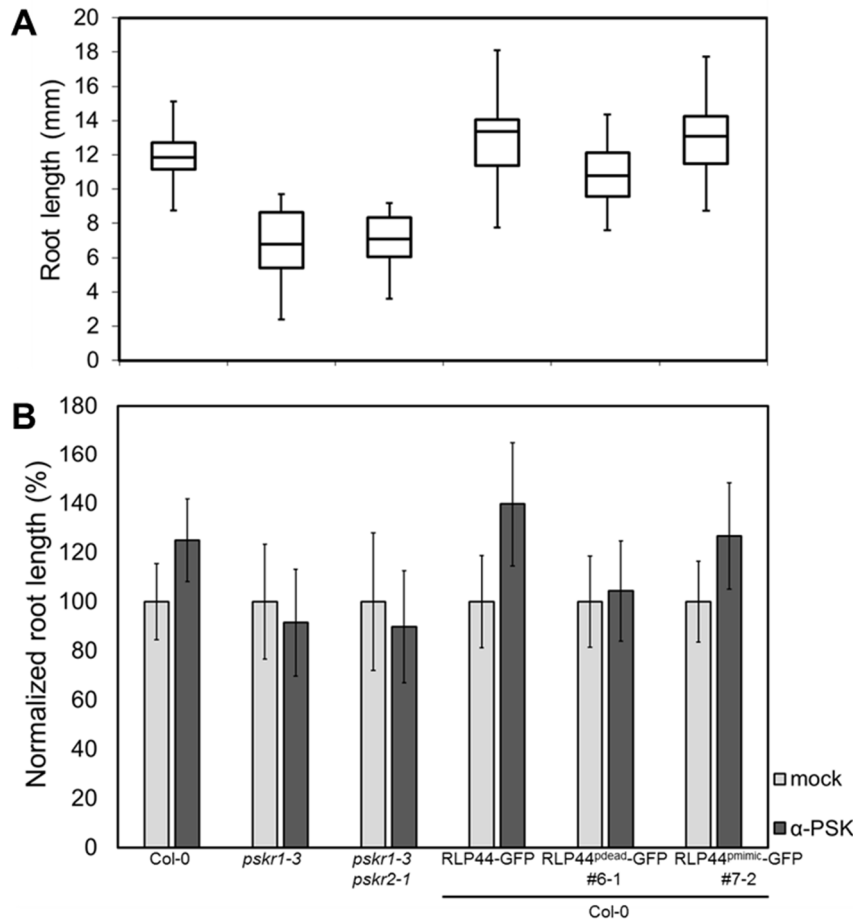


Figure 11. RLP44^{pdead}-GFP has a dominant negative effect over endogenous RLP44 in PSK response. **A.** RLP44-GFP but not RLP44^{pdead}-GFP trigger root length. Box-plots represents the root length in mm of mock treated 5-d old seedlings (n=30-57). **B.** RLP44^{pdead}-GFP (Col-0) is insensitive to PSK. Bars indicate normalized mean of the response in root length of 5-d-old seedlings to the treatment with PSK \pm SD (n=30-72). PSK: phytosulfokine.

Therefore, the effect of PSK in RLP44^{pmimic}-GFP and RLP44^{pdead}-GFP in *rlp44^{cnu2}* background was tested. After obtaining homozygous lines for the transgene as well for the *rlp44^{cnu2}* mutation, morphological phenotype of two lines for each of the phospho-versions together with a WT positive control was checked. *Rlp44^{cnu2}* is smaller than WT plants having smaller petioles length as well as a smaller rosette diameter. As expected, RLP44-GFP (*rlp44^{cnu2}*) was able to rescue the mutant phenotype as well as RLP44^{pmimic}-GFP (*rlp44^{cnu2}*) (Figure 12.A and 12.B). However, RLP44^{pdead}-GFP (*rlp44^{cnu2}*) failed to rescue the mutant phenotype maintaining the characteristic small phenotype (Figure 12.A and 12.B).

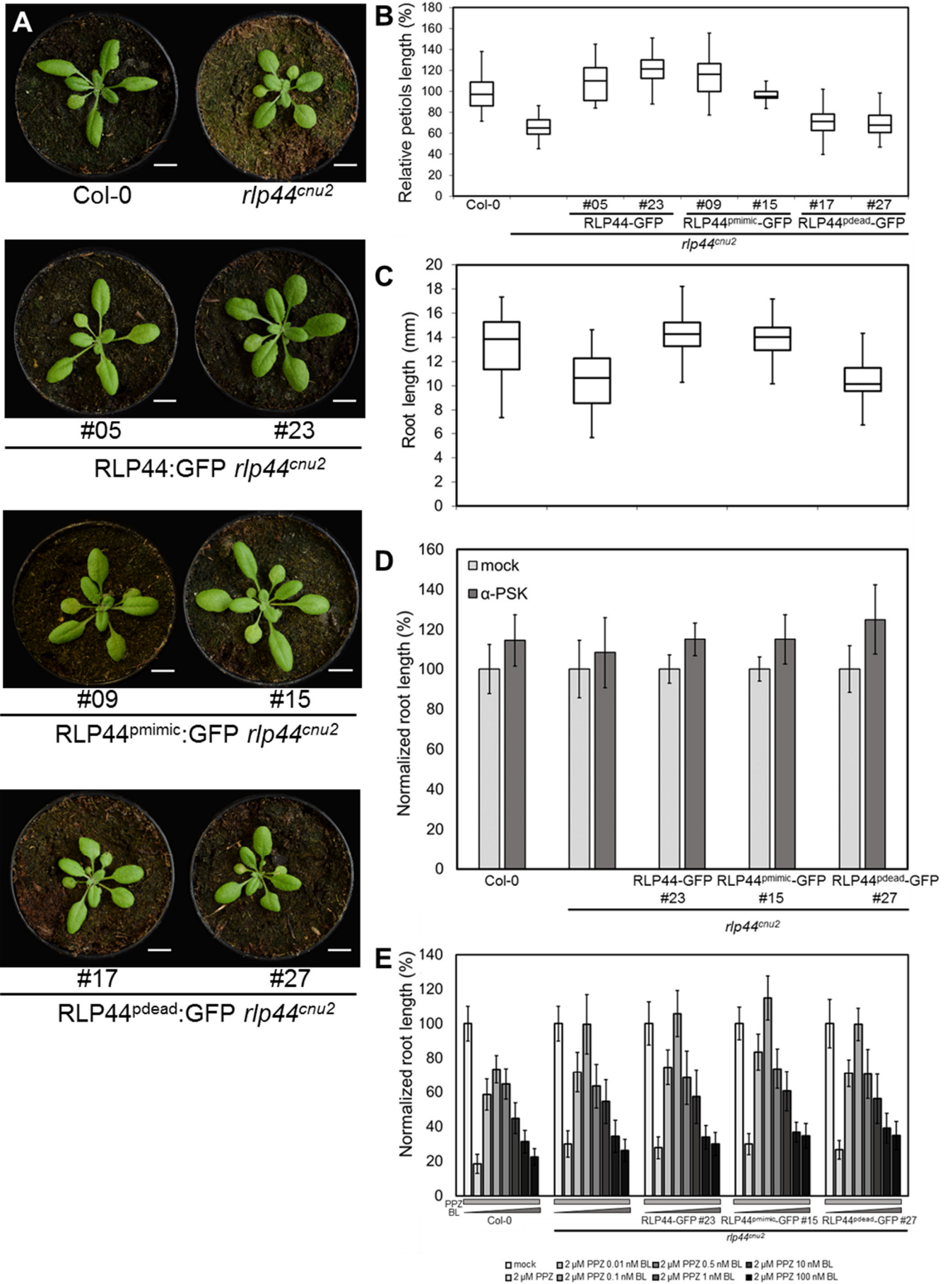


Figure 12. (Previous page) RLP44^{pdead}-GFP restores PSK in absence of endogenous RLP44. A. RLP44^{pdead}-GFP does not rescue macroscopic *rlp44^{cnu2}* phenotype in 21-d-old plants. Bar=1cm. **B.** Box-plot represents mean of the petioles length (n=18). **C.** RLP44^{pdead}-GFP does not rescue the shorter root length phenotype of *rlp44^{cnu2}*. Box-plot represents the root length in mm of mock treated 5-d old seedlings (n=27-61). **D.** RLP44^{pdead}-GFP (*rlp44^{cnu2}*) responds to PSK in a stronger manner than RLP44-GFP. Bars indicate normalized mean of the response in root length of 5-d-old seedlings to the treatment with PSK \pm SD (n=27-68). PSK: phytosulfokine. **E.** RLP44^{pdead}-GFP keeps the same response to BL as *rlp44^{cnu2}* and Col-0. Bars represent normalized response in root length to depletion of and exogenous addition of brassinosteroids \pm SD (n=25-43).

Moreover, *rlp44^{cnu2}* showed slightly shorter roots compared to Col-0. RLP44-GFP as well as RLP44^{pmimic}-GFP rescued the root length of the mutant in contrast to RLP44^{pdead}-GFP, which kept the same root length as the mutant (Figure 12.C) that might suggest that the root growth phenotype of RLP44 is BR dependent.

Afterwards, the response to PSK of the different RLP44 phospho-mutant lines in *rlp44^{cnu2}* background was tested. The mutant *rlp44^{cnu2}* partially lost the capability to promote root length upon PSK treatment when compared to Col-0 (Figure 12.D) suggesting again a role of RLP44 in PSK signaling. RLP44-GFP (*rlp44^{cnu2}*) as well as RLP44^{pmimic}-GFP (*rlp44^{cnu2}*) rescued RLP44 response to PSK and reached Col-0 response levels (Figure 12.D). Surprisingly, RLP44^{pdead}-GFP (*rlp44^{cnu2}*) also rescued *rlp44^{cnu2}* response to PSK in contrast with its effect in Col-0 background where RLP44^{pdead}-GFP were insensitive to PSK.

In addition, to test whether the presence of RLP44-GFP, RLP44^{pmimic}-GFP or RLP44^{pdead}-GFP affect the response to BL in *rlp44^{cnu2}* background, root length of the different phenotypes was measured upon increasing BL concentration in the ½ MS plates. In order to see complete response and not just growth depression, synthesis of endogenous BL synthesis has been blocked by applying 2 μ M PPZ to the media together with the different BL concentrations (from 0.01 nM to 100 nM). Col-0 and *rlp44^{cnu2}* had the same response to BL (Figure 12.E) and any of the constructs altered the response to BL in *rlp44^{cnu2}* background (Figure 12.E).

These results suggest that, contrary to the interaction with BRI1, the interaction between RLP44 and PSKR1 might not be dependent on RLP44 phosphorylation since there are no changes of interaction between the different phospho-mutants and RLP44^{pdead}-GFP is sensitive to PSK. Thus, is conceivable that RLP44 phosphorylation shifts the balance between its BR and PSK signaling promoting functions.

2.9. Gateway construct single phosphomutants show a nuclear localization

The RLP44 cytoplasmic tail presents four residues that could be putatively phosphorylated: Thr-256, Ser-268, Ser-270 and Tyr-274 (Figure 1.C). Among the four, only Ser-270 seems to be specific of *Brassicaceae* whereas the rest are conserved along phyla (Figure 1.A). Considering the impact of the modification of all those four amino acids together on RLP44 function, we were interested in understanding the individual contribution of these residues. To do so, the same approach using the Gateway system was followed for cloning all the different versions of RLP44 depicted in table 2.

2.10. Putative phosphosites are not detected by LC-MS

In parallel, a LC-MS analysis was carried out to identify *in-vivo* phosphorylation sites. 6 days-old RLP44-GFP (Col-0) plants grown in liquid medium were treated with 50 μ M Cantharidin or DMSO 3 hours before harvest the plant material. After immunopurification of RLP44-GFP using GFP beads, successful protein purification was checked by immunodetection with anti GFP antibody. Cantharidin has a phosphatase inhibiting activity, therefore phosphorylated proteins might be more stable than in a mock situation. In line with this, an enrichment on RLP44-GFP signal was detected after Cantharidin treatment when compared to DMSO control (Figure 14.A) Thus, the inhibition of phosphatases with Cantharidin could facilitate the retention of a phosphorylated RLP44 at the PM. Therefore, these samples could be potentially used for the determination of RLP44 phospho-residues.

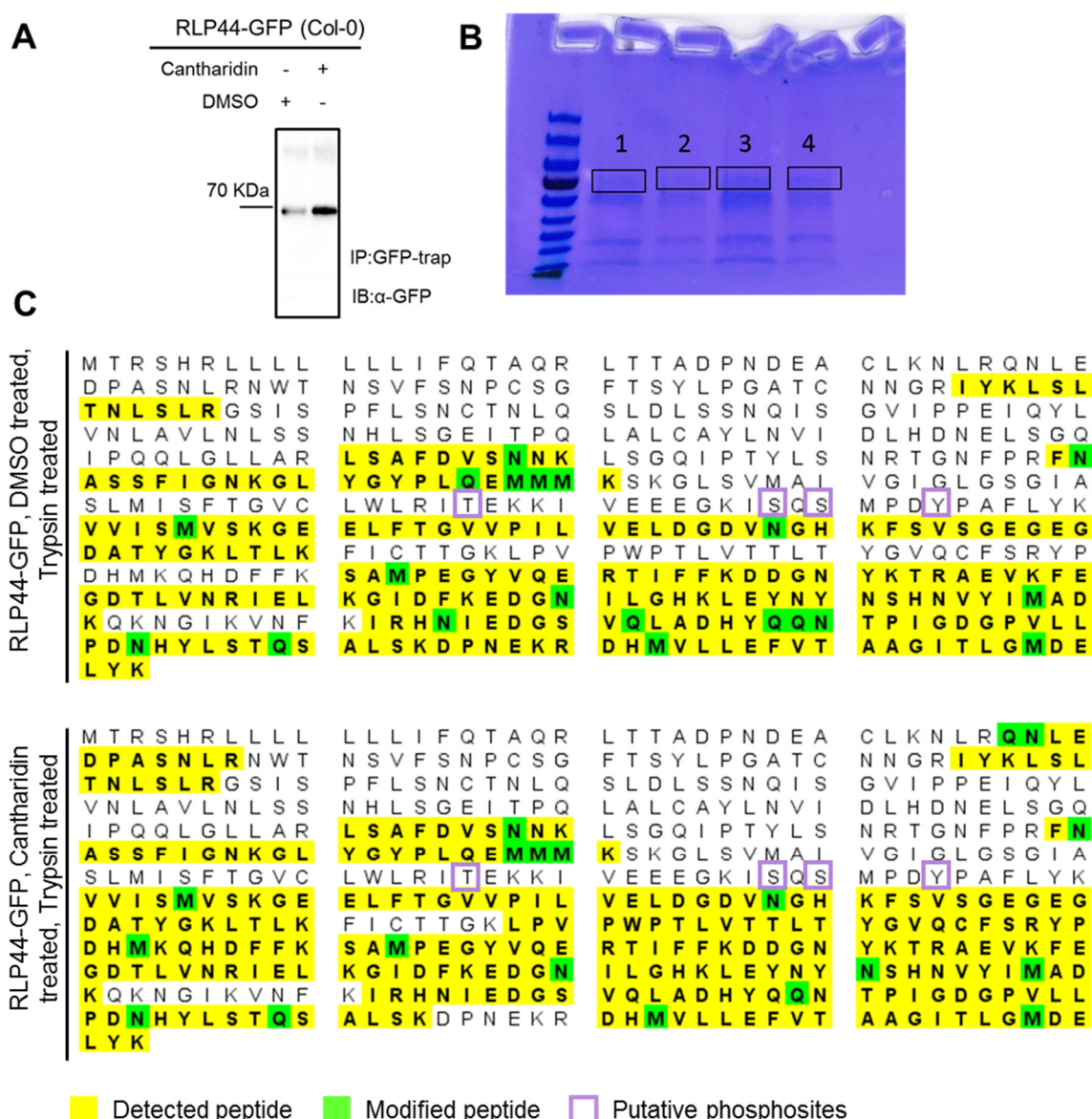


Figure 14. Proteomica analysis of RLP44-GFP by LC-MS. **A.** Cantharidin increases the detection of immunopurified RLP44-GFP from 7-d-old Col-0 seedlings. IP: immunoprecipitation against GFP. IB: Immunoblotting using GFP anti-serum. **B.** Immunopurified RLP44-GFP can be detected in Acrylamide gels stained with Coomassie. 1 and 3 lanes correspond with RLP44-GFP mock treated, 2 and 4 lanes correspond with RLP44-GFP cantharidin treated. **C.** Cantharidin treatment does not increase the number of detected peptides and it does not facilitate the detection of peptides including the putative phosphosites.

DMSO and Cantharidin treated samples were PAGE purified and in –gel digested with Trypsin and the resulted peptides were extracted and analyzed by LC-MS using Orbitrap-MS systems by the Core Facility for Mass Spectrometry and Proteomics (CFMP) at the ZMBH (Heidelberg, Germany). Analysis of the LC-MS samples by Scaffold V.4.7.5 Proteomics Software revealed the same level of detected peptides in RLP44-GFP on the two independent replicates of the two different samples (Cantharidin and DMSO treated seedlings). Samples were as well enriched in other proteins between 45 and 90 KDa, corresponding with the area of the gel that has been cut for the analysis and indicating that the procedure was successful (Figure 14.B). For the case of RLP44-GFP, the LC-MS analysis covered 44-53% of the protein sequence. Unfortunately, RLP44 sequences was poorly represented among all the peptides assigned to RLP44-GFP while the GFP sequence was well represented (Figure 14.C). Specially, RLP44 cytoplasmic tail was particularly underrepresented in the analysis (Figure 14.C). Therefore, it was not possible to determine the residues prone to be phosphorylated in the cytoplasmic tail of RLP44 by LC-MS and the protocol need to be improved for future experiments.

2.11. RLP44 is phosphorylated in a Brassinosteroid (BR)-dependent manner

RLPs, localized at the plasma membrane (PM), carry an extracellular domain able to sense different ligands but lack an evident cytoplasmic signaling part (Liebrand, van den Burg, and Joosten 2014). Therefore, RLPs need to interact with other plasma membrane proteins in order to activate an intracellular signaling cascade (Liebrand, van den Burg, and Joosten 2014).

In recent years, BAK1 has been described to have a crucial role in the integration and co-activation of different intracellular signaling pathways by phosphorylating multiple RECEPTOR-LIKE KINASES (RLKs) as BRI1 or FLAGELLIN SENSING 2 (FLS2), and other RLPs (Chinchilla et al., 2009; Albert et al., 2015; Ma et al., 2016). In the specific case of RLP44, the interaction with BAK1 and BRI1, the two co-receptors of the plant hormone brassinosteroid (BR), has been already described (Wolf et al., 2014; Holzwardt et al., In revision). Furthermore, RLP44 is able to activate BR signaling partially independent of BL perception and integrate cell wall and BR signaling (Wolf et al., 2014).

Since the RL44 Gateway constructs were not suited to the study of phosphorylation, to gain insight into the function of RLP44, plants were generated expressing a GFP-tagged RLP44 under the endogenous promoter (pRLP44:RLP44-(GS)₁₁-GFP) in *rlp44^{cnu2}* and wild-type (Col-0) backgrounds. The construct was created by the GreenGate cloning system (Lampropoulos et al., 2013). Plants carrying a single insertion of pRLP44:RLP44-(GS)₁₁-GFP are able to rescue the *rlp44^{cnu2}* phenotype and generate the characteristic RLP44 overexpression phenotype in the wild type background, previously observed with p35S:RLP44-RFP (RLP44ox from now on) (Figure 15.A). The RLP44ox phenotype is characterized by longer petioles and narrow leaf lades, similar to BRI1ox phenotype (Wolf et al., 2014; Wang et al., 2001).

To test if RLP44-(GS)₁₁-GFP is phosphorylated, the protein was immunopurified from 6-days-old RLP44-(GS)₁₁-GFP (Col-0) seedlings using GFPtrap beads. After immunodetection with a monoclonal antibody against GFP, two bands were observed corresponding to RLP44:GFP. To investigate if the nature of

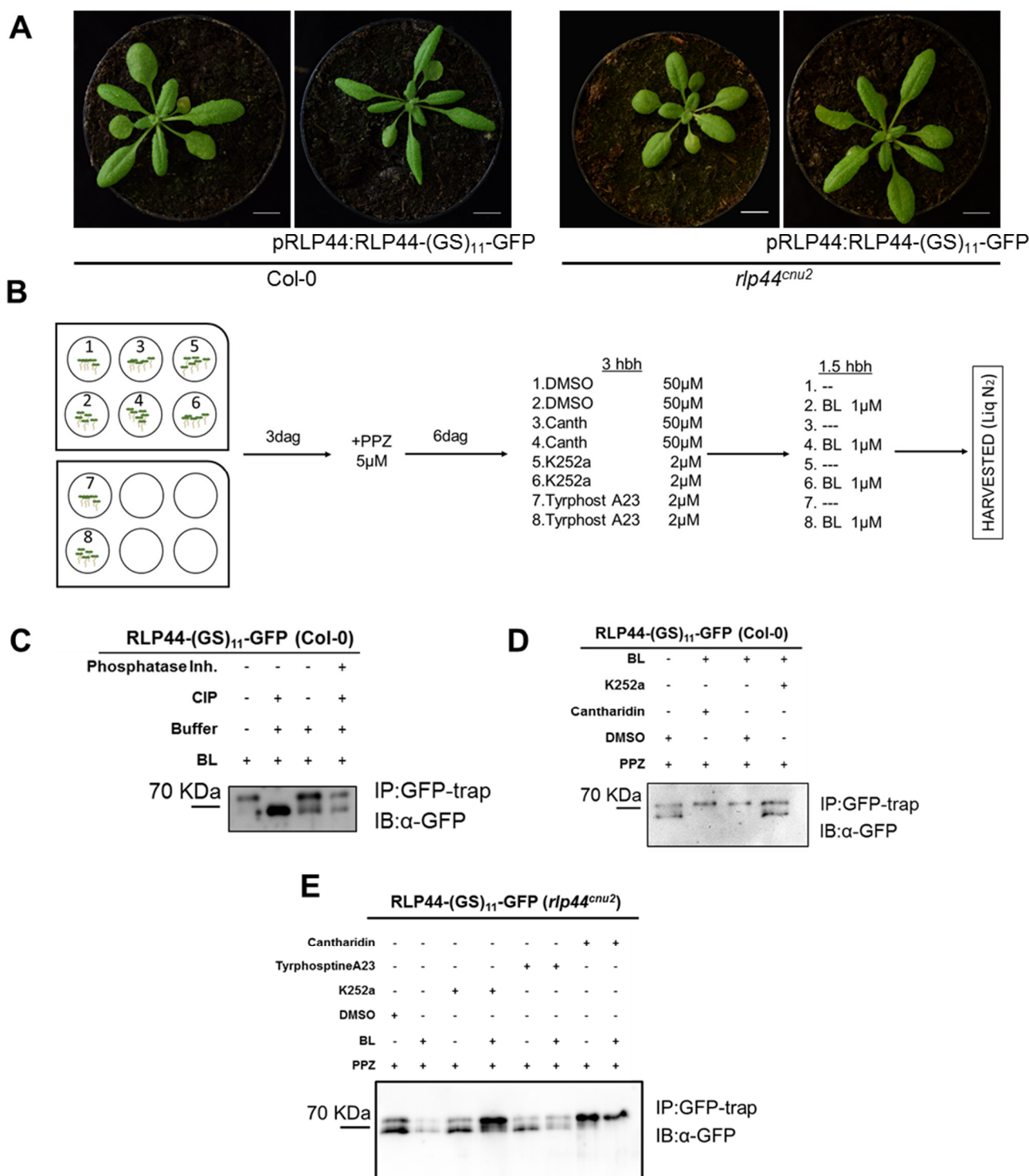


Figure 15. BL influences RLP44 phosphorylation. **A.** Schema of the $-(GS)_{11}$ -GFP linker used to potentiate phosphorylation of RLP44 cytoplasmic domain. In blue, RLP44 cytoplasmic domain, in grey, linker, in green, N-t of GFP. Phospho-residues in RLP44 cytoplasmic domain are highlighted in bold letters. **B.** RLP44 $-(GS)_{11}$ -GFP produce an overexpression phenotype in Col-0 and rescue *rlp44^{cnu2}* macroscopic phenotype in 21-d-old plants. **C.** Cartoon with the experimental procedure for phosphorylation experiments. BL (Brassinolide); PPZ (propiconazole, a BR synthesis inhibitor); Cantharidin (Phosphatase Inhibitor); K252a or Tyrphostine-A23 (Kinase inhibitor) or DMSO. **D.** Immunodetected RLP44 $-(GS)_{11}$ -GFP band are susceptible to switch mobility upon BL or CIP (Calf intestine phosphatase) treatment. **E** and **F.** Enrichment of the low-motion (phosphorylated) immunodetect RLP44 $-(GS)_{11}$ -GFP band in Col-0 (**E**) and *rlp44^{cnu2}* (**D**) changes upon BL, PPZ, Canth, K252 or TyrA23 application. IP: Immunoprecipitated against GFP, IB: Immunoblotting using GFP anti-serum.

these bands was related with phosphorylation, a phosphatase experiment was performed. Only a single band corresponding in size to the lower of the two bands in the control after CIP (calf intestine phosphatase) treatment was observed. The control situation was restored when CIP was added together with phosphatase Inhibitors (Figure 15.C). Thus, the pRLP44:RLP44-(GS)₁₁-GFP band pattern reflects different phospho-statuses of the protein.

To test if signaling could influence RLP44-GFP phosphorylation state, various chemicals that influences BR synthesis or signaling and kinase activity were applied. Seedlings of pRLP44:RLP44-(GS)₁₁-GFP (Col-0) were grown in ½ MS liquid medium and, three days after germination, treated with 5 µM propiconazole (PPZ), an inhibitor of endogenous BL synthesis. 6 days after germination and 3 hours before harvest plant material, these seedlings were treated with different kinase inhibitors (2 µM K252A, 100 µM tyrphostine A23), and a phosphatase inhibitor (50 µM cantharidin). Finally, 1.5 hours before harvesting 1 µM brassinolide (BL) was applied (Figure 15.B). After immunopurification and immunodetection using GFP antibodies, only treatment with BL produced an enrichment of the slow-moving band related to the phosphorylated version of RLP44. Besides, treatment with PPZ enriched the high mobility band (non-phosphorylated) after immunodetection (Figure 15.D, 15.E). As expected, kinase inhibitors led to a shift to the non-phosphorylated band and cantharidin to the phosphorylated one. BL treatment was able to revert the effect of kinase inhibitors and enhanced the cantharidin effect (Figure 15.D and 15.E). Taken together, we hypothesize that RLP44-(GS)₁₁-GFP is phosphorylated in a BR-dependent manner.

2.12. RLP44 phosphorylation depends on more than one kinase

RLP44 is able to interact with both co-receptors of the BR signaling pathway, BRI1 and BAK1 and promotes BR signaling. Thus, we sought to test if RLP44 might be phosphorylated by one or both BR co-receptors since both contain a kinase domain able to trans-phosphorylate proteins (Wang et al., 2005; Wang et al., 2008).

Therefore, pRLP44:RLP44-(GS)₁₁-GFP version was expressed in the *bri1-301*, *bri1^{cnu4}* and *bri1-null* backgrounds by crossing and selection of homozygous F3 lines. As described in Xu et al., 2008, *bri1-301* shows a hypomorphic phenotype since the specific mutation in the kinase domain (G989I) produce a less active BRI1 version. In turn, *bri1^{cnu4}* contains a mutation in the extracellular domain (G746S) that reduces BR sensitivity without totally blocking BRI1 function (Holzwardt et al., In revision). Finally, mutation in *bri1-null* fully blocks transcript accumulation and has a drastic effect on plant development (Jaillais et al., 2011). pRLP44:RLP44-(GS)₁₁-GFP was able to rescue the adult phenotype of *bri1^{cnu4}* completely and the phenotype of *bri1-301* partially (Figure 16.A). Furthermore, RLP44-(GS)₁₁-GFP subcellular localization in both backgrounds was similar to the one in Col-0 (Figure 16.B). Interestingly, *bri1^{cnu1}* has an intermediate BR-deficient phenotype similar to *bri1-301* (Wolf et al., 2012) but previous results showed that p35S:RLP44-RFP was not able to rescue *bri1^{cnu1}* phenotype (Wolf et al., 2014). Therefore, pRLP44:RLP44-(GS)₁₁-GFP (*bri1-301*) and pRLP44:RLP44-(GS)₁₁-GFP (*bri1^{cnu4}*) were further characterized. One of the phenotypical characteristics of *bri1-301* is its reduction on hypocotyl length in etiolated seedlings compared to Col-0 (Xu et al., 2008), therefore we checked if insertion of

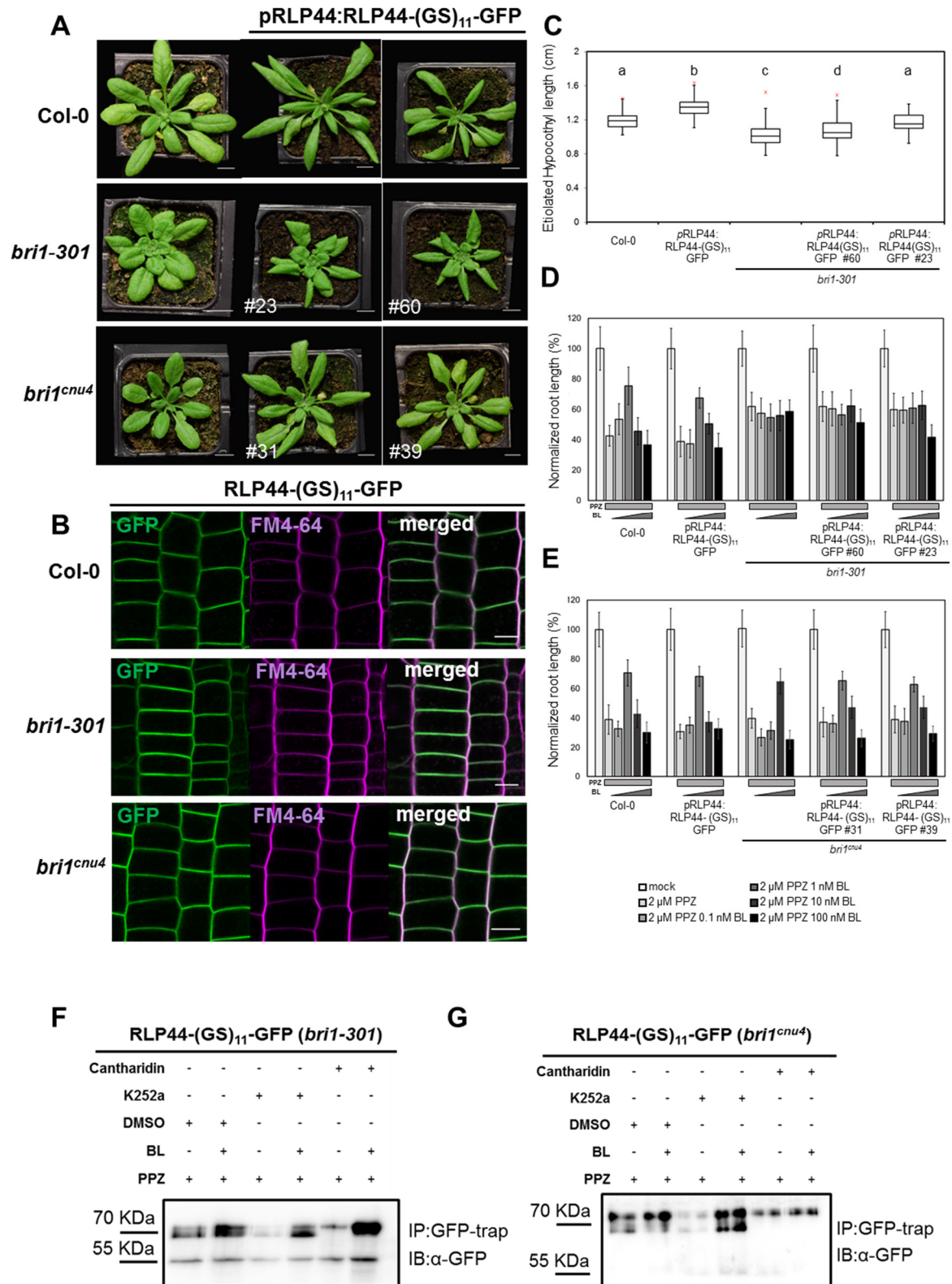


Figure 16. RLP44-(GS)₁₁-GFP is phosphorylated in *bri1-301* and *bri1^{cnu4}* backgrounds. A. RLP44-(GS)₁₁-GFP rescues *bri1^{cnu4}* but not *bri1-301* macroscopic phenotype of 21-d-old plants. Bars=1 cm. **B.** RLP44-(GS)₁₁-GFP localization in *bri1-301* and *bri1^{cnu4}* bars= 50 μm **C.** RLP44-(GS)₁₁-GFP rescues *bri1-301* hypocotyl length. Box-plots represent mean hypocotyl length. Letters indicated significant differences (p<0.001) determined by Tukey's test (ANOVA) (n=35-72). **D** and **E.** RLP44-(GS)₁₁-GFP restores BL response of *bri1^{cnu4}* but not *bri1-301*. Bars represent normalized response in root length to depletion of and exogenous addition of brassinosteroids ±SD (n=25-43). **F** and **G.** RLP44-(GS)₁₁-GFP is phosphorylated in *bri1^{cnu4}* and *bri1-301*. IB= Immunoprecipitation. IB=Immunoblotting with anti-GFP.

pRLP44:RLP44-(GS)₁₁-GFP would rescue the *bri1-301* hypocotyl length growth. Hypocotyls of pRLP44:RLP44-(GS)₁₁-GFP (Col-0) etiolated seedlings were longer than Col-0 and *bri1-301*. Moreover, dark-grown hypocotyls of two pRLP44:RLP44-(GS)₁₁-GFP (*bri1-301*) independent lines were significantly different to the mutant and, the line #23 even rescued to wild-type levels the length of dark-grown hypocotyls, supporting the observation that pRLP44:RLP44-(GS)₁₁-GFP might be able to rescue some aspects of the *bri1-301* phenotype (Figure 16.C). Previous reports showed that *bri1-301* is responding to BL only at high concentrations (W. Xu et al., 2008) very similar to *bri1^{cnu1}* (Wolf et al., 2012) whereas *bri1^{cnu4}* is only mildly insensitive to BL (Holzwardt et al., In revision). To test whether the presence of pRLP44:RLP44-(GS)₁₁-GFP could rescue the response to BL, root length of the different phenotypes was measured upon increasing BL concentration in the ½ MS plates. To avoid the variability on the measurements produced by the presence of endogenous BL, its synthesis has been blocked by applying 2 µM PPZ to the media together with the different BL concentrations (from 0.1 nM to 100 nM).

Upon blocking of the synthesis of endogenous BL by using PPZ, Col-0 seedlings were able to restore normal root length applying 1 nM BL (Figure 16.D). pRLP44:RLP44-(GS)₁₁-GFP (Col-0) plants behaved similarly to Col-0, in line with previous results described for the overexpression line RLP44ox (Wolf et al., 2014). On the other hand, *bri1^{cnu4}* did not restore normal root growth until exogenous application of 10 nM BL showing that even if the mutant was sensitive to BL, it was delayed when compared to WT. In contrast, in my experiments *bri1-301* was insensitive to BL (Figure 16.E). Interestingly, the expression of pRLP44:RLP44-(GS)₁₁-GFP in *bri1^{cnu4}* was able to restore the sensitivity to BL to WT levels, but not in the *bri1-301* lines, which remained insensitive to BL (Figure 16.D). Notably, the two hyposensitive mutants differ in the point mutation's localization. In the case of *bri1^{cnu4}* is in the extracellular domain of BRI1 and is thus unlikely to affect the kinase activity of the protein (Holzwardt et al., In revision), whereas in *bri1-301* is in the kinase domain of BRI1 (Xu et al., 2008). Thus suggest that RLP44 is only able to rescue phenotypes of BRI1 mutants where the kinase domain is functional. This result is in line with the incapacity of p35S:RLP44-GFP overexpression line to rescue *bri1^{cnu1}* (Wolf et al., 2014) another different hyposensitive mutant in the kinase domain of BRI1. Interestingly, even though pRLP44:RLP44-(GS)₁₁-GFP was not able to rescue the BL response of *bri1-301*, there was a rescue of the hypocotyl length as well as a mild rescue of the rosette phenotype. This observation could indicate a separate role of the RLP44-BRI1 interaction in cell expansion on different tissues.

In consequence, it was interesting to test if the absence of BRI1 in *bri1^{cnu4}* and *bri1-301* lines could influence pRLP44:RLP44-(GS)₁₁-GFP phosphorylation by studying the change on band pattern as previously described. Interestingly, after performing the experiment with kinase and phosphatase inhibitors, it was observed that RLP44 was still phosphorylated in both *bri1-301* and *bri1^{cnu4}* backgrounds (Figure 16.F and Figure 16.G). When the two bands upon BL treatment were compared, an enrichment of RLP44 phosphorylated form was observed in both backgrounds. Nevertheless, this enrichment seemed to be reduced in *bri1-301* when compared to *bri1^{cnu4}* (Figure 16.F and 16.G). However, even if RLP44 seems to be less phosphorylated in *bri1-301*, upon treatment with Cantharidin and BL, there is still a strong enrichment of RLP44 phosphorylated form (Figure 16.F and 16.G).

All together, we hypothesized that BRI1 might be important but other kinases might be involved in the phosphorylation of RLP44. Furthermore, we cannot rule out whether the two close functional homologs

BRI1-LIKE1 (BRL1) and BRI1-LIKE3 (BRL3) of BRI1, expressed exclusively in the vascular tissue (Caño-Delgado et al., 2004), could also participate in RLP44 activation. Moreover, it is possible that BAK1/SERK3 or its redundant homologs SOMATIC EMBRYGENESIS RECEPTOR KINASES 1 and 4 (SERK1/SERK4) (Gou et al., 2012) phosphorylate RLP44 as well.

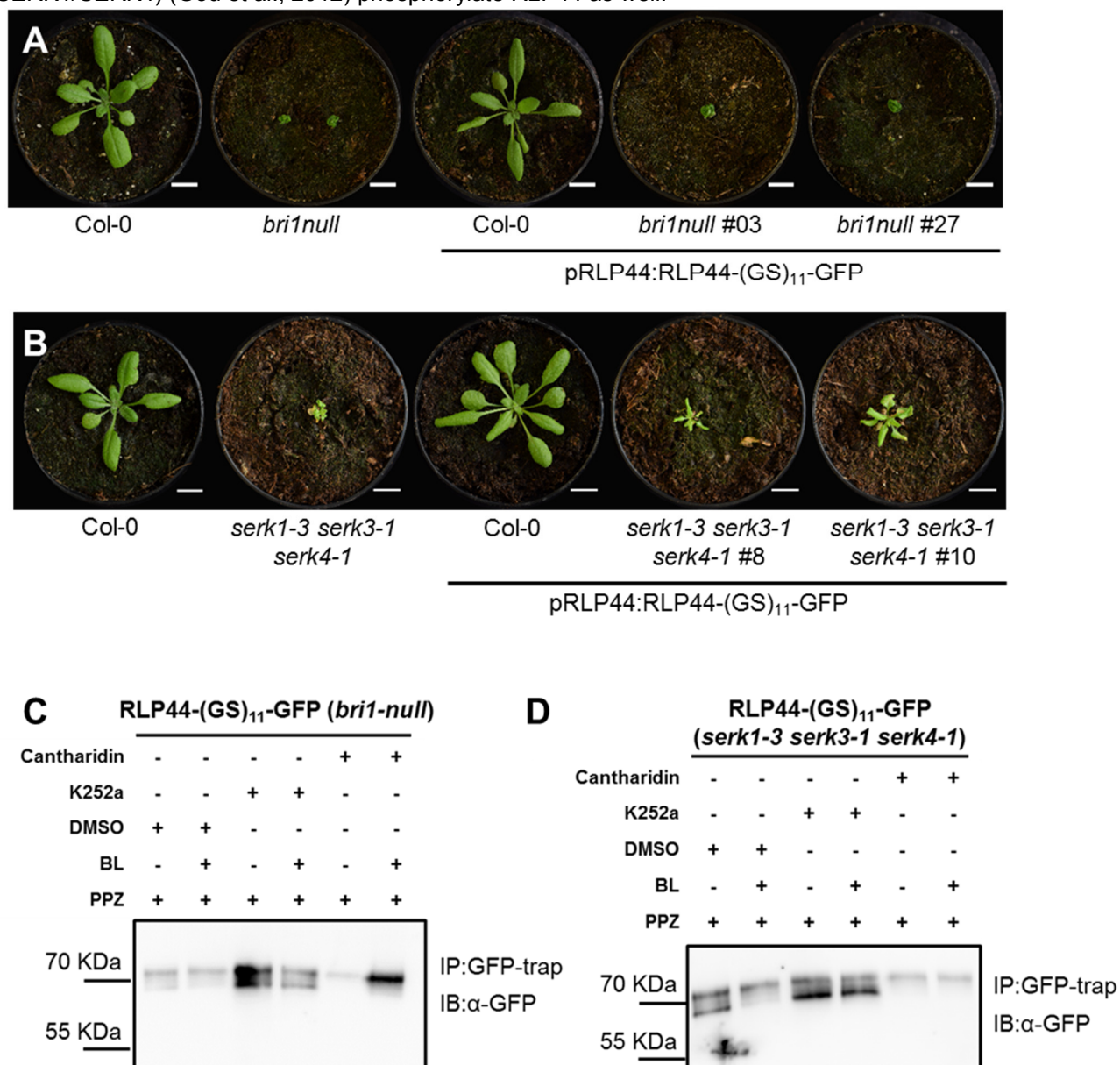


Figure 17. RLP44-(GS)₁₁-GFP is phosphorylated in *bri1-null* and *serk1-3 serk3-1 serk4-1* backgrounds. A and B. RLP44-(GS)₁₁-GFP cannot rescue the macroscopic phenotype of 21-d-old *bri1-null* and *serk1-3 serk3-1 serk4-1* plants. Bars=1 cm. **C and D.** RLP44-(GS)₁₁-GFP is phosphorylated in *bri1-null* and *serk1-3 serk3-1 serk4-1*. BL (Brassinolide); PPZ (propiconazole, a BR synthesis inhibitor); Cantharidin (Phosphatase Inhibitor); K252a (Kinase inhibitor) or DMSO. IB=Immunoprecipitation against GFP. IB=Immunoblotting with anti-GFP.

To unravel the contribution on RLP44 phosphorylation by BRI1 and/or other receptor-like kinase involved in BR signaling, homozygous lines of pRLP44:RLP44-(GS)₁₁-GFP in the *bri1-null* and *serk1-3 serk3-1 serk4-1* backgrounds were created. The study of the macroscopic phenotype of two independent mutant lines revealed that pRLP44:RLP44-(GS)₁₁-GFP was not able to rescue any of the characteristic dwarf phenotypes of *bri1-null* (Figure 17.A) but it was able to partially rescue the

macroscopic *serk1-3 ser3-1 serk4-1* phenotype (Figure 17.B, Supplemental Figure 6.A). Therefore, the phosphorylation of RLP44 was studied in those backgrounds following the approach previously described. After immunopurification and immunodetection using GFP antibodies, the double band of RLP44 was still observed in both mutants backgrounds in the sample treated with PPZ and DMSO meaning that RLP44 was still phosphorylated even if the BR signaling-related kinases BRI1 or SERK1 SERK3/BAK1 SERK4 were not present (Figure 17.C, Figure 17.D). In addition, in both cases, treatment with BL as able to rescue the partial block of phosphorylation produced by the K252a, a kinase inhibitor. Furthermore, BL stabilized the phosphorylated status upon inhibition of phosphatases by Cantharidin (Figure 17.C, Figure 17.D).

All data together suggest that RLP44 might be phosphorylated by more than one kinase. Presumably, BRI1 and its homologs together with the SERK kinases could phosphorylate RLP44 independently of the other ones. We cannot exclude that other kinases could phosphorylate RLP44 but those should be BL dependent since is the application of BL that modifies phosphorylation status in the different mutant backgrounds. However, it could be still possible that any of these kinases is involved and changes in RLP44 phosphorylation is an indirect effect of the mutations.

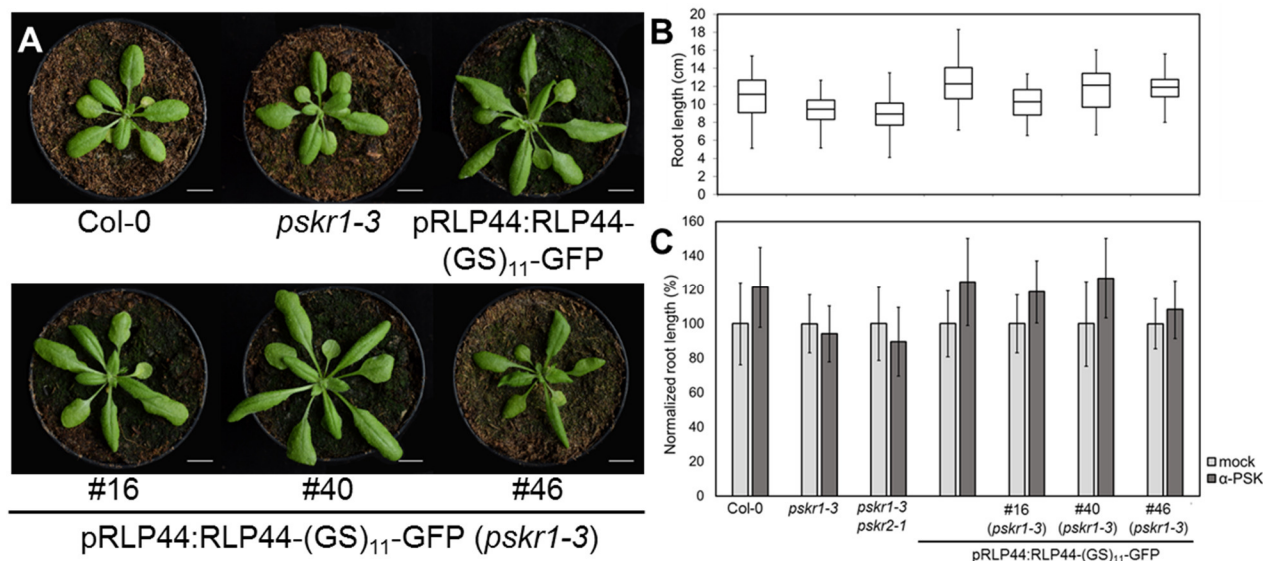
2.13. RLP44 phosphorylation is PSKR1 independent

RLP44 appeared to be involved in PSK signaling-dependent root growth promotion independently of its phosphorylation status. Nevertheless, it cannot be excluded that changes on RLP44 phosphorylation by other kinases as SERKs or BRI1 could have an impact on the functionality of the protein in the PSK signaling pathway. Therefore, we decided to study the effect of RLP44 phosphorylation in PSK mediated root growth.

To gain insight into the role of RLP44 phosphorylation by PSKR1, a *pskr1-3* mutant line (Kutschmar et al., 2009) expressing pRLP44:RLP44-(GS)₁₁-GFP was created. After genotyping, three homozygous F3 lines were selected and macroscopic phenotype was studied. The mutant *pskr1-3* is characterized by having a smaller rosette size compared to Col-0 (Hartmann et al., 2013). By contrast, pRLP44:RLP44-(GS)₁₁-GFP presents a phenotype characterized by longer petioles and leaves similar to the described phenotype of RLP44ox and in line with the BRI1ox phenotype (Wolf et al., 2014; Wang et al., 2001). Interestingly, pRLP44:RLP44-(GS)₁₁-GFP was able to rescue *pskr1-3* phenotype (Figure 18.A and 18.B). In addition, response to PSK in terms of root growth promotion was tested. Wild-type plants were able to increase root length when they grow for 6 days in medium containing 1 μ M PSK. In contrast, *pskr1-3* mutant as well as the double mutant *pskr1-3 pskr2-1* lost the capacity to respond to PSK whereas overexpression of RLP44 led to an increase of root length stronger than in Col-0 (Figure 18.C). Interestingly, *pskr1-3* lines expressing pRLP44:RLP44-(GS)₁₁-GFP rescued the response to PSK comparable to WT levels (Figure 18.C).

These observations suggest that RLP44 could have a central role in Phytosulfokine signaling helping in propagating the downstream signal. It cannot be discarded that in the pRLP44:RLP44-(GS)₁₁-GFP (*pskr1-3*) lines PSKR2 receptor is still functional. Nevertheless, the phenotypic difference in terms of

root length between the single and the double PSKR mutant was not big (Figure 18.C), suggesting that the effect on the signaling pathway of PSKR2 might be minor in comparison to PSKR1 and in line with previous results (Kutschmar et al., 2009; Hartmann et al., 2013). However, expressing RLP44 might have positive effect on PSKR2 expression.



The similarities between BRI1 and PSKR1 made interesting to test if the lack of PSKR1 might have an impact on RLP44 phosphorylation status. After treatment with PPZ, Cantharidin, K-252A and BL as previously described, RLP44-(GS)₁₁-GFP from 6-days-old *pskr1-3* seedlings carrying pRLP44:RLP44-(GS)₁₁-GFP were immunopurified with GFP beads. By immunodetection with GFP antibody RLP44-(GS)₁₁-GFP band pattern was checked. Treatment alone with BL produced an enrichment of the slow-moving band (phosphorylated RLP44) whereas treatment with PPZ enriched the fast mobility band (non-phosphorylated RLP44) in the same manner as RLP44-(GS)₁₁-GFP in a Col-0 background (Figure 19.A, Figure 15.E and 15.F). Additionally, kinase inhibitor K252A produced a shift to the non-phosphorylated band and cantharidin to the phosphorylated one similarly to Col-0 version (Figure 19.A). Furthermore, application of 1 μM of PSK 3 or 1.5 hours before harvesting in the same manner as BL application had no visible effect on band pattern (Figure 19.A).

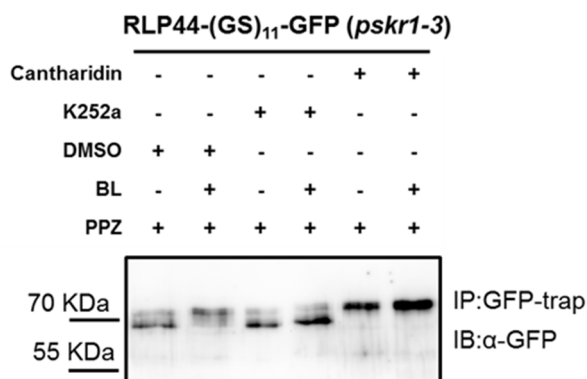


Figure 19. RLP44-(GS)₁₁-GFP is phosphorylated in *pskr1-3*. RLP44-(GS)₁₁-GFP is phosphorylated in *pskr1-3* a similar way to in Col-0 or *rlp44^{cnu2}* backgrounds. BL (Brassinolide); PPZ (propiconazole, a BR synthesis inhibitor); Cantharidin (Phosphatase Inhibitor); K252a (Kinase inhibitor) or DMSO. IB= Immunoprecipitation against GFP. IB=Immunoblotting with anti-GFP.

Phosphorylation status of RLP44 influences its function. Nevertheless, even if RLP44 seems to have a major role in PSK signaling, PSKR1 seemed not to have any effect on the phosphorylation of RLP44. In addition, changes on the phospho-residues from the RLP44 cytoplasmic domain did not influence in the interaction with PSKR1 or the response to PSK. On the other hand, modifications RLP44 phosphorylation was slightly modified in *bri1-null* and *serk1-3 serk3-1 serk4-1* backgrounds and RLP44^{pdead}-GFP was not able to interact with BRI1. Thus, we hypothesized that phosphorylation of RLP44 cytoplasmic domain might shift balance between its BR and PSK signaling promoting functions.

2.14. (GS)₁₁-GFP linker is presumably hyperphosphorylated

As previously mentioned, we made use of the GreenGate cloning system (Lampropoulos et al., 2013) to create a RLP44 version under its own promoter that turned out to be useful for the study of phosphorylation of RLP44. Therefore, to also try to detect differences in phospho-status, a phospho-mimic, a phospho-dead and single phospho-mutants RLP44 versions were created with the same cloning system (Table 4). Adult *cnu2* plants were transformed and after selection for single insertion lines, macroscopic phenotype together with the subcellular localization of the different constructs were studied on a T3 generation. The analysis of the macroscopic phenotype, showed that RLP44-(GS)₁₁-GFP and RLP44^{pmimic}-(GS)₁₁-GFP were able to rescue the *cnu2* phenotype in the same way the ubiquitously expressed lines did (Figure 20.A, Figure 2.B). Nevertheless, RLP44^{pdead}-(GS)₁₁-GFP was able as well to rescue the *cnu2* phenotype in contraposition with previous results. The subcellular localization of pRLP44:RLP44^{pdead}-(GS)₁₁-GFP showed as well a discrepancy with the localization displayed from RLP44^{pdead}-GFP (Figure 20.B, Figure 3.A). Specifically, while RLP44^{pdead}-GFP displayed an intracellular localization, RLP44^{pdead}-(GS)₁₁-GFP revealed preferential plasma membrane localization, similar to pRLP44:RLP44-(GS)₁₁-GFP and pRLP44:RLP44^{pmimic}-(GS)₁₁-GFP (Figure 20.B). In fact, the pRLP44:RLP44-(GS)₁₁-GFP already showed less intracellular localization that RLP44-GFP (Figure 20.B, Figure 4.A).

Table 4. (GS)₁₁-GFP linker constructs used for the study of RLP44 phosphorylation.



Name of the construct	Aminoacid change	Modification
pRLP44:RLP44-(GS) ₁₁ -GFP	---	WT version
pRLP44:RLP44 ^{pmimic} -(GS) ₁₁ -GFP	Four phospho-residues by Glu	Phospho-mimic version
pRLP44:RLP44 ^{pdead} -(GS) ₁₁ -GFP	Four phospho-residues by Ala or Pe	Phospho-dead version

Since the (GS)₁₁-GFP linker used for the GreenGate constructs was enriched in serine (Figure 20.D), there was the possibility that the phosphorylation of those serines would be useful to detect the different status of RLP44 phosphorylation by they could also mask the effect on the RLP44 phospho-residues mutations. Therefore, 7-days-old seedlings were used to extract and immunopurified the WT-,

Therefore, the (GS)₁₁-GFP linker is a useful tool to study the regulation of RLP44 phosphorylation but the phosphorylation of the additional linker masks modifications of RLP44 phospho-residues. Thus, the effect of these modifications in RLP44 phosphorylation should be study using a different non-phosphorylated linker as GAGA-GFP.

2.15. Phosphorylation of Ser-270 and Tyr-274 have a major effect on RLP44 function

Previous attempts to identify the crucial phospho-residues were unsuccessful as *cnu2* plants transformed with Gateway constructs showed a mislocalization of RLP44 (Figure 13.A). By using the (GS)₁₁-GFP linker in the constructs generated by GreenGate system, hyper phosphorylated versions of single-mutated RLP44 were created with which it was not possible to properly identify the crucial phospho-residues in RLP44 function (Figure 20). Therefore, to avoid the phosphorylation of the linker, the (GS)₁₁-GFP module was replaced by a new module containing a shorter and non-phosphorylated linker (GAGA-GFP) and it was used for the generation of new GreenGate constructs (Table 3).

Table 3. GAGA-GFP linker constructs used for the study of the contribution of single phospho-residues for the function of RLP44.



Name of the Construct	Aminoacid change	Modification
pRLP44:RLP44-GAGA-GFP	-	WT version
pRLP44:RLP44 ^{pmimic} -GAGA-GFP	Four residues by Glu	Phospho-mimic version
pRLP44:RLP44 ^{pdead} -GAGA-GFP	Four residues by Ala or Phe	Phospho-dead version
pRLP44:RLP44_ASSY-GAGA-GFP	Thr-256 by Ala	Single phospho-dead
pRLP44:RLP44_TASY-GAGA-GFP	Ser-268 by Ala	Single phospho-dead
pRLP44:RLP44_TSAY-GAGA-GFP	Ser-270 by Ala	Single phospho-dead
pRLP44:RLP44_TSSF-GAGA-GFP	Tyr-274 by Phe	Single phospho-dead

Adult *cnu2* plants were transformed with the new constructs depicted in Table 3 and the macroscopic phenotype of, at least, 30 plants from the T1 for each of the constructs, was directly analyzed. Phenotypic analysis was focused on the restoration or not of PMElox phenotype: organ convolution and fusion and reduction of fertility (Wolf et al., 2012). Interestingly, the new GAGA-GFP pRLP44:RLP44-GAGA-GFP, pRLP44:RLP44^{pmimic}-GAGA-GFP and pRLP44:RLP44^{pdead}-GAGA-GFP phenocopied the lines created with the Gateway versions under a ubiquitous promoter (Figure 21.A, Figure 2.B). Furthermore, only pRLP44:RLP44_TASY-GAGA-GFP was able to restore the PMElox phenotype in 90% of the T1 *cnu2* plants after transformation whereas wild-type construct only restore the phenotype in 50% of the cases (Figure 21.A), meaning that Ser-268 it is not crucial for the function of RLP44. In the other hand, absence of phosphorylation in Thr-256, Ser-270 and Tyr-274 might prevent RLP44 to be functional.

In addition, the localization of the fusion protein in T2 single insertion lines was checked to verify that this localization matches with previous observations and to ensure that the plasma membrane localization in the previous GreenGate constructs was due to the over phosphorylation of the (GS)₁₁-

GFP linker. Both RLP44-GAGA-GFP and RLP44^{pmimic}-GAGA-GFP rescued *cnu2* phenotype and had the PMElox root waving PMElox phenotype whereas RLP44^{pdead}-GAGA-GFP was not able to rescue the phenotype and it remained *cnu2*-like. These data were in line with the phenotype of the Gateway constructs in *cnu2* (Figure 2.B). In agreement with the phenotype observed in T1, only one of the single phospho-dead mutants, RLP44_TASY-GAGA-GFP, showed root waving PMElox phenotype. Lack of phosphorylation in Ser-270 and Tyr-274 did not rescue *cnu2* phenotype in the studied T2 lines. Unfortunately, none of the studied RLP44_ASSY-GAGA-GFP T2 lines were resistant to selective antibiotic, indicating either that the correspondent T1 lines were false positives or that the constructs in the T2 lines were silenced.

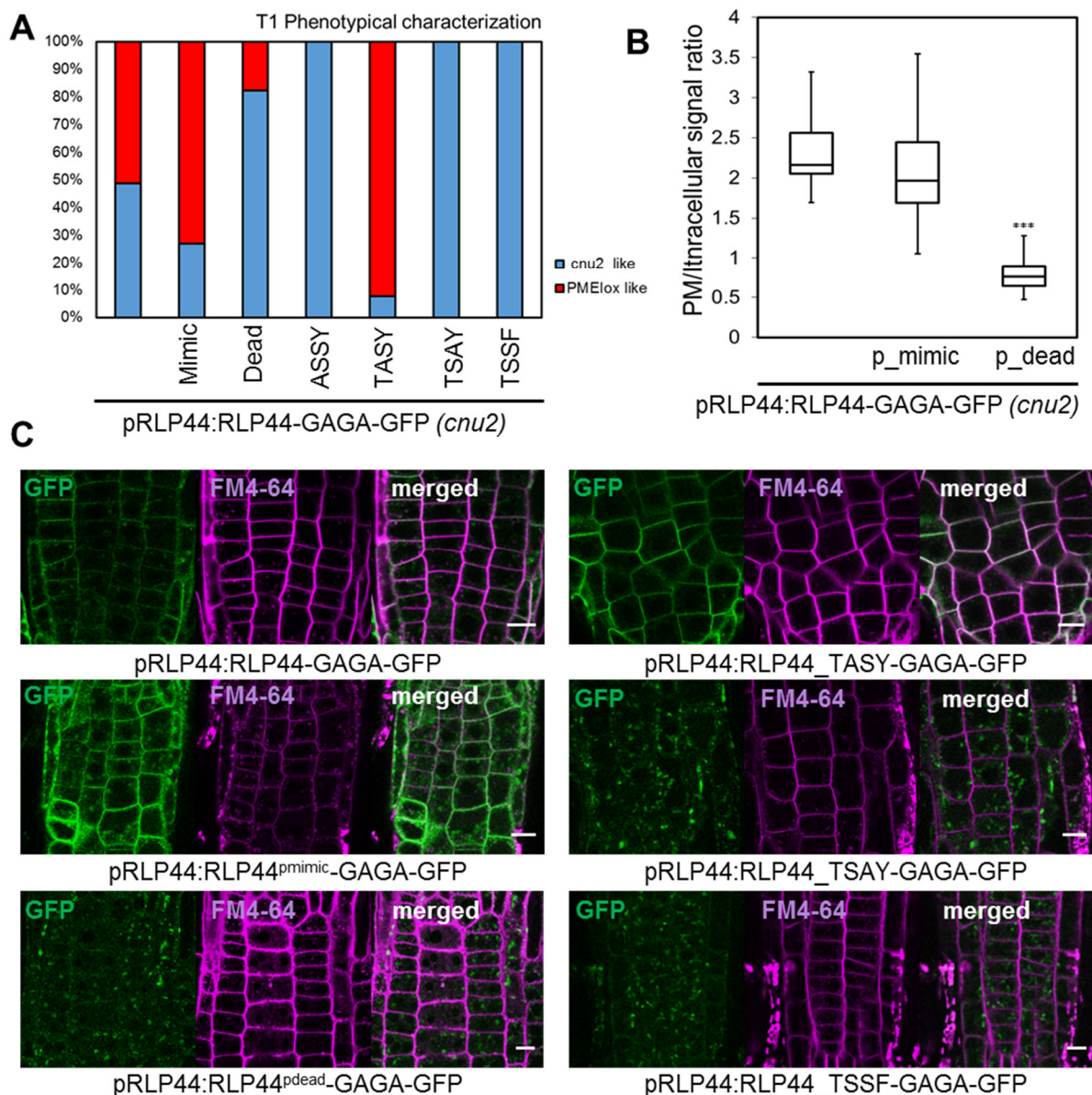


Figure 21. S270A and Y274F mutations produce non plasma membrane localization. A. Analysis of adult T1 *cnu2* plants transformed with GAGA-GFP shows that only mutation on S268A is able to reproduce PMElox phenotype. Graphic represents the percentage of T1 surviving plants with *cnu2* or PMElox phenotype (n=12-45). **B.** Analysis of single insertion T2 lines indicate a strong reduction of the GFP localization of RLP44^{pdead}-GAGA-GFP. Box-plot quantifies ratio of the mean value of the GFP fluorescence in the PM and intracellular. Asterisk indicate results significant differences p<0.001(***) determined by Tukey's test after a two-way ANOVA. (n=20-28). **C.** Representative image of intracellular localization in 6-d-old seedlings after 10 of staining with the endocytic tracer FM4-64. Bars= 50 μm.

Analysis of the subcellular localization showed PM localization and intracellular labeling of RLP44-GAGA-GFP (Figure 21.C) whereas vesicular localization was less abundant than in RLP44-GFP (*gnu2*) (Figure 3.A). RLP44^{pmimic}-GAGA-GFP also showed PM localization together with some vesicular signaling (Figure 21.C). However, RLP44^{pmimic}-GAGA-GFP did not show an increase of the PM/intracellular signaling ratio compared to RLP44-GAGA-GFP, contrary to the data observed for RLP44-GFP and RLP44^{pmimic}-GFP (Figure 21 .B, 21.C and Figure 3.B). On the other hand, RLP44^{pdead}-GAGA-GFP showed an increase of intracellular signal resulting in a reduction of the PM/intracellular signaling ratio compared to the WT and the phospho-mimic versions (Figure 21.B, 21.C). These data are in line with the previous observations in the p35S-driven lines and reinforced the idea that the nature of the -(SG)₁₁ linker affected the functionality and localization of RLP44.

Moreover, subcellular localization of the single phospho-dead single insertion lines was analyzed. RLP44_TASY-GAGA-GFP, in agreement with its capacity to restore PMElox phenotype, also showed a predominant PM localization (Figure 21.C). Interestingly, neither RLP44_TASY-GAGA-GFP nor RLP44_TSSF-GAGA-GFP showed a wild-type-like subcellular localization. RLP44_TASY-GAGA-GFP was localized predominantly in vesicles with strongly reduced PM signal (Figure 21.C). RLP44_TSSF-GAGA-GFP showed what seem to be ER localization without signal in vesicles or PM (Figure 21.C).

These data suggest that Ser-270 could be determinant for the role of RLP44 at the PM Tyr-274 could be needed for proper folding at the ER or the export of the protein. On the other hand, lack of phosphorylation in Ser-268 might inhibit RLP44 PM localization and therefore have also a determinant and opposite role to Ser-270 in RLP44 function.

2.16. RLP44 phosphorylation influences the control of vascular fate by BL and PSK signaling

Arabidopsis thaliana primary root presents in the central axis of the vascular tissue three metaxylem cells together with two peripheral protoxylem cells (De Rybel et al., 2015). Holzward et al., (In revision) showed that *rlp44^{gnu2}* presents an increased number of metaxylem cells compared to WT. This increase is even more pronounced in *bri1-null* mutants (Holzward et al., In revision). These findings suggest that RLP44 and BRI1 are needed to control the number of xylem cells. Interestingly, application of external PSK, perceived by PSKR1, rescued *rlp44^{gnu2}* xylem phenotype and, in addition, PSKR1 mutants also have an increased xylem cell number. Thus, RLP44 might balance PSK and BR signaling to control xylem differentiation during vascular development.

To gain insight into the mechanism of the balancing of PSK and BL signaling pathways by RLP44, we investigated whether phosphorylation of RLP44 might play a role in this particular function of RLP44, therefore homozygous lines expressing RLP44-GFP, RLP44^{pmimic}-GFP and RLP44^{pdead}-GFP in a *bri1-null* background were created. Macroscopically, none of the RLP44 constructs were able to restore the dwarf *bri1-null* phenotype (Figure 9.B). Afterwards, vascular development was studied visualizing the lignified secondary cell walls stained with fuchsin. Fully developed vascular tissue of Col-0 shows three metaxylem cells between two protoxylem cells making a total of five xylem cells (De Rybel et al., 2015)(Figure 22.A). Nevertheless, 20% of the Col-0 plants imaged displayed four metaxylem cells

(Figure 22.B and 22.C). As in Holzward et al., (In revision), *bri1-null* mutant typically displayed six-xylem cell in 50% of the cases (n=28), similar to *rlp44^{cnu2}* and distinguishable from Col-0 with only 20% (n=26) of cases (Figure 22.B and 22.C). RLP44-GFP was able to partially rescue the phenotype reducing the six-xylem cells event to 20% (n=26) and suggesting the effect of RLP44 in the control of vascular

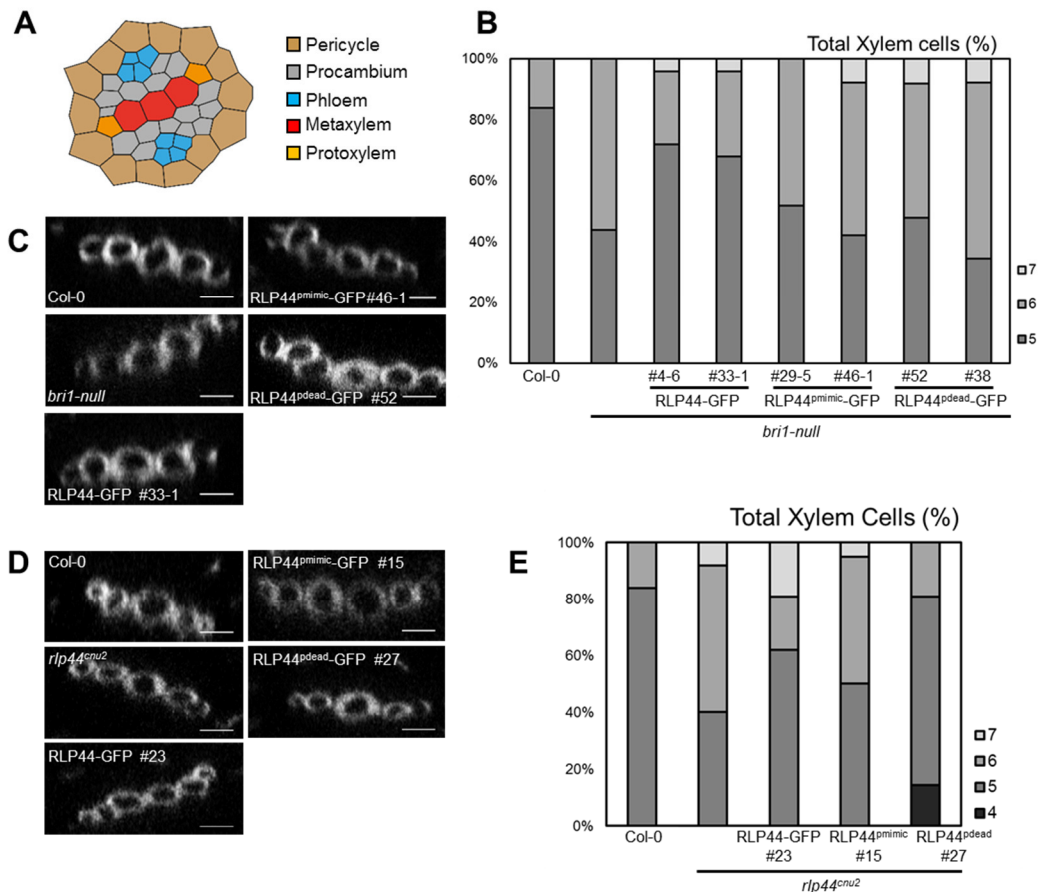


Figure 22. RLP44-GFP restores *bri1-null* and *rlp44^{cnu2}* xylem phenotype independently of phosphorylation. **A.** Schematic representation of the *Arabidopsis thaliana* stele. **B.** Bars represent the quantification of the frequency with the indicated number of metaxylem cells in *bri1-null* show the rescue exerted by the expression of RLP44-GFP (n=25-26). **C** and **D.** Representative orthogonal view of confocal stacks from studied genotypes used for the quantification of xylem cell numbers below the hypocotyl junction in 6-d-old *Arabidopsis* roots Bars=5 μ m. **E.** RLP44^{pdead}-GFP might rescue the *rlp44^{cnu2}* xylem phenotype. Bars indicate the frequency of indicated number of metaxylem cells in *rlp44^{cnu2}* mutant expressing the RLP44-GFP, RLP44^{pmimic}-GFP and RLP44^{pdead}-GFP (n=24-27).

development independent of BRI1 (Figure 22.B and 22.C). On the other hand, neither RLP44^{pmimic}-GFP nor RLP44^{pdead}-GFP were phenotypically distinguishable from *bri1-null* displaying six xylem cells in 50% of the cases (Figure 22.B and 22.C). Having in mind that RLP44ox in Col-0 have the same phenotype as *bri1-null* (Supplemental Figure 7.A and 7.B) and that RLP44^{pmimic}-GFP showed for other phenotypic analysis a stronger effect than RLP44-GFP (Figure 3.B, Supplemental Figure 2), it might be possible that RLP44^{pmimic}-GFP surpass the rescue of *bri1-null* and produce an RLP44ox phenotype. Strikingly, RLP44^{pdead}-GFP, showed a similar phenotype to *bri1-null* but also RLP44^{pmimic}-GFP that it could mean that either RLP44^{pdead}-GFP is not functional or it is as functional as the mimic version, maybe by the presence of the endogenous RLP44 in the lines. In addition, it could be possible that RLP44 might act with the BRI1 homologous BRL1 and BRL3 at the vascular level as (Caño-Delgado et al., 2004). Thus, this study should be also repeated in a triple *bri1-null bri1 bri3* background.

Therefore, it was interesting to study the vascular development by visualizing lignified secondary cell walls of RLP44-GFP, RLP44^{pmimic}-GFP and RLP44^{pdead}-GFP in *rlp44^{cnu2}* mutant background. Col-0, as previously described, showed five xylem cells (two protoxylem and three metaxylem) in around 85% (n=25) of the samples whereas *rlp44^{cnu2}* displayed five xylem cells only in 40%. Conversely, *rlp44^{cnu2}* had six xylem cells in 50% (n=25) of the samples and seven xylem cells in another 10% (Figure 22.D and 22.E). It is interesting to point out that the mutant and the overexpression line showed a similar phenotype, an increase the frequency of four or five metaxylem cells. 40% (n=25) of RLP44-GFP (*rlp44^{cnu2}*) and 45% (n=25) of RLP44^{pmimic}-GFP (*rlp44^{cnu2}*) showed an increase on xylem cell number, not as strong as *rlp44^{cnu2}* (60%) (Figure 22.D and 22.E). Having in mind that the *rlp44^{cnu2}* as well as the RLP44ox phenotype in terms of xylem cells is similar, two different scenarios are possible. On one hand, RLP44-GFP and RLP44^{pmimic}-GFP might not be able to fully rescue the *rlp44^{cnu2}* phenotype, and only slightly reduce the frequency of six xylem cells. On the other hand, the two constructs might be able to not only rescue *rlp44^{cnu2}* but also surpass WT signaling strength to partially behave as RLP44ox lines. Strikingly, RLP44^{pdead}-GFP fully restored the *rlp44^{cnu2}* xylem phenotype with around 60% of the cases with five xylem cells (Figure 22.D and 22.E). These results might indicate that RLP44^{pdead}-GFP, considered a non-functional version of RLP44, might still have an effect in the control of vascular development. Nevertheless, we cannot disentangle if the similar phenotype of RLP44^{pdead}-GFP (*bri1-null*) to RLP44^{mimic}-GFP (*bri1-null*) was simply the effect of strongly functional RLP44^{pdead}-GFP or it might be a dominant negative effect of RLP44^{pdead}-GFP over the endogenous RLP44 as it has been observed for the response to PSK in terms of root length (Figure 12.D). Therefore, the effect of RLP44 phosphorylation without the presence of both *bri1-null* and *rlp44^{cnu2}* was studied.

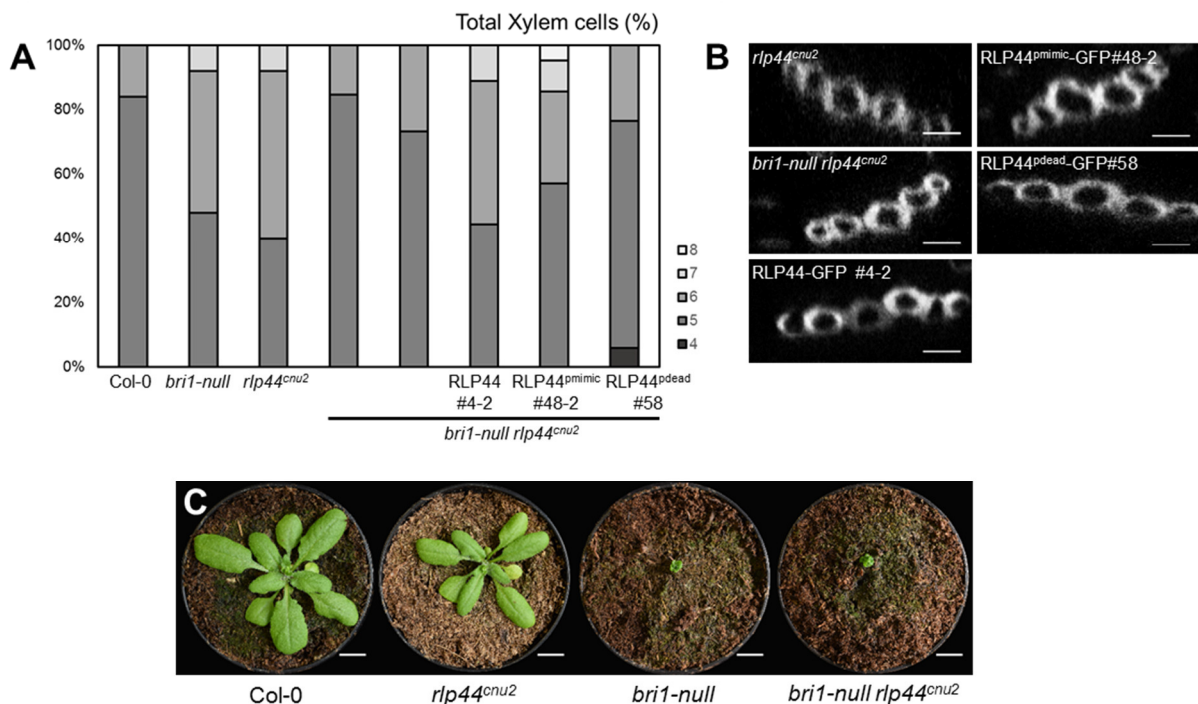


Figure 23. The *bri1-null rlp44^{cnu2}* phenotype might be the result of a compensatory response. A. *bri1-null rlp44^{cnu2}* rescue the xylem phenotype of the single mutants. Bars represent the quantification of the frequency with the indicated number of metaxylem cells in the double mutant *bri1-null rlp44^{cnu2}* background. (n=20-25) **B.** Representative orthogonal view of confocal stacks from studied genotypes used for the quantification of xylem cell numbers below the hypocotyl junction in 6-d-old *Arabidopsis* roots. Bars=5 μm **C.** *bri1-null rlp44^{cnu2}* does not rescue the dwarf *bri1-null* phenotype. Macroscopic phenotype of 21-d-old Col-0, *rlp44^{cnu2}*, *bri1-null*, *bri1-null rlp44^{cnu2}*. Bars=1 cm.

Homozygous lines expressing RLP44-GFP, RLP44^{pmimic}-GFP and RLP44^{pdead}-GFP in a *bri1-null rlp44^{cnu2}* background were created that were compared with Col-0, *bri1-null*, *rlp44^{cnu2}* and the double mutant *bri1-null rlp44^{cnu2}* by studying the vascular development of all of them. Identically to previous data, Col-0 showed five xylem cells in around 85% of the cases whereas *bri1-null* and *rlp44^{cnu2}* had a similar phenotype with an increase in total xylem cell number having six xylem cells in 40% of the cases and 7 xylem cells in 10% of the samples (Figure 23.A and 23.B). Holzwardt et al. (In revision) suggests that RLP44 and BRI1 participates together in the control of vascular cell fate. Unexpectedly, even if *bri1-null rlp44^{cnu2}* showed a macroscopic dwarf phenotype similar to *bri1-null* (Figure 23.C), in terms of total xylem cells, the double mutant was capable to restore the Col-0 phenotype (Figure 23.A and 23.B). Both RLP44-GFP and RLP44^{pmimic}-GFP complemented the lack of endogenous RLP44 restoring the increase on total xylem cell to *bri1-null* levels (Figure 23.A and 23.B). By contrast, RLP44^{pdead}-GFP xylem phenotype was still similar to Col-0 (Figure 23.A and 23.B). The unexpected results observed for the double mutant complicate the study of the contribution of phosphorylation in the control of vascular fate development. A compensatory response in the double mutant might explain the rescue of the xylem single phenotype and the differences in the different RLP44 lines thus, observations in *bri1-null rlp44^{cnu2}* might need to be complemented with the comparison and study of its transcriptome with the single mutants. In any case, these results suggest that phosphorylation could influence the control of vascular development exerted by RLP44.

To sum up, RLP44 is a conserved PM receptor which contains a particular cytoplasmic domain with four aminoacids predicted to be phosphorylated. In fact, phosphorylation of RLP44 cytoplasmic domain governs localization of the protein as well as the interaction with the BR co-receptors BRI1 and BAK1. Moreover, RLP44 phosphorylation is BL dependent and mutations on the different BR co-receptors alters RLP44 phosphorylation response. On the other hand, phosphorylation of RLP44 seems not to be important for the interaction with the PSK receptor PSKR1 and neither PSKR1 participates on the phosphorylation of the protein. Study of the contribution of each of the phospho-residues suggest that Ser-268 and Ser-270 might negative and positive, respectively, influence on RLP44 localization. In addition, phosphorylation might contribute to the control of vascular development by influencing on the interaction balance of RLP44 with BRI1 and PSKR1.

Chapter 2: RRE, a new saga of RLP44 suppressor mutants

2.17. RRE mutants are uncouple in the integration of RLP44 signal into the BL cascade

Cell wall composition and structure is continuously changing in order to allow cell growth. This makes essential the existence of accurate signaling cascades into the cell able to maintain cell wall in equilibrium (Wolf, Hématy, and Höfte 2012). In the last decade, several putative cell wall receptors have been described (Wolf 2017), but the downstream elements of the signal cascade are barely known. Among them, RLP44 presumably integrates information of changes in the cell wall into the BR signaling by interacting with BAK1 and BRI1 (Wolf et al., 2014, Holzward et al., In revision). However, the nature of RLP44 signaling upstream the interaction of BR receptors is still not characterized and RLP44 interacts as well with PSKR1 (Holzward et al., in revision) whose signaling cascade is unidentified. Thus, RLP44 signaling might suppose a more complex cascade with non-characterized components participating on the perception of cell wall changes and the integration into BL and PSK signaling.

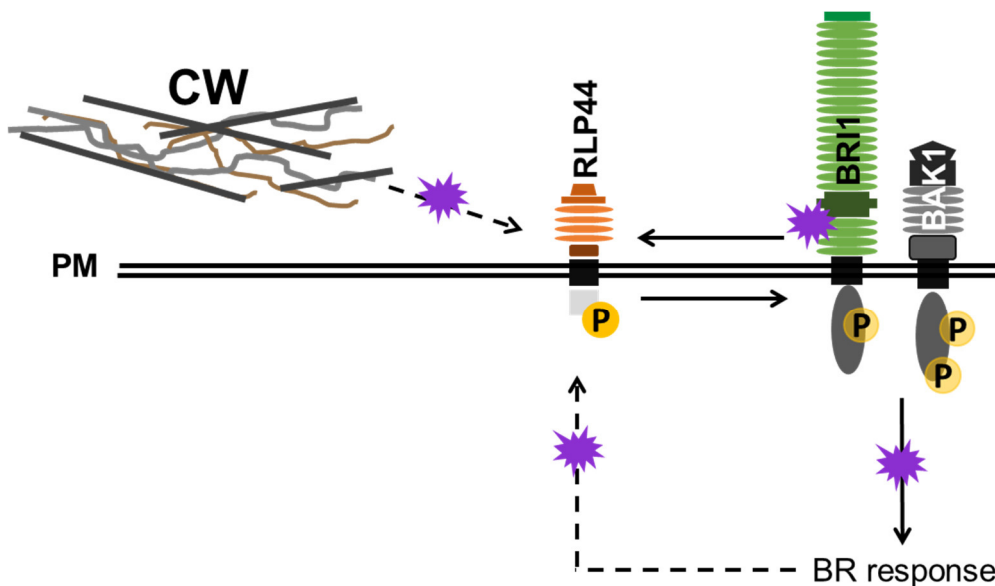


Figure 24. Diagram of expected mutations in the EMS suppressor screening. Mutations suppressing RLP44ox phenotype could occur in the cues labelled with purple balloons.

To try to identify new players in RLP44 signaling, RLP44:RFP (RLP44ox) seeds were mutagenized with EMS to identify suppressors of RLP44ox phenotype that is characterized for having longer petioles and leaves similar to BRI1ox. As depicted in Figure 24, mutations fulfilling this characteristic might occur in CW components that would affect the perception of the cue by RLP44, in the integration of the CW signal into BL receptors, in the BR cascade signaling or in putative BR response components that might respond to RLP44 perception. Having in mind a special interest for those mutations that specifically uncoupled the CW and BL signaling without affecting sensitivity to BL response, all mutations except the ones on the BR downstream signaling pathway were interested.

After seeds were mutagenized, plants were selected first based on their phenotype. Therefore, from 73 different M2 populations, all those plants that lost the RLP44ox phenotype returning into a WT-like phenotype were selected (Figure 25.A and 25.C) and named RRE (RLP44-RFP EMS mutants).

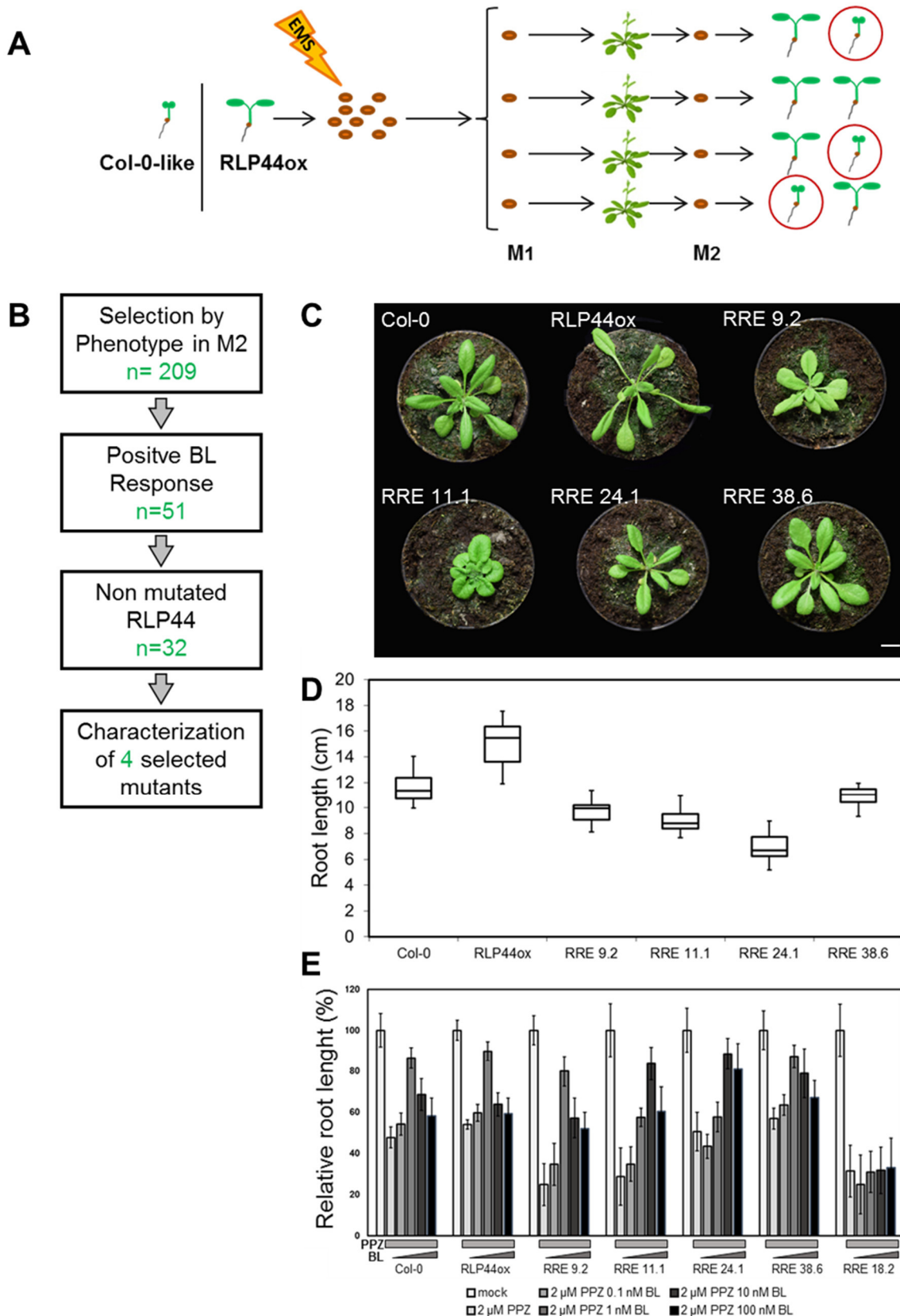


Figure 25. RRE mutants have no RLP44ox phenotype and are BL sensitive. **A.** Schematic representation of the M2 plants selected. **B.** Overview of steps followed for the selection of RRE mutants. In green, RRE mutants remained on each selection step. **C.** 21-d-old RRE plants lose RLP44ox macroscopic phenotype. Bars=1 cm. **D.** RRE mutants do not show characteristic increase on root length of RLP44 ox. Box-plot represent average of 6-d-old roots \pm SD ($n=14-23$). **E.** RRE mutants are BL sensitive. Bars represent normalized response in root length to depletion of and exogenous addition of brassinosteroids \pm SD ($n=14-27$).

Afterwards, the offspring of 209 selected plants without RLP44ox phenotype, were tested to their response to BL in terms of root length. To avoid the variability on the measurements produced by the presence of endogenous BL, its synthesis has been blocked by applying 2 μ M PPZ to the media together with the different BL concentrations (from 0.1 nM to 100 nM). Col-0 strongly reduced its root growth upon the application of 2 μ M PPZ alone. A progressive increase on BL concentration in the medium restored root growth having its peak at 1 nM BL and then progressively reduced again (Figure 25.E). RLP44ox behaved similarly to Col-0 but with increased resistance to PPZ. All mutants that were able to still respond to BL in the same manner as Col-0 were kept for further analysis (Figure 25.E). Subsequently, expression of the RLP44ox transgene was checked in all selected mutants by microscopy as well as its correct sequence by Sanger Sequencing. In addition, it was ensured that all selected suppressor mutants maintained a correct endogenous RLP44 sequence. At the end, out of the 209 initially selected plants, 32 were kept. Further studies were focused on four of those mutants: RRE 9.2, RRE 11.1, RRE 24.1 and RRE 38.6 (Figure 25.C).

Table 5. List of studied SNPs in the 4 selected RRE mutants

Chr.	Accession	Description	Discordant Chasity	Mutation Detected	Mutation In RLP44	Localization	Aminoacid modification
RRE 9.2							
3	At3g01130	Unkown	0.81	No	No	UTR	-
3	At3g04010	Unkown	0.65	No	No	UTR	-
3	At3g04490	Unkown	0.82	Yes C-T	No	Intron	N to N
3	At3g05280	Yip1 family protein	0.73	Yes C-T	No	Exon	R to R
3	At3g08900	RGP3, UDP-Arabinose	0.66	No	No	UTR	-
3	At3g09240	BSK9 Protein kinase	0.71	No	No	Exon	-
3	At3g14010	Hydroxyproline rich	0.67	Yes G-A	No	Exon	A to T
3	At3g01130	Unkown	0.81	No	No	UTR	-
RRE 11.1							
5	At5g05690	CPD	1	Yes G-A	No	Exon	K to K
5	At5g07225	Ring/U-box protein	0.95	No	No	Exon	-
5	At5g09890	Protein kinase	1	Yes G-A	No	Exon	K to K
RRE 24.1							
5	At5g02790	GSTL3 Glut. Transf.	0.75	No	No	Exon	-
5	At5g02880	UPL4 Ub-prot ligase	0.85	Yes G-A	No	Exon	G to E
5	At5g02910	F-box/RNI like	0.82	Yes G-A	No	Exon	E to K
5	At5g02950	Tudor superfamily	0.79	No	No	Exon	-
5	At5g04170	EF-hand family prot.	0.73	Yes C-T	No	Exon	S to S
5	At5g04480	BUP Glycosiltransf.	0.78	No	No	Exon	-
5	At5g05350	PLAC8	0.7	No	No	Exon	-
5	At5g05460	ENGase	0.71	No	No	Exon	-
RRE 38.6							
5	At5g04630	CYP77A9	0.93	Yes C-T	No	Exon	L to F
5	At5g07050	UMAMIT9	0.89	Yes G-A	No	Exon	G to S
5	At5g13580	ABCG16	0.91	Yes C-T	No	Exon	R to C
5	At5g13920	Unkown	1	No	No	Exon	-
5	At5g16210	Unkown	0.94	No	No	Exon	-

We hypothesized that mutations might be localized on the specific residues related with the interaction between BRI1 or BAK1 with RLP44. Therefore, to identify the point mutation of the four selected RRE mutants, the endogenous BAK1 and BRI1 were sequenced in the four RRE mutants. Interestingly, none of the four selected mutants showed a mutation in those genes even if some of the RRE mutants as RRE 11.1 presented a clear BR-deficiency phenotype (Figure 25.C). Thus, Next-generation EMS mutation mapping (NGM) (Austin et al., 2011) was used to localize the EMS induced point mutations in the RREs. Therefore, the four RRE mutants (in a Col-0 ecotype background) were crossed with *Landsberg erecta (Ler)* to generate a F2 mapping population. From the F2, all those plants carrying a mutant phenotype were selected, a pool of genomic DNA (gDNA) was generated, and it was sequenced by Illumina NGS platform. After the analysis of the NGM results, the likely chromosomal localization of the different mutations was determined and candidate SNPs were selected (Austin et al., 2010) (Table 4). Afterwards, the authenticity of the different selected SNPs was verified by Sanger sequencing in order to identify the causative mutation. At the end of this study, the putative SNPs were narrowed down without being able to disclose the one that generates the mutant phenotype (Table 5). Further experiments will be focus on determine the causative SNP by creating specific mutations by CRISPR genome editing tools in RLP44ox and compare the CRISPR phenotype with the suppressor ones. Once the causative mutation will be determined, further biochemistry and genetic analysis could be started to understand the relation of the RREs with RLP44.

2.18. RRE mutants present changes on the CW properties

In parallel to the genetic work, a characterization of different physiological and molecular aspects of the RRE mutants was started.

Since RLP44 is involved in perceiving changes of the cell wall, it was interesting to know if the mutation on the RRE could influence and/or modify the properties of their cell wall. It has been described that salt stress affects normal growth of plants and affects root growth and architecture (Galvan-Ampudia et al., 2011). This effect on plant growth is aggravated in mutants in the cell wall composition and organization (Benfey et al., 1993; Xu et al., 2008). Therefore, RRE seedlings were grown together with Col-0, RLP44ox and *cnu2* in $\frac{1}{2}$ MS medium with an increase from 0 to 150 mM NaCl and the effect of the different NaCl concentrations was analyzed by measuring the root length after 6 days under long-day growth conditions. Wolf et al., 2014 showed that the cell wall signaling mutant *rlp44^{cnu2}* was more sensitive to salt stress than WT. Col-0 experienced a gradual reduction of root growth correlated with an increase of salt concentration in the medium. In this study, *cnu2* mutant behaved similarly to Col-0 (Figure 26.B). This difference compared to *rlp44^{cnu2}* was expected since the *cnu2* mutant is in a PMElox background and the cell wall status is modified is already different to the Col-0, independently of the *cnu2* mutation. RLP44ox was more sensitive to salt concentrations than Col-0 and its growth was already blocked at 100 mM NaCl (Figure 26.B). RRE 9.2 and RRE 24.1 restored the Col-0 response to salt stress in agreement with its RLP44-suppressor nature (Figure 26.B). In contrast, RRE 11.1 and RRE 38.6 were sensitive to NaCl but while RRE 11.1 behaved similarly to RLP44ox, RRE 38.6 increased the salt sensitivity and its growth was inhibited already under 50 mM NaCl (Figure 26.B).

As some of the mutants presented growth deficiencies that could be related with changes in the CW status, it was decided to challenge it more specifically. Cellulose is the major component of plant CWs (Cosgrove 2005) and it is synthesized and exported to the extracellular matrix directly from the plasma membrane by the Cellulose Synthases (CESAs) (Arioli et al., 1998). Isoxaben alters the cell wall composition by specifically inhibiting the normal function of CESAs and their localization in the plasma membrane (Corio-Costet et al., 1991; Scheible et al., 2001; Desprez et al., 2002). Therefore, the effect of 10 mM Isoxaben on the RRE mutants' growth was tested by measuring the length of etiolated hypocotyl after 6 days in dark-growth conditions. Both Col-0 and RLP44ox were slightly sensitive to Isoxaben and they reduced its hypocotyl length when compared to mock conditions (Figure 26.A). RRE 24.1 experienced a depletion in hypocotyl growth similar to Col-0 and RLP44ox whereas RRE 9.2 and

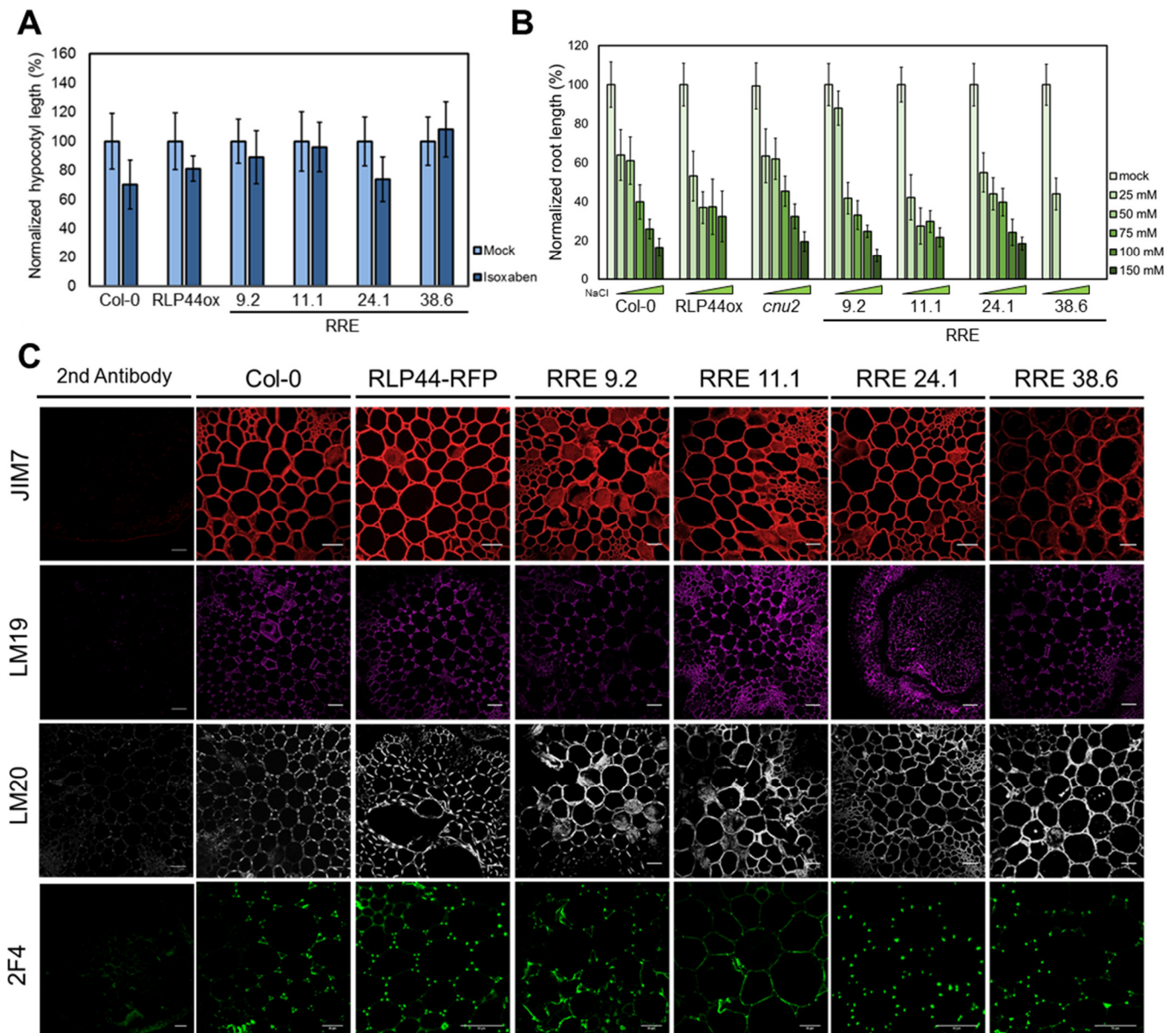


Figure 26. RRE 38.6 might present a perturbed CW. A. RRE 38.6 is resistant to the cell wall perturbation produced by Isoxaben. Bars represent normalized response in hypocotyl length to exogenous addition of Isoxaben \pm SD (n=25-32). **B.** RRE 38.6 is hypersensitive to salt stress. Bar represent normalized response in root length to progressive increase of salt in medium \pm SD (n=32-41). **C.** RRE 38.6 is enriched in methyl-esterified HG. Representative images of shoot cross-sections immunolabelled with antibodies recognized different HG epitopes. Bars= 50 μ m.

RRE 11.1 seemed insensitive to Isoxaben (Figure 26.A). Interestingly, RRE 38.6 was not only insensitive to Isoxaben but also showed a slightly better performance in hypocotyl growth when Isoxaben was present in the medium (Figure 26.A).

Since RLP44 is involved on sensing changes in balance between PECTIN METHYL ESTERASES (PMEs) and PECTIN METHYL ESTERASE INHIBITORS (PMEIs) (Wolf et al., 2014) my analysis was focused on possible modifications in pectins on the different RRE mutants compared to Col-0 and RLP44ox. Among all type of pectins, homogalacturonan (HG) is the most basic and well-known one (Ridley et al., 2001). HG, once synthesized in the Golgi, is exported to the extracellular region of plant cells in a highly methyl-esterified manner (Ridley et al., 2001) and there, the balance of activity between PMEs and PMEIs influences the methyl-esterification status of HG (Wolf et al., 2009). To unravel possible changes on HG methyl-esterification, we made use of a series of monoclonal antibodies that recognize different HG epitopes. JIM7 and LM20 are able to recognize partially methyl-esterified HG (Clausen et al., 2003; Verherbruggen et al., 2009), while LM19 recognizes preferentially un-esterified HG (Verherbruggen et al., 2009). 2F4, which recognize de-methyl-esterified HGs forming complexes through calcium bonds (Liners et al., 1992), was additionally used. RRE mutant shoot cross-sections were immunolabelled with the different HG antibodies and labelling pattern by fluorescence microscopy of the parenchyma (Miyashima et al., 2012) as studied. In this context, RLP44ox showed a stronger JIM7 and LM20 labelling when compares to Col-0. Furthermore, 2F4 labelling accumulated on the vertex of the typical 2F4 triangle-shape labelling produced in the point of contact between different pith cell walls (Figure 26.C). RRE 9.2 and RRE 24.1 showed a labelling for all the four antibodies with a very similar pattern as observed in RLP44ox (Figure 26.C). In contrast, RRE 11.1 differed from RLP44ox and Col-0 in the LM19 and 2F4 labelling. In both cases, labelling was expanded to all pith cell walls suggesting a change towards a more de-methyl esterified HG (Figure 26.C). In addition, RRE 38.6 showed an expanded LM20 labelling on the cell wall of pith cells (Figure 26.C), suggesting an enrichment of the methyl-esterified HG.

These data suggest that some of the characterized mutants, especially RRE 38.6, might modify the HG abundance or methyl-esterification when compared to RLP44ox by participating in the sensing of CW perturbation. Nevertheless, these changes might be up or downstream the perception process by RLP44 and therefore it is not possible to disentangle if RRE mutants participate on the integration of CW and BR cascades.

2.19. RRE mutants could uncouple the integration of CW and PSK signaling

RLP44 is not only able to interact with BRI1 but also with PSKR1 (Holzwardt et al., In revision). PSKR1 is the receptor for PSK activating a yet- unknown signaling pathway with a direct effect on plant and growth development (Matsubayashi et al., 2002; Hartmann et al., 2013). Therefore, the RLP44ox suppressor screening gave the opportunity to identify new players in the integration of the CW and PSK signaling.

To know if the different selected RRE mutants were affected only in the CW or also in the PSK signaling, the response to PSK of the different mutants was analyzed and compared to Col-0 and RLP44ox. RRE seedlings were grown for 6 days in agar medium supplied with either 1 μ M PSK or DMSO as mock control and the response was evaluated by measuring the changes in root length. PSK promoted root length in Col-0 and RLP44ox whereas the double mutant *pskr1-3 pskr2-1* was insensitive to the peptide (Figure 26.A). In the case of RRE mutants, PSK promoted the root growth of RRE 9.2 and RRE 11.1 similarly to RLP44ox (Figure 26.A). By contrast, RRE 24.1 and RRE 38.6 did not react to the presence of PSK (Figure 26.A) suggesting that some of the RRE mutants might disrupt the control that RLP44 exerts over the balance between BL and PSK signaling.

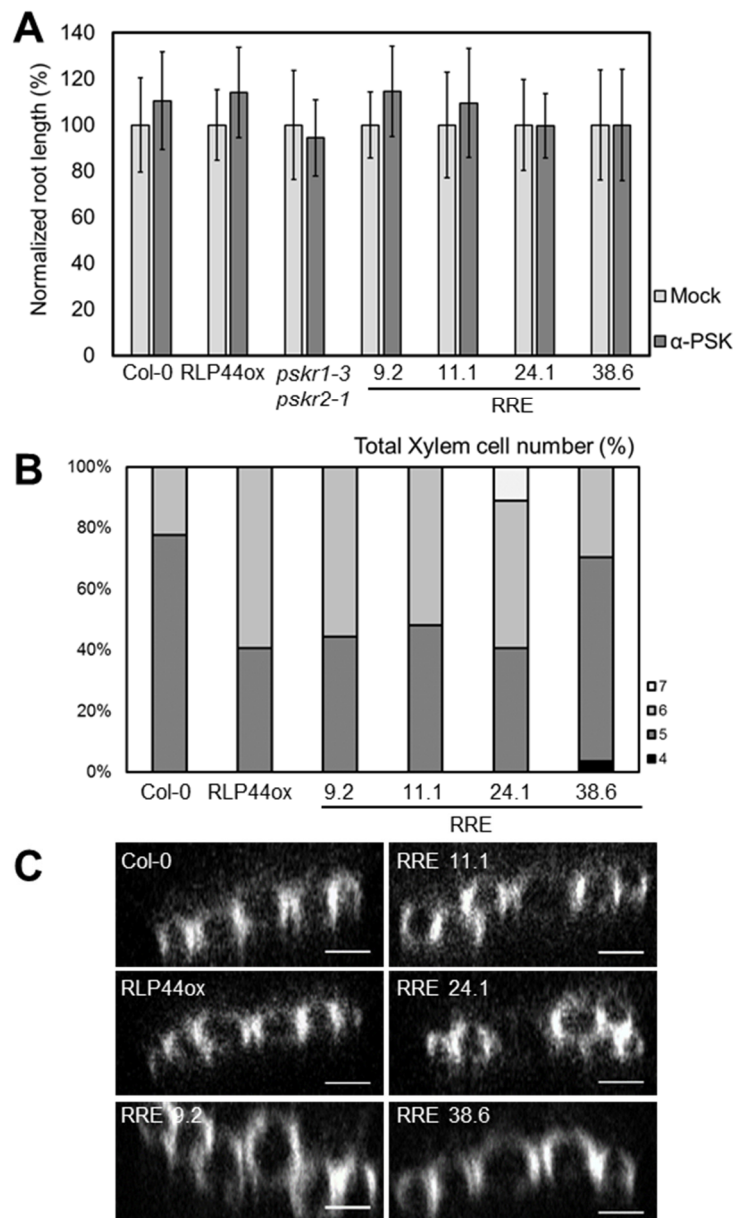


Figure 26. Mutations in RRE 24.1 and RRE 38.6 modifies PSK sensitivity and xylem phenotype to PSK. A. RRE 24.1 and RRE 38.6 are insensitive to PSK. Bars indicate normalized mean of the response in root length of 5-d-old seedlings treated with PSK \pm SD (n=43-51). **B.** RRE 24.1 intensify and RRE 38.6 rescue RLP44ox phenotype. Bars represent the quantification of the frequency with the indicated number of metaxylem cells in the RLP44ox background. (n=23-25) **C.** Representative orthogonal view of confocal stacks from studied genotypes used for the quantification of xylem cell numbers below the hypocotyl junction in 6-d-old *Arabidopsis* roots. Bars=5 μ m.

Intrigued by these results, we decided to investigate if the RRE mutants would affect the vascular phenotype of RLP44ox. Therefore, lignified secondary cell walls were visualized by staining with basic fuchsin 6 days-old seedlings. Col-0 presented developed root vasculature with five total xylem cells (three metaxylem and two protoxylem) in 85% (n=28) of the cases (Figure 26.B and 26.C). RLP44ox, as the rest of RLP44 overexpression lines, increased the cases where adult xylem contained six instead of five total xylem cells up to 60% (n=25) of the cases and therefore reducing the events with Col-0-like xylem phenotype (Figure 26.B and 26.C). RRE 9.2 and RRE 11.1 did not suppress RLP44ox xylem phenotype and they showed six total xylem cells in around 50-60% (n=25) of the cases studied (Figure 26.B and 26.C). Strikingly, RRE 24.1 and RRE 38.6, both insensitive to PSK, slightly modified the xylem phenotype. RRE 24.1 strengthened the RLP44ox phenotype by increasing by 10% (n=24) the cases with seven instead of five total xylem cells. By contrast, RRE 38.6 suppressed the RLP44ox phenotype reducing the cases with six total xylem cells and increasing up to 70% the samples where xylem consisted in five cells, similarly to Col-0 (Figure 26.B and 26.C).

These data might indicate that RRE 9.2 and RRE 11.1 might impair CW and BL signaling without affecting PSK signaling. Data also suggests that RRE 38.6 and RRE 24.1 could be downstream elements of PSK signaling with opposite effect on the integration of the RLP44 mediated signal.

To sum up, the RLP44ox suppressor screening has served to identify 32 mutants disturbing the integration of the CW into the BR signaling without altering the response to BL. Among those mutants, 4 has been further investigated to narrow down the localization of their mutation although more work is still needed to identify the causative one. In addition, the 4 mutants has been characterized in some aspects of CW perturbation, response to PSK and xylem phenotype. Interestingly, all mutants show divergent differences to what observed for RLP44ox that enhance their potential to understand the integration and monitoring of CW signals.

3. Discussion

3.1. RRE mutants suppose putative new player on the integration of CW signaling

RLP44 perceives cues from the cell wall and transduces the information to the cell via the interaction with the BR signaling pathway in a BL-independent manner (Wolf et al. 2014). At the beginning of this study, no other member of the RLP44 pathway was characterized. Therefore, it was interesting to narrow down candidates that could be part of this newly discovered cell wall signaling pathway by looking for mutants impaired on the integration of the CW and the BR pathway. For that purpose, RLP44-RFP EMS (RRE) mutants were selected from a suppressor screening in based on the loss of the RLP44ox phenotype (Figure 25.C) as well undisturbed BL sensitivity (Figure 25.E). In this way, we isolated mutants affecting the integration of CW signaling without modifying the BL cascade. The four RRE studied (RRE 9.2, RRE 11.1, RRE 24.1 and RRE 38.6) fulfill these premises, are not mutated in BRI1, BAK1 or both endogenous and transgene RLP44 and their causative mutation has been narrow down by Next Generation sequencing and analysis by Next Generation Mapping (Austin et al. 2011).

3.1.1. RRE 11.1 and RRE 38.6 have an altered CW

Analysis of the sensitivity of RRE to salt stress, which is often aggravated in cell wall mutants (Benfey et al. 1993) and their performance under Ixosaben, which alters cellulose synthesis (Corio-Costet et al., 1991) were helpful to unravel possible cell wall perturbations in RRE mutants. In addition, we studied possible modifications on homogalacturonan (HG) abundance and methylesterification by using monoclonal antibodies that recognizes different HG epitopes (Liners et al., 1992; Verherbruggen et al., 2009). Altogether, our results suggest that, at the cell wall level, neither RRE 9.2 nor RRE 24.1 seem to have a CW different from RLP44ox. However, the CW of RRE 11.1 and RRE 38.6 is different to the one of RLP44ox. RRE 11.1 is as sensible as RLP44 to salt stress but it is not sensitive to isoxaben. In addition, RRE 11.1 shows a more de-methyl-esterified HG that could indicate a change on the PME/PMEI balance towards a more active PME pool. Strikingly, *bri1* mutants as *bri1^{cnu1}* also show a similar 2F4 and LM19 pattern as RRE 11.1 (Sebastian Wolf, personal communication). In addition, RRE 11.1 shows a dwarf phenotype similar to hyposensitive BRI1 mutants as *bri1^{cnu1}* and *bri1-301* (Xu et al. 2008; Wolf et al. 2012) although RRE 11.1 is not mutated in BRI1. Sequencing of RRE 11.1 showed an SNP, confirmed by Sanger sequencing, in CONSTITUTIVE PHOTOMORPHOGENIC DWARF (CPD) involved in the synthesis of endogenous BL (Szekeres et al., 1996). Since it has been already shown that CPD and BRI1 mutant phenotypes are similar (Szekeres et al., 1996; Jaillais et al., 2011), it would not surprising that also the CW pattern would be the same. In any case, the causative mutation of the different RRE mutants has to be shown. Undoubtedly, RRE 38.6 seems to be the mutant showing the biggest differences in terms of cell wall composition. It is hypersensitive to salt stress but resistant to ixosaben treatment and it seems to have a more methyl-esterified HG. Even if all these data can correspond with an anomalous CW, lack of experiments specifically quantifying the different cell wall components complicate the connection of the different phenotypes. In addition, since RRE 38.6 has not an extreme macroscopic phenotype, RRE 38.6 might compensate their cell wall composition as in other cell wall synthesis mutants as *prc1-1*, *pom1-1* or *xxt1 xxt2* (Hauser et al., 1995; Fagard et al., 2000;

Cavalier et al., 2008). If we assume that RRE 38.6 is part of the RLP44 cell wall signaling, it could be possible that the observed cell wall phenotype is an effect of an interrupted signaling cascade that would lead to an unbalanced cell wall, specially having in mind the results obtained with the HG-epitopes antibodies. It could be also possible that CW changes observed in RRE 38.6 prevents the RLP44ox morphology independent of the RLP44 signaling by, for example, restricting the elongation that defines RLP44ox phenotype. However, it cannot be exclude either that the cell wall changes might be due to a compensatory or a secondary effect produced by the unknown mutation

3.1.2. RRE 24.1 and RRE 38.6 might participate in the control of vascular fate by RLP44

Holzwardt et al. (In revision) recently demonstrated that the balance of BL and PSK signaling by the interaction of RLP44 with BRI1 and PSKR1 might control the xylem differentiation during vascular development. A wild-type developed xylem contains on its central axis three metaxylem and two protoxylem cells (Figure 26.A and 26.B), whereas RLP44ox shows an increase in the number of metaxylem cells, which might be produced by a deregulation on the BL-PSK balance due to an excess of RLP44. RRE 9.2 and RRE 11.1 did not increased xylem number compared to RLP44ox and both were still sensitive to PSK (Figure 26.A and 26.B). Thus, RRE 9.2 and RRE11.1 might not interfere with the integration of RLP44 and PSKR1. On the other hand, neither RRE 24.1 nor RRE 38.6 were sensitive to PSK. In addition, RRE 24.1 slightly strengthened the RLP44 xylem phenotype whereas RRE 38.6 restored a normal Col-0 phenotype (Figure 26.A and 26.B). Therefore, it would suggest that RRE 24.1 and RRE 38.6 could be downstream elements of the PSK signaling pathway. RRE 24.1 could be a repressor of PSK signaling under positive control of RLP44 and lack of RRE 24.1 would suppose an increase on xylem cells. Interestingly, from the confirmed SNPs in RRE 24.1, two unknown proteins could have a function on signaling: a F-box/RNI like protein (At5g02910) that is related with protein-protein interaction and usually couples with other motifs as LRR (Kipreos and Pagano 2000) or a EF-hand family protein (At5g04170) involved in intracellular Ca²⁺ signaling (Lewit-Bentley and Réty 2000). Interestingly, upon PSK perception, PSKR1 interacts with BAK1 and the cation channel CNGC17 that could allow the increase of Ca²⁺ on the cytosol and activate this EF-hand protein (Ladwig et al. 2015). In addition, RRE 24.1 mutation could localize in proteins that negative regulates RLP44 activity. Again, two of the confirmed SNPs could fit to this possibility. UPL4 (At5g02880) is an E3 ubiquitin-protein ligase that could participate in the regulation by ubiquitination of RLP44. Interestingly, UPL3, its closest homolog, was demonstrated to participate in the regulation of trichome development (Downes et al. 2003). In addition, F-box proteins have been also described as members of the E3 ubiquitin-ligase complex in mammals that can recruit previously phosphorylated substrates (Skowyra et al. 1997). However, it has been already demonstrated that RLP44 phosphorylation overrules ubiquitination (Kolbeck 2015, Master thesis). On the other hand, RRE 38.6 suppresses RLP44ox xylem phenotype. Taking to account that RRE 38.6 also presumably presents CW defects and that the proteins derived from genes showing confirmed SNPs in RRE 38.6 are predicted to localize to the CW or the PM, RRE 38.6 might be a late target of the RLP44 signaling or a CW component that participates in the perception of the signal. Interestingly, confirmed SNPs are localized in CYP77A9 (At5g04630) involved in the biosynthesis of the cuticle (Yeats and Rose 2013), UMAMIT9 (At5g07050) related with transport at the

PM (Müller et al. 2015) and ABCG16 (At5g13580) that belongs to a family related with the proper synthesis of suberin (Yadav et al., 2014).

3.2. Phosphorylation of the highly conserved AtRLP44 C-terminal domain impact on protein function

3.2.1. RLP44 C-terminal domain is highly conserved

Arabidopsis RLP44 (At3g49750) is a plasma membrane (PM) protein with a leucine-rich domain (LRR) on its extracellular domain, and a small cytoplasmic domain (Wolf et al. 2014). RLPs have been shown to play an important role in both developmental and defense-signaling processes in a broad variety of species (Wang et al. 2008). In line with this observation, RLP44 is well conserved across the plant kingdom and *AtRLP44* is more similar to RLP44 orthologs from other *Brassicaceae* than to its paralog RLP57 (Figure 1.A). It has been shown that RLP44 is important for vascular development in *Arabidopsis thaliana* (Holzwardt et al., in revision). However, it is also conserved in lower plants such as mosses where no vascular tissue exists. Therefore, it would be interesting to investigate if the role of RLP44 extends beyond cell wall integrity signaling although it is not shown whether RLP44 vascular function is connected with its role in cell wall signaling. Another indicator that the role of RLP44 might change across species is the high degree of variability found in the LRR domain in the extracellular region, which is much more variable than the cytoplasmic domain of RLP44 which is quite conserved (Figure 1.B). These modifications might act to change the type of putative signals the receptor could sense and subsequently produce divergent signaling outputs. Additionally, from the four putative phosphorylated residues in the *AtRLP44* cytoplasmic domain, Thr-256, Ser-268, Ser-270 and Tyr-274 (Sup. Figure 1), *Brassicaceae*s have exclusively acquired an extra serine residue, Ser-270, that could potentially regulate a distinct signaling pathway in *Arabidopsis*. For that reason, it would be interesting to test if the RLP44 orthologs, lacking this specific residue, could recapitulate the PMElox phenotype in *Arabidopsis cnu2* mutants. Interestingly, RLP57, the closest RLP44 paralog in *Arabidopsis thaliana*, has a similar expression pattern in roots than RLP44 (Brady et al., 2007). Moreover, the *rlp57-1* mutant has higher xylem cell numbers, similar to what has been observed for *rlp44^{cnu2}* (Huerta 2016 Master thesis, Holzwardt et al., in revision). Therefore, it is possible that RLP44 and RLP57 have redundant developmental roles. However, more work is needed in order to decipher the relation between the two RLPs, such as evaluating the contribution of the double mutant towards the xylem phenotype or the capacity of RLP57 to rescue the *cnu2* mutant. Moreover, the RLP44 cytoplasmic domain contains two predicted ubiquitination-sites at Lys-258 and Lys-266. The importance of ubiquitination as a label for endocytosis of PM-localized proteins has already been shown for the LRR-RLKs BRI1 and FLS2, and the auxin efflux carrier, PIN2 (Lu et al. 2011; Martins et al. 2015; Kleine-Vehn et al. 2008). However, ubiquitination does not appear to be essential for the regulation of RLP44. RLP44 constructs with single or double point mutations on Lys-258 and Lys-266, were used to transform the *cnu2* mutant (Wolf et al. 2014). All constructs were able to restore the PMElox phenotype in the *cnu2* background indicating that those residues do not interfere with the integration of CW into BR signaling (Kolbeck 2015, Master thesis).

3.2.2. Mutations on putative phospho-sites in RLP44 C-terminus domains alters protein function

The role of phosphorylation in RLP44 was assessed by creating mutants where the four putative phospho-residues -T256, S268, S270 and Y274- were exchanged by alanine, generating a phospho-dead version RLP44^{pdead}-GFP or exchanged by glutamate, generating a phospho-mimic version RLP44^{pmimic}-GFP. RLP44-GFP and RLP44^{pmimic}-GFP recapitulated all physiological and transcriptional aspects of the PMElox phenotype in transformed *cnu2* plants (Figure 2), including the previously described physiological alterations described by Wolf et al., 2012 and the expression of BR-regulated genes such as *DWF4* and *EXPA8*. In contrast, RLP44^{pdead}-GFP failed to complement these *cnu2* mutants phenotypes (Figure 2.). In addition, the functionality of RLP44-GFP, RLP44^{pdead}-GFP or RLP44^{pmimic}-GFP were also tested in *rlp44^{cnu2}* plants, a mutant carrying the *cnu2* point mutation of RLP44 in the absence of PMElox transgene (Wolf et al. 2014). RLP44-GFP and RLP44^{pmimic}-GFP rescued the shorter root and petiole length of *rlp44^{cnu2}* to wild-type levels, whereas RLP44^{pdead}-GFP did not (Figure 12.A,12.B and 12.C). In addition, *cnu2* plants expressing GFP-tagged phospho-mimic, phospho-dead RLP44 under its own promoter with a non-phosphorylated linker (GAGA) (pRLP44:RLP44-GAGA-GFP) also showed that RLP44-GAGA-GFP and RLP44^{pmimic}-GAGA-GFP recapitulated PMElox phenotype whereas RLP44^{pdead}-GAGA-GFP did not (Figure 21.A), supporting previous results. These data suggest that the four putative phospho-residues in the cytoplasmic tail of RLP44 are important for the function of RLP44 and its activation of BR signaling. These data are in line with what has been observed for different PM-localized proteins in which phosphorylation is required for their proper function. For instance, the auto- and trans-phosphorylated of SERKs in Thr, Ser and Tyr residues is fundamental for the activation of the different signaling processes they are involve in (Karlova et al. 2009). BRI1 and FLS2 are similarly auto- and trans-phosphorylated in order to activate their signaling pathways (Oh et al., 2000; X. Wang et al., 2008; Schulze et al., 2010). All before mentioned examples of phosphorylated PM-localized proteins have long, cytosolic kinase domains whereas RLP44 lacks such a domain and is therefore reliant on the catalytic activity of an associated protein for its phosphorylation. CLV2/RLP10 or TMM/RLP17 are well characterized RLPs, but in contrast to RLP44, they seem not to possess a cytoplasmic domain with active phosphorylation (Jeong et al.,1999; Nadeau et al.,2002; Wang et al., 2008). RLP23 and RLP30 are well characterized MAMP-perceiving RLPs, sensing peptides involved in initiating immune responses (Zhang et al., 2013; Albert et al., 2015; Couto and Zipfel 2016). These two RLPs contain a cytoplasmic domain similar in length to that of RLP44 but only RLP30 was predicted to be phosphorylated (Wang et al., 2008; Kolbeck 2015, Master thesis). Moreover, RLP44 cytoplasmic domain differs from the rest of RLPs in its biochemical characteristics being acidic instead of basic and lacking an occurrence of the characteristic Trp-Phe sequence in RLPs (Gust and Felix 2014). Therefore, the phosphorylation of RLP44 and its importance for protein function is the first described example in RLPs and is a step forward for the understanding of the role of RLPs in the intracellular propagation of signals upon the perception of ligands at the plasma membrane.

3.2.3. Specific phosphorylation of the RLP44 C-terminus is still unidentified

The specific *in vivo* phosphorylation pattern of RLP44 is still not clearly described. Previous results using specific anti-pSer antibodies after immunopurification of RLP44, suggest that the protein RLP44 could

be phosphorylated on serine residues (Wolf et al. 2014). However, the specific contribution of the S268 and S270 as well as the contribution of T256 and Y272 is yet unknown. In order to identify the phosphorylated residues on the cytoplasmic domain of RLP44, and LC-MS analysis with RLP44-GFP has been performed (Figure 14.A) but among all the peptides obtained, none of them covered the cytoplasmic domain where T256, S268, S270 and Y274 are located (Figure 14.C). Therefore, the observation of phosphorylated peptides was not possible. In addition, phosphorylation was assessed in RLP44-GFP, RLP44^{pdead}-GFP and RLP44^{pmimic}-GFP (*cnu2*) by using anti p-Ser, p-Thr and p-Tyr antibodies upon the immunopurification of RLP44 proteins. Unfortunately, detection was not successful even if phosphorylation with p-Ser antibodies was previously performed in RLP44-RFP plants (Wolf et al. 2014). Interestingly, *cnu2* plants expressing GFP-tagged single phospho-dead RLP44 under its own promoter with a non-phosphorylated linker (GAGA) (pRLP44:RLP44-GAGA-GFP) showed that the S268A mutation recapitulated PMElox phenotype whereas T256A, S270A or Y274F did not. These results suggest that phosphorylation in different residues differentially affect RLP44 function and therefore, future studies with these lines might facilitate elucidation of the biochemical mechanism of RLP44 function. In any case, the results concerning LC-MS or p-Ser antibodies do not reject the existence of phosphorylation but further experiments need to be performed to confirm protein phosphorylation *in vivo* and detect the specific residues where RLP44 is phosphorylated in the cytoplasmic domain. LC-MS analysis could be performed using the same line previously used but under treatments that could potentiate the presence of residues phosphorylated such as treatments with anti-phosphatases. In addition, to potentiate the recognition of the peptides containing the predicted phospho-residues, a new construct containing an artificial lysine on the linker sequence with GFP could be generated to create a cutting site for Trypsin and assure the presence of the desired peptide. In addition, it would be interesting to improve the use of anti-phospho antibodies to test not only the presence or not of phosphorylation in phospho-mimic, phospho-dead and single phospho-mutants but also to test differences on phosphorylation pattern in different backgrounds. Comparing phosphorylation of RLP44-GFP (Col-0) and RLP44-GFP (*cnu2*), with putative differences on the perturbation of the cell wall status, could be useful for understanding if the signal perception promotes posttranslational changes in the cytoplasmic domain as it has been already shown for other PM proteins (Offringa and Huang 2013; Dubeaux and Vert 2017).

3.3. Phosphorylation controls RLP44 clathrin-mediated endocytosis

Plasma membrane proteins are often subjected to continuous endocytosis to control protein levels, but endocytosis can also play a part in signal propagation and regulation (Irani and Russinova 2009). Posttranslational modifications, particularly phosphorylation and ubiquitination, have been observed to play a crucial role in the regulation of signaling by influencing protein localization as observed for multiple PM proteins (Barberon et al., 2011a; Irani et al., 2012; Ortiz-Morea et al., 2016; Mbengue et al., 2016). In addition, we demonstrated that RLP44 phosphorylation and not ubiquitination is important for the protein function.

3.3.1. Phosphorylation does not interfere with protein vesicular trafficking

RLP44 localizes to the PM and undergoes endocytosis as suggested by co-localization assays with the endocytic tracer FM4-64 (Wolf et al. 2014) and with the late endosome marker ARA7 (Kolbeck 2015 Master thesis). Interestingly, modification of the putative phospho-residues of RLP44 was enough to alter RLP44 localization. In *gnu2* background, RLP44-GFP displayed PM and vesicular localization whereas RLP44^{pmimic}-GFP was dramatically increased at the PM (Figure 3.A and 3.B). Oppositely, RLP44^{pdead}-GFP showed exclusively a vesicular localization. In *gnu2* plants carrying the non-ubiquitous versions RLP44-GAGA-GFP, RLP44^{pmimic}-GAGA-GFP and RLP44^{pdead}-GAGA-GFP also showed PM or intracellular localization, respectively (Figure 21.B). Interestingly, RLP44^{pdead}-GFP localizes to the cell plate during cytokinesis, a process which is characterized by increased protein trafficking to the PM (Reichardt et al., 2007). These results are indicative of one of two things: phosphorylation is required for trafficking to the PM or phosphorylation inhibits endocytosis. We tested if phosphorylation of RLP44 serves as a PM retention signal using two pharmacological inhibitors of the endocytic pathway: BFA and Wortmannin. WM increased PM localization in RLP44^{pdead}-GFP and the formation of ring structures (Figure 4.A) similar to what is observed in RLP44-GFP and RLP44^{pmimic}-GFP (Supplemental figure 4.A and 4.B). In addition, RLP44^{pmimic}-GFP showed a reduction in accumulation of GFP signal in BFA bodies and an increase in GFP signal RLP44^{pdead}-GFP (Figure 4.B and 4.C), suggesting that RLP44 phosphorylation does not interfere with the vesicular trafficking of the protein since the response to BFA and WM application is similar to RLP44-GFP in both RLP44^{pmimic}-GFP and RLP44^{pdead}-GFP. In addition, these data support the hypothesis that phosphorylation triggers PM localization. On one hand, a slight RLP44^{pdead}-GFP increase in PM localization upon WM treatment could be in line with known effects WM has in perturbing the endocytic pathway of plants (Ito et al., 2012). On the other hand, the differences of in BFA-localized GFP signal between RLP44^{pmimic}-GFP and RLP44^{pdead}-GFP could indicate that RLP44^{pmimic} is retained at the PM for a longer time, and therefore is present in BFA bodies in lower quantities. In addition, the PM localization of RLP44^{pdead}-(GS)₁₁-GFP, containing the same phospho-dead cytoplasmic domain but a hyper-phosphorylated linker, confirm that phosphorylation triggers PM localization. However, since BFA bodies are defined as an accumulation of TGN/EE vesicles, it could also be possible that the difference in GFP co-localization reflects a higher rate of RLP44^{pdead}-GFP transport from the ER due to a lack of RLP44 at the PM. To try resolving these two possibilities, BFA treatment should be complemented with a Concanamycin A (ConcA) treatment. ConcA is an antibiotic that specifically inhibits proton transport by blocking V-ATPases, and traps newly synthesized PM proteins within Golgi (Robinson et al., 2008). A comparison of both treatments would be useful to decipher if BFA bodies co-localization corresponds to endocytic vesicles as has been observed with BRI1 (Irani et al., 2012).

3.3.2. RLP44 undergoes clathrin-mediated endocytosis

The effect of phosphorylation on the endocytosis of RLP44 was pursued with the study of stable RLP44-GFP and RLP44^{pdead}-GFP lines containing an inducible TPLATE amiRNA cassette (amiR-TPL). TPLATE is a core member of the TPLATE adaptor complex (TPC) that has a crucial role in nucleation and coat assembly during clathrin-mediated endocytosis (CME) (Gadeyne et al., 2014). Measurements of mean GFP signal were used to calculate the plasma membrane/intracellular signal ratios. Upon

amiRNA induction, RLP44-GFP experienced an increase in the PM/intracellular ratio, indicating a reduction of endocytosis (Figure 5.A and 5.C). Interestingly, the PM/intracellular ratio of RLP44^{pdead}-GFP also increased upon induction, indicating that RLP44^{pdead}-GFP is also retained in the PM (Figure 5.A and 5.C). This suggests that RLP44^{pdead}-GFP is normally integrated in the PM but the absence of phosphorylated residues on the cytoplasmic domain triggers a fast endocytosis of the protein. Phosphorylation is primarily described as a signal for CME cargo to facilitate protein ubiquitination (Traub and Bonifacino 2014) as is the case with IRT1, BRI1 and FLS2 upon ligand binding (Schulze et al. 2010; Lu et al. 2011; Barberon et al., 2011; Martins et al., 2015). RLP44^{pmimic}-GFP and RLP44^{pdead}-GFP are ubiquitinated in a similar way as RLP44-GFP (Kolbeck 2015, Master thesis) suggesting that phosphorylation supersedes ubiquitination in the case of RLP44 and as such, it would be unlikely that phosphorylation recruits the ubiquitination of RLP44. Thus, phosphorylation might promote the stable localization of RLP44 in the PM, allowing it to integrate perceived signal(s) into the BL- and/or PSK-dependent signaling pathways. If true, RLP44 would be one of a few described proteins in plants, which are retained in the PM by phosphorylation. Some other examples in plants include the apical localization of PIN1 which depends on a proper phosphorylation of the protein although the absence of phosphorylation only prevents the specific apical positioning in the cell rather than the localization at the PM (Huang et al., 2010). In addition, some proteins undergo endocytosis or PM stabilization depending on the specific residues which are phosphorylated as in the case of the polymeric immunoglobulin receptor pIgR that mediates the transport of IgA from blood to saliva in the salivary glands (Ofringa and Huang 2013). In any case, even if phosphorylation stabilize a protein in the PM, upon perception of the ligand a subsequent posttranscriptional modification, usually ubiquitination, could also facilitate endocytosis (Ofringa and Huang 2013). In the case of RLP44, the stable retention and endocytosis observed for RLP44^{pmimic}-GFP and RLP44^{pdead}-GFP respectively, might be a result of the total absence or presence of phosphorylation. Differential phosphorylation of RLP44, in one or more phospho-residues simultaneously, could balance the PM stabilization and endocytosis of the protein.

3.3.3. Ser-268 and Ser-270 regulates the localization of RLP44

Monitoring the differences in localization of single RLP44 phospho-mutants could be of great interest if we wish to understand the role of differential phosphorylation in RLP44 regulation. Study of the subcellular localization of the single phospho-dead RLP44-GAGA-GFP mutants revealed that mutation of S268A leads to a RLP44 PM localization whereas mutation in S270A and Y274F leads to an intracellular localization of RLP44 (Figure 21.C). These observations reinforce the importance of Ser-268, Ser-270 and Tyr-274 for the function of RLP44. RLP44 Y274F displays what appears to be ER localization that is commonly observed for those proteins that undergo an incorrect folding (Ellgaard et al., 2016). Therefore, it could be possible that Tyr-274 is involved in the correct folding of the protein. If that would be the case, it is surprising that RLP44^{pdead}-GAGA-GFP is not retained in the ER since it also has the same mutation. However, the localization needs to be confirmed by crossing with specific marker lines for ER as NIP1;1 (Boursiac et al., 2005; Geldner et al., 2009). In addition, the contribution of Thr-256 to the function of RLP44 needs confirmation since it was not possible to study the subcellular localization of the T2 lines. More interestingly, the two serine seem opposite in function. The S270 is crucial for function as mutation of alanine of this residue was sufficient to not prevent complementation

of *gnu2* plants. Strikingly, Ser-270 is the only putative phospho-residue that is not conserved. In fact, Ser-270 is exclusive for brassicaceas species whereas the rest of RLP44 orthologs contain a leucine, chemically different to serine and non-posttranslational modified (Hashiguchi and Komatsu 2017). Thus, although the function of other RLPs as TMM seemed to be conserved (Peterson et al., 2010), it could be possible that the acquisition of the Ser-270 at the cytoplasmic domain benefited the generation of a new phospho-active site and subsequently the acquisition of a new feature for RLP44 function. On the other hand, Ser-268 is a residue conserved among RLP44 orthologs and S268A mutation recapitulates PMElox phenotype in *gnu2* plants. However, RLP44-GAGA-GFP carrying the S268A or S270A mutation leads to a different subcellular localization of the protein. The S268A mutant version in RLP44 is strongly present in the PM and the S270A version is mainly localized in vesicular bodies. It could be possible that the two serines play opposite roles controlling the localization of RLP44. In this scenario, phosphorylation of Ser-270 would be important to keep the PM localization of RLP44 whereas Ser-268 would have a negative effect on this localization. As it has been discussed, it has been already described in mammals how sequential phosphorylation in different residues can govern the stabilization in the PM or endocytosis as described for AQP2, EGFR or plgR (Offringa and Huang 2013). For instance, in the case of plgR, a specific phosphorylation on a serine triggers the endocytosis of the receptor whereas the phosphorylation on a different serine promotes the localization of the protein at the apical PM for the transmission of the signal ligand (Hirt et al., 1993; Okamoto et al., 1994). Therefore, it is possible that differential phosphorylation in Ser-268 and Ser-270 would govern the localization the protein to create a phospho-code that would determine RLP44 functionality. How this phosphorylation is regulated could be the focus of future research. Thus, experiments should focus on addressing if the two serines really oppositely regulate the localization of RLP44 by creating specific phospho-mimic mutants that should present an opposite localization to the phospho-dead ones. It would be also interesting to decipher if the two residues are phosphorylated by the same or a different kinase or if these specific mutations could facilitate the balance of interaction with BRI1, BAK1 or PSKR1. In addition, it could be interesting to study if the two mutations have a differential activity in both BL- and PSK-mediated signaling.

3.4. RLP44 phosphorylation controls the integration of CW signals into the BL signaling cascade

Our results suggest that RLP44 phosphorylation plays a major role in its function although the mechanism underlying the regulation of phosphorylation is unknown. Since RLP44 interacts with several PM kinases such as BRI1, BAK1 or PSKR1 (Wolf et al., 2014; Holzwardt et al., In revision) and those can trans-phosphorylate other PM proteins (Wang et al., 2008; Schwessinger et al., 2011), it could be possible that one or more of them phosphorylate RLP44.

3.4.1. RLP44 phosphorylation is BL dependent

Immunodetection of RLP44-(GS)₁₁-GFP, a GFP-tagged RLP44 controlled by its endogenous promoter, with anti-GFP antibodies revealed the presence of a double band that could correspond to a phosphorylated (slow-moving band) or un-phosphorylated (fast-moving band) RLP44 (Figure 15.C).

This assumption was confirmed by the application of calf intestine phosphatase (CIP) which fully eliminated the slow-moving band whereas a double band was observed upon the treatment of CIP together with phosphatase inhibitors (Figure 15.C). This observation suggest that the double pattern band detected for RLP44-(GS)₁₁-GFP corresponds indeed with RLP44 phosphorylation status. Interestingly, application of BL during seedling growth triggered an enrichment of the slow-moving band whereas treatment with PPZ promoted the non-phosphorylated band, suggesting that RLP44-(GS)₁₁-GFP phosphorylation status might be BL-dependent. By applying BL in combination with cantharidin (a phosphatase inhibitor) or K252a (a kinase inhibitor) the effect of BL enriching phosphorylated RLP44-(GS)₁₁-GFP was strengthen or alleviated, respectively. Cantharidin, is a specific inhibitor of the PP2A phosphatase, which it has been reported to inhibit BRI1 function (Wang et al., 2015); and K252a is a potent kinase inhibitor, which could influence BRI1 function. Therefore, chemicals that affect BRI1 activity in turn influence the BL-dependent RLP44 phosphorylation thus, it could be possible that BRI1 is the kinase responsible for RLP44 phosphorylation. However, it is important to remark that PP2A also controls BAK1 activity (Segonzac et al. 2014), thus BAK1 could also be involved in phosphorylation of RLP44. The effect on RLP44 phosphorylation by the different kinases was tested by expressing RLP44-(GS)₁₁-GFP in different mutants backgrounds: *bri1-301*, *bri1^{cnu4}*, *bri1-null*, *serk1-3 serk3-1 serk4-1* which were subjected to BL in combination with cantharidin and K252A treatments. Strikingly, total abolishment of RLP44 phosphorylation was not observed in any of the mutants studied when compared to *rlp44^{cnu2}* background although differences on phosphorylation pattern were appreciable among them (Figures 15.D, 15.E, 16.F, 16.G, 17.C, 17.D). Phosphorylation of RLP44-(GS)₁₁-GFP in *bri1-301* seemed to be partially insensible to BL treatment and prone to be un-phosphorylated under this conditions (Figure 16.F). By contrast, RLP44-(GS)₁₁-GFP phosphorylation in *bri1^{cnu4}* does not differ from in *rlp44^{cnu2}* (Figure 16.G). In addition, RLP44-(GS)₁₁-GFP rescued *bri1^{cnu4}* but not *bri1-301* macroscopic phenotype and BL response (Figure 16.D and 16.E). Differences between *bri1-301* and *bri1^{cnu4}* could be explained by their different mutation. *Bri1-301* carries a mutation in the kinase domain whereas *bri1^{cnu4}* is mutated in the extracellular domain (Xu et al., 2008; Holzwardt et al., in revision). Therefore, since the kinase domain in *bri1^{cnu4}* might not be altered, RLP44 phosphorylation could still be possible. Furthermore, RLP44-(GS)₁₁-GFP phosphorylation in *bri1-null* and *serk1-3 serk3-1 serk4-1* still responded to BL treatment alone but not in presence of kinase inhibitors (Figure 17.C and 17.D). These results suggest that neither BRI1 nor SERKs seem to be the only kinase participating in the phosphorylation of RLP44 since it is still presenting switches between the phosphorylated and unphosphorylated bands. One possible explanation could be that BRI1 and SERKs are both phosphorylating RLP44. The effect of K252A in *bri1-null* or *serk1-3 serk3-1 serk4-1* would be the closest situation to a lack of both BRI1 and SERKs. Interestingly, BL does not counteract the K252A effect on RLP44-(GS)₁₁-GFP phosphorylation in these two mutants when it compares to the same effect in *rlp44^{cnu2}*. As mentioned, BRI1 and SERKs activity is controlled by PP2A (Segonzac et al., 2014; Wang et al., 2015), whose effect is inhibited by Cantharidin. Thus, phosphorylation of RLP44-(GS)₁₁-GFP in *bri1-null* or *serk1-3 serk3-1 serk4-1* is enhanced in presence of BL when Cantharidin is applied, especially in *bri1-null* what it would also suggest that stabilization of the remaining kinase would facilitate RLP44-(GS)₁₁-GFP phosphorylation. However, *in vitro* phosphorylation experiments should be carried out in order to decipher the role of both BRI1 and SERKs in the phosphorylation of RLP44. In addition, it cannot be excluded that BRL1 and

BRL3, BRI1 homologs (Caño-Delgado et al., 2004), could also phosphorylate RLP44 thus, RLP44 phosphorylation in *bri1-116 bri1 bri3* (Vragović et al., 2015) should be also tested. Moreover, RLP44 interacts with PSKR1 (Holzwardt et al., in revision) therefore, we cannot rule out that also it takes part in RLP44 phosphorylation. Nevertheless, the immunodetection with GFP antibody of a double band in RLP44-(GS)₁₁-GFP is probably the result of the hyperphosphorylation of the sequence linker between RLP44 C-terminal and N-terminal GFP, enriched in serine residues (GS)₁₁ (Figure 20.D). The observation of a double band in RLP44^{pmimic}-(GS)₁₁-GFP and RLP44^{pdead}-(GS)₁₁-GFP which, ideally, should only present a non-phosphorylated band, strongly support this assumption. Therefore, the results obtained for the phosphorylation of RLP44 with RLP44-(GS)₁₁-GFP have to be taken with caution and repeated with mutants carrying the RLP44-GAGA-GFP version where the sequence linker before GFP does not contain residues that could be phosphorylated.

3.4.2. RLP44 triggers the formation of BRI1 and BAK1 complex

Co-immunoprecipitation experiments in *Arabidopsis* to analyze the amount of BAK1 coimmunoprecipitated with BRI1 in the presence or not of RLP44 were fundamental to gain insight on the effect of RLP44 in the BAK1-BRI1 complex formation. In fact, more BAK1 could be detected in immunoprecipitates of BRI1 in the presence of RLP44 (Figure 7.B), suggesting that RLP44 promotes the formation of BRI1-BAK1 complexes, presumably by the activation of the downstream signaling. Intriguingly, RLP44 activation of BR signaling is BR-independent (Wolf et al. 2014) whereas the activation of BRI1 and the subsequent BR-signaling cascade requires BR (Jaillais et al., 2011; Wang et al., 2015). However, rather than producing an allosteric activation of the kinase domain, BL acts as molecular glue allowing BRI1 and BAK1 to be in close proximity and allows the trans-phosphorylation of their kinases domains (Wang et al., 2008; Santiago et al., 2013). Therefore, it is possible that RLP44 could favor the activation of BR signaling by promoting the BAK1-BRI1 interaction and its activation by proximity as a scaffold. Another possible scenario could be that the presence of RLP44 stabilizes BRI1 and BAK1 at the PM by hindering the activity of PP2A, a phosphatase that attenuates BRI1 and BAK1 activity (Segonzac et al. 2014; R. Wang et al. 2016). More work is needed in order to understand the mechanism governing the interaction between RLP44, BAK1 and BRI1 and the formation of the complex. Further experiments should focus on challenging the observed RLP44-mediated increase in complex formation through the depletion of BR with drugs such as Propiconazol, which inhibit BR synthesis.

Strikingly, the interaction of PSKR1 and BAK1 is also promoted by the presence of RLP44 (Holzwardt et al., in preparation). Thus, RLP44 might promote the activation of two different signaling cascades, how this is regulated would be the focus of future research. It might be possible that RLP44 perceives different signals from the cell wall and switches between the two RLKs depending on that signal. The RLP, TMM, changes its interaction with different ER or ERL depending on the signal perceived and modulates stomata development accordingly (Lin et al. 2017). However, TMM interacts with proteins all belonging to the homologous receptors whereas RLP44 is interacting with two RLKs that, even if they are structurally similar (Wang et al., 2015), activate two independent cascades. Intriguingly, the extracellular domain of RLP44 is not able to form a complex with either BRI1 or PSKR1 *in vitro* or in transient CoIP experiments in *N. benthamiana* leaves, whereas the cytoplasmic tail of RLP44 does

(Michael Hothorn and Eleonore Holzward, personal communication). It seems that the interaction between RLP44 and different RLKs occurs at the cytoplasmic level, possibly relying on the posttranslational modification of the cytoplasmic domain upon signal perception. However, at this point in time it cannot be excluded that RLP44 senses various signals that together produce differential phosphorylation of the cytoplasmic domain and subsequently allows for unique interaction patterns.

3.4.3. RLP44 phosphorylation modifies the interaction with BRI1 but not with BAK1

Phosphorylation of PM proteins cytoplasmic domain can produce changes of their conformation and facilitate the interaction with other proteins and signaling cascade propagation (Ofringa and Huang 2013). The effect of RLP44 phosphorylation on the capacity to interact with BAK1 and BRI1 was assessed by using the generated *cnu2* lines expressing RLP44-GFP, RLP44^{pmimic}-GFP and RLP44^{pdead}-GFP and analyzing the possible differences of interaction by immunodetecting the presence of BRI1 and BAK1 after immunopurification of RLP44. In addition, we also tested the interaction of RLP44 with BRI1 and BAK1 by using ratiometric Bimolecular Fluorescent Complementation (BiFC) (Grefen and Blatt 2014). By Co-IP, both RLP44^{pmimic}-GFP and RLP44^{pdead}-GFP formed a complex with BRI1 and BAK1 (Figure 7) whereas BiFC showed interaction of RLP44^{pmimic} and RLP44^{pdead} with BAK1 but only interaction of RLP44^{pmimic} with BRI1 (Figure 8). These results suggest that RLP44 phosphorylation influence the interaction with BRI1 but not BAK1. CoIP reflects what is happening on the specific moment when the samples were taken. In addition, since the results of the coimmunoprecipitation reflect the formation of a complex, we cannot exclude that the detection of BRI1 in RLP44^{pdead} samples is an effect of an indirect interaction with a third component of the complex. Moreover, it was described that BRI1 is constantly going into endocytosis, independent of the ligand (Irani et al., 2012) and RLP44^{pdead}-GFP localization is enriched in vesicular bodies (previously discussed). Thus, it could also be possible that the coimmunoprecipitation of BRI1 with RLP44^{pdead} would be the result of being in the same complex on a vesicle and subsequently, it would not reflect the real role of phosphorylation for RLP44 activity in the PM. On the other hand, BiFC is assumed to reflect the direct interaction of two proteins, which becomes irreversible after the fluorophore is reconstituted. Taking into account the results of BiFC, RLP44^{pdead} did not interact with BRI1 whereas the interaction between RLP44^{pdead} and BAK1 still occurs. Thus, BiFC results suggest that RLP44 phosphorylation is important for complex formation rather than its stability. Therefore, we speculate that the phospho-residues in the cytoplasmic tail of RLP44 are not fundamental for the interaction with BAK1 since either RLP44^{pmimic} and RLP44^{pdead} interact with BAK1 in both experiments. However, the interaction with BRI1 might depend on the phosphorylation of those residues. In this scenario, RLP44^{pdead} would still interact with BAK1, but not with BRI1, as observed for BiFC. In addition, since BAK1 and BRI1 are forming a complex, the coimmunoprecipitation of BRI1 together with RLP44^{pdead} might be an effect of the presence of BAK1. Furthermore, these results would be in line with the observation that RLP44^{pmimic}-GFP and not RLP44^{pdead}-GFP is able to recapitulate the PMElox phenotype in *cnu2* as well as rescue the *rlp44^{cnu2}* phenotype. However, all RLP44 phospho-versions had a similar BL-response to the control independently of being in Col-0 or *rlp44^{cnu2}* background (Figure 12.E, Supplemental Figure 3), indicating that the phosphorylation of RLP44 did not interfere with the BL sensitivity of BRI1. However, the lack of interaction between BRI1 and RLP44^{pdead} in BiFC can also be explained by a rare presence of both proteins at the PM. Furthermore, results with RLP44^{pdead}-(GS)₁₁-

GFP showed that PM localization but not the modification of the residues were required for the interaction with BRI1. In addition, the cytosolic domain of RLP44 alone is able to coimmunoprecipitate BRI1 and PSKR1 in transient ColP experiments (Elenore Holzward, personal communication), it would be interesting to also test if the RLP44^{pdead} and RLP44^{pmimic} cytoplasmic domains coimmunoprecipitate BRI1. In addition, to restrict the study to the complexes present at the PM, coimmunoprecipitation could be done after a purification of plasma membranes.

3.4.4. RLP44 stabilization of BR signaling requires the presence of BRI1

Interestingly, RLP44^{pmimic}-GFP had a stronger phenotype in Col-0, *cnu2* and *rlp44^{cnu2}* background when compared to RLP44-GFP in the same backgrounds. In addition, RLP44^{pmimic}-GFP showed an increase of the PM localization that could relate with a more active form of RLP44. If RLP44 activates BR signaling by acting as a scaffold for BAK1 and BRI1 and the function of RLP44 depends on its stabilization at the PM, it might be possible that a more active version of RLP44 (RLP44^{pmimic}-GFP) could help to compensate for the lack of BR signaling. The expression of RLP44-GFP, RLP44^{pmimic}-GFP or RLP44^{pdead}-GFP in *bri1-301* and *bri1-null* backgrounds (Xu et al., 2008; Jaillais et al., 2011) did not rescue the macroscopic dwarfs phenotypes of both BRI1 mutants (Figure 9.A and 9.B). In addition, the unresponsiveness to BL of the BRI1 mutants was neither rescued by any of the transgenic lines expressing the different RLP44 phospho-versions (Holzward et al. in preparation). Moreover, RLP44-(GS)₁₁-GFP, which is presumably more active than RLP44-GFP since its residence in PM is also increased, cannot rescue either the macroscopic phenotype of *bri1-null* or *bri1-301* or the unresponsiveness to BL (Figure 16.A, 16.D and 17.A). By contrast, RLP44-(GS)₁₁-GFP can rescue the macroscopic phenotype as well as the BL response of *bri1^{cnu4}* (Figure 16.A and 16.E) where the kinase activity of BRI1 is presumably not limiting. In addition, localization of RLP44 seems to depend also on the presence of an active BRI1 since the PM/intracellular signal ratios of RLP44^{pmimic}-GFP shows a strong increased intracellular localization in *bri1-null* when compares to Col-0 reducing the PM/intracellular ratio to WT levels (Figure 6.A and 6.B). These data suggest that RLP44 needs the presence of a functional BRI1 localized in the PM in order to be stabilized at the PM, independently on the phosphorylation status of the RLP44 cytoplasmic domain. In contrast, RLP44-RFP is capable to rescue *bak1-4* phenotype (Wolf et al. 2014) although the lack of BAK1 could be compensated for the presence of its homologs SERK1 and SERK4 that interact with BRI1 during BR signaling (Gou et al., 2012). However, the expression of RLP44-(GS)₁₁-GFP in a *serk1-3 serk3-1 serk4-1* background partially rescues the mutant phenotype (Figure 17.B) which argues against the putative compensation of SERK1 and SERK4. These observations strengthen the idea that RLP44 phosphorylation is important for the stabilization of the protein at the PM rather its activation and that BRI1 and not BAK1 is important for the integration of RLP44 into the BR signaling. Alternatively, it could be possible that RLP44 interacts with downstream elements of the BR signaling cascade, as it has been observed for other PM proteins as OCTOPUS (OPS) that can interact and sequesters BIN2 from the nucleus to activate BR signaling in a BL-independent manner (Anne et al., 2015). In that way, RLP44 could activate the signal independently of BL and BRI1 interaction. However, none of the RLP44 phospho-versions seems to interact with BIN2 (Data not shown). Therefore, these data also support the hypothesis that the integration of RLP44 information into the BR signaling happens at the PM in a BRI1 dependent manner.

3.5. Activation of PSK signaling is independent of RLP44 phosphorylation

Since RLP44 interacts also with PSKR1 (Holzwardt et al., in preparation), we also investigated if RLP44 is phosphorylated by PSKR1 and if RLP44 phosphorylation will also interfere with PSKR1 interaction. Regarding the effect of PSKR1 in phosphorylation of RLP44, we conclude that PSKR1 is not necessary since RLP44-(GS)₁₁-GFP in *pskr1-3* presented similar band pattern to *rlp44^{cnu2}* phosphorylation upon the treatment with BL together with Cantharin and K262A treatments (Figure 19). In addition, RLP44-(GS)₁₁-GFP in *pskr1-3* was able to restore to wild-type levels the small *pskr1-3* macroscopic phenotype as well as to restore the defective PSK response in *pskr1-3* (Figure 18.B). Furthermore, switch to a slow-moving band (phosphorylated) in RLP44-(GS)₁₁-GFP *rlp44^{cnu2}* was not appreciated upon PSK treatment as it was shown for BL (Data not shown). These data presumably indicate that the phosphorylation of RLP44 is independent of PSKR1 and that RLP44 could still participate in PSK signaling independently of its phosphorylation status. In fact, transient CoIP experiments suggest that RLP44-GFP, RLP44^{pmimic}-GFP and RLP44^{pdead}-GFP formed a complex with PSKR1 (Figure 10) supporting the independence of phosphorylation of RLP44 to interact with PSKR1. However, PSKR1 is forming a complex with BAK1 (Ladwig et al. 2015) thus, it cannot be excluded that the coimmunopurification of PSKR1 is due to the existence of a complex with BAK1 which interaction it has been shown to not be affected by the phosphorylation status of RLP44.

In addition, RLP44-GFP expressed in Col-0 promoted root length in presence of PSK similarly to the overexpression of PSKR1 (Figure 11.B) (Hartmann et al. 2013) whereas *rlp44^{cnu2}* is partially insensitive to PSK response, sensitivity can be restored upon RLP44-GFP expression in *rlp44^{cnu2}* (Figure 12.D). This data suggest that RLP44 might not only interact with PSKR1 but it might also participate in perception of the peptide in line with what is observed for other RLPs. RLP23 and RLP30 directly bind to MAMPs to activate innate immunity responses (Zhang et al., 2013; Albert et al., 2015). Moreover, CLV2 not only directly binds to CLV3 in the SAM but also is required for the perception of CLE peptides in the root (Hazak et al., 2017) and TMM not only perceives different EPFLs but also specify the response depending on which it perceives (Lin et al., 2017). Therefore, even if more experiments are needed for confirmation of this hypothesis, it is possible that the ECD of RLP44 is not only able to interact with the cell wall but also with PSK. Strikingly, the phosphorylation of RLP44 did not affect the activation of PSK signaling. Expression of RLP44^{pmimic}-GFP or RLP44^{pdead}-GFP in *rlp44^{cnu2}* also supposed the restoration of PSK response in a similar manner than RLP44-GFP (Figure 12.D). Interestingly, RLP44^{pdead}-GFP restored the response to PSK by promoting root length but without restoring the shorter root length of *rlp44^{cnu2}* compared to Col-0, phenotype that probably depend on BR-response (Figure 12.C and 12.D). These data suggest that the phosphorylation of RLP44 is not necessary for the activation of PSK signaling. However, when the same experiment was performed in Col-0 lines expressing the same constructs, RLP44-GFP and RLP44^{pmimic}-GFP still promoted root length upon PSK treatment whereas RLP44^{pdead}-GFP was as insensitive as *pskr1-3 pskr2-1* (Figure 12.D). This result might indicate a dominant negative effect of the RLP44^{pdead}-GFP over the endogenous RLP44 alleviated in *rlp44^{cnu2}*. In addition, the expression of RLP44^{pdead}-GFP could trigger an unknown compensatory response. Further genetics and biochemical studies on the PSKR1-RLP44 interaction as well as the

comparison of *rlp44^{cnu2}* and *pskr1-3* transcriptomes would help to gain insight into their role on the PSK signaling as well as the real function of RLP44 phosphorylation.

Interestingly, the RLP44 cytoplasmic domain interacts with both BRI1 and PSKR1. In addition, RLP44^{pdead}-GFP does not restore BR-dependent phenotypes and does not interact with BRI1 (Figure 12.E, Supplemental Figure 3) whereas RLP44^{pdead}-GFP restores the PSK effect on root length and form a complex with PSKR1. Thus, these differences might indicate that the interaction with BRI1 and PSKR1 and therefore the control of RLP44 over the balance between BL and PSK signaling could be governed by its phosphorylation. Furthermore, the observed differences on localization of the mutants in single residues Ser-268 and Ser-270 suggest a phospho-code for protein stabilization in the PM and, therefore functionality of the protein, that could be control by the kinase activity of BRI1 and/or BAK1 but not PSKR1. This phospho-code in the both serines could be translated into differences on interaction with PSKR1 and BRI1 and govern the mentioned balance BL and PSK signaling. The importance of these two residues in the PM localization and balance of RLP44 function will be the focus of future research.

3.6. RLP44 phosphorylation balance BL and PSK signaling in vascular fate control

The vascular tissue of *Arabidopsis thaliana* primary roots presents in the center five xylem cells aligned in the axis: three metaxylem cells with two protoxylem cells on the periphery (De Rybel et al., 2015). Recent results from the lab showed that *rlp44^{cnu2}* shows increased number of metaxylem cells as well as *bri1* and *pskr1-3* mutants (Holzwardt et al., in revision). The *rlp44^{cnu2}* xylem phenotype can be rescued with the external application of PSK (Holzwardt et al., in revision). RLP44 might balance PSK and BR signaling to control xylem differentiation during vascular development in which BL signaling controls cell proliferation and PSK procambial identity (Holzwardt et al., in revision). Interestingly, it has been discussed that RLP44 phosphorylation seem to be important for the integration of RLP44 signaling with BL but not PSK signaling thus, phosphorylation could also influence the balance between the two pathways on the context of vascular development. Col-0 presents in around 85% of the cases 5 xylem cells and only a low percentage of increase xylem cell number. By contrast, lack of BRI1 in *bri1-null* leads to an increase of up to 50% of roots with 6 xylem cells (Figure 22.B and 22.C). The expression of RLP44-GFP, RLP44^{pmimic}-GFP and RLP44^{pdead}-GFP in *bri1-null* showed that none of the constructs rescued the *bri1-null* dwarf phenotype or the response to BL (Figure 9) (Holzwardt et al., in revision). However, RLP44-GFP was able to restore the xylem phenotype of *bri1-null* suggesting that RLP44-GFP is in the same pathway with BRI1 for xylem cell fate. By contrast, RLP44^{pmimic}-GFP and RLP44^{pdead}-GFP did not restored xylem phenotype. However, it has been already shown (Holzwardt et al., in revision) that overexpression of RLP44 also triggers an increase of xylem cells similar to what was observed for *bri1-null* and *rlp44^{cnu2}*. Moreover, RLP44^{pmimic}-GFP presents a stronger phenotype than RLP44-GFP in the activation of BR signaling (Figure 2). Therefore, the phenotype of RLP44^{pmimic}-GFP might be either the failure to rescue the *bri1-null* mutant or the surpass of WT signaling strength. By contrast, RLP44^{pdead}-GFP does not activate BR signaling (Figure 2). The situation in which RLP44^{pdead}-GFP might be active and surpass could be explained by the fact that the endogenous RLP44 is still present and it could sum its activity to the one of the transgene. However, it does not explain why RLP44-GFP does not have the

same summatory effect as RLP44^{pdead}-GFP. In addition, in the vascular tissue, not only BRI1 but also its homologs BRL1 and BRL3 are expressed (Caño-Delgado et al., 2004). Therefore, it could be possible that presence of BRL1 and BRL3 could also influence the activity of RLP44. Thus, even if RLP44^{pdead}-GFP does not interact with BRI1, the interaction with BRL1 and BRL3 has to be checked. In any case, to elucidate the role of BRL1 and BRL3 together with RLP44 phosphoverions, the xylem phenotype need to be studied in *bri1-116 bri1 bri3* (triple *bri1*) mutants expressing RLP44-GFP, RLP44^{pmimic}-GFP and RLP44^{pdead}-GFP. Interestingly, RLP44^{pdead}-GFP still interacts with PSKR1 (Figure 9) and it seems to have a dominant negative effect on the response to PSK when endogenous RLP44 is present (Figure 11.B) which could explain the incapability of RLP44^{pdead}-GFP to restore procambial identity in *bri1-null*. In this scenario, RLP44-GFP rescues *bri1-null* phenotype, RLP44^{pmimic}-GFP acts as RLP44ox and RLP44^{pdead}-GFP has a dominant negative effect. To rule out the effect of endogenous RLP44, we expressed the same constructs in *rlp44^{cnu2}*, which has the same xylem phenotype as *bri1-null*. RLP44-GFP slightly rescued *rlp44^{cnu2}* whereas RLP44^{pmimic}-GFP showed an increase on xylem cell. Surprisingly, RLP44^{pdead}-GFP fully rescued the *rlp44^{cnu2}* to wild-type xylem phenotype (Figure 22.D and 22.E). These data support the hypothesis that RLP44^{pdead}-GFP can activate PSK but no BR signaling. In a *rlp44^{cnu2}* background, RLP44^{pdead}-GFP would trigger PSK signaling, and the absence of endogenous RLP44 would prevent the activation of BR signaling. Thus, wild-type xylem phenotype observed in RLP44^{pdead}-GFP in *rlp44^{cnu2}* background would be the result of a predisposition on the activation of PSK signaling and subsequently maintenance of procambial identity. By contrast, RLP44^{pmimic}-GFP, presumably more active, would surpass the wild-type xylem phenotype independently of the presence of endogenous RLP44. In addition, differences in RLP44-GFP xylem phenotype between *bri1-null* and *rlp44^{cnu2}* could be explained if we take in consideration that RLP44 might be phosphorylated by BRI1 but not PSKR1. In *bri1-null* background, RLP44-GFP would not be phosphorylated and thus, prevent xylem differentiation whereas in *rlp44^{cnu2}* RLP44-GFP, presumably more active, would destabilize the balance in the control of vascular fate and promote an increase in xylem cell number. In any case, to assume this true, RLP44-GFP phosphorylation should be independent of BRI1 homologs, BRL1 and BRL3, assumption that need to be checked by study the phosphorylation of RLP44 as well as the xylem phenotype of *bri1-116 bri1 bri3* mutants expressing RLP44-GFP. In order to precisely understand the effect of phosphorylation in the balance of vascular fate exerted by RLP44, we expressed the same constructs in in a *bri1-null rlp44^{cnu2}* double mutant. The two single mutants have an increased xylem number phenotype and therefore the double mutant was expected to have the same phenotype since RLP44 and BRI1 are in the same pathway to control xylem cell fate. However, *bri1null rlp44^{cnu2}* is capable to rescue the phenotype of *bri1null* or *rlp44^{cnu2}*, and restore the wild-type xylem cell number (Figure 23.A and 23.B). In this double mutant background, RLP44^{pdead}-GFP roots also presented a wild-type xylem number phenotype. By contrast, RLP44^{pmimic}-GFP and RLP44-GFP restored the *bri1null rlp44^{cnu2}* roots to a *bri1-null* xylem cell number phenotype what it would mean that RLP44^{pdead}-GFP is, in fact, not active or that would have a dominant negative effect, similar to what observed for the root length response to PSK (Figure 23.A and 23.B). On one hand, the phenotype of *bri1-null rlp44^{cnu2}* could be the result of a compensatory response in PSK cascade that we could only asses by analyzing the transcriptome of these mutants together with *pskr1-3 pskr2-1*. Other possible explanation for this observation could be the existence of an interaction balance between the different receptors

participating in xylem differentiation. Both scenarios could explain the apparent dominant negative effect of RLP44^{pdead}-GFP. BAK1 interacts not only with BRI1 and PSKR1 but also with FLS2 and other RLPs as RLP23 or RLP30 (Ma et al. 2016), therefore interaction of BAK1 with the different receptors need to be extremely controlled as it has been recently reported for BAK1 interaction with BRI1 and FLS2 (Imkampe et al., 2017). Since BAK1 forms a complex with both BRI1 and PSKR1 and is interacting with RLP44 independently of its phosphorylation status (Figure 7.C and 8.A), it might be possible that BAK1 helps RLP44 to interact with either PSKR1 or BRI1. Moreover, reduction on the responsiveness to PSK and the unchanged responsiveness to BL of *rlp44^{cnu2}* when compared to Col-0 (Figure 12D and 12E), suggests that RLP44 is necessary for the activation of PSK but not BL signaling. Absence of endogenous RLP44 would block the activation of PSKR1 and produce an increase of xylem as observed in *rlp44^{cnu2}*. RLP44-GFP and RLP44^{pmimic}-GFP, capable of be phosphorylated and presumably more active than endogenous RLP44, would overpass wild-type phenotype. By contrast, RLP44^{pdead}-GFP would only interact with PSKR1 and therefore, it would maintain the inhibition of xylem proliferation. The absence of BRI1 would allow BAK1 to easily interact with other PM receptors. If in that case, BAK1 could strongly interact with RLP44 and it could sequester RLP44 to prevent interaction with PSKR1. In this situation, we should assume that phosphorylation of RLP44 promotes a stronger interaction with BAK1 and not with PSKR1. RLP44-GFP might rescue *bri1-null* phenotype since it is the unique constructs that would be correctly phosphorylated and properly balance its interaction between BAK1 and PSKR1. RLP44^{pmimic}-GFP would be fully sequestered by BAK1 and therefore it would promote xylem differentiation. RLP44^{pdead}-GFP should preferable interact with PSKR1. However, RLP44^{pdead}-GFP might have a dominant negative effect over endogenous RLP44 that could explain its xylem cell phenotype in *bri1-null* phenotype. In the absence of RLP44 and BRI1 (*bri1-null, rlp44^{cnu2}*), BAK1 would freely interact with PSKR1, promoting procambial identity, and therefore *bri1-null rlp44^{cnu2}* would have a wild-type xylem cell number. RLP44-GFP and RLP44^{pmimic}-GFP would destabilize BAK1 and PSKR1 interaction and restore xylem differentiation. Whereas RLP44^{pdead}-GFP, without the presence of the endogenous RLP44, would trigger PSK signaling activation and maintain procambial identity as observed in RLP44^{pdead}-GFP (*bri1-null, rlp44^{cnu2}*). In any case, further studies of the xylem phenotype of different BAK1 and SERK mutants as well as the effect of the expression of RLP44 in those mutants for the xylem phenotype is needed. In addition, it is necessary to shed light on the biochemical mechanism that governs the interaction and balance of RLP44 with the PSK and BL cascades, especially on the contribution of single residues of RLP44 cytoplasmic domain for the control of vascular phenotype.

4. Conclusion

RLP44 is a plasma membrane localized (PM) receptor-like protein (RLP) that senses the perturbations from the cell wall (CW) and transduce this information into the cell via a balanced interaction with BRI1 and PSKR1 (Holzwardt et al., in revision). This thesis investigates the biochemical mechanism that regulates RLP44 function during the integration of CW information into Brassinosteroid (BR) and Phytosulfokine (PSK) signaling cascades.

AtRLP44 contains a highly conserved cytoplasmic domain in which two putatively ubiquitinated and four putatively phosphorylated residues have been predicted *in silico*. While ubiquitination of the cytoplasmic domain has no a significant impact on RLP44 function, phosphorylation is responsible for the protein localization and, subsequently, for the protein function. Non-phosphorylated RLP44 promotes the clathrin-mediated endocytosis of the protein without affecting its secretory trafficking, whereas phosphorylation of the cytoplasmic domain retains the protein at the PM where it can interact with BRI1, BAK1 and PSKR1. RLP44 phosphorylation is BL dependent, thus, BRI1 and BAK1 but not PSKR1 are potentially responsible for protein phosphorylation. RLP44 facilitates the interaction between BRI1 and BAK1 by acting as a scaffold that promotes the close proximity of the two BR co-receptors and subsequently activates BR-signaling cascade, depending on a non-compromised kinase activity of BRI1. A similar mechanism might be expected for the interaction of PSKR1 and BAK1. Phosphorylation of the RLP44 cytoplasmic domain affects the interaction with BRI1, but not that with BAK1 and PSKR1. However, lack of phosphorylation impacts differently on the activation of BR- and PSK- signaling cascades. Phosphorylation of RLP44 seems to be necessary for the activation of BR-signaling cascade whereas activation of PSK response by RLP44 is independent of its activation. This discriminative nature of RLP44 phosphorylation might be a determining factor for the balance between BL and PSK signaling cascades that RLP44 exerts during the regulation of xylem differentiation and vascular cell fate control. Interestingly, the localization of the protein at the PM and its functionality, might be regulated by differential phosphorylation in two serines in the cytoplasmic domain, Ser-268 and Ser-270. Ser-268 phosphorylation might negatively regulate localization of RLP44 at the PM whereas Ser-270 trigger the stabilization of RLP44 at the PM. How these two residues influence the localization of RLP44 and how their phosphorylation is regulated could be the focus of future research.

In addition, four new RLP44ox suppressor mutants, RRE 9.2, RRE 11.1, RRE 24.1 and RRE 38.6 have been described to be impaired in the integration of the CW- and BR-signaling. RRE 9.2 and especially RRE 38.6 present disturbed cell wall composition when compared to RLP44ox and wild-type. In addition, RRE 24.1 and RRE 38.6 modify the RLP44ox xylem phenotype as well as PSK responsiveness, which turn them into attractive candidates for studying the biochemical mechanism that is involved in the integration of CW signals into BL and PSK-dependent cascades.

5. Material and Methods

5.1. Cloning procedures and Plasmid Construct

5.1.1. Gateway™ Cloning

Some of the plasmid constructs were generated by the Gateway™ system (Gateway™ BP Clonase™ II Clonase Enzyme Mix and Gateway™ LR Clonase™ II Clonase Enzyme, ThermoFisher), following the manufacturer recommendations. The PCR products were amplified with primers specific (Table 5) for the desired targeted DNA, separated on a 1% Agarose gel to verify fragment size. Thereafter, PCR products were purified (GeneJet Gel Extraction kit, ThermoFisher), following the manufacturer's protocol and recommendations. Point mutations in the cytoplasmic domain of RLP44 were introduced with the reverse oligo. The purified PCR products were integrated into pDNOR207® by Gateway™ BP Clonase reaction following standardized protocol. After the recombination reaction, plasmids were used to transform chemically competent *Escherichia coli* XL1 Blue cells, which were then grown in Luria-Bertani (LB) medium, supplemented with the adequate antibiotic (Table 1). Correct fragment insertion was tested by check-PCR using proper primers (Table 5) and confirmed by sequencing of plasmids extracted from colonies transferred to liquid culture after miniprep extraction (GenElute™ Plasmid Miniprep Kit, Sigma-Aldrich) following manufacturer's procedure. After sequence confirmation, pDNOR207® were used to perform the Gateway™ LR clonase reaction using pK7RWG2, pK7FWG2 or pGWB14 (Karimi et al., 2002; Nakagawa et al., 2007). After the second recombination reaction, vectors were used to transform chemically competent *Escherichia coli* XL1 Blue cells which were grown in selection LB media. Correct fragment insertion was tested by check-PCR using proper primers (Table 5), colonies with correct inserted fragment were amplified by transferring them to liquid culture and plasmids for subsequent transformation of Agrobacteria were extracted from amplified colonies with a miniprep extraction (GenElute™ Plasmid Miniprep Kit, Sigma-Aldrich) following manufacturer's procedure.

For BiFC studies, the generated PCR product were integrated first in pDNOR221® P1P4 or pDNOR221® P2P3 by Gateway™ BP Clonase and after cloning and sequence verification, into pBiFCT 2in1-CC (Grefen and Blatt, 2014) by Gateway™ LR.

Luria-Bertani Medium: 0,5% (w/v) Bacto™ yeast extract (Roth), 1% Bacto™ tryptone (BD Biosciences), 1% (w/v) KCl. For preparing solid LB Medium, 1% of Bacto™ Agar (BD Biosciences) were added.

Antibiotics: 50 µg/ml Gentamycin, Spectinomycin or Kanamycin were added to the medium.

Table 1. Gateway constructs.

Construct	Plasmid	Selection marker	Comment	Cloning Technique
BRI1oSTOP	pDONR207	Gent+	Wolf et al., 2014	Gateway
BAK1oSTOP	pDONR207	Gent+	Holzward et al., In revision	Gateway
Lti6BoSTOP	pDONR201	Kan+	Holzward et al., In revision	Gateway
RLP44oSTOP	pDONR207	Gent+	Wolf et al., 2014	Gateway
BRI1:GFP	pK7FWG2	Spec+	Wolf et al., 2014	Gateway
BAK1:HA	pGWB14	Kan+	Holzward et al., In revision	Gateway
GFP:Lti6B	pK7FWG2	Spec+	Holzward et al., In revision	Gateway
RLP44:GFP	pK7FWG2	Spec+	Wolf et al., 2014	Gateway
RLP44:RFP	pK7RWWG2	Spec+	Wolf et al., 2014	Gateway
RLP44oSTOPoY	pDONR207	Gent+	Generated by S. Wolf	Gateway
RLP44oSTOPoY pdead	pDONR207	Gent+	Generated by S. Wolf	Gateway
RLPoSTOPoY SS-AA	pDONR207	Gent+	Generated by S. Wolf	Gateway
RLP44oSTOPoY T256A	pDONR207	Gent+	Generated by S. Wolf	Gateway
RLP44oSTOPoY S270A	pDONR207	Gent+	Generated by S. Wolf	Gateway
RLP44oSTOPoY S268A	pDONR207	Gent+	Generated by S. Wolf	Gateway
RLP44oSTOPoY Y274F	pDONR207	Gent+	Generated by S. Wolf	Gateway
RLP44oSTOPoY pmimic	pDONR201	Kan+	Generated by S. Wolf	Gateway
RLP44oSTOPoY SS-EE	pDONR207	Gent+	This study	Gateway
RLP44oSTOPoY T256E	pDONR207	Gent+	This study	Gateway
RLP44oSTOPoY S268E	pDONR207	Gent+	This study	Gateway
RLP44oSTOPoY S270E	pDONR207	Gent+	This study	Gateway
RLP44oSTOPoY Y272E	pDONR207	Gent+	This study	Gateway
RLP44oY:GFP	pK7FWG2	Spec+	Generated by S. Wolf	Gateway
RLP44oY:GFP pdead	pK7FWG2	Spec+	Generated by S. Wolf	Gateway
RLP44oY:GFP SS-AA	pK7FWG2	Spec+	Generated by S. Wolf	Gateway
RLP44oY:GFP T256A	pK7FWG2	Spec+	Generated by S. Wolf	Gateway
RLP44oY:GFP S268A	pK7FWG2	Spec+	Generated by S. Wolf	Gateway
RLP44oY:GFP S270A	pK7FWG2	Spec+	Generated by S. Wolf	Gateway
RLP44oY:GFP Y274F	pK7FWG2	Spec+	Generated by S. Wolf	Gateway
RLP44:GFP pmimic	pK7FWG2	Spec+	Generated by S. Wolf	Gateway
RLP44:GFP SS-EE	pK7FWG2	Spec+	This study	Gateway
RLP44oY:GFP T256E	pK7FWG2	Spec+	This study	Gateway
RLP44oY:GFP S268E	pK7FWG2	Spec+	This study	Gateway
RLP44oY:GFP S270E	pK7FWG2	Spec+	This study	Gateway
RLP44oY:GFP Y274E	pK7FWG2	Spec+	This study	Gateway

5.1.2. GreenGate Cloning

5.1.2.1. Entry module creation

The PCR products amplified with primers specific (Table 2) for the target DNA, separated on a 1% Agarose gel to verify fragment size, and the PCR products were purified (GeneJet Gel Extraction kit, ThermoFisher) following manufacturer's protocol and recommendations. Purified PCR product and empty entry vector (pGGC000) were independently digested with *Eco31I* FD (ThermoFisher) at room temperature, gently mixed and incubated at 37°C for 5 min.

Both digestion products were purified (GeneJet Gel Extraction kit, ThermoFisher) according to the manufacturer. Subsequently, 20-50 ng of digested empty vector a 2-3 fold excess of digested PCR product and digested empty vector were ligated using Instant Sticky-end Ligase Master Mix (New England Biolabs). After ligation, resulting plasmids were used to transform *Escherichia coli* strains DH5 α by performing a heat-shock at 42 °C for 45 s. After incubation at 37 °C with vigorous shaking (160 rpm) for 1-2 hours in LB medium, *E. coli* culture was centrifuged at 6000 rpm for 2 min, supernatant discarded and pellet gently resuspended, spread over LB-Agar medium supplied with 50 μ g/ml Ampicillin and incubated at 37 °C overnight. Correct fragment insertion was tested by check-PCR using proper primers (Table 5) and correct sequence was confirmed by sequencing of plasmids extracted from colonies transferred to liquid culture after miniprep extraction (GenElute™ Plasmid Miniprep Kit, Sigma-Aldrich) following manufacturer's procedure.

single colonies after miniprep extraction (GenElute™ Plasmid Miniprep Kit, Sigma-Aldrich) following manufacturer procedure.

5.1.2.2. Destination module creation

100 ng of the module containing the CDS of the gene-of-interest (module C) was mixed with 1.5 μ l of the rest of modules: module A (containing promoter), module B (containing an N-tag or a dummy sequence), module D (containing a C-tag or a dummy sequence), module E (containing a terminator) and module F (containing the Resistance) (Lampropoulos et al., 2013). 1 μ l of an empty destination module (pGGZ001 or pGGZ003) was added to the mix together with 1 μ l of *Eco31I* FD (ThermoFisher), 2 μ l of FastDigest buffer (ThermoFisher), 1.5 μ l of 10 mM ATP (ThermoFisher) and 1 μ l T4 DNA ligase (ThermoFisher). The reaction mix was subject to the following cycle in a PCR thermocycle (Biometra, AnalytikJena):

Temp. (°C)	time (s)	
37	120	30x
16	120	
50	300	
80	300	

After the thermocycling, 5 μ l of the resulting destination vector was used to transform chemically competent *Escherichia coli* strains DH5 α by performing a heat-shock at 42 °C for 45 s. After incubation at 37 °C with vigorous shaking (160 rpm) for 1-2 hours in LB medium, *E. coli* culture was centrifuged at 6000 rpm for 2 min, supernatant discarded and pellet gently resuspended, spread over LB-Agar

medium supplied with 50 µg/ml Kanamycin and incubated at 37 °C overnight. Correct fragment insertion was confirmed by PCR (primers depicted in Table 5) and sequencing of positive single colonies after miniprep extraction (GenElute™ Plasmid Miniprep Kit, Sigma-Aldrich) following manufacturer procedure.

Table 2. GreenGate constructs.

pSW 362	pRLP44:RLP44-(GS)₁₁-GFP			Holzwart et al.,
	<i>Name</i>	<i>Internal name</i>	<i>Source</i>	<i>Primers</i>
“Promoter” module	pRLP44	pSW299	Holzwart et al., In revision	
“N-tag” module	B-dummy	pGGB003	Lampropoulos et al., 2013	
“CDS” module	RLP44	pSW334	Holzwart et al., In revision	SW1179-1205
“C-tag” module	(GS) ₁₁ -GFP	pGGD001	Lampropoulos et al., 2013	
“Terminator” module	tUBQ10	pGGE009	Lampropoulos et al., 2013	
“Resistance” module	pMAS::BastaR::tMAS	pGGF001	Lampropoulos et al., 2013	
Destination vector		pGGZ0001	Lampropoulos et al., 2013	
pSW 567	pRLP44:RLP44^{pmimic}-(GS)₁₁-GFP			This study
	<i>Name</i>	<i>Internal name</i>	<i>Source</i>	<i>Primers</i>
“Promoter” module	pRLP44	pSW299	Holzwart et al., In revision	
“N-tag” module	B-dummy	pGGB003	Lampropoulos et al., 2013	
“CDS” module	RLP44 ^{pmimic}	pSW519	This study	SW1179-1368
“C-tag” module	(GS) ₁₁ -GFP	pGGD001	Lampropoulos et al., 2013	
“Terminator” module	tUBQ10	pGGE009	Lampropoulos et al., 2013	
“Resistance” module	SulfR	pGGF006	Lampropoulos et al., 2013	
Destination vector		pGGZ0001	Lampropoulos et al., 2013	
pSW 566	pRLP44:RLP44^{pdead}-(GS)₁₁-GFP			This study
	<i>Name</i>	<i>Internal name</i>	<i>Source</i>	<i>Primers</i>
“Promoter” module	pRLP44	pSW299	Holzwart et al., In revision	
“N-tag” module	B-dummy	pGGB003	Lampropoulos et al., 2013	
“CDS” module	RLP44 ^{pdead}	pSW518	This study	SW1179-1367
“C-tag” module	(GS) ₁₁ -GFP	pGGD001	Lampropoulos et al., 2013	
“Terminator” module	tUBQ10	pGGE009	Lampropoulos et al., 2013	
“Resistance” module	SulfR	pGGF006	Lampropoulos et al., 2013	
Destination vector		pGGZ0001	Lampropoulos et al., 2013	

pSW 731	pRLP44:RLP44-GAGA-GFP			This study
	<i>Name</i>	<i>Internal name</i>	<i>Source</i>	<i>Primers</i>
“Promoter” module	pRLP44	pSW299	Holzward et al., In revision	
“N-tag” module	B-dummy	pGGB003	Lampropoulos et al., 2013	
“CDS” module	RLP44	pSW334	Holzward et al., In revision	SW1179-1205
“C-tag” module	GAGA-GFP	pSW620	This study	SW1491-1492
“Terminator” module	tUBQ10	pGGE009	Lampropoulos et al., 2013	
“Resistance” module	SulfR	pGGF006	Lampropoulos et al.,2013	
Destination vector		pGGZ0001	Lampropoulos et al.,2013	
pSW 729	pRLP44:RLP44^{pmimic}-GAGA-GFP			This study
	<i>Name</i>	<i>Internal name</i>	<i>Source</i>	<i>Primers</i>
“Promoter” module	pRLP44	pSW299	Holzward et al., In revision	
“N-tag” module	B-dummy	pGGB003	Lampropoulos et al., 2013	
“CDS” module	RLP44 ^{pmimic}	pSW519	This study	SW1179-1368
“C-tag” module	GAGA-GFP	pSW620	This study	SW1491-1492
“Terminator” module	tUBQ10	pGGE009	Lampropoulos et al., 2013	
“Resistance” module	SulfR	pGGF006	Lampropoulos et al.,2013	
Destination vector		pGGZ0001	Lampropoulos et al.,2013	
pSW 727	pRLP44:RLP44^{pdead}-GAGA-GFP			This study
	<i>Name</i>	<i>Internal name</i>	<i>Source</i>	<i>Primers</i>
“Promoter” module	pRLP44	pSW299	Holzward et al., In revision	
“N-tag” module	B-dummy	pGGB003	Lampropoulos et al., 2013	
“CDS” module	RLP44 ^{pdead}	pSW518	This study	SW1179-1367
“C-tag” module	GAGA-GFP	pSW620	This study	SW1491-1492
“Terminator” module	tUBQ10	pGGE009	Lampropoulos et al., 2013	
“Resistance” module	SulfR	pGGF006	Lampropoulos et al.,2013	
Destination vector		pGGZ0001	Lampropoulos et al.,2013	
pSW 736	pRLP44:RLP44_ASSY-GAGA-GFP			This study
	<i>Name</i>	<i>Internal name</i>	<i>Source</i>	<i>Primers</i>
“Promoter” module	pRLP44	pSW299	Holzward et al., In revision	
“N-tag” module	B-dummy	pGGB003	Lampropoulos et al., 2013	
“CDS” module	RLP44_ASSY	pSW523	This study	SW1179-1205
“C-tag” module	GAGA-GFP	pSW620	This study	SW1491-1492
“Terminator” module	tUBQ10	pGGE009	Lampropoulos et al., 2013	
“Resistance” module	SulfR	pGGF006	Lampropoulos et al.,2013	
Destination vector		pGGZ0001	Lampropoulos et al.,2013	

pSW 737	pRLP44:RLP44_TASY-GAGA-GFP			This study
	<i>Name</i>	<i>Internal name</i>		<i>Name</i>
“Promoter” module	pRLP44	pSW299	“Promoter” module	pRLP44
“N-tag” module	B-dummy	pGGB003	“N-tag” module	B-dummy
“CDS” module	RLP44_TASY	pSW521	“CDS” module	RLP44_TASY
“C-tag” module	GAGA-GFP	pSW620	“C-tag” module	GAGA-GFP
“Terminator” module	tUBQ10	pGGE009	“Terminator” module	tUBQ10
“Resistance” module	SulfR	pGGF006	“Resistance” module	SulfR
Destination vector		pGGZ0001	Destination vector	
pSW 738	pRLP44:RLP44_TSAY-GAGA-GFP			This study
	<i>Name</i>	<i>Internal name</i>		<i>Name</i>
“Promoter” module	pRLP44	pSW299	“Promoter” module	pRLP44
“N-tag” module	B-dummy	pGGB003	“N-tag” module	B-dummy
“CDS” module	RLP44_TSAY	pSW592	“CDS” module	RLP44_TSAY
“C-tag” module	GAGA-GFP	pSW620	“C-tag” module	GAGA-GFP
“Terminator” module	tUBQ10	pGGE009	“Terminator” module	tUBQ10
“Resistance” module	SulfR	pGGF006	“Resistance” module	SulfR
Destination vector		pGGZ0001	Destination vector	
pSW 739	pRLP44:RLP44_TSSF-GAGA-GFP			This study
	<i>Name</i>	<i>Internal name</i>		<i>Name</i>
“Promoter” module	pRLP44	pSW299	“Promoter” module	pRLP44
“N-tag” module	B-dummy	pGGB003	“N-tag” module	B-dummy
“CDS” module	RLP44_TSSF	pSW522	“CDS” module	RLP44_TSSF
“C-tag” module	GAGA-GFP	pSW620	“C-tag” module	GAGA-GFP
“Terminator” module	tUBQ10	pGGE009	“Terminator” module	tUBQ10
“Resistance” module	SulfR	pGGF006	“Resistance” module	SulfR
Destination vector		pGGZ0001	Destination vector	

5.1.3. Transformation of competent *Agrobacterium tumefaciens*

For transformation of agrobacteria with different final Gateway™ vectors, *Agrobacterium tumefaciens* C58C1 containing the Ti-Plasmid pGV2260 was used. 2 µl of vector was pipetted into the competent *Agrobacterium* vial, carefully mixed and kept on ice for 2 minutes and transferred into an electrocuvette. *Agrobacterium* were subjected to an electrotransformation at 1.80 kV during 4-5 ms using an electroporator (BioRad MicroPulser™). Immediately, SOC medium was added into electrocuvette and the transformed *Agrobacterium* were transferred into a 1.5 ml Eppendorf containing SOC medium and incubated at 28°C with vigorous shaking (200 rpm) for 2-3 hours.

For the transformation with agrobacteria with the GreenGate final modules, chemically competent *A. tumefaciens* strain ASE (pSOUP⁺) were used. 5 µl of the GreenGate final module was pipetted into an

Agrobacterium vial, gently mixed and directly frozen into liquid Nitrogen for 5 min and incubated for other 5 additional minutes at 37°C. Afterwards, LB medium was added and *Agrobacterium* was incubated at 28°C with vigorous shaking (200 rpm) for 2-3 hours.

In both cases, after incubation, *Agrobacterium* were centrifuged at 6000 rpm for 2 minutes, the supernatant was mostly removed and the pellet gently resuspended using the remaining supernatant. Finally, the *Agrobacterium* resuspension was spread over a LB-Agar plate supplied with the corresponding antibiotics and grown at 28°C for 2 days.

SOC medium: 0.5% (w/v) Bacto™ yeast extract (Roth), 2% Bacto™ tryptone (BD Biosciences), 10 mM NaCl, 2.5 mM KCl, 10 mM MgCl₂, 10mM MgSO₄ and 20 mM Glucose.

Antibiotics: For C58C1 strain 50 µg/ml of Carbenicillin (Ti-plasmid) and 100 µg/ml of Rifampicin (genomic resistance) were added. Additionally, 50 µg/ml of Kanamycin or 100 µg/ml Spectinomycin depending on the vector. For ASE strain 50 µg/ml of Chloramphenicol, Kanamycin (genomic resistance), Tetracyclin (pSOUP resistance) were added and Spectinomycin (vector resistance).

5.1.4. Stable transformation of *Arabidopsis thaliana*

All constructs described in Table 1 and Table 2 were used to generate stable expressing lines of *Arabidopsis thaliana* ecotype Col-0 and mutant *cnu2*. For that purpose, a single positive *Agrobacterium* colony was regrown in a LB-Agar medium plate supplied with the correspondent antibiotics and grown for 2 days at 28 °C in order to generate a master plate. From the master plate, *Agrobacterium* were spread on a LB-agar selective plate and grown for other 2 days at 28 °C. 2 days before transformation, *Agrobacterium* were re streaked on 2 fresh selective LB-Agar plates and grown at 28 °C. 15 mL of fresh LB medium was added to each plate and *Agrobacterium* were scraped into a 16 cm² plastic container. *Agrobacterium* enriched LB medium was added to 120 mL of transformation solution. This suspension was used to transform approx. 5-week-old *Arabidopsis* plants via floral dip (Clough and Bent 1998). Bolting plants with a large number of young, unopened flowers were dipped for 1 min in the *Agrobacterium* solution. Afterwards, plants were sprayed with water and covered with a lid to maintain the humidity and transferred to a light-protected place for 24 h. This process was repeated with same plants 5-7 days later to increase transformation efficiency. After that, plants were grown in under long day conditions at 22 °C.

Selection of transformed seeds was done on sterile plant agar plates containing ½ MS, 1 % Sucrose, pH 5.8 and 0.7 % phytoagar supplied with 100 µg/ml of the corresponding selective agent. Seedlings were grown for 8-10 days. Resistant plants were transferred to soil and grown at long day conditions at 22 °C.

Transformation solution: 5% (w/v) Sucrose, 0.03 % (v/v) Silwet L-77 (Lehle Seeds).

5.2. Plant material and growth conditions

5.2.1. General growth conditions

Seeds were sterilized in a solution containing 70% ethanol and 10% sodium hypochlorite for 5 minutes and washed twice with absolute ethanol for an additional 2 minutes. After removing ethanol, seeds were dried under aseptic conditions for 2 hours.

Seeds were grown on half-strength Murashine-Skoog (MS) medium (Duchefa) supplemented with 0.7 or 0.9% (w/v) plant agar (Duchefa) and 1% (w/v) Sucrose (Roth) when needed. Medium pH was adjusted to 5.8 with KOH. All seed were stratified for 48 hours in the dark at 4°C and plates with seedlings were placed to growth chambers (Conviron) with long day conditions (16 hours photoperiod, 100 $\mu\text{E m}^{-2} \text{s}^{-1}$ light intensity, 60-70% humidity and 22°C) for 6-7 days in a vertical position unless otherwise stated.

Seedlings were transferred to CLT-SM substrate (Enheiterde Classic) after 6-7 days into a growth room under long day conditions (16 hours photoperiod, 100 $\mu\text{E m}^{-2} \text{s}^{-1}$ light intensity, 65% humidity and 22°C). Pictures of rosettes were taken 18-20 days after plants were transferred to soil. Soon after bolting, seed collectors were placed over the plants and they were kept until seed collection after plants were dried.

5.2.2. Crossing *A. thaliana*

Bolting 4-weeks-old plants were used for crossing. On one of the two parent plants, a healthy looking inflorescence were chosen, all the already formed siliques and all but the 4-5 largest flowers buds were removed. Of the remaining buds, the sepals, petals and stamens were removed carefully with sharped forceps under a stereo dissecting microscope. Anthers of the other parental plant were rubbed on the carpel until it was completely covered with pollen. Crossed plants were kept in long day conditions and successfully crossed siliques harvested once dried.

5.2.3. Transgenic lines

The following *Arabidopsis thaliana* transgenic lines, T-DNA insertions and genetic backgrounds were used in this study:

Table 3. Mutant alleles and transgenic lines.

Ecotype or line	Source/Reference
Col-0 (Columbia-0) ecotype	Arabidopsis biological resource center (ABRC, Ohio state University, OH)
Ler (Landsberg erecta) ecotype	Arabidopsis biological resource center (ABRC, Ohio state University, OH)
<i>rlp44^{cnu2}</i>	Wolf et al., 2014
<i>bri1-301</i>	Li and Nam et al., 2002
<i>bri1^{cnu4}</i>	Holzwardt et al., In revision
<i>bri1-null</i>	Jaillais et al.,
<i>serk1-3 serk3-1 serk4-1</i>	donated by Dr. Santiago-Cuellar
<i>pskr1-3</i>	Kutschmar et al., 2009
<i>pskr1-3 pskr2-1</i>	Kutschmar et al., 2009
PMElox	Wolf et al., 2012
<i>cnu2</i>	Wolf et al., 2014

Ecotype or line	Source/Reference
amiR-TPLATE	Gadeyne et al., 2014
Lti6B-GFP	Cutler et al., 2000
35S:RLP44-RFP	Wolf et al., 2014
<i>bri1null rlp44^{cnu2}</i>	This study
pRLP44:RLP44-(GS) ₁₁ -GFP (Col-0)	Holzward et al., In revision
pRLP44:RLP44-(GS) ₁₁ -GFP (<i>rlp44^{cnu2}</i>)	Holzward et al., In revision
pRLP44:RLP44-(GS) ₁₁ -GFP (<i>bri1-301</i>)	This study
pRLP44:RLP44-(GS) ₁₁ -GFP (<i>bri1^{cnu4}</i>)	This study
pRLP44:RLP44-(GS) ₁₁ -GFP (<i>bri1-null</i>)	This study
pRLP44:RLP44-(GS) ₁₁ -GFP (<i>serk1-3 serk3-1 serk4-1</i>)	This study
pRLP44:RLP44-(GS) ₁₁ -GFP (<i>pskr1-3</i>)	This study
pRLP44:RLP44-(GS) ₁₁ -GFP (<i>cnu2</i>)	This study
pRLP44:RLP44pmimic-(GS) ₁₁ -GFP (<i>cnu2</i>)	This study
pRLP44:RLP44pdead-(GS) ₁₁ -GFP (<i>cnu2</i>)	This study
35S:RLP44-GFP (<i>cnu2</i>)	This study
35S:RLP44-GFP phospho-mimic (<i>cnu2</i>)	This study
35S:RLP44-GFP phospho-dead (<i>cnu2</i>)	This study
35S:RLP44_ASSY-GFP (<i>cnu2</i>)	This study
35S:RLP44_TASY-GFP (<i>cnu2</i>)	This study
35S:RLP44_TSAY-GFP (<i>cnu2</i>)	This study
35S:RLP44_TSSF-GFP (<i>cnu2</i>)	This study
35S:RLP44_TAAAY-GFP (<i>cnu2</i>)	This study
35S:RLP44_ESSY-GFP (<i>cnu2</i>)	This study
35S:RLP44_TESY-GFP (<i>cnu2</i>)	This study
35S:RLP44_TSEY-GFP (<i>cnu2</i>)	This study
35S:RLP44_TSSE-GFP (<i>cnu2</i>)	This study
35S:RLP44_TEEY-GFP (<i>cnu2</i>)	This study
pRLP44:RLP44-GAGA-GFP (<i>cnu2</i>)	This study
pRLP44:RLP44pmimic-GAGA-GFP (<i>cnu2</i>)	This study
pRLP44:RLP44pdead-GAGA-GFP (<i>cnu2</i>)	This study
pRLP44:RLP44_ASSY-GAGA-GFP (<i>cnu2</i>)	This study
pRLP44:RLP44_TASY-GAGA-GFP (<i>cnu2</i>)	This study
pRLP44:RLP44_TSAY-GAGA-GFP (<i>cnu2</i>)	This study
pRLP44:RLP44_TSSF-GAGA-GFP (<i>cnu2</i>)	This study
35S:RLP44-GFP (amiR-TPLATE)	This study
35S:RLP44-GFP phospho-dead (amiR-TPLATE)	This study
35S:BRI1-GFP	Frierichsen et al., 2000
pBRI1:BRI1-mCit, pBAK1:BAK1-HA (<i>bri1-null</i>)	donated by Prof. M. Hothorn
pBRI1:BRI1-mCit, pBAK1:BAK1-HA, 35S:RLP44-RFP (<i>bri1-null</i>)	This study
35S:RLP44-GFP (Col-0)	This study
35S:RLP44-GFP phospho-mimic (Col-0)	This study
35S:RLP44-GFP phospho-dead (Col-0)	This study
35S:RLP44-GFP (<i>bri1-301</i>)	This study
35S:RLP44-GFP phospho-mimic (<i>bri1-301</i>)	This study
35S:RLP44-GFP phospho-dead (<i>bri1-301</i>)	This study
35S:RLP44-GFP (<i>bri1-null</i>)	This study
35S:RLP44-GFP phospho-mimic (<i>bri1-null</i>)	This study
35S:RLP44-GFP phospho-dead (<i>bri1-null</i>)	This study
35S:RLP44-GFP (<i>rlp44^{cnu2}</i>)	This study
35S:RLP44-GFP phospho-mimic (<i>rlp44^{cnu2}</i>)	This study
35S:RLP44-GFP phospho-dead (<i>rlp44^{cnu2}</i>)	This study
35S:RLP44-GFP (<i>bri1-null rlp44^{cnu2}</i>)	This study
35S:RLP44-GFP phospho-mimic (<i>bri1-null rlp44^{cnu2}</i>)	This study
35S:RLP44-GFP phospho-dead (<i>bri1-null rlp44^{cnu2}</i>)	This study
RRE 9.2	This study
RRE 11.1	This study
RRE 24.1	This study
RRE 38.6	This study

5.2.4. gDNA Extraction

Isolation of Arabidopsis DNA was performed according to (Edwards et al., 1991) with modifications. Around 100 mg of young leaf tissue, previously frozen with liquid nitrogen directly after harvest, were homogenized by a tissue lyser (TissueLyserII, Qiagen). 400 µl of gDNA extraction buffer were added to the sample and the homogenate was centrifuged at 13.000 rpm for 10 min. 150 µl of supernatant were transferred to a fresh Eppendorf tube and mixed with 1 volume of Isopropanol and centrifuged for 10 min at 13.000 rpm. The pellet was washed with 150 µl of 70% (v/v) of ethanol by centrifugation at 13.000 rpm for 5 min. 70% Ethanol was discarded, the pellet air dried and dissolved with 30 µl of low TE buffer.

gDNA Extraction Buffer: 150 mM Tris-HCl (pH 8), 250 mM NaCl, 25 mM EDTA 0.5% (w/v) SDS.

low TE buffer: 10 mM Tris-HCl (pH 8), 0.5 mM EDTA.

5.2.5. Genotyping

Presence of the *rlp44^{cnu2}* mutation was assessed by a CAPS marker using primers at3g49750_SP1_F and rlp44-4_CAPS_R and subsequent HinfI digestion. The *bri1-301* mutation was genotyped with the primers bri1-301_CAPS_F and bri1-301_CAPS_R followed by Bsp143I digestion. The *bri1^{cnu4}* mutation was detected by using bri1cnu4_CAPS_F and bri1cnu4_CAPS_R followed by a digestion with BseLI. For the genotyping of *bri1-null* t-DNA insertion line, BRI1-GK_WT_F and primer BRI1_3'UTR_R were used for detection of the wild-type allele. Presence of the t-DNA insertion was assessed with primers GK-o8409 and BRI1_GK-134E10_R. For genotyping *pskr1-3* t-DNA insertion line, pskr1-3_F and pskr1-3_R primers were used to assess wild-type allele; and LBb1.3 and pskr1-3_R to assess the t-DNA insertion. The *serk1-3* t-DNA insertion was genotyped using serk1-3_F and GK-o8409 for the WT allele and serk1-3_F and serk1-3_R. The *serk3-1* mutation was checked using serk3-1_LP and serk3-1_RP for the WT allele or LBb1.3 and serk3-1_RP for the t-DNA insertion. To assess *serk4-1* mutation, serk4-1_LP and serk4-1_RP primers were used for the WT allele or LBb1.3 and serk4-1_RP for t-DNA insertion. Gateway insertions were checked by using attB1 and attB2 primers. Greengate insertions were analyzed by using pGG-Bdummy_F and pGGA/C000_R.

5.3. Root length measurements

To study the response to different growth conditions, root length of seedlings was measured by plating them in half strength MS medium supplied with 1% Sucrose and 0.9% phytoagar. For BL root growth response, plates were supplied with 2 µM Propiconazole (PPZ, Sigma-Aldrich) without or together with 0.1, 1, 10 and 100 nM of Brassinolide (BL, Santa Cruz Biotech), respectively. For PSK response, plates were supplied with 10 nM α-PSK (PolyPeptide). For salt stress response, medium was prepared together with 25, 50, 75 and 150 mM of NaCl (Sigma-Aldrich).

After stratification, plates were placed in growth chambers and scanned after 6 days of growth in long day conditions. Images were analyzed with the image-processing program *Image J* (<https://imagej.nih.gov/ij/>), by measuring the length of the root from the root tip to the transition to hypocotyl. Average or average normalized to the mock control together with the standard deviations of, at least 50 plants, were plotted for each experiment.

Chemicals stocks: PPZ (Sigma-Aldrich) 100 mM stock dissolved in Dimethylsulfoxid (DMSO); BL (Santa Cruz Biotech) 10 mM stock in 80% Ethanol. α -PSK (PolyPeptide): 10 mM stock in desalted water.

5.4. Hypocotyl length measurements

To determine seedlings hypocotyl length, seeds were plated in half strength MS medium supplied with 0.7% phytoagar. For agravitropic response, plates were supplied with 2 μ M PPZ (Sigma-Aldrich) together with 5, 10, 100, 500 or 1000 nM of BL (Santa Cruz Biotech) For isoxaben response, plates were supplied with 100 μ M isoxaben (Sigma-Aldrich) from a 1 mM stock solution.

After Stratification, plates were exposed to light for 6 hours on a horizontal position and afterwards wrapped with aluminum foil. After 5 days of growth in darkness, plates were scanned and images analyzed with *ImageJ* by measuring the length of the hypocotyls from the apical meristem to the point to transition to the root. The average and standard deviations of at least 30 plants were plotted for each experiment.

Chemicals stocks: PPZ (Sigma-Aldrich) 100 mM stock dissolved in DMSO; BL (Santa Cruz Biotech) 10 mM stock in 80% Ethanol. Isoxaben (Sigma-Aldrich) 10 mM stock in Ethanol.

5.5. Phosphorylation studies

To study the phosphorylation status of RLP44 in different mutant backgrounds, around 100 seeds per well were disposed in 6-well-plates (Corning) containing 5 mL of liquid $\frac{1}{2}$ MS medium supplied with 1% sucrose. After stratification, plates were placed into growth chambers with long day conditions and kept in agitation (100 rpm). 3-days-after germination, seedlings were treated with 5 μ M PPZ (Sigma-Aldrich). 6-days-after germination and 3-hours-before harvesting, seedlings were treated independently with 50 μ M Cantharidin (Sigma-Aldrich), 2 μ M K-252a (Enzo Life Sciences) or 50 μ M of DMSO. 1.5-hours-before harvesting, seedlings were treated with 1 μ M BL or 80% Ethanol. Afterwards, plant material was carefully collected, weight and directly froze in liquid N₂.

Chemicals stocks: PPZ (Sigma-Aldrich) 100 mM stock dissolved in DMSO; Cantharidin (Sigma-Aldrich) 100 mM stock in DMSO, K-252a (Enzo Life Sciences) 1 mM stock in DMSO BL (Santa Cruz Biotech) 10 mM stock in 80% Ethanol.

5.6. EMS mutation mapping

5.6.1. EMS mutation procedure

For the generation of suppressor mutants of the 35S:RFP44-RFP (Col-0) (RFP44ox) phenotype, around 30.000 seeds placed on 50 mL Falcon® were mutagenized by keeping them for 10 h on 0.3% (w/v) Ethyl Methanesulfonate (EMS) (Sigma-Aldrich) aqueous solution in a rotational shaker. Seeds were washed 15 times for 5 minutes with water and seeds were transferred to ½ MS pH 5.8 plates supplied with 0.1 % (w/v) of phytoagar. Around 2000 seeds were sown per 72 independent pools and grown under long day conditions. After bolting and silique production, the total amount of seeds per pool was harvest independently. Screening of M2 seedlings was performed by checking for seedlings with an RFP44ox suppressor phenotype grown for 7 days on ½ MS pH 5.8 plates supplied with 0.9 % phytoagar and the correspondent antibiotic. Selected plants were transferred to soil and grown in long day conditions and their seeds were collected for subsequent analysis.

5.6.2. Population creation for Next Generation Sequencing (NGS)

Selected RRE mutants (in a Col-0 background) were crossed with *Arabidopsis thaliana* Ler-0 ecotype. F1 plants were grown and seeds collected independently. F2 seeds were grown in ½ MS 0.9% (w/v) phytoagar supplied with Kanamycin for 7 days in long day conditions. Resistant plants were then transferred to soil and subjected to phenotypic selection. 150 to 200 plants for each RRE mutant showing a suppressor-like phenotype (Not RFP44ox) were selected. Sample material of each plant was taken, combined, frozen on Liquid N₂ and stored at -80°C. Genomic DNA was extracted using the DNeasy® DNA Extraction kit (Qiagen) following manufacturer recommendations. At least, 100 ng/µl of DNA per sample was used for NGS by Illumina HiSeq 2500 system (Eurofins Genomics).

5.6.3. Analysis of SNPs

Sequences of the F2 pooled population were analyzed by Next Generation Mapping (NGM) similar to (Austin et al., 2011). Using Bowtie2 (<http://bowtie-bio.sourceforge.net/bowtie2>), the entire short reads acquired by Illumina were aligned and mapped to the reference *Arabidopsis thaliana* genome available (TAIR10). Alignments were pileup and refined and SNPs were called and filtered to generate a bam file by Samtools (<http://samtools.sourceforge.net/>). BAM file were used for the localization of Chromosome region of the mutation and selection of candidate SNPs using the web-based tool for NGM available in www.bar.utoronto.ca/ngm/. Candidate SNPs were further confirmed by Sanger sequencing.

5.7. RNA extraction and qPCR

For RNA analysis, a maximum of 100 mg of frozen *Arabidopsis thaliana* seedlings material was ground in an eppendorf tube with the aid of a pre-cooled tissue lyser (TissuelyserII, Qiagen). RNA from ground tissue was extracted with the RNA purification Kit (Roboklon), following the manufacturer instructions. The obtained RNA was quantified in a NANODROP. For cDNA synthesis, 1µg of RNA was mixed in 5,75 µl RNAase free water and 0,625 µl 10mM dNTPs (Sigma-Aldrich) and 0,625 µl 40µM Oligo(dT)

(ThermoFisher Technologies). The mix was incubated at 65°C for 5 minutes and kept on ice for another additional 5 min. Immediately after, 2 µl 5x RT Reaction Buffer (EURx), 0.5 µl RNase inhibitor 40u/µl, 0.5 µl DTT (Sigma-Aldrich) and 0.25 µl of AMV Reverse Transcriptase (EURx), were added to the mix. Reaction was incubated for 1 h at 42°C followed by 5 min at 85°C. The cDNA generated, was stored at -20°C. The cDNA reaction was diluted 1:10 in water and used for qPCR analysis with primers specific to the desired genes. The SYBR® Green I nucleic acid gel stain (Sigma-Aldrich) was used for amplification, with the CLATHRIN (At1g10730) gene used as internal control. qPCR reactions were run in a Rotor-Gene Q 2plex (Qiagen) and the amplification data analyzed by the 75 Rotor-Gene Q 2plex software.

5.8. Transient expression studies

For Agroinfiltration of *Nicotiana benthamiana* leaves, *Agrobacterium tumefaciens* strains C58C1 (for Gateway constructs) or ASE (For Greengate constructs), transformed according to previously described method (section 5.1.3) written method, were used. As pre culture, single positive *Agrobacterium* colonies were grown in 5 mL of LB medium supplied with the corresponding antibiotics overnight at 28 °C with gently agitation (200 rpm). The main culture was started by transferring 100 µl of the pre culture into 30 mL of LB medium supplied with the corresponding antibiotics. The main culture was grown overnight at 28 °C with vigorous shaking (200 rpm). Thereafter, the *Agrobacterium* culture was centrifuged for 30 min at 3000 rpm, the supernatant discarded and the pellet resuspended in 10 mL of distilled water. Re-suspended culture was starved for 1 h at RT under moderate agitation (100 rpm). *Agrobacterium* concentration at OD₆₀₀ was measured and adjusted to OD₆₀₀ of 1 when necessary.

2-3 weeks old *Nicotiana benthamiana* plants were grown under long day conditions (16 hours photoperiod, 100 µE m⁻² s⁻¹ light intensity, 65% humidity and 25°C). 3 h before agro infiltration, plants were move to lab light and kept under humid conditions. For simple transient expression or BiFC studies, independent *Agrobacterium* cultures carrying different constructs were used. For co-immunoprecipitation studies, suspensions combining *Agrobacterium* with different constructs at the same concentration were used. In all cases, infiltration of the abaxial side of *N. benthamiana* leaves using a 1.5 mL syringe was performed. After agroinfiltration, *N. benthamiana* leaves were kept in a humid and light protected environment overnight and transferred to long day conditions afterwards.

Two days after infiltration, leaf discs were used for confocal microscope observation of fluorescent signal and BiFC or several leaves were collected and frozen in liquid nitrogen for subsequent protein extraction.

5.9. BiFC (Bi-molecular Fluorescent Complementation)

The different pENTRY™ constructs generated by Gateway technology are depicted in table 4 and were used for the generation of destination vectors using the plasmid pBiFCT 2in1-CC (Grefen and Blatt, 2014), a constructs carrying the paired genes of interest linked to nYFP or cYFP together and also

containing 35S:RFP to use for normalization of the YFP signal. To test interaction, the different pBiFCT 2in1-CC constructs were agroinfiltrated in *N. benthamiana* leaves. Leaf discs were analyzed under confocal microscopy (Zeiss LSM 510 Meta) for YFP and RFP activity. 4 positives images were taken per disc, 2 disc leaves per leaf were analyzed and 9 different leaves in 3 independent experiments were considered for the image analysis.

Table 4. BiFC constructs.

Construct	Plasmid	Selection marker	Comment	Cloning Technique
BRI1 nYFP	pDONR221 P2P3	Kan+	This study	Gateway
BRI1 cYFP	pDONR221 P1P4	Kan+	This study	Gateway
BAK1 nYFP	pDONR221 P2P3	Kan+	This study	Gateway
FLS2 cYFP	pDONR221 P1P4	Kan+	This study	Gateway
FLS2 nYFP	pDONR221 P2P3	Kan+	This study	Gateway
RLP44_WT cYFP	pDONR221 P1P4	Kan+	This study	Gateway
RLP44pmimic cYFP	pDONR221 P1P4	Kan+	This study	Gateway
RLP44pdead cYFP	pDONR221 P1P4	Kan+	This study	Gateway
BAK1nYFP-BRI1cYFP	pBiFCT 2in1-CC	Spec+	This study	Gateway
BRI1nYFP-FLS2cYFP	pBiFCT 2in1-CC	Spec+	This study	Gateway
BAK1nYFP-RLP44_WTcYFP	pBiFCT 2in1-CC	Spec+	This study	Gateway
BAK1nYFP-RLP44pmimic-cYFP	pBiFCT 2in1-CC	Spec+	This study	Gateway
BAK1nYFP-RLP44pdead-cYFP	pBiFCT 2in1-CC	Spec+	This study	Gateway
BRI1nYFP-RLP44_WTcYFP	pBiFCT 2in1-CC	Spec+	This study	Gateway
BRI1nYFP-RLP44pmimic-cYFP	pBiFCT 2in1-CC	Spec+	This study	Gateway
BRI1nYFP-RLP44pdead-cYFP	pBiFCT 2in1-CC	Spec+	This study	Gateway
FLS2nYFP-RLP44_WTcYFP	pBiFCT 2in1-CC	Spec+	This study	Gateway
FLS2nYFP-RLP44pmimic-cYFP	pBiFCT 2in1-CC	Spec+	This study	Gateway
FLS2nYFP-RLP44pdead-cYFP	pBiFCT 2in1-CC	Spec+	This study	Gateway

5.10. Co-immunoprecipitation (Co-IP) and Western blotting

For protein analysis, *A. thaliana* seedlings or *N. benthamiana* leaves frozen in liquid nitrogen and stored at -80 °C were ground to powder with the aid of a mortar pre-cooled with liquid nitrogen and extracted with 1:2 (w/v) of protein extraction buffer. Extracts were always kept on ice and clarified by centrifugation at 13000 rpm during 15 min at 4 °C. Supernatants were carefully collected into a new tube and centrifuged again for 10 min at 13000 rpm to remove all plant debris. 20 µl of the protein extract were separated in a new tube to be used as an input fraction. The rest of extract was incubated with 20 µl of 50% slurry anti-tag MicroBeads (Chromotek GFP-Trap® or RFP-Trap®, depending on the tag attached to the protein of interest) for 2-3 h at 4 °C with continuous rotation. Before incubation with extract, anti-tag beads were equilibrated for 2 minutes in 1 mL protein extraction buffer, after which the supernatant was removed by centrifugation at 4 °C and 500 rpm. After incubation with extract, the beads were pelleted for 5 min at 4 °C and 500 rpm, the supernatant was discarded, and 1 mL of washing buffer was

added at 4 °C for 5 minutes under continuous rotation. This washing procedure was repeated three times. After removal of the supernatant of the last washing step, 1:2 ratio (v/v) of commercial SDS-PAGE loading buffer (Roti®-Load 1, CarlRoth) was added to the input and bead samples, heated at 95 °C for 10 min and conserved at 4 °C.

For western blot analysis, adjusted inputs and beads fractions were loaded in self-prepared SDS-PAGE gels (12 or 10% gels for RLP44 and LT16B detection, 8% for BAK1 and 6% for BRI1 or PSKR1). After running SDS-PAGE gels in running buffer, proteins were transferred to a PVDF membrane (Immobilon-P, Millipore) using a semidry Transfer blot system. The PVDF membrane was blocked for 1 h at RT with 5 % BSA (CarlRoth) in 1X TBST buffer and subsequently probed with the correspondent primary antibody, diluted in 1 % BSA in 1X TBST buffer, overnight at 4 °C. Membranes were washed 8 times for 5 min with 1X TBST buffer and incubated with the corresponding secondary antibody (coupled to horseradish peroxidase) diluted in 1% BSA 1X TBST buffer for 1 h at RT. Membranes were again washed 8 times for 5 minutes before being imaged.

Protein Extraction Buffer: 100 mM Tris-HCl (pH 8.0), 150 mM NaCl, 10% (v/v) Glycerol. Added fresh: 5 mM EDTA (Sigma-Aldrich), 2 mM DTT (Sigma-Aldrich), 2 mM PMSF (Sigma-Aldrich), 1% (v/v) Protease Inhibitor Cocktail (Bimake), 2% (v/v) Igepal CA-630 (Sigma-Aldrich).

Washing Buffer: 100 mM Tris-HCl (pH 8.0), 150 mM NaCl, 10% (v/v) Glycerol. Added fresh: 2 mM DTT (Sigma-Aldrich), 1% (v/v) Protease Inhibitor Cocktail (Bimake), 0.2% (v/v) Igepal CA-630 (Sigma-Aldrich).

10X Running Buffer: 250 mM Tris, 1.92 M Glycine, 35 mM SDS.

Semidry buffer: 20% (v/v) Methanol (HPLC-rate, Sigma-Aldrich), 48 mM Tris, 39 mM Glycin, 0.0375 % (v/v) SDS (Sigma-Aldrich).

10X TBST buffer: 0.2 M Tris-HCl (pH 7.4), 1.5 M NaCl, 0.5% (v/v) Tween®-20 (Panreac).

Antibodies: **anti-GFP** (Biolegend) Purified mouse monoclonal IgG. Dilution 1:10000; **anti-RFP** (Karin Schumacher) Purified rabbit polyclonal IgG. Dilution 1:10000; **anti-HA** (F-7, SantaCruz Biotechnology) Purified mouse monoclonal IgG. Dilution 1:5000; **anti-BRI1** (Bojar et al., 2014) Purified rabbit polyclonal IgG. Dilution 1:5000; **anti-BAK1** (Bojar et al., 2014) Purified rabbit polyclonal IgG. Dilution 1:5000; **anti-rabbit IgG** (Thermo-Fisher) Purified goat polyclonal IgG horseradish peroxidase conjugate. Dilution 1:10000; **anti-mouse IgG** (Sigma-Aldrich) Purified rabbit polyclonal IgG horseradish peroxidase conjugate. Dilution 1:10000.

Western detection: For antibody detection, the membranes were incubated with the SuperSignal™ west pico chemiluminescent Substract (ThermoFisher Scientific) or the SuperSignal™ west femto chemiluminescent Substract (ThermoFisher Scientific), and exposed using an ECL Imager (INTAS).

5.11. Confocal microscopy

5.11.1. Confocal laser scanning microscopy

Confocal laser scanning microscopy (CLSM) of *Arabidopsis thaliana* roots and *Nicotiana benthamiana* leaf discs was performed on a TCS SP5 II inverted Confocal Laser Scanning Microscope (Leica) or a LSM 510 Meta Confocal Laser Scanning Microscope (Zeiss). In the first case a HCX PL APO lambda blue 63.0x1.20 water immersion objective (Leica) was used. In the second case, a Plan-Neofluar 5.0x1.05, Plan-Neofluar 25.0x0.80 water immersion and C-Apochromat 63.0x1.20 water immersion objectives were used. Excitation bandwidth was set at 488 nm for GFP, at 514 for YFP and 561 nm for RFP or mCherry with VIS-Argon (Leica) or VIS-DPSS 561 (Leica) lasers for TCS SP5 CLSM and LSM-Argon (Zeiss) or LSM-He-Ne (Zeiss) for LSM 510 CLSM. Emission was detected at 500-545 nm for GFP, at 545-573 nm for YFP and 620-670 nm for RFP or mCherry using HyD hybrid detectors (Leica) or photomultipliers (PMT) detectors (Zeiss).

5.11.2. Inhibitor treatments

6 days-old seedlings of the previously indicated *Arabidopsis thaliana* transgenic lines were incubated in 12-well plates using liquid ½ MS pH 5.8 supplied with 20 µM Wortmannin (WM) (Sigma-Aldrich) or 50 µM of Brefeldin A (BFA) (Sigma-Aldrich). As control, same volume of DMSO (Sigma-Aldrich) was applied. Incubation for both inhibitors took place at 22°C and in the dark 165 min (for WM) or 120 min (for BFA) before imaging.

5.11.3. FM4-64 staining

FM4-64 staining was performed in liquid ½ MS, pH 5.8 with 1 µM FM4-64 (Molecular probes) for 15 min. Seedlings were imaged with CLSM using 561 nm laser line for excitation and 670-750 nm range for emission detection.

5.11.4. Basic Fuchsin staining

6 days-old seedlings of indicated *Arabidopsis thaliana* transgenic lines were fixed in 6-well plates in Methanol (Sigma-Aldrich) for 3 h at RT. Methanol was exchanged with 10% (v/v) NaOH and seedlings were incubated for 3 h at 65°C. NaOH was removed and seedlings were stained with 0.01% (w/v) of Basic Fuchsin (Sigma-Aldrich) for 5 min. Fuchsin was removed and seedlings destained in 70% (v/v) Ethanol for 10 min. Ethanol was exchanged with 50% (v/v) Glycerol and seedlings on 6-well plates stored overnight at 4 °C. Seedlings were mounted on slides with 50% (v/v) glycerol and sealed. Seedlings were imaged with CLSM (Zeiss LSM 510 Meta) using 514 nm laser line for excitation and detected with 420-480 nm band pass filter. e. Basic fuchsin staining of xylem tissue was visualized by taking z-stack with transverse root sections imaged 1 mm below the collet.

5.11.5. Cell Wall polysaccharides antibodies staining

10-to-12 cm long shoots of recently bolted *Arabidopsis thaliana* EMS mutated plants were cut and the 2 cm closer to rosette embedded in 7% (w/v) Agarose. Fixed shoots were cut manually with a razor blade to obtain 1-2 mm cross-sections and then conserved at 4°C in absolute Ethanol in 24-well plates.

Prior to staining process, cross-sections were washed with distilled water for 10 min. For immunolabeling with 2F4 antibody, cross-sections were rinsed in 2F4 Buffer for 10 minutes. Samples were then incubated with 2F4 antibody diluted 1:250 (v/v) in 2F4 buffer with 5% milk for one hour under gentle shaking. Cross-sections were washed three times and incubated with secondary antibody (anti-mouse) diluted 1:1000 in 2F4 buffer supplied with 5% milk for 3 hours in the dark and then washed three times with 2F4 buffer. For immunolabeling with JIM7, LM19 and LM20, cross-sections were first washed for 10 minutes in 1X PBS buffer and then incubated with the different antibodies diluted 1:25 in 1X PBS buffer supplied with 1% (w/v) BSA and 0.05% (v/v) Tween20 (Sigma-Aldrich) for 1h at RT and constant shaking. Cross-sections were washed 3 times with 1X PBS and then incubated with secondary antibody (anti-rat) diluted 1:1000 in 1X PBS for 3h in darkness. Cross-sections were washed 3 times.

Z-Stacks of Cross-sections were taken with Zeiss CLSM 510 Meta using 495 nm laser line for excitation of 2F4 immunolabeled samples and 562 nm for excitation of JIM7, LM19 and LM20.

2F4 Buffer: (20mM Tris-HCl (pH 8,2), 0.5 mM CaCl₂, 150 mM NaCl).

Antibodies: **2F4** (Anti-homogalacturonan, PlantProbes) Unpurified mouse monoclonal IgG1. Dilution 1:1000; **JIM7** (Anti-homogalacturonan, PlantProbes) Purified rat monoclonal IgA. Dilution 1:30; **LM19** (Anti-homogalacturonan, PlantProbes) Purified rat monoclonal IgM. Dilution 1:30; **LM20** (Anti-homogalacturonan, PlantProbes) Purified rat monoclonal IgM. Dilution 1:30; **anti-Mouse** (ThermoFischer) Purified polyclonal goat IgG anti-Mouse (H+L) antibody Alexa-Fluor 488 © conjugated. Dilution 1:1000; **anti-rat** (ThermoFisher) Purified polyclonal IgG anti-rat (H+L) antibody Cyanine3 (Cy3) conjugated.

5.12. Image analysis

5.12.1. Non-quantitative analysis

Images for non-quantitative analysis were processed using "Image J". When necessary, background was subtracted with a rolling ball radius of 50.0 pixels and images were transformed to 16-bit. Finally, images were processed with Gaussian-Blur filter with a 1.0 sigma radius. All images were arranged with Power Point.

5.12.2. BFA compartments measurement

Images for were processed using "Image J". Background was subtracted with a rolling ball radius of 50.0 pixels. 8 to 10 cells per image were chosen for measurement. BFA bodies were selected by using the ImageJ Wand Tool and Area of those ROIs was measured. Area of all cells of, at least, 15 independent plants were charted on a box-plot graph (Vertex42 LLC, www.vertex42.com).

5.12.3. Plasma membrane-Intracellular signal ratio measurement

Images for were processed using "Image J". Background was subtracted with a rolling ball radius of 50.0 pixels. 8 to 10 cells per image were chosen for measurements and the same ROI covering the Plasma Membrane (PM) was used to measure Area, Mean Grey Value, Minimum and Maximum Grey

Value. Same parameters were measured on the corresponding intracellular region per each PM ROI. Ratio was obtained dividing the mean gray value of the PM for its correspondent intracellular mean value. Data of all cells of, at least, 12 independent plants were combined and plotted on a box-plot graph (Vertex42 LLC, www.vertex42.com).

5.12.4. YFP/RFP ratio measurements for BiFC

Images for were processed using “Image J”. Background was subtracted with a rolling balls radius of 50.0 pixels. Full images were used to measure Area, Mean Grey Value, Minimum and Maximum Grey Value for both YFP and RFP channels. Images with a Maximum Grey Value of 256 were discarded. BiFC values were obtained by dividing the YFP and RFP Mean Grey Value. All non-discarded values of the three independent biological replicates were combined and plotted on a box-plot graph (Vertex42 LLC, www.vertex42.com).

5.13. Bioinformatics

5.13.1. *In silico* phosphorylation and ubiquitination prediction

RLP44 protein sequence has been used to predict the putative phospho-sites in the cytosolic domain using NetPhos 3.1 server (www.cbs.dtu.dk/services/NetPhos/). For the analysis of putative ubiquitinated residues, CKSAAP_UbSite server (www.protein.cau.edu.cn/cksaap_ubsite/) has been used.

5.13.2. Tree and protein alignments

Protein sequences were retrieved from NCBI data base. Tree Alignment run with a Blosum62 cos matrix with a gap open penalty of 12 and a gap extension penalty of 3. For building the tree, genetic distances were analyzed under the Jukes-Canto model with a Neighbor-Joining method using as an out group *Pohlia nutans*.

A Clustal W multiple alignment of nucleotides sequences has been performed with a BLOSUM cost matrix with a gap open cost of 10 and a gap extend cost of 0.1.

5.14. Statistical analysis

Significant differences were tested applying a one-factor analysis of variance (ANOVA) (performing Tukey’s test as post-hoc analysis) or Student’s t-test (p, 0.05), using the GraphPad Prism 7 Software.

Primers used for Genotyping				
Primer name	Internal name	Sequence (5' → 3')	Gene target	Observations
rlp44-4_CAPS_F	SW503	AATCTACAACTCTCACTCAC	At3g49750	Hinfl
rlp44-4_CAPS_R	SW504	CTGACCGGATAATTCGTTATC	At3g49750	Hinfl
at3g49750_SP1_F	SW315	AGCAATCAATTC AATTTAATC	At3g49750	Hinfl
bri1cnu4_CAPS_F	SW1158	TCAGGAGCTCATGTATGTCA	At4g39400	BseLI
bri1cnu4_CAPS_R	SW1159	TCCAATTGGTGTGTAGCAG	At4g39400	BseLI
bri1-301_CAPS_F	SW1426	GGTTTGGAGATGTTTACAAAG	At4g39400	Bsp143I
bri1-301_CAPS_R	SW1427	AAAATCCGGTGAATCCGTTG	At4g39400	Bsp143I
GK-o8409	SW1377	ATATTGACCATCATACTCATTGC		GABI-KAT insertions
BRI1-GK_WT_F	SW129	AACTATGGCTGAATATGTTAG		
BRI1_3'UTR_R	SW134	AAACGAAAACATTACAAATCC		<i>bri1null</i> WT allele
GK-134E10_F	SW1378	TAGCGGAAAACAAAATCAGTGG	At4g39400	<i>bri1null</i>
GK-134E10_R	SW1379	TCGTTCCATTGAAGAGATTGG	At4g39400	<i>bri1null</i>
serk1-3_F	SW1585	AGCAATTTTGTTCAGAAAAGT	At1g71830	<i>serk1-3 serk3-1 serk4-1</i>
serk1-3_R	SW1586	ATATTGACCATCATACTCATTGC	At1g71830	<i>serk1-3 serk3-1 serk4-1</i>
serk3-1_LP	SW1587	GAAAAACAGTTTAGCCGACCC	At4g33430	<i>serk1-3 serk3-1 serk4-1</i>
serk3-1_RP	SW1588	CATTCTTCCAGAACCAATCCG	At4g33430	<i>serk1-3 serk3-1 serk4-1</i>
serk4-1_LP	SW1589	TGGCTCAGAAGAAAACACAG	At2g13790	<i>serk1-3 serk3-1 serk4-1</i>
serk4-1_RP	SW1590	CTGCTCCACTTCTGTTCCAC	At2g13790	<i>serk1-3 serk3-1 serk4-1</i>
pskr1-3_F	SW1754	CTCGCTTCTGGTATGACGAG	At2g02220	<i>pskr1-3</i>
pskr1-3_R	SW1746	TCCGAAACTATACATCCGCC	At2g02220	<i>pskr1-3</i>
LbB1.3	SW230	ATTTTGCCGATTTCCGAAC		SALK insertions
attB1	SW905	ACAAGTTTGTACAAAAAGCAGGCT		For Gateway Constructs
attB2	SW906	ACCACTTTGTACAAGAAAGCTGGGT		For Gateway Constructs
pGG-Bdummy_F	SW1202	GTATTCAGTCGACTGGTACCAAC		For GreenGate Constructs
pGGA/C000_R	SW1137	CAGATTGACTGAGAGTGCACC		For GreenGate Constructs

Primers used for BiFC			
Primer name	Internal name	Sequence (5' → 3')*	Gene target
BRI1nYFP_F	SW1357	<u>GGGGACA</u> ACTTTGTATAATAAAGTTGATGAAGAC TTTTTCAAGCTTCTT	At4g39400
BRI1nYFP_R	SW1358	<u>GGGGACC</u> ACTTTGTACAAGAAAGCTGGGTTTAA TTTTCTTCCAGGAATTCTT	At4g39400
BAK1nYFP_F	SW890	<u>GGGGACA</u> ACTTTGTATAATAAAGTTGATGGAAC GAAGATTAATGATC	At4g33430
BAK1nYFP_R	SW891	<u>GGGGACC</u> ACTTTGTACAAGAAAGCTGGGTTTCT TGGACCCGAGGGTATTC	At4g33430
FLS2 cYFP_F	SW1361	<u>GGGGACA</u> AGTTTGTACAAAAAGCAGGCTATGA AGTTACTCTCAAAGAC	At5g46330
FLS2 cYFP_R	SW1362	<u>GGGGACA</u> ACTTTGTATAGAAAAGTTGGGTGTAA CTTCTCGATCCTCGTTACG	At5g46330
BRI1cYFP_F	SW887	<u>GGGGACA</u> AGTTTGTACAAAAAGCAGGCTATGA AGACTTTTTCAAGCTTCTT	At4g39400
BRI1cYFP_R	SW888	<u>GGGGACA</u> ACTTTGTATAGAAAAGTTGGGTGTAA ATTTCTTCCAGGAATTCTT	At4g39400
RLP44_wt_cYFP_F	SW372	<u>GGGGACA</u> AGTTTGTACAAAAAGCAGGCTATGA CAAGGAGTCACCGTTAC	At3g49750
RLP44_wt_cYFP_R	SW889	<u>GGGGACA</u> ACTTTGTATAGAAAAGTTGGGTGTGT AATCAGGCATAGATTGAC	At3g49750
RLP44 PM cYFP_F	SW372	<u>GGGGACA</u> AGTTTGTACAAAAAGCAGGCTATGA CAAGGAGTCACCGTTAC	At3g49750
RLP44 PM cYFP_R	SW1360	<u>GGGGACA</u> ACTTTGTATAGAAAAGTTGGGTGGTT CATCAGGCATTTCTTGTTT	At3g49750
RLP44 PD cYFP_F	SW372	<u>GGGGACA</u> AGTTTGTACAAAAAGCAGGCTATGA CAAGGAGTCACCGTTAC	At3g49750
RLP44 PD cYFP_R	SW1359	<u>GGGGACA</u> ACTTTGTATAGAAAAGTTGGGTGGGA AATCAGGCATAGCTTGAG	At3g49750
FLS2 nYFP_F	SW1363	<u>GGGGACA</u> ACTTTGTATAATAAAGTTGATGAAGTT ACTCTCAAAGAC	At5g46330
FLS2 nYFP_R	SW1364	<u>GGGGACC</u> ACTTTGTACAAGAAAGCTGGGTTAAC TTCTCGATCCTCGTTACG	At5g46330

* Underlined nucleotides correspond with the sequences needed for the building of recombinant extremes for Gateway® Cloning.

Primers used for qPCR			
<i>Primer name</i>	<i>Internal name</i>	<i>Sequence (5' → 3')</i>	<i>Gene target</i>
AtEXP8_F	SW521	CCGAAATAACTAACCCCTCCTC	At2g40610
AtEXP8_R	SW522	TAGCCACAAGCTCCGCCCAT	At2g40610
DWF4_F	SW803	CAACAGCAAAACAACGGAGCG	At3g50660
DWF4_R	SW804	TCTGAACCAGCACATAGCCTTG	At3g50660
Clath_F	SW1015	TCGATTGCTTGGTTTGAAGAT	At1g10730
Clath_R	SW1016	GCACTTAGCGTGGACTCTGTTTGC	At1g10730

6. Supplemental Figures

A RLP44 At3g49750 OS=Arabidopsis thaliana

```

MTRSHRLLLLLLLLIFQTAQRLLTADPNDEACLKLNLRQNLDPASNLRNWTNSVFSNPGSGFTSYLPGATCNGRIYKLSL      80
TNLSLRGSI SPFLSNCTNLQSLDLSSNQISGVIPPEIQYLVNLAVLNLSSNHLSGEITPQLALCAYLNVIDLHDNELSGQ      160
IPQQLGLLARLSAFDVSNNKLSGQIPTYLSNRTGNFPRFNASSFIGNKGLYGYPLQEMMMKSKGLSVMAIVGIGLGSGIA      240
SLMISFTGVCLWLRITTEKKIVEEEGKISQSMPDY                                                    320
.....TT.....S.....
...S...S.....Y.....S...T.....
.....S.....S.....Y.....S.....
.....T.....S.S...Y

```

Phosphorylation sites predicted: Ser: 9 Thr: 4 Tyr: 3

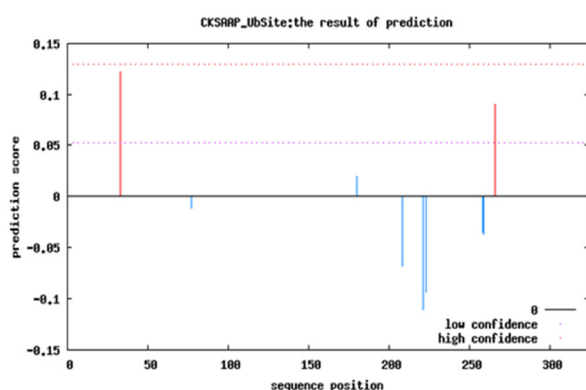
Name	Pos	Context	Score	Pred
tr_Q9M2Y3_Q	256	WLRIT EKKI	0.734	*T*
tr_Q9M2Y3_Q	268	EGKISQ SMP	0.954	*S*
tr_Q9M2Y3_Q	270	KISQ SMPDY	0.964	*S*
tr_Q9M2Y3_Q	274	SMPDY----	0.973	*Y*

B >RLP44 At3g49750 OS=Arabidopsis thaliana

```

MTRSHRLLLLLLLLIFQTAQRLLTADPNDEACLKLNLRQNLDPASNLRNWTNSVFSNPGSGFTSYLPGATCNGRIYKLSL
TNLSLRGSI SPFLSNCTNLQSLDLSSNQISGVIPPEIQYLVNLAVLNLSSNHLSGEITPQLALCAYLNVIDLHDNELSGQ
IPQQLGLLARLSAFDVSNNKLSGQIPTYLSNRTGNFPRFNASSFIGNKGLYGYPLQEMMMKSKGLSVMAIVGIGLGSGIA
SLMISFTGVCLWLRITEKKRIVEEEGKISQSMPDY

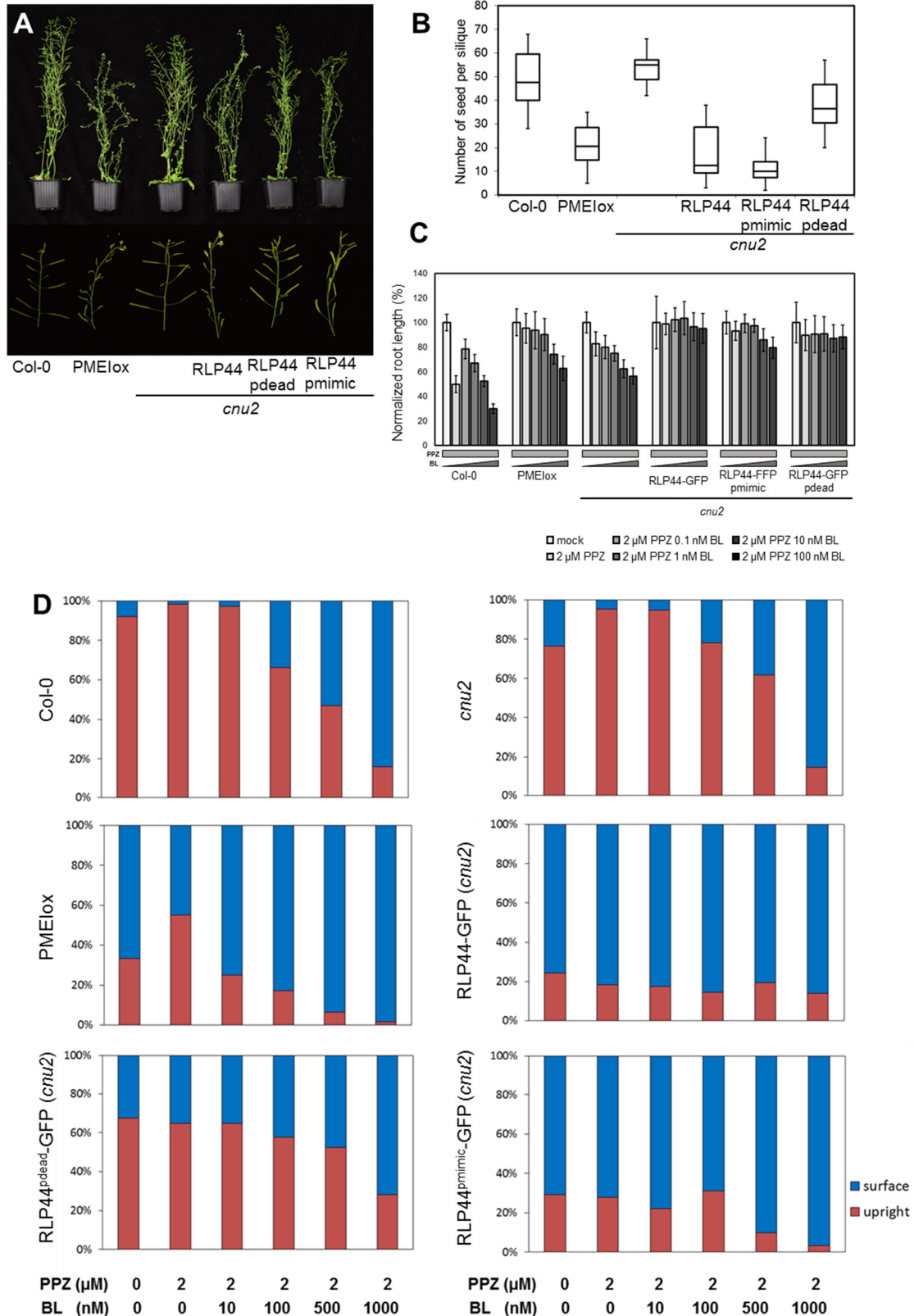
```



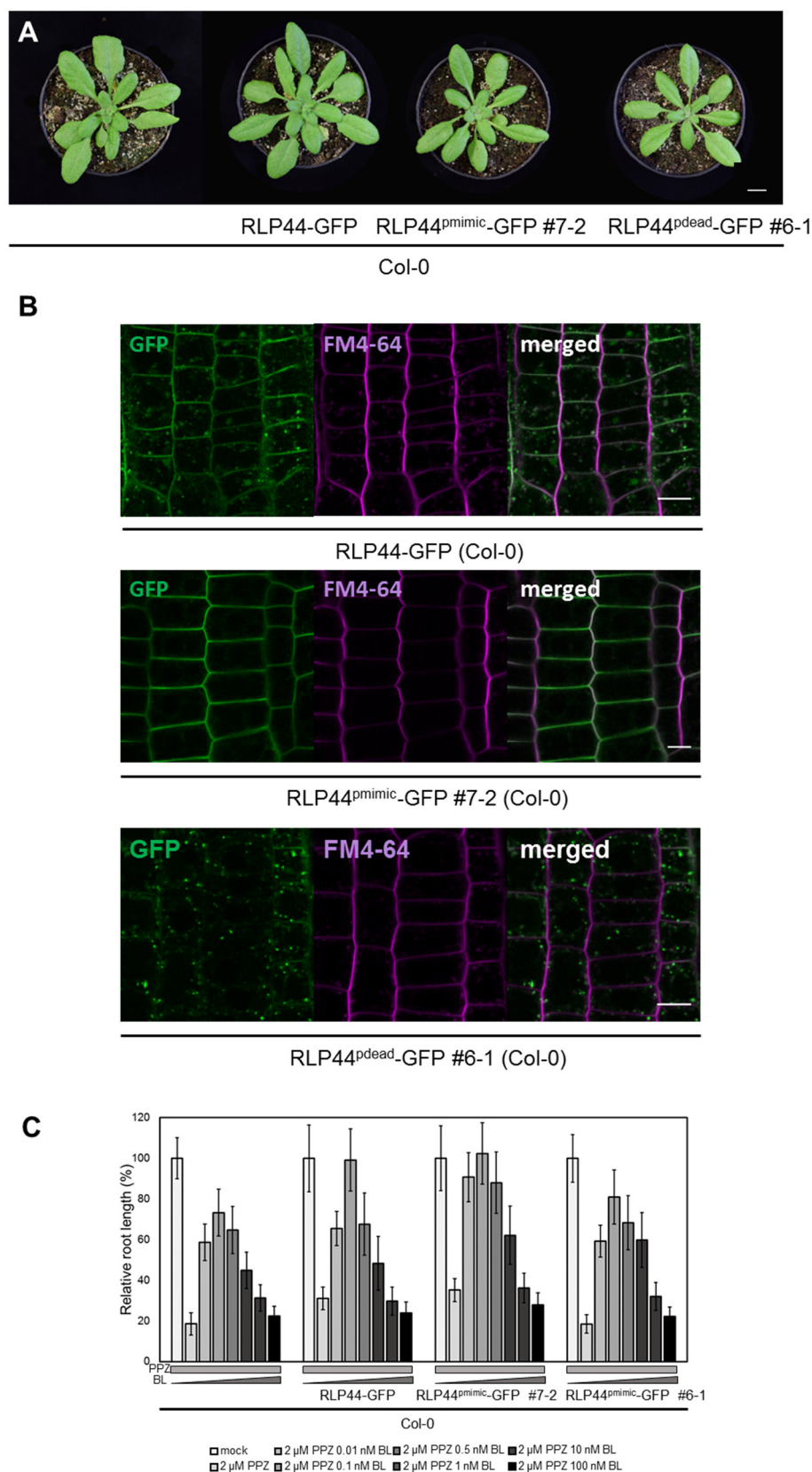
Output:

Residue	Score	Ubiquitinated
33	0.59	No
77	0.26	No
180	0.53	No
208	0.44	No
221	0.69	Yes Medium confidence
223	0.52	No
258	0.52	No
259	0.59	No
266	0.84	Yes High confidence

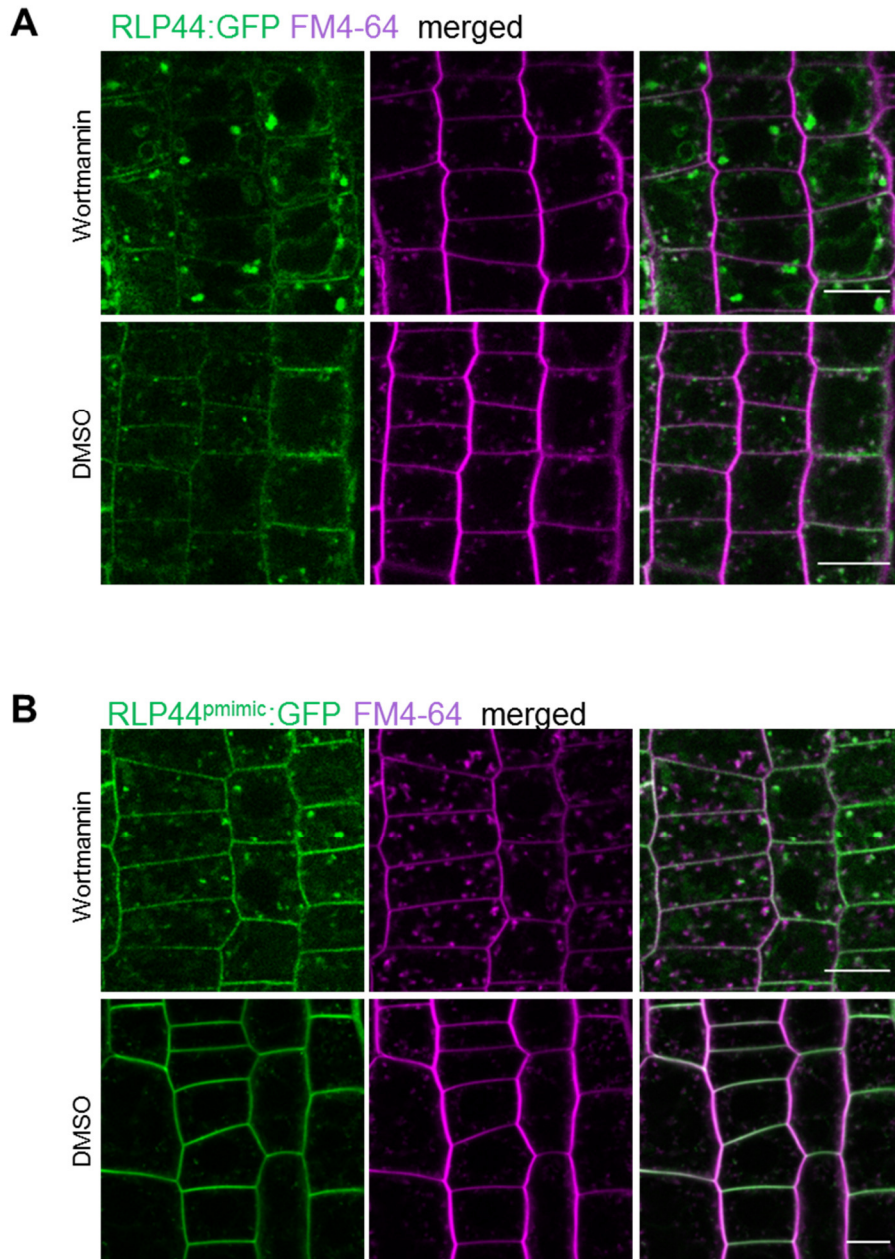
Supplemental Figure 1. Phosphorylation and Ubiquitination prediction of RLP44 cytoplasmic domain. **A.** To identify putative phosphorylation sites in RLP44, full sequence was subjected to an *in silico* software prediction (NetPhos 3.1) but only cytoplasmic sequence was considered in this study. In green, RLP44 cytoplasmic domain. **B.** Prediction of possible ubiquitinated lysines in RLP44 sequence was performed *in silico* by prediction software (CKSAAP_UbSite).



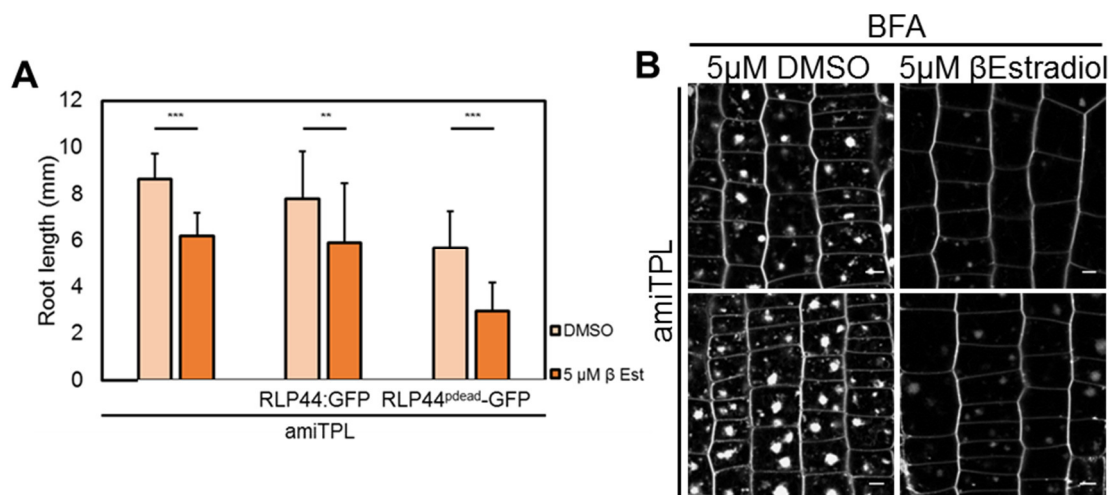
Supplemental Figure 2. Modification of RLP44 phospho-residues influence protein function. A. Adult plant phenotype of RLP44-GFP, RLP44^{pmimic}-GFP and RLP44^{pdead}-GFP in *gnu2* background. **B.** RLP44^{pmimic}-GFP present a strong reduction on fertility. Box-plots represent average number of seed per silique ±SD (n=12-15). **C.** Bars represent normalized response in root length to depletion of and exogenous addition of brassinosteroids ±SD (n=21-27). **D.** RLP44^{pmimic}-GFP agravitropically response as PMElox. Bars represent percentage of dark-grown hypocotyls growing upright or over the surface in response to depletion of and exogenous addition of brassinosteroids (n=90-112).



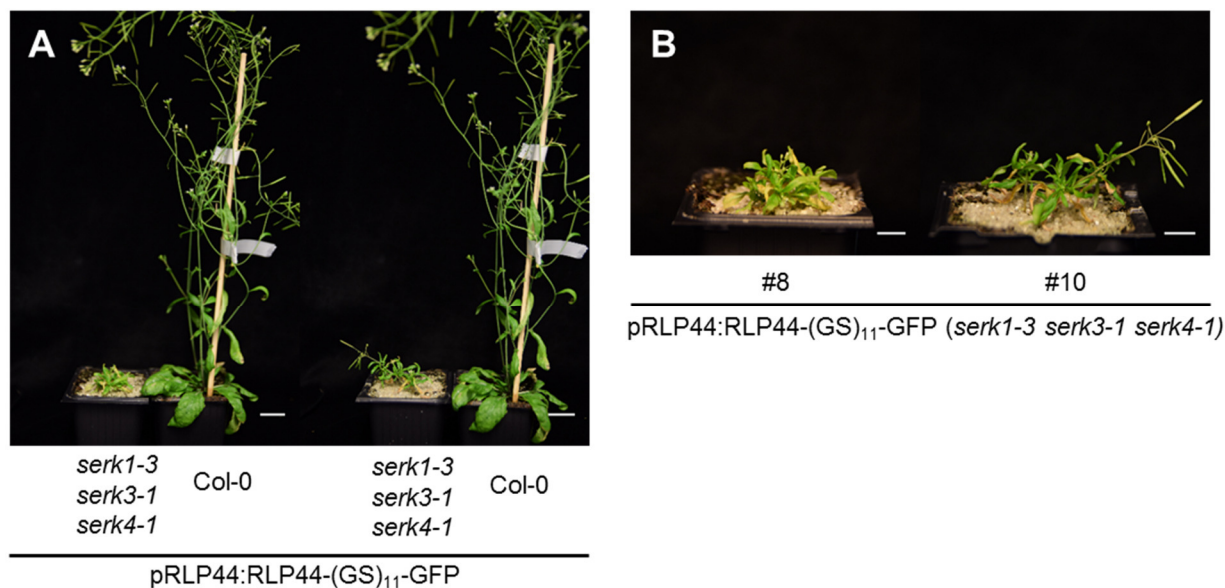
Supplemental Figure 3. RLP44^{pmimic}-GFP and RLP44^{pdead}-GFP in Col-0. **A.** 21-d-old macroscopic phenotype of RLP44^{pmimic}-GFP and RLP44^{pdead}-GFP in Col-0. Bars=1 cm. **B.** RLP44^{pmimic}-GFP and fluorescence signal of 7-day-old seedlings roots and merged fluorescence after 10 min of staining with endocytic tracer dye FM4-64 shows an enrichment on PM localization or when compares WT. Bars=10 μm **C.** BL-response is not altered in RLP44^{pmimic}-GFP or RLP44^{pdead}-GFP. Bars represent normalized response in root length to depletion of and exogenous addition of brassinosteroids ±SD (n=43-55).



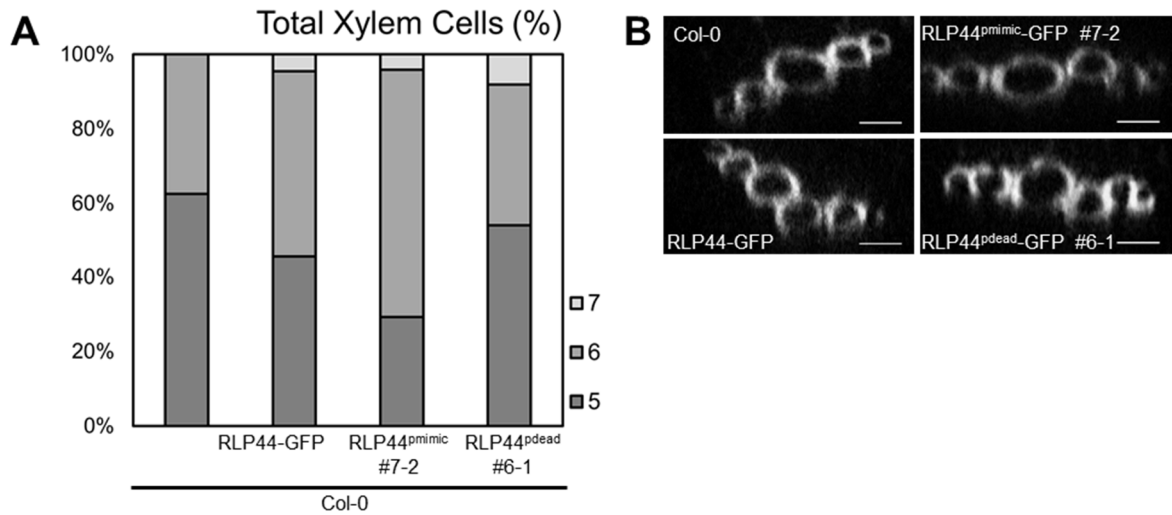
Supplemental Figure 4. RLP44-GFP and RLP44^{pmimic}-GFP present normal VB formation. A and B. 7day-old RLP44-GFP *cnu2* (A) and RLP44^{pmimic}-GFP (B) seedlings upon the treatment with 30 μ M Wortmannin for 165 min or DMSO for 165 min ; followed by the staining with the endocytic tracer dye FM4-64 for 20min (n=18) bars= 10 μ m.



Supplemental Figure 5. Induction of amiR-TPL dramatically reduce endocytosis. **A.** Upon induction of amiR-TPL root growth is depleted. Bars indicate the response in root length of 5-d-old seedlings treated with DMSO or β -estradiol \pm SD (n=25-33). Asterisk indicate results of a two-tailed t-test with $p < 0.05$ (*), $p < 0.01$ (**), $p < 0.001$ (***) **B.** BFA bodies formation is reduced upon the induction of amiR-TPL. Representative images of 5-d-old seedlings upon β -estradiol induction and subsequent treatment with 50 μ M BFA for 120 min or DMSO for 165 min, followed by the staining with the endocytic tracer dye FM4-64 for 20min, bars=10 μ m.



Supplemental Figure 6. RLP44-(GS)₁₁-GFP cannot rescue *serk1-3 serk3-1 serk4-1* macroscopic phenotype. **A.** Comparison of adult phenotype of RLP44-(GS)₁₁-GFP in *serk1-3 serk3-1 serk4-1* or Col-0 background. Bars=1 cm. **B.** Detailed view of adult phenotype of RLP44-(GS)₁₁-GFP (*serk1-3 serk3-1 serk4-1*). Bars=1 cm.



Supplemental Figure 7. RLP44 phosphomutants have RLP44ox xylem phenotype. A. RLP44^{pmimic}-GFP and RLP44^{pdead}-GFP have same xylem phenotype as RLP44-GFP in Col-0 plants. Bars represent the quantification of the frequency with the indicated number of metaxylem cells (n=25-26) **B.** Representative orthogonal view of confocal stacks from studied genotypes used for the quantification of xylem cell numbers below the hypocotyl junction in 6-d-old *Arabidopsis* roots. Bars=5 μ m.

7. References

- Afzal, Ahmed J., Andrew J. Wood, and David A. Lightfoot.** 2008. "Plant receptor-like serine threonine kinases: roles in signaling and plant defense." *Molecular Plant-Microbe Interactions* **21** (5): 507–17.
- Albert, Isabell, Hannah Böhm, Markus Albert, Christina E. Feiler, Julia Imkampe, Niklas Wallmeroth, Caterina Brancato, et al.** 2015. "An RLP23–SOBIR1–BAK1 complex mediates nlp-triggered immunity." *Nature Plants* **1** (10): 15140.
- Ali, Olivier, and Jan Traas.** 2016. "Force-driven polymerization and turgor-induced wall expansion." *Trends in Plant Science* **21** (5): 398–409.
- Amano, Y., H. Tsubouchi, H. Shinohara, M. Ogawa, and Y. Matsubayashi.** 2007. "Tyrosine-sulfated glycopeptide involved in cellular proliferation and expansion in arabidopsis." *Proceedings of the National Academy of Sciences* **104** (46): 18333–38.
- Amsbury, Sam, Lee Hunt, Nagat Elhaddad, J Paul Knox, Andrew J Fleming, and Julie E Gray.** 2016. "Report stomatal function requires pectin de-methyl- esterification of the guard cell wall." *Current Biology* **26** (21): 2899–2906.
- Anne, Pauline, Marianne Azzopardi, Lionel Gissot, Sébastien Beaubiat, Kian Hématy, and Jean-Christophe Palauqui.** 2015. "OCTOPUS Negatively Regulates BIN2 to Control phloem differentiation in arabidopsis thaliana." *Current Biology* **25** (19): 2584–90.
- Arioli, Tony, Liangcai Peng, Andreas S Betzner, Joanne Burn, Werner Wittke, Werner Herth, Christine Camilleri, et al.** 1998. "Molecular analysis of cellulose biosynthesis in arabidopsis." *Science* **279** (5351): 717–20.
- Atmodjo, Melani A, Zhangying Hao, and Debra Mohnen.** 2013. "Evolving views of pectin biosynthesis." *Annu. Rev. Plant Biol* **64** (4): 747–79.
- Augustin, Sebastian.** 2015. "Structure-function analysis of the arabidopsis thaliana receptor-like protein 4." *Master Thesis Presented to the Faculty of Bioscience of the Ruprecht-Karls-Universität.*
- Austin, Ryan S., Danielle Vidaurre, George Stamatiou, Robert Breit, Nicholas J. Provart, Dario Bonetta, Jianfeng Zhang, et al.** 2011. "Next-generation mapping of arabidopsis genes." *Plant Journal* **67** (4): 715–25.
- Barberon, Marie, Enric Zelazny, Stéphanie Robert, Geneviève Conéjéro, and Cathy Curie.** 2011a. "Monoubiquitin-dependent endocytosis of the transporter controls iron uptake in plants." *Proceedings of the National Academy of Sciences* **108** (32): E450–58.
- Bashline, Logan, Shundai Li, Xiaoyu Zhu, and Ying Gu.** 2015. "The TWD40-2 Protein and the AP2 complex cooperate in the clathrin-mediated endocytosis of cellulose synthase to regulate cellulose biosynthesis." *Proceedings of the National Academy of Sciences* **112** (41): 12870–75.
- Belkhadir, Youssef, and Joanne Chory.** 2006. "Brassinosteroid signaling: a paradigm for steroid hormone signaling from the cell surface." *Science* **314** (5804): 1410–12.
- Belkhadir, Youssef, and Yvon Jaillais.** 2015. "The molecular circuitry of brassinosteroid signaling." *New Phytologist* **26** (2): 522–40.
- Benfey, Philip N., Paul J. Linstead, Keith Roberts, John W. Schiefelbein, Marie-Theres Hauser, and Roger A. Aeschbacher.** 1993. "Root Development in arabidopsis: four mutants with dramatically altered root morphogenesis." *Development* **119**: 57–70.
- Bichet, Adeline, Thierry Desnos, Simon Turner, Olivier Grandjean, and Herman Hofte.** 2001. "BOTERO1 Is required for normal orientation of cortical microtubules and anisotropic cell expansion in arabidopsis." *The Plant Journal* **25** (2): 137–48.
- Boisson-Dernier, Aurélien, Sharon A Kessler, and Ueli Grossniklaus.** 2011. "The walls have ears : the role of plant CrRLK1Ls in sensing and transducing extracellular signals." *Journal of Experimental Botany* **62** (5): 1581–91.

- Boisson-Dernier, Aurélien, Dmytro S. Lituiev, Anna Nestorova, Christina Maria Franck, Sharme Thirugnanarajah, and Ueli Grossniklaus.** 2013. "ANXUR receptor-like kinases coordinate cell wall integrity with growth at the pollen tube tip via NADPH oxidases." *PLoS Biology* **11** (11): e1001719.
- Boisson-Dernier, Aurélien, Sucharita Roy, Konstantinos Kritsas, Monica A Grobei, Miloslawa Jaciubek, Julian I Schroeder, and Ueli Grossniklaus.** 2009. "disruption of the pollen-expressed FERONIA homologs ANXUR1 and ANXUR2 triggers pollen tube discharge." *Development* **136** (19): 3279–88.
- Boursiac, Yann, Sheng Chen, Doan-trung Luu, Mathias Sorieul, Niels Van Den Dries, and Christophe Maurel.** 2005. "Early effects of salinity on water transport in arabidopsis roots . molecular and cellular features of aquaporin expression." *Plant Physiology* **139** (2): 790–805.
- Brady, Siobhan M, David A Orlando, J-Young Lee, Jean Y Wang, Jeremy Koch, José R Dinneny, Daniel Mace, Uwe Ohler, and Philip N Benfey.** 2007. "A high-resolution root spatiotemporal map reveals dominant expression patterns." *Science* **318** (5851): 801–6.
- Brand, Ulrike, Jennifer C Fletcher, Martin Hobe, and Elliot M Meyerowitz.** 2000. "dependence of stem cell fate in arabidopsis on a feedback loop regulated by CLV3 activity." *Science* **289** (5479): 617–19.
- Burd, Christopher, and Peter J Cullen.** 2014. "Retromer : a master conductor of endosome sorting." *Cold Spring-Harbor Perspectives in Biology* **6** (2): 1–14.
- Caño-Delgado, Ana, Yanhai Yin, Cong Yu, Dionne Vafeados, Santiago Mora-García, Jin-Chen Cheng, Kyoung Hee Nam, Jianming Li, and Joanne Chory.** 2004. "BRL1 and BRL3 are novel brassinosteroid receptors that function in vascular differentiation in arabidopsis." *Development* **131** (21): 5341–51.
- Castro, María De, Asier Largo-Gosens, Jesús Miguel Alvarez, Penélope García-Angulo, and José Luis Acebes.** 2014. "Early cell-wall modifications of maize cell cultures during habituation to Dichlobenil." *Journal of Plant Physiology* **171** (2): 127–35.
- Cavalier, David M., and Kenneth Keegstra.** 2006. "Two Xyloglucan xylosyltransferases catalyze the addition of multiple xylosyl residues to cellohexaose." *Journal of Biological Chemistry* **281** (45): 34197–207.
- Cavalier, David M, Olivier Lerouxel, Lutz Neumetzler, Kazuchika Yamauchi, Antje Reinecke, Glenn Freshour, Olga a Zobotina, et al.** 2008. "Disrupting two arabidopsis thaliana xylosyltransferase genes results in plants deficient in xyloglucan, a major primary cell wall component." *The Plant Cell* **20** (6): 1519–37.
- Chinchilla, Delphine, Libo Shan, Ping He, Sacco de Vries, and Birgit Kemmerling.** 2009. "One for all: the receptor-associated kinase BAK1." *Trends in Plant Science* **14** (10): 535–41.
- Cho, Hyunwoo, Hojin Ryu, Sangchul Rho, Kristine Hill, Stephanie Smith, Dominique Audenaert, Joonghyuk Park, et al.** 2014. "A secreted peptide acts on BIN2-mediated phosphorylation of ARFs to potentiate auxin response during lateral root development." *Nature Cell Biology* **16** (1): 66–76.
- Chow, Brenda, and Peter Mccourt.** 2008. "Plant hormone receptors : perception is everything." *Genes and Development* **20** (6): 1998–2008.
- Clark, Steven E, Robert W Williams, and Elliot M Meyerowitz.** 1997. "The CLAVATA1 gene encodes a putative receptor kinase that controls shoot and floral meristem size in arabidopsis." *Cell* **89** (4): 575–85.
- Clausen, Mads H., William G T Willats, and J. Paul Knox.** 2003. "Synthetic methyl hexagalacturonate hapten inhibitors of anti-homogalacturonan monoclonal antibodies LM7, JIM5 and JIM7." *Carbohydrate Research* **338** (17): 1797–1800.
- Clough, Steven J, and Andrew F Bent.** 1998. "Floral Dip : a simplified method for agrobacterium-mediated transformation of Arabidopsis thaliana." *The Plant Journal* **16** (6): 735–43.

- Corio-Costet, Marie-France, Muriel Dall Agnese, and Reni Scalla.** 1991. "Effects of Lsoxaben on Sensitive and tolerant plant cell cultures." *Pesticide Biochemistry and Physiology* **40** (14): 246–54.
- Cosgrove, Daniel J.** 2005. "Growth of the plant cell wall." *Nature Reviews* **6** (11): 850–61.
- Cosgrove, Daniel J.** 2015. "Plant cell wall extensibility: connecting plant cell growth with cell wall structure, mechanics and the action of wall-modifying enzymes." *Journal of Experimental Botany* **67** (2): 463–76.
- Couto, Daniel, and Cyril Zipfel.** 2016. "Regulation of pattern recognition receptor signalling in plants." *Nature Reviews* **16** (9):537-52.
- Cutler, S. R., D. W. Ehrhardt, J. S. Griffitts, and C. R. Somerville.** 2000. "Random GFP::cDNA fusions enable visualization of subcellular structures in cells of arabidopsis at a high frequency." *Proceedings of the National Academy of Sciences* **97** (7): 3718–23.
- De Rybel, Bert, Ari Pekka Mähönen, Yrjö Helariutta, and Dolf Weijers.** 2016. "Plant Vascular development: from early specification to differentiation." *Nature Reviews* **17** (1). 30–40.
- Decreux, Annabelle, and Johan Messiaen.** 2005. "Wall-associated kinase WAK1 interacts with cell wall pectins in a calcium-induced conformation." *Plant and Cell Physiology* **46** (2): 268–78.
- Delay, Christina, Nijat Imin, and Michael A Djordjevic.** 2013. "Regulation of arabidopsis root development by small signaling peptides." *Frontiers in Plant Science* **4** (9): 1–6.
- Desprez, Thierry, Samantha Vernhettes, Mathilde Fagard, Guislaine Refrégier, Thierry Desnos, Estelle Aletti, Nicolas Py, Sandra Pelletier, and Herman Höfte.** 2002. "Resistance against herbicide isoxaben and cellulose deficiency caused by distinct mutations in same cellulose synthase isoform CESA6." *Plant Physiology* **128** (2): 482–90.
- Donaldson, Julie G, and Catherine L Jackson.** 2011. "ARF family G proteins and their regulators : roles in membrane transport , development and disease." *Nature Reviews* **12** (6): 362–75.
- Downes, Brian P, Robert M Stupar, Derek J Gingerich, and Richard D Vierstra.** 2003. "The HECT Ubiquitin-Protein Ligase (UPL) family in arabidopsis: UPL3 Has a specific role in trichome development." *The Plant Journal* **35** (6): 729–42.
- Doyle, Siamsa M, Ash Haeger, Thomas Vain, Adeline Rigal, Corrado Viotti, and Qian Ma.** 2015. "An early secretory pathway mediated by GNOM-LIKE 1 and GNOM is essential for basal polarity establishment in arabidopsis thaliana." *Proceedings of the National Academy of Sciences* **112** (7): E806–15.
- Dubeaux, Guillaume, and Grégory Vert.** 2017. "Zooming into plant ubiquitin-mediated endocytosis." *Current Opinion in Plant Biology* **40** (12): 56–62.
- Edwards, K, C Johnstone, and C Thompson.** 1991. "A simple and rapid method for the preparation of plant genomic DNA for PCR analysis." *Nucleic Acids Research* **19** (6): 1349-50.
- Ellgaard, Lars, Nicholas Mccauley, Anna Chatsisvili, and Ineke Braakman.** 2016. "Co- and post-translational protein folding in the ER." *Traffic* **17** (6): 615–38.
- Fagard, Mathilde, Thierry Desnos, Thierry Desprez, Florence Goubet, Guislaine Refregier, Gregory Mouille, Maureen Mccann, Catherine Rayon, Samantha Vernhettes, and Herman Höfte.** 2000. "PROCUSTE1 Encodes a cellulose synthase required for normal cell elongation specifically in roots and dark-grown hypocotyls of arabidopsis." *The Plant Cell* **12** (12): 2409–23.
- Fan, Lusheng, Huaiqing Hao, Yiqun Xue, Liang Zhang, Kai Song, Zhaojun Ding, Miguel A Botella, Haiyang Wang, and Jinxing Lin.** 2013. "Dynamic analysis of arabidopsis AP2 σ subunit reveals a key role in clathrin-mediated endocytosis and plant development." *Development* **140** (18): 3826–37.
- Fernandez-Borja, Mar, Richard Wubbolts, Jero Calafat, Hans Janssen, Nullin Divecha, Simone Dusseljee, and Jacques Neefjes.** 1999. "Multivesicular body morphogenesis requires phosphatidylinositol 3-kinase activity." *Current Biology* **9** (1): 55–58.

- Ferrari, Simone, Daniel V Savatin, Francesca Sicilia, Giovanna Gramegna, Felice Cervone, and Giulia De Lorenzo.** 2013. "Oligogalacturonides : Plant damage-associated molecular patterns and regulators of growth and development." *Frontiers in Plant Science* **4** (4): 1–9.
- Friedrichsen, Danielle M, Claudio A P Joazeiro, Jianming Li, Tony Hunter, and Joanne Chory.** 2000. "Brassinosteroid-Insensitive-1 is a ubiquitously expressed leucine-rich repeat receptor serine/threonine kinase." *Plant Physiology* **123** (4): 1247–56.
- Frost, Megan.** 1981. "In Vivo Chemical Sensors :." *Annual Review of Biochemistry* **50** (5): 783–814.
- Fujimoto, Masaru, Shin-ichi Arimura, Takashi Ueda, Hideki Takanashi, Yoshikazu Hayashi, Akihiko Nakano, and Nobuhiro Tsutsumi.** 2010. "Arabidopsis dynamin-related proteins DRP2B and DRP1A Participate together in clathrin-coated vesicle formation during endocytosis." *Proceedings of the National Academy of Sciences* **107** (13): 6094–99.
- Gadeyne, Astrid, Clara Sánchez-Rodríguez, Steffen Vanneste, Simone Di Rubbo, Henrik Zauber, Kevin Vanneste, Jelle Van Leene, Nancy De Winne, Dominique Eeckhout, Geert Persiau, Eveline Van De Slijke, et al.** 2014. "The TPLATE Adaptor complex drives clathrin-mediated endocytosis in plants." *Cell* **156** (4): 691–704.
- Gallego-Bartolome, J., E. G. Minguet, F. Grau-Enguix, M. Abbas, a. Locascio, S. G. Thomas, D. Alabadi, and M. a. Blazquez.** 2012. "Molecular mechanism for the interaction between gibberellin and brassinosteroid signaling pathways in arabidopsis." *Proceedings of the National Academy of Sciences* **109** (33): 13446–51.
- Galvan-Ampudia, Carlos S., and Christa Testerink.** 2011. "Salt Stress signals shape the plant root." *Current Opinion in Plant Biology* **14** (3): 296–302.
- Gampala, Srinivas S, Tae-wuk Kim, Jun-xian He, Wenqiang Tang, Zhiping Deng, Mingyi-yi Bai, Shenheng Guan, et al.** 2007. "Article an essential role for 14-3-3 proteins in brassinosteroid signal transduction in arabidopsis." *Developmental Cell* **13** (2): 177–89.
- Geldner, N., and S. Robatzek.** 2008. "Plant Receptors go endosomal: a moving view on signal transduction." *Plant Physiology* **147** (4): 1565–74.
- Geldner, Niko, Valérie Déneraud-Tendon, Derek L. Hyman, Ulrike Mayer, York Dieter Stierhof, and Joanne Chory.** 2009. "Rapid, combinatorial analysis of membrane compartments in intact plants with a multicolor marker set." *Plant Journal* **59** (1): 169–78.
- Ghelis, Thanos.** 2011. "Signal Processing by protein tyrosine phosphorylation in plants." *Plant Signaling & Behavior* **6** (7): 942–51.
- Gomez-Gomez, Lourdes, and Boller, Thomas.** 2000. "FLS2 : An LRR receptor – like kinase involved in the perception of the bacterial elicitor flagellin in arabidopsis." *Molecular Cell* **5** (6): 1003–11.
- Gou, Xiaoping, Hongju Yin, Kai He, Junbo Du, Jing Yi, Shengbao Xu, Honghui Lin, and D Steven.** 2012. "Genetic evidence for an indispensable role of somatic embryogenesis receptor kinases in brassinosteroid signaling." *PLoS Genetics* **8** (1): e1002452.
- Grefen, Christopher, and Michael R Blatt.** 2014. "A 2in1 cloning system enables ratiometric bimolecular fluorescence complementation (rBiFC)." *Biotechniques* **56** (5): 311–14.
- Guo, Hongqing, Lei Li, Maneesha Aluru, Sriniva Aluru, and Yanhai Yin.** 2013. "Mechanisms and networks for brassinosteroid regulated gene expression." *Current Opinion in Plant Biology* **16** (5): 545–53.
- Gupta, A., M. Singh, A. M. Jones, and A. Laxmi.** 2012. "Hypocotyl directional growth in arabidopsis: a complex trait." *Plant Physiology* **159** (4): 1463–76.
- Gust, Andrea a, and Georg Felix.** 2014. "Receptor like proteins associate with SOBIR1-Type of adaptors to form bimolecular receptor kinases." *Current Opinion in Plant Biology* **21** (10): 104–11.
- Hartmann, Jens, Nils Stührwohldt, Renate I. Dahlke, and Margret Sauter.** 2013. "Phytosulfokine control of growth occurs in the epidermis, is likely to be non-cell autonomous and is dependent on brassinosteroids." *Plant Journal* **73** (4): 579–90.

- Haruta, Miyoshi, Grzegorz Sabat, Kelly Stecker, Benjamin B Minkoff, and Michael R Sussman.** 2014. "A peptide hormone and its receptor." *Science* **343** (6169): 408–11.
- Hashiguchi, A, and S Komatsu.** 2017. Posttranslational modifications and plant – environment interaction. *Methods in Enzymology*. Vol. **586**.
- Hauser, Marie-theres, Atsushi Morikami, and Philip N Benfey.** 1995. "Conditional root expansion mutants of arabidopsis." *Development* **121** (4): 1237–52.
- Hazak, Ora, Benjamin Brandt, Pietro Cattaneo, Julia Santiago, Antia Rodriguez-villalon, Michael Hothorn, and Christian S Hardtke.** 2017. "Perception of root-active CLE peptides requires CORYNE function in the phloem vasculature." *EMBO Reports* **346** (6207): 343–46.
- He, Jun-xian, Joshua M Gendron, Yanli Yang, Jianming Li, and Zhi-yong Wang.** 2002. "The GSK3-like kinase BIN2 Phosphorylates and destabilizes BZR1, a positive regulator of the brassinosteroid signaling pathway in arabidopsis." *Proceedings of the National Academy of Sciences* **99** (15): 10185–90.
- Hématy, Kian, Pierre Etienne Sado, Ageeth Van Tuinen, Soizic Rochange, Thierry Desnos, Sandrine Balzergue, Sandra Pelletier, Jean Pierre Renou, and Herman Höfte.** 2007. "A receptor-like kinase mediates the response of arabidopsis cells to the inhibition of cellulose synthesis." *Current Biology* **17** (11): 922–31.
- Heyman, Jefri, Toon Cools, Filip Vandebussche, Ken S Heyndrickx, Jelle Van Leene, Dominique Van Der Straeten, and Lieven De Veylder.** 2013. "ERF115 controls root quiescent center cell division and stem cell replenishment." *Science* **342** (6160): 860–64.
- Hirakawa, Yuki, Hidefumi Shinohara, Yuki Kondo, Asuka Inoue, Ikuko Nakanomyo, Mari Ogawa, Shinichiro Sawa, Kyoko Ohashi-Ito, Yoshikatsu Matsubayashi, and Hiroo Fukuda.** 2008. "non-cell-autonomous control of vascular stem cell fate by a CLE peptide/receptor system." *Proceedings of the National Academy of Sciences* **105** (39): 15208–13.
- Hirt, Robert P, Graham J Hughes, Séverine Frutiger, Pierre Michetti, Christine Perregaux, Odile Poulain-godefroy, Nathalie Jeanguenat, Marian R Neutra, and Jean P Kraehenbuhl.** 1993. "Transcytosis of the polymeric ig receptor requires phosphorylation of serine 664 in the absence but not the presence of dimeric IgA." *Cell* **74** (2): 245–55.
- Hocq, Ludivine, Jérôme Pelloux, and Valérie Lefebvre.** 2016. "Connecting homogalacturonan-type pectin remodeling to acid growth." *Trends in Plant Science* **22** (1): 20–29.
- Höfte, Herman.** 2015. "The Yin and Yang of cell wall integrity control : brassinosteroid and FERONIA signaling." *Plant & Cell Physiology* **56** (2): 224–31.
- Holzwarth E, Huerta Al, Glöckner N, Garnelo Gómez B, Ladwig F, Augustin S, Askani JC, Harter K, Wolf S.** In revision. "Integration of brassinosteroid and phyto-sulfokine signalling controls vascular cell fate in the Arabidopsis root." *Developmental Cell*.
- Hosmer, Kerry, and Debra Mohnen.** 2009. "The Structure , function , and biosynthesis of plant cell wall pectic polysaccharides." *Carbohydrate Research* **344** (14): 1879–1900.
- Huang, Fang, Marcelo Kemel Zago, Lindy Abas, Arnoud Van Marion, Carlos Samuel Galva, and Remko Offringa.** 2010. "Phosphorylation of conserved PIN motifs directs arabidopsis PIN1 polarity and auxin transport." *The Plant Cell* **22** (4): 1129–42.
- Huck, Norbert, James M Moore, Michael Federer, and Ueli Grossniklaus.** 2003. "The Arabidopsis mutant feronia disrupts the female gametophytic control of pollen tube reception." *Development* **130** (10): 2149–59.
- Huerta, Aponio.** 2016. "The Receptor-like Protein , RLP44 , Regulates root xylem differentiation through a yet unknown signaling pathway and mediates differential phosphorylation of BAK1-BRI1 complexes." *Master Thesis Presented to the Faculty of Bioscience of the Ruprecht-Karls-Universität Heidelberg*.
- Humphrey, Tania V., Dario T. Bonetta, and Daphne R. Goring.** 2007. "Sentinels at the wall: cell wall receptors and sensors." *New Phytologist* **176** (1): 7–21.

- Ibañes, Marta, Norma Fàbregas, Joanne Chory, and Ana I Caño-Delgado. 2009. "Brassinosteroid signaling and auxin transport are required to establish the periodic pattern of arabidopsis shoot vascular bundles." *Proceedings of the National Academy of Sciences* **106** (32): 13630–35.
- Igarashi, Daisuke, Kenichi Tsuda, and Fumiaki Katagiri. 2012. "The peptide growth factor , phyto-sulfokine , attenuates pattern-triggered immunity." *The Plant Journal* **71** (2): 194–204.
- Imkamke J, Halter T, Huang S, Schulze S, Mazzota S, Schmidt N, Manstretta R, Postel S, Wierzba M Yang Y, van Dongen W, Stahl M, Zipfel C, Goshe MB, Clouse S, de Vries SC, Tax F, Wang X Kemmerling B. 2017. "The Arabidopsis leucine-rich repeat receptor kinase BIR3 negatively regulates BAK1 receptor complex formation and stabilizes BAK1". *Plant Cell* **29** (9).
- Irani, Niloufer G, Simone Di Rubbo, Evelien Mylle, Jos Van den Begin, Joanna Schneider-Pizoń, Jaroslava Hniliková, Miroslav Šiša, et al. 2012. "Fluorescent castasterone reveals BRI1 signaling from the plasma membrane." *Nature Chemical Biology* **8** (6): 583–89.
- Irani, Niloufer G, and Eugenia Russinova. 2009. "Receptor endocytosis and signaling in plants." *Current Opinion in Plant Biology* **12** (6): 653–59.
- Ito, Emi, Masaru Fujimoto, Kazuo Ebine, Tomohiro Uemura, Takashi Ueda, Akihiko Nakano. 2012. "Dynamic behavior of clathrin in arabidopsis thaliana unveiled by live imaging." *The Plant Journal* **69** (2): 204–16.
- Jackson, Catherine L, and James E Casanova. 2000. "Turning on ARF: The Sec7 Family of exchange factors." *Trends in Cell Biology* **6** (99): 60–67.
- Jaillais, Yvon, Youssef Belkhadir, Emilia Balsemão-Pires, Jeffery L Dangel, and Joanne Chory. 2011. "Extracellular leucine-rich repeats as a platform for receptor/coreceptor complex formation." *Proceedings of the National Academy of Sciences* **108** (20): 8503–7.
- Jaillais, Yvon, Michael Hothorn, Youssef Belkhadir, Tsegaye Dabi, Zachary L Nimchuk, Elliot M Meyerowitz, and Joanne Chory. 2011. "Tyrosine phosphorylation controls brassinosteroid receptor activation by triggering membrane release of its kinase inhibitor." *Genes & Development* **25** (3): 232–37.
- Jaillais, Yvon, and Grégory Vert. 2012. "Brassinosteroids, gibberellins and light-mediated signalling are the three-way controls of plant sprouting." *Nature Cell Biology* **14** (8): 788–90.
- Jaillais, Yvon, and Grégory Vert. 2016. "Brassinosteroid signaling and BRI1 dynamics went underground." *Current Opinion in Plant Biology* **33** (10): 92–100.
- Jeong, S, A E Trotochaud, and S E Clark. 1999. "The Arabidopsis CLAVATA2 gene encodes a receptor-like protein required for the stability of the CLAVATA1 receptor-like kinase." *Plant Cell* **11** (10): 1925–34.
- Jiang, Lixi, Shu-Lan Yang, Li-Fen Xie, Ching San Pua, Xue-Qin Zhang, Wei-Cai Yang, Venkatesan Sundaresan, and De Ye. 2005. "VANGUARD1 encodes a pectin methylesterase that enhances pollen tube growth in the arabidopsis style and transmitting tract." *The Plant Cell* **17** (2): 584–96.
- Kajava, Andrey V. 2002. "Assessment of the ability to model proteins with leucine-rich repeats in light of the latest structural information." *Protein Science* **11** (5): 1082–90.
- Kang, Hyangju, Soo Youn Kim, Kyungyoung Song, Eun Ju Sohn, Yongjik Lee, Dong Wook Lee, Ikuko Hara-nishimura, and Inhwan Hwang. 2012. "Trafficking of vacuolar proteins: the crucial role of arabidopsis vacuolar protein sorting 29 in recycling vacuolar sorting receptor." *The Plant Cell* **24**: 5058–73.
- Karimi, M, D Inze, and A Depicker. 2002. "GATEWAY vectors for agrobacterium-mediated plant transformation." *Trends in Plant Science* **7** (5): 193–95.
- Karlova, Rummyana, Sjef Boeren, Walter van Dongen, Mark Kwaaitaal, Jose Aker, Jacques Vervoort, and Sacco de Vries. 2009. "Identification of in vitro phosphorylation sites in the arabidopsis thaliana somatic embryogenesis receptor-like kinases." *Proteomics* **9** (2): 368–79.

- Khaled, Sara Ben, Jelle Postma, and Silke Robatzek.** 2015. "A moving view : subcellular trafficking processes in pattern recognition receptor – triggered plant immunity." *Annual Review of Phytopathology* **53**: 379–402.
- Khan, Mamoona, Wilfried Rozhon, Jean Bigeard, Delphine Pflieger, Sigrid Husar, Andrea Pitzschke, Markus Teige, Claudia Jonak, Heribert Hirt, and Brigitte Poppenberger.** 2013. "Phosphorylate mitogen-activated protein (MAP) Kinase kinases , which control stomata development in arabidopsis thaliana." *The Journal of Biological Chemistry* **288** (11): 7519–27.
- Khoury, George A, Richard C Baliban, and Christodoulos A Floudas.** 2011. "Proteome-wide post-translational modification statistics: frequency analysis and curation of the swiss-prot database." *Scientific Reports* **1** (90): 1–5.
- Kim, Tae-Wuk, Shenheng Guan, Alma L Burlingame, and Zhi-Yong Wang.** 2011. "The CDG1 kinase mediates brassinosteroid signal transduction from BRI1 receptor kinase to BSU1 phosphatase and GSK3-like kinase BIN2." *Molecular Cell* **43** (4): 561–71.
- Kim, Tae-Wuk, Shenheng Guan, Yu Sun, Zhiping Deng, Wenqiang Tang, Jian-Xiu Shang, Ying Sun, Alma L Burlingame, and Zhi-Yong Wang.** 2009. "Brassinosteroid signal transduction from cell-surface receptor kinases to nuclear transcription factors." *Nature Cell Biology* **11** (10): 1254–60.
- Kim, Tae-wuk, Marta Michniewicz, Dominique C Bergmann, and Zhi-yong Wang.** 2012. "Brassinosteroid regulates stomatal development by GSK3-mediated inhibition of a MAPK pathway." *Nature* **482** (7385): 419–22.
- Kipreos, Edward T, and Michele Pagano.** 2000. "The F-Box Protein Family." *Genome Biology*, 1–7.
- Kleine-Vehn, Jürgen, Johannes Leitner, Marta Zwiewka, Michael Sauer, Lindy Abas, Christian Luschig, and Jirí Friml.** 2008. "Differential degradation of PIN2 auxin efflux carrier by retromer-dependent vacuolar targeting." *Proceedings of the National Academy of Sciences* **105** (46): 17812–17.
- Kohorn, Bruce D.** 2016. "Cell wall-associated kinases and pectin perception." *Journal of Experimental Botany* **67** (2): 489–94.
- Kolbeck, Andreas.** 2015. "Cell wall integrity signal propagation: localisation and turnover of RLP44." *Master Thesis Presented to the Faculty of Bioscience of the Ruprecht-Karls-Universität Heidelberg*.
- Kondo, Yuki, Tasuku Ito, Hirofumi Nakagami, Yuki Hirakawa, Masato Saito, Takayuki Tamaki, Ken Shirasu, and Hiroo Fukuda.** 2014. "Plant GSK3 proteins regulate xylem cell differentiation downstream of TDIF-TDR signalling." *Nature Communications* **5** (3504).
- Krupková, Eva, Peter Immerzeel, Markus Pauly, and Thomas Schmu.** 2007. "The TUMOROUS SHOOT DEVELOPMENT2 gene of arabid- oopsis encoding a putative methyltransferase is required for cell adhesion and co-ordinated plant development." *The Plant Journal* **50** (4): 735–50.
- Kutschmar, A, G Rzewuski, N Stührwohldt, G T Beemster, D Inze, and M Sauter.** 2009. "PSK-Alpha promotes root growth in arabidopsis." *New Phytologist* **181** (4): 820–31.
- Ladwig, Friederike, Renate I Dahlke, Nils Stührwohldt, Jens Hartmann, Klaus Harter, and Margret Sauter.** 2015. "Phytosulfokine regulates growth in arabidopsis through a response module at the plasma membrane that includes CYCLIC NUCLEOTIDE-GATED CHANNEL17, H + -ATPase, and BAK1." *The Plant Cell* **27** (6): 1718–29.
- Lampropoulos, Athanasios, Zoran Sutikovic, Christian Wenzl, Ira Maegele, Jan U Lohmann, and Joachim Forner.** 2013. "GreenGate- a novel, versatile, and efficient cloning system for plant transgenesis." *PloS One* **8** (12): e83043.
- Lemmon, Mark A, and Joseph Schlessinger.** 2010. "Cell signaling by receptor tyrosine kinases." *Cell* **141** (7): 1117–34.
- Lewit-Bentley, Anita, and Stéphane Réty.** 2000. "EF-Hand calcium-binding proteins." *Current Opinion in Structural Biology* **10** (6): 637–43.

- Li, Jia, Jiangqi Wen, Kevin a. Lease, Jason T. Doke, Frans E. Tax, and John C. Walker.** 2002. "BAK1, an Arabidopsis LRR receptor-like protein kinase, interacts with BRI1 and modulates brassinosteroid signaling." *Cell* **110** (2): 213–22.
- Li, Jianming, and Joanne Chory.** 1997. "A putative leucine-rich repeat receptor kinase involved in brassinosteroid signal transduction." *Cell* **90**: 929–38.
- Liebrand, Thomas, Hannes Schwandt, Baiping Wang, Zilai Wang, Qinxu Guo, Katsuhiko Tabuchi, Robert E Hammer, et al.** 2013. "Receptor-like kinase SOBIR1/EVR Interacts with receptor-like proteins in plant immunity against fungal infection." *Proceedings of the National Academy of Sciences* **110** (24): 10010–15.
- Liebrand, Thomas W H, Harrold A. van den Burg, and Matthieu H A J Joosten.** 2014. "Two for all: receptor-associated kinases SOBIR1 and BAK1." *Trends in Plant Science* **19** (2): 123–32.
- Lin, Guangzhong, Liang Zhang, Zhifu Han, Xinru Yang, Weijia Liu, Ertong Li, Junbiao Chang, Yijun Qi, Elena D Shpak, and Jijie Chai.** 2017. "A receptor-like protein acts as a specificity switch for the regulation of stomatal development." *Genes & Development* **31** (10): 927–38.
- Liners, Françoise, Jean-François Thibault, and Pierre Van Cutsem.** 1992. "Influence of the degree of polymerization of oligogalacturonates and of esterification pattern of pectin on their recognition by monoclonal antibodies." *Plant Physiology* **99** (3): 1099–1104.
- Logeat, Frédérique, Christine Bessia, Christel Brou, Odile LeBail, Sophie Jarriault, Nabil G Seidah, and Alain Israël.** 1998. "The Notch1 receptor is cleaved constitutively by a furin-like convertase." *Proceedings of the National Academy of Sciences* **95** (14): 8108–12.
- Lu, Dongping, Wenwei Lin, Xiquan Gao, Shujing Wu, Cheng Cheng, Julian Avila, Antje Heese, Timothy P Devarenne, Ping He, and Libo Shan.** 2011. "Direct Ubiquitination of pattern recognition receptor FLS2 attenuates plant innate immunity." *Science* **332** (6036): 1439–42.
- Lucas, William J, Andrew Groover, Raffael Lichtenberger, Kaori Furuta, Shri-ram Yadav, Xinqiang He, Hiroo Fukuda, et al.** 2013. "The plant vascular system : evolution , development." *Journal of Integrative Plant Biology* **55** (4): 294–388.
- Luschnig, Christian, and Grégory Vert.** 2014. "The dynamics of plant plasma membrane proteins: PINs and beyond." *Development* **141** (15): 2924–38.
- Ma, Xiyu, Guangyuan Xu, Ping He, and Libo Shan.** 2016. "SERKING coreceptors for receptors." *Trends in Plant Science* **21** (12). Elsevier Ltd: 1017–33.
- Manfield, Iain W., Caroline Orfila, Lesley McCartney, Jesper Harholt, Adriana J. Bernal, Henrik Vibe Scheller, Philip M. Gilmartin, Jorn D. Mikkelsen, J. Paul Knox, and William G T Willats.** 2004. "Novel cell wall architecture of isoxaben-habituated arabidopsis suspension-cultured cells: global transcript profiling and cellular analysis." *Plant Journal* **40** (2): 260–75.
- Martins, Sara, Esther M N Dohmann, Anne Cayrel, Alexander Johnson, Wolfgang Fischer, Florence Pojer, Béatrice Satiat-Jeunemaitre, et al.** 2015. "Internalization and vacuolar targeting of the brassinosteroid hormone receptor BRI1 are regulated by ubiquitination." *Nature Communications* **6**: 6151.
- Matsubayashi, Y.** 2006. "Disruption and overexpression of arabidopsis phyto-sulfokine receptor gene affects cellular longevity and potential for growth." *Plant Physiology* **142** (1): 45–53.
- Matsubayashi, Y., and Y. Sakagami.** 1996. "Phyto-sulfokine, Sulfated peptides that induce the proliferation of single mesophyll cells of *Asparagus officinalis* L." *Proceedings of the National Academy of Sciences* **93** (15): 7623–27.
- Matsubayashi, Y, M Ogawa, A Morita, and Y Sakagami.** 2002. "An LRR receptor kinase involved in perception of a peptide plant hormone, phyto-sulfokine." *Science* **296** (5572): 1470–72.
- Matsubayashi, Yoshikatsu.** 2014. "Posttranslationally Modified Small-Peptide Signals in Plants." *Annual Review of Plant Biology* **65** (1): 385–413.

- Matsubayashi, Yoshikatsu, Leiko Takagi, Naomi Omura, Akiko Morita, and Youji Sakagami.** 1999. "The Endogenous sulfated pentapeptide phyto-sulfokine- a stimulates tracheary element differentiation of isolated mesophyll cells of *Zinnia*." *Plant Physiology* **120** (August): 1043–48.
- Mbengue, Malick, Gildas Bourdais, Fabio Gervasi, Martina Beck, Ji Zhou, Thomas Spallek, Sebastian Bartels, et al.** 2016. "Clathrin-dependent endocytosis is required for immunity mediated by pattern recognition receptor kinases." *Proceedings of the National Academy of Sciences* **113** (39): 11034–39.
- McMahon, Harvey T H.T., and Emmanuel Boucrot.** 2011. "Molecular mechanism and physiological functions of clathrin-mediated endocytosis." *Nature Reviews* **12** (8): 517–33.
- Mellerowicz, Ewa J, and Björn Sundberg.** 2008. "Wood cell walls : biosynthesis , developmental dynamics and their implications for wood properties." *Current Opinion in Plant Biology* **11**: 293–300.
- Miyashima, Shunsuke, Jose Sebastian, Ji-Young Lee, and Yka Helariutta.** 2012. "Stem cell function during plant vascular development." *The EMBO Journal* **32** (2): 178–93.
- Mouille, Grégory, Marie-christine Ralet, Alan Marchant, and Herman Höfte.** 2007. "Homogalacturonan Synthesis in *Arabidopsis thaliana* requires a golgi-localized protein with a putative methyltransferase domain." *The Plant Journal* **50**: 605–14.
- Müller, Benedikt, Astrid Fastner, Julia Karmann, Andrea Bleckmann, Thomas Dresselhaus, Ulrich Z Hammes, Benedikt Mu, et al.** 2015. "Amino acid export in developing *Arabidopsis* seeds depends on umamit facilitators." *Current Biology* **35** (23): 3126–31.
- Müller, Ralf, Andrea Bleckmann, and Rüdiger Simon.** 2008. "The receptor kinase CORYNE of *Arabidopsis* transmits the stem cell – limiting signal CLAVATA3 independently of CLAVATA1." *The Plant Cell* **20** (April): 934–46.
- Nadeau, Jeanette a, and Fred D Sack.** 2002. "Control of stomatal distribution on the *Arabidopsis* leaf surface." *Science* **296** (2001): 1697–1700.
- Nakagami, Hirofumi, Naoyuki Sugiyama, Keiichi Mochida, Arsalan Daudi, Yuko Yoshida, Tetsuro Toyoda.** 2010. "Large-Scale comparative phosphoproteomics identifies conserved phosphorylation sites in plants." *Plant Physiology* **153** (3): 1161–74.
- Nakagawa, Tsuyoshi, Takayuki Kurose, Takeshi Hino, Katsunori Tanaka, Makoto Kawamukai, Yasuo Niwa, Kiminori Toyooka, Ken Matsuoka, Tetsuro Jinbo, and Tetsuya Kimura.** 2007. "Development of series of gateway binary vectors, pGWBs, for realizing efficient construction of fusion genes for plant transformation." *Journal of Bioscience and Bioengineering* **104** (1): 34–41.
- Neumetzler, Lutz, Tania Humphrey, Shelley Lumba, Stephen Snyder, Trevor H Yeats, Björn Usadel, Aleksandar Vasilevski, et al.** 2012. "The FRIABLE1 gene product affects cell adhesion in *Arabidopsis*." *Plos One* **7** (8): e42914..
- Nimchuk, Zachary L, Paul T Tarr, Carolyn Ohno, Xiang Qu, and Elliot M. Meyerowitz.** 2011. "Plant Stem cell signaling involves ligand-dependent trafficking of the CLAVATA1 receptor kinase." *Current Biology* **21** (5): 345–52.
- Oda, Yoshihisa, and Hiroo Fukuda.** 2012. "Secondary cell wall patterning during xylem differentiation." *Current Opinion in Plant Biology* **15** (1): 38–44.
- Offringa, Remko, and Fang Huang.** 2013. "Phosphorylation-dependent trafficking of plasma membrane proteins in animal and plant cells." *Journal of Integrative Plant Biology* **55** (9): 789–808.
- Oh, Eunkyoo, Jia-ying Zhu, and Zhi-yong Wang.** 2012. "Interaction between BZR1 and PIF4 Integrates brassinosteroid and environmental responses." *Nature Cell Biology* **14** (8): 802–9.
- Oh, Man-ho, William K Ray, Steven C Huber, John M Asara, Douglas A Gage, and Steven D Clouse.** 2000. "Recombinant brassinosteroid insensitive 1 receptor-like kinase autophosphorylates on serine and threonine residues and phosphorylates a conserved peptide Motif in Vitro ." *Plant Physiology* **124** (2): 751-66.

- Okamoto, Curtis T, Wenxia Song, Morgane Bomsel, and Keith E Mostov.** 1994. "Rapid internalization of the polymeric immunoglobulin receptor requires phosphorylated serine 726." *The Journal of Biological Chemistry* **269** (22): 15676–82.
- Ortiz-Morea, Fausto Andres, Daniel V. Savatin, Wim Dejonghe, Rahul Kumar, Yu Luo, Maciej Adamowski, Jos Van den Begin, et al.** 2016. "Danger-associated peptide signaling in *arabidopsis* requires clathrin." *Proceedings of the National Academy of Sciences* **113** (39): 11028–11033.
- Paez Valencia, Julio, Kaija Goodman, and Marisa S Otegui.** 2016. "Endocytosis and endosomal trafficking in plants." *Annual Review of Plant Biology* **67**: 309–35.
- Paredes, Alexander R, Christopher R Somerville, and David W Ehrhardt.** 2006. "Visualization of Cellulose Synthase Demonstrates Functional Association with Microtubules." *Science* **312** (5779): 1491–95.
- Park, Yong Bum, and Daniel J Cosgrove.** 2015. "Xyloglucan and its interactions with other components of the growing cell wall." *Plant & Cell Physiology* **56** (2): 180–94.
- Peaucelle, Alexis, Siobhan a. Braybrook, Laurent Le Guillou, Emeric Bron, Cris Kuhlemeier, and Herman Höfte.** 2011. "Pectin-induced changes in cell wall mechanics underlie organ initiation in *arabidopsis*." *Current Biology* **21** (20): 1720–26.
- Peaucelle, Alexis, Raymond Wightman, and Herman Höfte.** 2015. "The control of growth symmetry breaking in the *arabidopsis* hypocotyl." *Current Biology* **25** (13):1746–52.
- Pelloux, Jérôme, Christine Rustérucci, and Ewa J Mellerowicz.** 2007. "New insights into pectin methylesterase structure and function." *Trends in Plant Science* **12** (6): 267–77.
- Perrot-Rechenmann, Catherine.** 2010. "Cellular responses to auxin : division versus expansion." *Cold Spring-Harbor Perspectives in Biology* **2** (1): 1–16.
- Peterson, K M, A L Rychel, and K U Torii.** 2010. "Out of the Mouths of Plants: The molecular basis of the evolution and diversity of stomatal development." *Plant Cell* **22** (2): 296–306.
- Reichardt, Ilka, York-dieter Stierhof, Ulrike Mayer, Sandra Richter, Heinz Schwarz, and Karin Schumacher.** 2007. "Report plant cytokinesis requires de novo secretory trafficking but not endocytosis." *Current Biology* **17** (23):2047–53.
- Reyes, Francisca C, Rafael Buono, and Marisa S Otegui.** 2011. "Plant endosomal trafficking pathways." *Current Opinion in Plant Biology* **14** (6): 666–73.
- Richter, Sandra, Niko Geldner, Jarmo Schrader, Hanno Wolters, York-dieter Stierhof, Gabino Rios, Csaba Koncz, David G Robinson, and Gerd Ju.** 2007. "Functional diversification of closely related ARF-GEFs in protein secretion and recycling." *Nature* **448** (7152): 488–93.
- Ridley, Brent L, Malcolm A O'Neill, and Debra Mohnen.** 2001. *Pectins: Structure, Biosynthesis, and Oligogalacturonide-Related Signaling. Phytochemistry. Vol. 57.*
- Robert, Stéphanie, Jürgen Kleine-Vehn, Elke Barbez, Michael Sauer, Tomasz Paciorek, Pawel Baster, Kenichiro Hayashi, et al.** 2010. "ABP1 Mediates auxin inhibition of clathrin-dependent endocytosis in *arabidopsis*." *Cell* **143** (1): 111–21.
- Robinson, D. G., L. Jiang, and K. Schumacher.** 2008. "The endosomal system of plants: charting new and familiar territories." *Plant Physiology* **147** (4): 1482–92.
- Robinson, David G, Peter Pimpl, David Scheuring, York-dieter Stierhof, Silke Sturm, and Corrado Viotti.** 2012. "Trying to Make Sense of Retromer." *Trends in Plant Science* **17** (7): 431–39.
- Santiago, Julia, Benjamin Brandt, Mari Wildhagen, Ulrich Hohmann, Ludwig A Hothorn, Melinka A Butenko, and Michael Hothorn.** 2016. "Mechanistic Insight into a peptide hormone signaling complex mediating floral organ abscission." *eLife* **5** (e15075): 1–19.
- Santiago, Julia, Christine Henzler, and Michael Hothorn.** 2013. "Molecular Mechanism for plant steroid receptor activation by somatic embryogenesis co-receptor kinases." *Science* **341** (6148): 889–93.

- Schallus, Thomas, Christine Jaeckh, Krisztina Fehér, Angelina S Palma, Yan Liu, Jeremy C Simpson, Mukram Mackeen, et al.** 2008. "Malectin : A novel carbohydrate-binding protein of the endoplasmic reticulum and a candidate player in the early steps of protein N -Glycosylation." *Molecular Biology of the Cell* **19**: 3404–14.
- Scheible, W R, R Eshed, T Richmond, D Delmer, and Christopher R Somerville.** 2001. "Modifications of cellulose synthase confer resistance to isoxaben and thiazolidinone herbicides in arabidopsis ixr1 mutants." *Proceedings Of The National Academy Of Sciences* **98** (18): 10079–84.
- Scheller, Henrik Vibe, and Peter Ulvskov.** 2010. "Hemicelluloses." *Annual Review of Plant Biology* **61** (1): 263–89.
- Schulze, Birgit, Tobias Mentzel, Anna K Jehle, Katharina Mueller, Seraina Beeler, Thomas Boller, Georg Felix, and Delphine Chinchilla.** 2010. "rapid heteromerization and phosphorylation of ligand-activated plant transmembrane receptors and their." *The Journal of Biological Chemistry* **285** (13): 9444–51.
- Schwessinger, Benjamin, Milena Roux, Yasuhiro Kadota, Vardis Ntoukakis, Jan Sklenar, Alexandra Jones, and Cyril Zipfel.** 2011. "Phosphorylation-dependent differential regulation of plant growth, cell death, and innate immunity by the regulatory receptor-like kinase BAK1." *PLoS Genetics* **7** (4): e1002046.
- Segonzac, Cécile, Alberto P Macho, Maite Sanmartín, Vardis Ntoukakis, José Juan Sánchez-serrano, and Cyril Zipfel.** 2014. "Negative control of BAK 1 by protein phosphatase 2 A during plant innate immunity." *The EMBO Journal* **33** (18): 2069–79.
- Sénéchal, Fabien, Christopher Wattier, Christine Rustérucci, and Jérôme Pelloux.** 2014. "Homogalacturonan-modifying enzymes : structure, expression , and roles in plants" *Journal of Experimental Botany* **65** (18): 5125-5160.
- Shen, Yunping, and Andrew C. Diener.** 2013. "Arabidopsis Thaliana RESISTANCE TO FUSARIUM OXYSPORUM 2 Implicates tyrosine-sulfated peptide signaling in susceptibility and resistance to root infection." *PLoS Genetics* **9** (5) e1003525.
- Shih, Han-wei, Nathan D Miller, Cheng Dai, Edgar P Spalding, and Gabriele B Monshausen.** 2014. "Report the receptor-like kinase FERONIA is required for mechanical signal transduction in arabidopsis seedlings." *Current Biology* **24** (16): 1887–92.
- Skowrya, Dorota, Karen L Craig, Mike Tyers, Stephen J Elledge, and J Wade Harper.** 1997. "F-Box proteins are receptors that recruit phosphorylated substrates to the SCF ubiquitin-ligase complex." *Cell* **91** (2): 209–19.
- Somerville, Chris.** 2006. "Cellulose synthesis in higher plants." *Annu. Rev. Cell Dev. Biolo* **22**: 53–78.
- Somssich, Marc, Andrea Bleckmann, and Rüdiger Simon.** 2016. "Shared and distinct functions of the pseudokinase CORYNE (CRN) in shoot and root stem cell maintenance of Arabidopsis." *Journal of Experimental Botany* **67** (16): 4901–15..
- Stahl, Yvonne, H Wink, Gwyneth C Ingram, and Rüdiger Simon.** 2009. "Report a signaling module controlling the stem cell niche in arabidopsis root meristems." *Current Biology* **19** (11): 909–14.
- Sun, Yu, Xi Ying Fan, Dong Mei Cao, Wenqiang Tang, Kun He, Jia Ying Zhu, Jun Xian He, et al.** 2010. "Integration of brassinosteroid signal transduction with the transcription network for plant growth regulation in Arabidopsis." *Developmental Cell* **19** (5): 765–77.
- Suslov, D, and JP Verbelen.** 2006. "Cellulose orientation determines mechanical anisotropy in onion epidermis cell walls." *Journal of Experimental Botany* **57** (10): 2183–92.
- Sweitzer, Sharon M, and Jenny E Hinshaw.** 1998. "Dynamin Undergoes a GTP-dependent conformational change causing vesiculation." *Cell* **93** (6): 1021–29.
- Szekeres, Miklos, Kinga Németh, Zsuzsanna Koncz-Kálmán, Jaideep Mathur, Annette Kauschmann, Thomas Altmann, Ferenc Nagy, Jeff Schell, George P Rédei, and Csaba Koncz.** 1996. "Brassinosteroids rescue the deficiency of CYP90 , a Cytochrome P450, controlling cell elongation and de-etiolation in arabidopsis." *Cell* **85** (2): 171–82.

- Takano, Junpei, Mayuki Tanaka, Atsushi Toyoda, Kyoko Miwa, Koji Kasai, Kentaro Fuji, and Hitoshi Onouchi.** 2010. "Polar localization and degradation of arabidopsis boron transporters through distinct trafficking pathways." *Proceedings of the National Academy of Sciences* **107** (11): 5220–25.
- Tang, Wenqiang, Tae-wuk Kim, Juan A Oses-prieto, Yu Sun, Zhiping Deng, Ruiju Wang, Alma L Burlingame, and Zhi-yong Wang.** 2009. "Brassinosteroid-signaling kinases (BSKs) mediate signal transduction from the receptor kinase BRI1 in Arabidopsis." *Science* **321** (5888): 557–60.
- Tanz, Sandra K, Ian Castleden, Cornelia M Hooper, Michael Vacher, Ian Small, and Harvey A Millar.** 2013. "SUBA3: A database for integrating experimentation and prediction to define the subcellular location of proteins in Arabidopsis." *Nucleic Acids Research* **41** (11): 1185–91.
- Taylor, Neil G, Rhian M Howells, Alison K Huttly, Kate Vickers, and Simon R Turner.** 2003. "Interactions among three Distinct CesA proteins essential for cellulose synthesis." *Proceedings of the National Academy of Sciences* **100** (3): 1450–55.
- Traub, Linton M, and Juan S Bonifacino.** 2014. "Cargo recognition in clathrin-mediated endocytosis." *Cold Spring-Harbor Perspectives in Biology* **5** (11): 1–23.
- Verger, Stéphane, Salem Chabout, Emilie Gineau, and Grégory Mouille.** 2016. "Cell adhesion in plants is under the control of putative o-fucosyltransferases." *Development* **143** (14): 2536–40.
- Verhertbruggen, Yves, Susan E. Marcus, Ash Haeger, José J. Ordaz-Ortiz, and J. Paul Knox.** 2009. "An extended set of monoclonal antibodies to pectic homogalacturonan." *Carbohydrate Research* **344** (14): 1858–62.
- Vert, Grégory, and Joanne Chory.** 2006. "Downstream nuclear events in brassinosteroid signalling." *Nature* **441** (7089): 96–100.
- Vragović, Kristina, Ayala Sela, Lilach Friedlander-Shani, Yulia Fridman, Yael Hacham, Neta Holland, Elizabeth Bartom, Todd C Mockler, and Sigal Savaldi-Goldstein.** 2015. "Translatome analyses capture of opposing tissue-specific brassinosteroid signals orchestrating root meristem differentiation." *Proceedings of the National Academy of Sciences* **112** (3): 923–28.
- Wagner, Tanya A, and Bruce D Kohorn.** 2001. "Wall-associated kinases are expressed throughout plant development and are required for cell expansion." *The Plant Cell* **13** (2): 303–18.
- Walker, John C., and Ren Zhang.** 1990. "Relationship of a putative receptor protein kinase from maize to the s-locus glycoproteins of Brassica." *Nature* **345**: 743–46.
- Wang, G., U. Ellendorff, B. Kemp, J. W. Mansfield, a. Forsyth, K. Mitchell, K. Bastas, et al.** 2008. "A Genome-wide functional investigation into the roles of receptor-like proteins in arabidopsis." *Plant Physiology* **147** (2): 503–17.
- Wang, Jizong, Hongju Li, Zhifu Han, Heqiao Zhang, Tong Wang, Guangzhong Lin, Junbiao Chang, Weicai Yang, and Jijie Chai.** 2015. "Allosteric Receptor activation by the plant peptide hormone phytosulfokine." *Nature* **525** (7568): 265–68.
- Wang, Li, Hong Li, Xueqin Lv, Tong Chen, Ruili Li, Yiqun Xue, Jianjun Jiang, et al.** 2015. "Spatiotemporal dynamics of the BRI1 receptor and its regulation by membrane microdomains in Living Arabidopsis Cells." *Molecular Plant* **8** (9): 1334–49.
- Wang, Ruiju, Mengmeng Liu, Min Yuan, Juan A. Oses-Prieto, Xingbo Cai, Ying Sun, Alma L. Burlingame, Zhi Yong Wang, and Wenqiang Tang.** 2016. "The brassinosteroid-activated BRI1 receptor kinase is switched off by dephosphorylation mediated by cytoplasm-localized PP2A B' Subunits." *Molecular Plant* **9** (1): 148–57.
- Wang, Tuo, Yong Bum Park, Daniel J Cosgrove, and Mei Hong.** 2015. "Cellulose-pectin spatial contacts are inherent to never-dried arabidopsis primary cell walls: evidence from solid-state nuclear magnetic resonance." *Plant Physiology* **168** (3): 871–84.
- Wang, Xiaofeng, Michael B Goshe, Erik J Soderblom, Brett S Phinney, Jason A Kuchar, Jia Li, Tadao Asami, Shigeo Yoshida, Steven C Huber, and Steven D Clouse.** 2005. "Identification and functional analysis of in vivo phosphorylation sites of the arabidopsis receptor kinase." *The Plant Cell* **17** (6): 1685–1703.

- Wang, Xiaofeng, Uma Kota, Kai He, Kevin Blackburn, Jia Li, Michael B. Goshe, Steven C. Huber, and Steven D. Clouse.** 2008. "Sequential transphosphorylation of the BRI1/BAK1 receptor kinase complex impacts early events in brassinosteroid signaling." *Developmental Cell* **15** (2): 220–35.
- Wang, Z Y, H Seto, S Fujioka, S Yoshida, and J Chory.** 2001. "BRI1 is a critical component of a plasma-membrane receptor for plant steroids." *Nature* **410** (6826): 380–383.
- Wolf, S, K Hématy, and H Höfte.** 2012. "Growth control and cell wall signaling in plants." *Annual Review of Plant Biology* **63** (1): 381–407.
- Wolf, Sebastian.** 2017. "Plant cell wall signalling and receptor-like kinases." *Biochemical Journal* **474** (4): 471–92.
- Wolf, Sebastian, Grégory Mouille, and Jérôme Pelloux.** 2009. "Homogalacturonan methylesterification and plant development." *Molecular Plant* **2** (5): 851–60.
- Wolf, Sebastian, Jozef Mravec, Steffen Greiner, Grégory Mouille, and Herman Höfte.** 2012. "Plant cell wall homeostasis is mediated by brassinosteroid feedback signaling." *Current Biology* **22** (18): 1732–37.
- Wolf, Sebastian, Dieuwertje van der Does, Friederike Ladwig, Carsten Sticht, Andreas Kolbeck, Ann-Kathrin Schürholz, Sebastian Augustin, et al.** 2014. "A Receptor-like protein mediates the response to pectin modification by activating brassinosteroid signaling." *Proceedings of the National Academy of Sciences* **111** (42): 15261–66.
- Wu, Guang, Xiuling Wang, Xianbin Li, Yuji Kamiya, and Marisa S Otegui.** 2011. "Methylation of a Phosphatase Specifies Dephosphorylation and Degradation of Activated Brassinosteroid Receptors." *Sci Signal* **4** (172): 1–25.
- Xiao, Chaowen, Tian Zhang, Yunzhen Zheng, Daniel J Cosgrove, and Charles T Anderson.** 2016. "Xyloglucan deficiency disrupts microtubule stability and cellulose biosynthesis in arabidopsis , altering cell growth and morphogenesis." *Plant Physiology* **170** (1): 234–49.
- Xu, S.-L., A. Rahman, T. I. Baskin, and J. J. Kieber.** 2008. "Two Leucine-rich repeat receptor kinases mediate signaling, linking cell wall biosynthesis and ACC Synthase in Arabidopsis." *The Plant Cell* **20** (11): 3065–79.
- Xu, Weihui, Juan Huang, Baohua Li, Jiayang Li, and Yonghong Wang.** 2008. "Is kinase activity essential for biological functions of BRI1?" *Cell Research* **18** (4): 472–78.
- Yadav, Vandana, Isabel Molina, Kosala Ranathunge, Indira Queralta-Castillo, Steven J Rothstein, and Jason W Reed.** 2014. "ABCG Transporters are required for suberin and pollen wall extracellular barriers in Arabidopsis." *The Plant Cell* **26** (9): 3569–88.
- Yamaguchi, Yasuka L, Takashi Ishida, and Shinichiro Sawa.** 2016. "CLE Peptides and their signaling pathways in plant development." *Journal of Experimental Botany* **67** (16): 4813–26.
- Yamaguchi, Yube, and Alisa Huffaker.** 2011. "Endogenous peptide elicitors in higher plants." *Current Opinion in Plant Biology* **14** (4): 351–57.
- Yamaguchi, Yube, Alisa Huffaker, Anthony C Bryan, Frans E Tax, and Clarence A Ryan.** 2010. "PEPR2 is a second receptor for the Pep1 and Pep2 peptides and contributes to defense responses in Arabidopsis." *The Plant Cell* **22** (2): 508–22.
- Yang, Heping, Yoshikatsu Matsubayashi, Kenzo Nakamura, and Youji Sakagami.** 1999. "Oryza Sativa PSK gene encodes a precursor of phytosulfokine- alfa , a sulfated peptide growth factor found in plants." *Proceedings of the National Academy of Sciences* **96** (23): 13560–65.
- Yeats, Trevor H, and Jocelyn K C Rose.** 2013. "The formation and function of plant cuticles." *Plant Physiology* **163** (1): 5–20.
- Yeats, Trevor H, Hagit Sorek, David E Wemmer, and Chris R Somerville.** 2016. "Cellulose deficiency is enhanced on hyper accumulation of sucrose by a h + -coupled sucrose symporter." *Plant Physiology* **171** (1): 110–24.
- Zhang, Heqiao, Zhifu Han, Wen Song, and Jijie Chai.** 2016. "Structural insight into recognition of plant peptide hormones by receptors." *Molecular Plant* **9** (11): 1454–63.

- Zhang, Weiguo, Malou Fraiture, Dagmar Kolb, Birgit Löffelhardt, Yoshitake Desaki, Freddy F G Boutrot, Mahmut Tör, Cyril Zipfel, Andrea A Gust, and Frédéric Brunner.** 2013. "Arabidopsis RECEPTOR-LIKE PROTEIN30 and receptor-like kinase SUPPRESSOR OF BIR1-1/ EVERSHED mediate innate immunity to necrotrophic fungi." *The Plant Cell* **25** (10): 4227–41.
- Zhang, Zhenzhen, Jia-ying Zhu, Jeehee Roh, Yu Sun, Wenfei Wang, Zhi-yong Wang, Seong-ki Kim, Christian Meyer, and Yu Sun.** 2016. "Report TOR signaling promotes accumulation of bsr1 to balance growth with carbon availability in arabidopsis." *Current Biology* **26** (14): 1854–60.
- Zhu, Yingfang, Yuqing Wang, Ruili Li, Xiufen Song, Qinli Wang, Shanjin Huang, Jing Bo Jin, Chun-ming Liu, and Jinxing Lin.** 2010. "Analysis of interactions among the CLAVATA3 receptors reveals a direct interaction between CLAVATA2 and CORYNE in Arabidopsis." *The Plant Journal* **61** (2): 223–33.
- Zientara-rytter, Katarzyna, and Agnieszka Sirko.** 2016. "To deliver or to degrade – an interplay of the ubiquitin – proteasome system , autophagy and vesicular transport in plants." *The FEBS Journal* **283** (19): 3534–55.
- Zipfel, Cyril, Gernot Kunze, Delphine Chinchilla, Anne Caniard, Jonathan D G Jones, Thomas Boller, and Georg Felix.** 2006. "Perception of the bacterial PAMP EF-Tu by the receptor EFR restricts agrobacterium -mediated transformation." *Cell* **125** (4): 749–60.

Acknowledgments

We say in Spanish “es de bien nacido ser agradecido”, something that according to google translator should be “gratitude is the sign of noble souls” in English. Therefore, trying to make myself an honorable human I would like to thank to all those people that went with me along this road to the PhD.

I am extremely thankful to Dr. Sebastian Wolf. Thanks for invite me to Heidelberg and give me the opportunity to start this adventure. Thank you for guiding me along this journey and giving me free hands to explore, to learn and to mistake but also for being there to solve any doubt or even some drama. It has been a pleasure to achieve my PhD as a member of your team.

I would like to thank to Prof. Jan Lohmann and Prof. Karin Schumacher for all the support, discussion and ideas during the TAC as well as for taking their time to be part of my thesis committee defense. I also immensely grateful to Prof. Steffen Lemke for not doubt even a second to accept being part of my committee and go along the awesome world of plant cell wall.

I might be quite subjective, but I no doubt when I write that I had the best colleagues in the lab during this time. Actually, this experience it would not be the same without all the motivation bubbles, frustration killers and burning away lab monkeys. Eli, it has been a long way since the “we are not to close” to the “daily Tinder updates”. I don’t know what I could do without your spontaneity and without the “fights” for having the reason. What I will not miss at all is your infiltration protocol. Thank you very much for being as authentic as you are. Zhenni, toujours la voix de la raison. Merci pour me calmer dans les pire moments, merci pour rasionaliser mes drama attaques et bien sûr pour accoître ma capacité pour filtrer en chinoises, même si j’ai appris le faux genre. Anka, gracias por todo, especially for being able to make me smile in the desperation moments, to stay strong when my foul mood was around and to be the best sporty partner. Nobody is able to fill so efficiently an ambulance with my furniture. I would like to also thank the rest of AG Wolf members along these years: John, Augustin, Leonie, Nabila and specially Polo. Not only for all your scientific input and help with the writing, also for every single discussion about everything and to be the first one offering a beer when it was needed. I would also like to put into words my gratitude to Heike, to be patience enough to control me when I was wander around totally lost.

I would like to also thanks the rest of colleges from AG Schumacher, AG Maizel and COS. An honest and especial thanks to Rainer, Görkem, Upendo, Jana, Noah, Paula, Zhaoxue, Michi, Cristophe, Vadir, Mouli, Francesca, Sanja and Lúa, for all the scientific ideas, support and good moments around. But overall, I would like to thanks to those who not only shared bench issues but also life experiences. Belén, thanks for bringing time to time the sunny south back to the lab, your biotec spirit always keep me alive. Paola, thank you for taking over the role of a mom and control that this oso peludo does not harm himself, your hugs have always reloaded my energy in the hardest moments. However, we still need to solve the “zapato con z” issue, it is not going well by now. Anne-Laure, I really missed your post-it in the last year even if we shortened distances with those long trans-border calls. Thanks to be crazy enough to give free rein to our stupidities an make every event unforgettable. Amaya, ay Amaya. Thank you very much to try to integrate me in HD life from the very beginning and keep supporting me along this time with all the mimos and good advices, despite all my cat moments and our little disputations. I am

really looking forward to continue judging your outfits although you learnt and improved. Andrea, trying to write a line about you is quite complicated, simply because there are some many great moments together with you that they make difficult to summarize it here. In any case, thanks to be ready to share all the fun but also to be the first one to not hesitate on helping when was needed. Zaida, who would tell us that we would share endless experiences the day you brought me that letter that mistakenly arrive to your house? I am deeply grateful for all your help with the bench work and the writing process but specially for letting this proud berciano share with you concerts, game nights, tones of laughs and most important, a friendship. To all of you, thank you. Your friendship is probably one of the best treasures I got in Heidelberg. I would like to thank also to all that universe outside of the lab. Thanks to the “Big Thing” and especially to Deni, Shafak, Emil, Asha and Veli. Theatre has been not only the best stress release machinery but also a factory of wonderful moments and crazy scientific discussions.

I am thankful to all my friends, to all those who keep feeding my life even when the only way was behind a WhatsApp group. From all the biofrikis, I am especially thankful to Laura, to be not only the one who took the responsibility to be my family here, but also the best scientific reviewer, English proofreader and musical critic. To Sara, for being a “scientific lamp” as well as a never-ending source of smiles and frikadas. To Blanca, Brandán and Marta, because you are always ready for every crazy idea. To Ana, for all the “Buenos días”, without exception, that fulfill with happiness the grey german mornings. To Laura Junco, to be that undiscovered treasure from Fisio-lab, thank you for being my bigger contributor to my special book collection and for becoming an indispensable person. To Vero, because since our first practical/fight-for-colors together, you never stopped to help me to become a better scientist. Special mention to Africa. I would not only like to thank all our experiences sharing bench troubles, buses to the Atlas mountains or hours spelling the Rodalies stops. I would like to also thank her the last three years of continuous support, endless skype sessions and constant supervision of my “garneladas”. Y ya sabes, olvida todos los prejuicios. From the Erasmus tribe, thanks to Lis and Laura to share the same concept of life as me. I always find on you the most trustable words. We have still tones of experiences ahead. To Esther, because I would not be the same hipster without you. To Ana and Emiliano, because you are the example that time and distance do not alter the important things of life. From “El Bierzo, Esencia del Noroeste”, to Jose, Rebe, Stéphanie, Bea, Anna, Raquel, Patri y Laura. I guess that the entire life sharing everything is enough to be here.

Last but not least, to my family. Gracias mamá y papá por darme alas para volar tan alto como quisiera. Gracias por vuestro constante esfuerzo para permitirme alcanzar cada una de las metas que han ido apareciendo a lo largo del camino. Gracias por vuestor apoyo eterno, por vuestras palabras de aliento y por vuestra dedicación. Andrés, no te lo digo mucho, pero gracias. Por quererme a nuestra manera, por ser un ejemplo. Irene, aunque nuestro rollo sea el refunfuño, gracias por leerme como solo tú me lees. A ti Candela, por traer la alegría cuando más la necesitaba. Y también a ti, abuelo. Que nos enseñaste a todos que lo importante de la vida es disfrutarla. Nada de lo que haga en esta vida será suficiencia para devolveros todo lo que os debo.